

# Investigation of the Pathophysiology and In-Utero Treatment of Gastroschisis-Related Intestinal Dysfunction

Helen Kristina Carnaghan

Thesis submitted in fulfilment for the requirements of the degree of Doctor of  
Philosophy, University College London, December 2018

## **Declaration**

I, Helen Kristina Carnaghan, confirm that the work presented in this thesis is my own. Where information has been derived from other sources, I confirm that this has been indicated in the thesis.

Signed:

Date: 16<sup>th</sup> December 2018

## **Abstract**

**Background:** Gastroschisis is a paraumbilical abdominal wall defect through which the bowel herniates. The bowel is in direct contact with the amniotic fluid. At birth the bowel is often thickened and shortened. The main gastroschisis-related morbidity is that of intestinal dysmotility but the mechanism(s) underlying this are poorly understood and no treatment advances have occurred since the advent of parenteral nutrition. Human studies have shown that the third trimester amniotic fluid of gastroschisis pregnancies is proinflammatory. In addition, in animal models of gastroschisis and human pathological gut tissue interstitial cells of Cajal (ICC – pacemaker cells of the gut) have been found to be decreased in number and immature within gastroschisis bowel.

**Hypotheses:** Gastroschisis-related intestinal dysfunction (GRID) is secondary to deficient, immature bowel wall ICC.

**Aims:** My primary aim in this thesis was to investigate the development of ICC in gastroschisis utilising genetic animal models and human pathological gut tissue. Additionally, I aimed to determine the overall morphology of gastroschisis bowel wall, the impact of inflammatory modulation on bowel wall development and the impact of clinical antenatal interventions on infant outcomes.

**Methods:** Quantitative analysis of bowel wall ICC, enteric neurons and architecture were performed utilising genetic animal gastroschisis models and human pathological tissue. Modulation of in-utero inflammation was performed through in-utero injections of IL-8 (pro-inflammatory protein) in a genetic animal gastroschisis model. Finally, retrospective clinical data on gastroschisis were collected from three paediatric surgical centres to determine whether early delivery or administration of maternal antenatal corticosteroids could improve infant morbidity.

**Results:** Phenotypic analysis of the Scribble knockout mouse model revealed the expressed abdominal wall defect (AWD) to be that of exomphalos rather than gastroschisis. Additionally, phenotypic analysis of the aortic carboxypeptidase-like protein (ACLP) knockout mouse showed the AWD was not characteristic of

gastroschisis as the externalised bowel was free floating within exocoelomic fluid and not the amniotic fluid. Bowel wall ICC were architecturally normal but reduced in number in AWD fetuses compared to controls. In-utero injection of IL-8 further reduced ICC numbers. In contrast, analysis of human pathological gut tissue showed no difference in the number or architecture of bowel wall ICC between gastroschisis and control tissue. However, the gastroschisis bowel wall was significantly thicker than that of controls with evidence of smooth muscle hyperplasia and deficiency of  $\alpha$ -smooth muscle actin within the longitudinal muscle layer.

The clinical retrospective data showed that early delivery of gastroschisis fetuses did not improve bowel function and was associated with prolonged time to full enteral feeds and length of hospital stay. Additionally, there was no evidence that administration of maternal antenatal corticosteroids improved time to full enteral feeds or length of hospital stay in gastroschisis infants.

**Conclusions:** Phenotypic analysis of abdominal wall defects in murine models is challenging. However, accurate delineation of the defect anatomy is essential to ensure appropriate result reporting and data analysis. The presented data suggests the ICC may be less important as the cause of GRID than originally expected. However, another potential cause for GRID is bowel wall thickening comprising of smooth muscle hyperplasia and possible bowel myopathy for which there are several hypothesised triggers. Additionally, the data presented in this thesis do not support early delivery of gastroschisis fetuses or the administration of maternal antenatal corticosteroids as methods to improve gastroschisis infant outcomes.

The results of this thesis have generated some important findings and have highlighted a number of novel hypotheses for the trigger of GRID. Further research on the basis of these findings within an appropriate animal model and through prospective non-invasive human studies are required in order to develop a targeted antenatal therapy to improve gastroschisis infant bowel function and clinical outcomes.



## Impact Statement

The research presented in this thesis significantly adds to the scientific literature on the pathophysiology of gastroschisis-related intestinal dysfunction (GRID) and has been presented at international conferences and published in peer review journals. In particular, the data presented contradicts the current literature on the pathophysiology of GRID providing evidence for a potential alternative mechanism and reclassifies the phenotypic description of two genetic mouse abdominal wall defect models that have previously been reported as gastroschisis in the literature. This will enable future research to build on this knowledge and potentially help develop novel therapies for GRID shortening the time to full enteral feeds, duration of parenteral nutrition and length of hospital stay for gastroschisis infants. The clinical data generated from the large retrospective cohort studies will help provide guidance to clinicians treating women with a gastroschisis pregnancy in fetal medicine centres and enable more informed discussions when counselling the expectant parents.

Methodologically this thesis describes a novel micro-MRI technique for the phenotyping of fetal mouse abdominal wall defects, which could be of value for the phenotyping of other structural abnormalities of the abdominal wall and also other organ systems in fetal genetic mouse models. Additionally, robust cell quantification techniques were developed during this research for the analysis of bowel wall interstitial cells of Cajal and enteric neurons, which will be of value to other researchers within this field and may help standardise cell quantification making data more comparable and reproducible.

This research adds to the literature, which aims to improve gastroschisis infant outcomes and the lives of the patient and their families. As the scientific knowledge of the cause of GRID grows this brings the scientific and medical community closer to helping affected infants to achieve enteral autonomy and leave hospital sooner. This will not only improve the health of the infant and reduce the risk of complications such as sepsis but will reunite families quicker. Frequently parents have to travel long distances or live away from home during their newborns hospital stay due to the care required being located in tertiary referral centres that may be a long distance from home. A shorter hospital stay will allow families to bond quicker,

reduce parental expense of travelling/accommodation and the stress of living apart  
improving the lives of not just the infant but their family too.

# Table of Contents

Declaration .....	2
Abstract .....	3
Impact Statement.....	5
Table of Contents .....	7
Table of Figures .....	20
Table of Tables.....	30
Acknowledgements .....	35
Abbreviations .....	36
Definitions .....	38
Chapter 1: Introduction .....	39
1.1 Overview .....	39
1.2 Normal Function and Structure of the Gut.....	39
1.2.1 Functions of the Gut.....	39
1.2.2 Structure of the Gastrointestinal Tract Wall .....	40
1.2.3 Gut Motility.....	43
1.2.4 Intestinal Smooth Muscle.....	44
1.2.5 Enteric Nervous System.....	45
1.2.6 Interstitial Cells of Cajal .....	46
1.3 Overview of Human Embryological and Fetal Development .....	48
1.3.1 Overview of the Embryonic and Fetal Period.....	48
1.3.2 Terminology of Pregnancy.....	48
1.3.3 The Placenta, Fetal Membranes, Umbilical Cord, and Amniotic Fluid... .....	49
1.4 Development of the Gastrointestinal Tract and Abdominal Wall.....	50
1.4.1 General Development of the Gastrointestinal Tract.....	50

1.4.2	Ventral Abdominal Wall Closure and Development of the Midgut Intestinal Loops .....	53
1.4.3	Neuromuscular Development of the Gut .....	55
1.5	Human Congenital Anomalies .....	56
1.5.1	Overview of Congenital Anomalies .....	56
1.5.2	Congenital Ventral Abdominal Wall Defects .....	57
1.5.3	Congenital Gastrointestinal Defects .....	61
1.6	Gastroschisis .....	63
1.6.1	Overview and Characteristic Features .....	63
1.6.2	Concomitant Congenital Defects .....	65
1.6.3	Pathogenesis .....	66
1.6.4	Aetiology, Incidence and Risk Factors .....	67
1.6.5	Mortality .....	68
1.6.6	Morbidity .....	69
1.6.7	Clinical Management of Gastroschisis .....	70
1.6.7.1	Antenatal Management of Gastroschisis .....	70
1.6.7.2	Neonatal and Surgical Management of Gastroschisis .....	76
1.6.7.3	Surgical Management .....	77
1.7	Current Understanding of Gastroschisis-Related Intestinal Dysfunction ...	80
1.7.1	Gastroschisis versus Exomphalos: Gut Function and Anatomy .....	81
1.7.2	Gastroschisis Antenatal Bowel Morphological Changes and Amniotic Fluid Composition .....	81
1.7.3	Amniotic Fluid and Fetal Inflammatory Markers .....	82
1.7.4	Bowel Wall Thickening .....	83
1.7.5	Deficiency of the Interstitial Cells of Cajal .....	86
1.7.6	ICC Plasticity and Response to Inflammation .....	90
1.8	Clinical Therapeutic Strategies Trialled in Humans to Improve GRID .....	91
1.8.1	Amnioexchange .....	91

1.8.2	Early Delivery .....	92
1.8.3	Fetoscopic Surgery.....	92
1.8.4	Postnatal Prokinetics .....	94
1.9	Animal Models .....	95
1.9.1	Overview of Animal Research.....	95
1.9.2	Types of Animal Models.....	95
1.9.3	Induced Models of Human Pathology.....	96
1.9.3.1	Surgical Animal Models.....	96
1.9.3.2	Genetically Modified Animal Models.....	96
1.9.3.3	Chemically Induced Animal Models.....	97
1.9.4	Animal Models of Gastroschisis .....	100
1.9.4.1	Surgical Animal Models of Gastroschisis .....	100
1.9.4.2	Genetic Mouse Models of Gastroschisis .....	100
1.9.5	Surgical Versus Genetic Gastroschisis Animal Models.....	104
1.10	Summary.....	104
1.11	Hypotheses.....	105
1.12	Thesis Aims .....	105
1.13	Outline of Work to be undertaken .....	105
1.13.1	Gastroschisis Bowel Wall Morphology .....	106
1.13.2	Impact of Inflammatory Modulation on Gastroschisis Bowel Wall Morphology and Bowel Contractility .....	106
1.13.3	Impact of Simple Clinical Antenatal Measures on Clinical Outcomes.... .....	106
Chapter 2: Materials and Methods .....		107
2.1	Animal Models General Methods .....	107
2.1.1	Ethics Statement.....	107
2.1.2	Selected Animal Models .....	107
2.1.3	Model Source and Creation of Null Fetuses .....	107
2.1.3.1	Scribble Knockout Mouse Model.....	107

2.1.3.2	ACLP Knockout Model.....	108
2.1.4	Animal Husbandry .....	108
2.1.4.1	Housing of Mouse Colonies .....	108
2.1.4.2	Pinworm treatment .....	108
2.1.4.3	Breeding Pairs .....	109
2.1.4.4	Timed Mating .....	109
2.1.4.5	Fetal Collection .....	109
2.1.5	Genotyping.....	109
2.1.5.1	Tissue for Genotyping .....	109
2.1.5.2	DNA extraction .....	110
2.1.5.3	Genotyping by PCR.....	110
2.1.5.4	Gel Electrophoresis .....	112
2.1.5.5	Electrophoresis Bands .....	113
2.1.6	Abdominal Wall Defect Phenotyping .....	114
2.1.6.1	Fetal Preparation.....	114
2.1.6.2	Microdissection and Imaging .....	115
2.1.6.3	In-Amnio Fetal Micro-MRI.....	115
2.1.6.4	In-Amnio Paraffin Embedded Cross-Sections .....	116
2.1.7	Experimental Groups .....	118
2.1.7.1	Scribble Knockout Mouse Model Experiments .....	118
2.1.7.2	ACLP Knockout Mouse Model Experiments .....	118
2.1.8	Intra-Amniotic Injections .....	119
2.1.8.1	Timing of injections .....	119
2.1.8.2	Procedure.....	119
2.1.8.3	IL-8 Dose-Finding Study.....	120
2.1.9	Gut Tissue Gross Dissection, Handling and Specimen Numbers .....	120
2.1.9.1	Harvest Timing, Number and Coding of Gut Specimens.....	120
2.1.9.2	Gut Length and Weight .....	121
2.1.10	Gut Motility Studies .....	121
2.1.10.1	Gut Preparation .....	121
2.1.10.2	Motility Imaging .....	121
2.1.10.3	Gut Edge Detection and Spatiotemporal Mapping .....	123

2.1.10.4	Frequency of Gut Contractions.....	125
2.1.10.5	Statistical Analysis of Gut Motility .....	125
2.2	Archived Human Gut Tissue General Methods .....	127
2.2.1	Ethics Statement.....	127
2.2.2	Sample Selection Criteria.....	127
2.2.3	Specific Inclusion and Exclusion Criteria.....	128
2.2.3.1	Inclusion Criteria for ICC and Enteric Neuron Analysis .....	129
2.2.3.2	Exclusion Criteria for ICC and Enteric Neuron Analysis .....	129
2.2.3.3	Inclusion Criteria for Bowel Wall Morphological Analysis .....	129
2.2.3.4	Exclusion Criteria for Bowel Wall Morphological Analysis .....	130
2.2.4	Specimen Identification .....	130
2.2.5	Specimen Pseudonymisation.....	130
2.2.6	Clinical Data Collection.....	130
2.2.7	Specimen Sectioning.....	130
2.3	ICC and Enteric Neuron Quantification (Animal and Human Tissue) .....	131
2.3.1	Outcome Measures.....	131
2.3.2	ICC and Enteric Neuron Quantification Method Selection .....	132
2.3.3	Animal Gut Tissue Preparation for Immunofluorescence .....	132
2.3.3.1	Transverse Cross-Sectioned Ileal Tissue.....	133
2.3.3.2	Whole Mount Ileal Tissue .....	133
2.3.4	Human Gut Tissue Preparation for Immunofluorescence.....	134
2.3.5	Immunofluorescence Protocols.....	134
2.3.5.1	Interstitial Cells of Cajal.....	134
2.3.5.2	Enteric Neurons .....	135
2.3.5.3	Nuclei .....	136
2.3.5.4	Immunofluorescence Staining Protocol for Cross-Sectioned Tissue ... .....	136
2.3.5.5	Immunofluorescence Staining Protocol for Whole Mount Tissue.	138
2.3.6	Immunofluorescence Imaging.....	139
2.3.6.1	Cross-Sectioned Tissue .....	140

2.3.6.2	Whole Mount Tissue .....	140
2.3.7	ICC and Enteric Neuron Quantification.....	141
2.3.7.1	Cross-Sectioned Tissue .....	141
2.3.7.2	Whole Mount Tissue .....	143
2.4	Bowel Wall Thickness and Morphology (Animal and Human Tissue) ...	145
2.4.1	Animal Gut Tissue Preparation Morphological Studies .....	145
2.4.2	Human Gut Tissue Preparation for Morphological Studies.....	146
2.4.3	Histology Staining Protocols .....	146
2.4.3.1	H&E Staining Protocol.....	146
2.4.3.2	Immunohistochemistry and Picrosirius Red Staining Protocols ....	146
2.4.4	Histology Imaging.....	147
2.4.4.1	Imaging of H&E Cross-Sections.....	147
2.4.4.2	Imaging of Immunohistochemistry Cross-sections.....	147
2.4.5	Morphological Bowel Wall Analysis.....	148
2.4.5.1	Bowel Wall Measurements and Muscle Fibre Quantification .....	148
2.4.5.2	$\alpha$ -SMA, PS and TGF $\beta$ 3 quantification.....	150
2.4.5.3	Ki67 Quantification.....	154
2.4.6	Statistical Analysis ICC, Enteric Neurons and Morphological Data .	155
2.5	Clinical Retrospective Multicentre Cohort Studies.....	156
2.5.1	Institutional Approval .....	156
2.5.2	Inclusion Criteria.....	157
2.5.2.1	Timing of Delivery and Impact on Gastroschisis Infant Outcomes Study.....	157
2.5.2.2	Maternal Antenatal Corticosteroid Administration and Impact on Gastroschisis Infant Outcomes Study .....	157
2.5.2.3	Predicting Infant Outcomes with Antenatal Bowel Dilatation Study .. .....	157
2.5.3	Exclusion Criteria.....	158
2.5.4	Patient Management.....	158
2.5.5	Identification of Patients .....	159
2.5.6	Data Collection.....	159



2.5.7	Outcome Measures .....	160
2.5.8	Confidentiality .....	160
2.5.9	Statistical Analysis .....	160
2.5.9.1	Timing of Delivery and Impact on Gastroschisis Infant Outcomes Study.....	160
2.5.9.2	Maternal Antenatal Corticosteroid Administration and Impact on Gastroschisis Infant Outcomes Study .....	161
2.5.9.3	Predicting Infant Outcomes with Antenatal Bowel Dilatation Analysis .....	161
<b>Chapter 3: Phenotypic and ICC Characterisation in the Scribble Knockout Mouse</b>		
	<b>Model of an Abdominal Wall defect.....</b>	<b>162</b>
3.1	Introduction .....	162
3.2	Results .....	162
3.2.1	Gross Characterisation of Scribble Knockout Fetuses.....	162
3.2.2	Abdominal Wall Defect Phenotype .....	164
3.2.2.1	Timing of Abdominal Wall Phenotyping.....	164
3.2.2.2	Visualisation of Intra-Amniotic Fetuses.....	164
3.2.2.3	Microdissection .....	167
3.2.2.4	In-Amnio Fetal Micro-MRI.....	169
3.2.3	Gross Bowel Morphology .....	170
3.2.4	ICC and Enteric Neurons .....	171
3.2.4.1	Immunofluorescence Staining Protocol .....	171
3.2.4.2	ICC Architecture and Numbers .....	172
3.2.4.3	Enteric Neuron Architecture and Numbers .....	172
3.3	Discussion .....	173
3.3.1	Abdominal Wall Phenotype .....	173
3.3.1.1	Exomphalos Phenotype .....	173
3.3.1.2	A Case of Mistaken Identity.....	174
3.3.1.3	Importance of Accurate Phenotyping.....	175
3.3.1.4	Concomitant Pathology and Penetrance.....	176
3.3.2	The Use of In-Amnio Micro-MRI for Fetal Structural Phenotyping.	176

3.3.3	Bowel Development.....	177
3.3.3.1	Gross Bowel Development.....	177
3.3.3.2	ICC and Enteric Neuron Development .....	178
3.3.4	ICC Quantification.....	178
3.4	Conclusion.....	179
Chapter 4: Aortic Carboxypeptidase-Like Protein (ACLP) Knockout Mouse Model: Phenotypic Characterisation and Impact of Inflammation on ICC Development and Gut Motility.....		
4.1	Introduction .....	180
4.2	Results .....	181
4.2.1	Gross Characterisation of ACLP Knockout Fetuses.....	181
4.2.2	Abdominal Wall Defect Phenotype .....	182
4.2.2.1	Timing of Abdominal Wall Defect Phenotyping .....	182
4.2.2.2	Visualisation of Intra-Amniotic Fetuses.....	182
4.2.2.3	Microdissection .....	183
4.2.2.4	Fetal In-Amnio Paraffin Embedded Cross-Sections .....	184
4.2.2.5	Fetal Expression of ACLP and TGF $\beta$ .....	191
4.2.3	In-Utero IL-8 Injections .....	194
4.2.4	Gross Bowel Morphology.....	194
4.2.4.1	Pre-injection Comparison of Untreated Phenotypically Normal and Untreated AWD Fetuses .....	194
4.2.4.2	Statistical Comparison between Experimental Groups .....	195
4.2.5	ICC and Enteric Neurons .....	198
4.2.5.1	Intact Gut Tube Whole Mount Preparation Technique .....	198
4.2.5.2	ICC Architecture and Numbers: Comparison of Untreated Phenotypically Normal and AWD Fetuses .....	199
4.2.5.3	ICC Architecture and Numbers: IL-8 Injected Groups .....	199
4.2.5.4	Enteric Neuron Architecture and Numbers: Comparison of Untreated Phenotypically Normal and AWD Fetuses .....	201
4.2.5.5	Enteric Neuron Architecture and Numbers: IL-8 Injected Groups .....	202
4.2.6	Motility Studies.....	203

4.2.6.1	Experimental Groups.....	203
4.2.6.2	Pattern of Contractions.....	204
4.2.6.3	Contraction Strength.....	204
4.2.6.4	Frequency of Contractions .....	207
4.3	Discussion .....	210
4.3.1	Abdominal Wall Phenotype.....	210
4.3.1.1	An Unusual Exomphalos Phenotype? .....	210
4.3.1.2	Another Case of Mistaken Identity .....	212
4.3.1.3	Failed Umbilical Cord Formation and Abdominal Wall Closure ..	213
4.3.2	Bowel Wall Development.....	214
4.3.2.1	Comparison of Untreated Control and Untreated AWD Fetuses ...	214
4.3.2.2	Impact of IL-8 In-Utero Injections.....	215
4.3.2.3	Bowel Contractility and ICC Numbers .....	216
4.3.3	Limitations of the Study.....	217
4.3.3.1	ACLP Knockout Model.....	217
4.3.3.2	Experimental Numbers and Treatment for Pinworm .....	218
4.3.3.3	Motility Study Analysis Optimisation.....	219
4.3.4	Conclusion .....	221
Chapter 5: Analysis of Gastroschisis ICC and Enteric Neurons in Infant Human		
Pathological Gut Tissue .....		
5.1	Introduction .....	222
5.2	Results .....	222
5.2.1	Study Population and Demographics.....	222
5.2.2	ICC and Enteric Neurons .....	224
5.2.2.1	Optimisation of Immunofluorescence ICC Staining Protocols .....	224
5.2.2.2	ICC and Enteric Neuron Architecture .....	225
5.2.2.3	ICC and Enteric Neuron Numbers .....	226
5.2.2.4	ICC and Enteric Neuron Numbers and Age at Bowel Resection...	226
5.2.2.5	ICC and Enteric Neuron Numbers and Time to Full Enteral Feeds	228
5.2.2.6	ICC in Meconium Ileus .....	229
5.3	Discussion .....	231

5.3.1	Tissue Selection for Inclusion in the Study.....	231
5.3.2	ICC and Enteric Neuron Numbers and Architecture .....	231
5.3.3	Quantification of ICC and Enteric Neurons.....	232
5.3.4	Comparison with Other Studies .....	232
5.3.5	Limitations of the Current Study.....	234
5.4	Conclusion.....	234
Chapter 6: Analysis of Gastroschisis Bowel Wall Morphology in Infant Human		
	Pathological Gut Tissue .....	236
6.1	Introduction .....	236
6.2	Results .....	236
6.2.1	Study Population and Demographics.....	236
6.2.2	Bowel Wall Thickness .....	239
6.2.2.1	Bowel Wall H&E Qualitative Description.....	243
6.2.2.2	Bowel Wall Thickness and Age at Bowel Resection.....	245
6.2.2.3	Bowel Wall Thickness and Time to Full Enteral Feeds.....	246
6.2.2.4	$\alpha$ -Smooth Muscle Actin .....	247
6.2.2.5	Collagen.....	250
6.2.2.6	Ki67 Staining.....	253
6.2.2.7	Transforming Growth Factor-Beta 3 Staining.....	254
6.3	Discussion .....	256
6.3.1	Bowel Wall Thickness and Mucosal Morphology.....	256
6.3.2	Bowel Wall Architecture and Composition .....	256
6.3.3	Hypothesised Cause of Bowel Wall Thickening .....	258
6.3.4	Smooth Muscle $\alpha$ -SMA Deficiency and Chronic Idiopathic Intestinal Pseudo-Obstruction.....	262
6.3.5	Limitations of the Study.....	262
6.4	Conclusion.....	263
Chapter 7: Gestational Age at Delivery and Maternal Corticosteroid Administration: Association with Outcomes in Gastroschisis .....		
		264

7.1	Introduction .....	264
7.1.1	Timing of Delivery.....	264
7.1.2	Maternal Antenatal Corticosteroids .....	265
7.1.3	Hypothesis, Aims and Study Design.....	266
7.2	Results .....	267
7.2.1	Timing of Delivery and Impact on Time to Full Enteral Feeds and Length of Hospital Stay .....	267
7.2.1.1	Study Population and Demographics .....	267
7.2.1.2	Linear Regression Analysis.....	270
7.2.1.3	Group Univariate Analysis.....	271
7.2.1.4	Cox Regression Analysis.....	272
7.2.1.5	Timing of Delivery and Impact on Macroscopic Bowel Wall Inflammation.....	275
7.2.2	Maternal Antenatal Corticosteroid Administration and Impact on Infant Outcomes .....	276
7.2.2.1	Demographics.....	276
<b>7.2.3</b>	<b>Postnatal Outcomes.....</b>	<b>278</b>
7.2.3.1	<i>Univariate analysis</i> .....	278
7.2.3.2	<i>Post-hoc Exploratory Analyses</i> .....	282
7.3	Discussion .....	284
7.3.1	Timing of Delivery and Impact on Postnatal Outcomes.....	284
7.3.2	Relationship between Maternal Antenatal Corticosteroid Administration and Gastroschisis Outcomes .....	284
7.3.3	Impact of Other Factors on Gastroschisis Outcomes.....	285
7.3.4	Timing of Delivery Review of the Literature .....	285
7.3.5	Hypothesised Reason for Prolonged Postnatal Outcomes at Lower Birth Gestational Age.....	290
7.3.6	Hypothesised Reason for Lack of Effect from Maternal Antenatal Corticosteroid Administration.....	290
7.3.7	Limitations of the Study.....	291

7.3.8	Strength of the Study.....	292
7.4	Conclusion.....	292
Chapter 8: Does Antenatally Detected Bowel Dilation Predict Gastroschisis Infant Outcomes? .....		
		294
8.1	Introduction .....	294
8.2	Results .....	295
8.3	Discussion .....	300
8.3.1	Predictive Value of Antenatal Bowel Dilatation.....	300
8.3.2	Implications of Findings .....	300
8.3.3	Literature Review.....	301
8.3.4	Limitations of the Study.....	305
8.3.5	Strength of the Study.....	305
8.3.6	Conclusion .....	306
Chapter 9: Summary, Discussion and Concluding Remarks .....		
		307
9.1	Discussion .....	307
9.1.1	Gastroschisis Bowel Wall Morphology .....	307
9.1.2	Impact of Inflammatory Modulation on Gastroschisis Bowel Wall Morphology.....	309
9.1.3	Impact of Clinical Antenatal Interventions on Infant Outcomes .....	310
9.1.4	Other Findings.....	312
9.2	Future Research .....	314
9.2.1	Modulation of Inflammation .....	315
9.2.2	Regulation of the Hippo Pathway .....	316
9.2.3	Growth Factors.....	317
9.2.4	Prospective Cohort Study.....	318
9.3	Concluding Statement .....	319
References .....		320

Appendix 1: Publications and Presentations Arising from the Work Contributing to this Thesis .....	344
Publications .....	344
International Invited Speaker .....	344
International Oral Presentations .....	344
International Poster Presentations .....	346
Appendix 2: The Long-Term Impact of Parenteral Nutrition on Growth in Surgical Infants.....	347

## Table of Figures

<b>Figure 1-1:</b> General structure of the gastrointestinal tract. Showing (from luminal surface outwards) the convoluted mucosal surface, submucosa, muscularis externa composed of the inner circular smooth muscle and outer longitudinal smooth muscle between which is the myenteric plexus and interstitial cells of Cajal and finally the outermost layer is the serosa. ....	41
<b>Figure 1-2:</b> Structure of jejunal and ileal villi, demonstrating simple columnar epithelia with microvilli brush border, villus crypts and a central blind ending lymphatic vessel (lacteal) and blood capillary network. ....	42
<b>Figure 1-3:</b> <b>A.</b> Schematic of ileum. <b>B.</b> Immuofluorescence image of the myenteric plexus (red) and nuclei (blue) showing the interconnecting network of enteric neurons and glial cells. ....	46
<b>Figure 1-4:</b> <b>A.</b> Schematic of ileum. <b>B.</b> Immuofluorescence image of the ICC (green) network at the level of the myenteric plexus and nuclei (blue) showing the branching network of ICC. ....	47
<b>Figure 1-5:</b> Primitive digestive tract showing the developing foregut, midgut and hindgut with the respective arterial supply and the vitelline duct, which temporarily connects the gut tube to the yolk sac (Gest, 2002). ....	52
<b>Figure 1-6:</b> Physiological herniation and development of the midgut. <b>A.</b> Rapid elongation of the primary intestinal loop during the 6 <sup>th</sup> week of development. <b>B.</b> Rotation of the bowel during physiological herniation. <b>C.</b> Return and rotation of the intestinal loops into the abdominal cavity. <b>D.</b> Initial returning loops lie on the left side of the abdomen. <b>E.</b> Later returning loops come to lie on the right side of the abdomen and the caecal bud comes to lie in the right iliac fossa. Physiological herniation resolves around 10 <sup>th</sup> week of development (Larsen, 1997). ....	54
<b>Figure 1-7:</b> Types of survivable congenital ventral abdominal wall defects. <b>A.</b> Gastroschisis showing a ventral abdominal wall defect to the right of the umbilicus and externalised gut without a covering membrane. <b>B.</b> Exomphalos showing a large central abdominal wall defect with gut herniating into the base of the umbilical cord providing a protective membrane. <b>C.</b> Bladder exstrophy showing a lower midline central abdominal wall defect exposing the bladder plate and associated epispadias (Coran et al., 2012). ....	60



<b>Figure 1-8:</b> Schematic representation of gastrointestinal pathologies. <b>A.</b> Atresia depicting blind ending proximal and distal bowel. <b>B.</b> Stenosis depicting narrowed bowel lumen. <b>C.</b> Perforation depicting a hole in the bowel wall. ....	62
<b>Figure 1-9:</b> Schematic illustration of an in-utero gastroschisis fetus. ....	64
<b>Figure 1-10:</b> Schematic illustration of the gastroschisis abdominal wall defect in transverse section. ....	65
<b>Figure 2-1:</b> <i>Scrib</i> and <i>scrib<sup>lox-neo</sup></i> allele gel electrophoresis, including DNA ladder and control DNA from a known heterozygote fetus. <b>A.</b> Gel electrophoresis for <i>Scrib</i> (WT) allele, box highlights positive allele bands. <b>B.</b> Gel electrophoresis for <i>scrib<sup>lox-neo</sup></i> (knockout) allele, box highlights positive allele bands. ....	113
<b>Figure 2-2:</b> <i>ACLP</i> and <i>ACLP<sup>-</sup></i> allele gel electrophoresis, including DNA ladder and control DNA from a known heterozygote fetus. <b>A.</b> Gel electrophoresis for <i>ACLP</i> (WT) allele, box highlights positive allele bands. <b>B.</b> Gel electrophoresis for <i>ACLP<sup>-</sup></i> (knockout) allele, box highlights positive allele bands. ....	114
<b>Figure 2-3:</b> Gut motility recording. <b>A.</b> One frame taken from a 60 second recording of ileal motility. The ileum appears white in this black and white image. Also evident are numerous air bubbles generated from oxygenation of the organ bath. <b>B.</b> Reference image of graph paper with 1mm increments. ....	122
<b>Figure 2-4:</b> Ileal edge detection using MATLAB software. <b>A.</b> Original frame from ileal recording. <b>B.</b> Vertically inverted light intensity image created in MATLAB. Ileum appears yellow, the pink line indicates the ileal edge and the green line is the centre point of the bowel. <b>C.</b> Graph representing change from mean diameter (mm) against vertical slice bowel incremental point (mm) with time (seconds). ....	124
<b>Figure 2-5:</b> analysis of frequency of gut contractions using MATLAB software. <b>A.</b> Change in ileal diameter over time for one vertical slice analysis. <b>B.</b> Fast Fourier transform (FFT) highlighting the most dominant frequency of contraction. <b>C.</b> FFT converted from frequency to contractions per minute. ....	126
<b>Figure 2-6:</b> Sample selection criteria. <b>A.</b> Inclusion of grossly normal resection margins. <b>B.</b> Exclusion of grossly abnormal resection margins. ....	128
<b>Figure 2-7:</b> Random image orientation leads to differing myenteric plexus lengths and would give different counts for the same tissue region. <b>A.</b> Horizontal orientation. <b>B.</b> Diagonal orientation. <b>C.</b> Vertical orientation. ....	140

<b>Figure 2-8: A.</b> Schematic of ileum, rectangle indicating the region imaged at high power (40x objective). Maximum intensity project images of confocal z-stacks. <b>B.</b> Anti-CD117 green, DAPI blue. <b>C.</b> Anti-PGP9.5 red, DAPI blue.....	141
<b>Figure 2-9:</b> ImageJ anti-CD117 (ICC, green) and DAPI (nuclei, blue) combined image and ImageJ cell counter software. Magenta markers (indicated with white circles) highlighting counted ICC cell bodies.....	142
<b>Figure 2-10:</b> ImageJ anti-HuC/D (enteric neuron, red) and DAPI (nuclei, blue) combined image and ImageJ cell counter software. Green markers (indicated with white circles) highlighting counted ICC cell bodies.....	143
<b>Figure 2-11:</b> ImageJ ICC maximum intensity project (anti-CD117, ICC, green and DAPI, nuclei, blue) and ImageJ cell counter software. Magenta markers (indicated with white circles) highlighting counted ICC cell bodies.....	144
<b>Figure 2-12:</b> ImageJ enteric neuron maximum intensity project (Anti-PGP9.5, enteric neurons, red and DAPI, nuclei, blue) and ImageJ cell counter software. Green markers (indicated with white circles) highlighting counted enteric neuron cell bodies. ....	145
<b>Figure 2-13:</b> Mouse bowel wall measurements performed using Zeiss ZEN lite imaging software.....	149
<b>Figure 2-14:</b> Human bowel wall measurements performed using Zeiss ZEN lite imaging software.....	149
<b>Figure 2-15:</b> $\alpha$ -SMA quantification macro written for ImageJ software.....	150
<b>Figure 2-16:</b> Quantification protocol for $\alpha$ -SMA. <b>Step 1:</b> Convert image to RGB and draw region of interest (bounded by the yellow line). <b>Step 2:</b> Colour deconvolution using methyl green DAB vector. <b>Step 3:</b> Automated colour thresholding of resultant brown colour image. <b>Step 4:</b> Convert to a binary image. <b>Step 5:</b> Data output. ....	152
<b>Figure 2-17:</b> Manual colour thresholding following colour deconvolution for TGF $\beta$ 3 quantification.....	153
<b>Figure 2-18:</b> Quantification protocol for Ki67. <b>Step 1:</b> Convert image into RGB and apply Gaussian blur. <b>Step 2:</b> Draw ROI (bounded by the yellow line). <b>Step 3:</b> Adjust maxima settings to detect all nuclei within ROI (imaged zoomed in). <b>Step 4:</b> Manually count Ki67 positively stained nuclei (magenta marker) with cell counting software (image zoomed in).....	155
<b>Figure 3-1:</b> Gross phenotypic characterisation of the floxed <i>Scrib</i> ( <i>Scrib<sup>fl</sup></i> ) mouse model.....	163

**Figure 3-2:** Intra-amniotic fetuses including intact placenta (P) at 17.5 dpc, 0.8x objective. **A.** Phenotypically normal fetus. **B.** Fetus with small AWD. The herniated viscera (HV) is contained within a membraneous sac. Also evident in this image is failed closure (FC) of the cranium and blood stained amniotic fluid. **C.** Fetus with large AWD. Externalised viscera (EV) appear to be free floating. There is evidence of an intra-amniotic membraneous structure (MS) compartmentalising the intra-amniotic cavity. This fetus additionally had a concomitant NTD (not visible on this image due to orientation) and blood stained amniotic fluid..... 166

**Figure 3-3:** Scribble mutant mouse abdominal wall phenotypes at 17.5 dpc, magnification 0.8x objective. **A.** Normal phenotype with intact abdominal wall and structurally normal umbilical cord (UC) that inserts centrally on the abdominal wall. The placenta (P) also remains intact. **B.** Small AWD with membrane covered herniated liver and bowel into the base of the umbilical cord (UC) consistent with exomphalos (E). **C.** Large AWD with evisceration of liver, gut and spleen. A ruptured thin membrane (TM) is present associated with the abdominal viscera and exhibits vascular attachments to the amniotic membrane (AM). The placenta (P) and umbilical cord (UC) have been left intact. **D.** Large ventral wall defect with intact thin membrane (TM) covering herniated abdominal viscera (superior pole of the membrane was iatrogenically ruptured (IR) during dissection) consistent with exomphalos (E). ..... 168

**Figure 3-4:** In-amnio micro-MRI of intra-amniotic fetuses at 17.5 dpc. **A.** Sagittal image of a phenotypically normal fetuses. **B.** Sagittal image of characteristic exomphalos (E) AWD phenotype showing herniation of abdominal viscera contained within an intact membrane. Also evident is craniorachischisis (CR) with failed neural tube closure from the cranium to sacrum. **C.** Sagittal image of the large AWD phenotype showing externalised abdominal viscera (EAV) with no discernable membrane covering. The craniorachischisis defect is also evident. **D.** Contrast enhanced axial image of the large AWD. The externalised liver is associated with a membranous structure (blue arrow). **E.** Contrast enhanced sagittal image of the large AWD. The externalised liver is associated with a membranous structure (blue arrows). **F.** Contrast enhanced coronal image of the large AWD showing the presence of a normal placental (P) and umbilical cord (UC). ..... 170

**Figure 3-5:** **A.** Low powered (10x objective) composite image of entire gut cross-section (anti-CD117 green, anti-TUJ1 red, DAPI blue), rectangle showing region

imaged at high power. <b>B.</b> High powered (40x objective) image of ICC (indicated by arrow). <b>C.</b> High powered (40x objective) image of enteric neurons (indicated by arrow). .....	171
<b>Figure 3-6:</b> Whole mount 18.5 dpc ileal specimens stained for ICC with anti-CD117 (A and C) and enteric neurons with anti-TUJ1(B and D) images acquired by confocal microscopy, 40x objective, maximum intensity project of z-stack images. <b>A and B.</b> Specimen from control mouse. <b>C and D.</b> Specimen from large AWD mutant mouse. ....	173
<b>Figure 4-1:</b> Intra-amniotic fetuses at 18.5 dpc, 0.6x objective. <b>A.</b> Phenotypically normal fetus. <b>B.</b> Fetus with AWD exhibiting externalised, free floating bowel and liver. ....	183
<b>Figure 4-2:</b> Microdissection images of ACLP phenotypically normal and AWD fetuses at 18.5 dpc, orientated with tail inferiorly, 0.6x objective. <b>A.</b> Phenotypically normal fetus with a structurally normal umbilical cord (UC), consisting of 3 blood vessels, covered by the amniotic membrane, which inserts centrally on a closed abdominal wall. <b>B-D.</b> AWD fetuses. The amniotic membrane (AM) attaches directly to the ventral wall defect edge (DE) and the externalised gut (G) and liver (L) are free floating within the exocoelomic cavity separated from the amniotic fluid by the amniotic membrane. <b>B.</b> Direct view of the ventral abdominal wall defect with the amniotic membrane (AM) lying flat against the abdominal wall. <b>C.</b> The amniotic membrane is displaced superiorly away from the abdominal wall to reveal the direct attachment to the inferior defect edge. <b>D.</b> The amniotic membrane is displaced inferiorly away from the abdominal wall to reveal the direct attachment to the superior defect edge. <b>A, C and D.</b> The placenta (P) was grossly normal in all fetuses. ....	184
<b>Figure 4-3:</b> 13.5 dpc phenotypically normal in-amnio paraffin embedded fetus, H&E stained, sagittal cross-section through the umbilicus, imaged with Zeiss AxioScan Z1 slide scanner with 40x objective. This shows normal physiological herniation of the gut. <b>A.</b> Original AxioScan image. <b>B.</b> Schematic representation of fetal anatomy overlaid on the original image. ....	186
<b>Figure 4-4:</b> 18.5 dpc phenotypically normal in-amnio paraffin embedded fetus, H&E stained, sagittal cross-section through the umbilicus, imaged with Zeiss AxioScan Z1 slide scanner with 40x objective. Showing normal abdominal wall closure and a	

centrally inserted umbilical cord. **A.** Original AxioScan image. **B.** Schematic representation of fetal anatomy overlaid on the original image..... 187

**Figure 4-5:** 13.5 dpc AWD in-amnio paraffin embedded fetus, H&E stained, sagittal cross-section through the umbilicus, imaged with Zeiss AxioScan Z1 slide scanner with 40x objective. This shows failed abdominal wall closure and failed attachment of the amniotic membrane to the umbilical cord resulting in the externalised bowel lying within the exocoelomic cavity separated from the amniotic fluid by the amniotic membrane. **A.** Original AxioScan image. **B.** Schematic representation of fetal anatomy overlaid on the original image..... 189

**Figure 4-6:** 18.5 dpc AWD in-amnio paraffin embedded fetus, H&E stained, sagittal cross-section through the umbilicus, imaged with Zeiss AxioScan Z1 slide scanner with 40x objective. This shows failed abdominal wall closure and failed attachment of the amniotic membrane to the umbilical cord resulting in the externalised bowel lying within the exocoelomic cavity separated from the amniotic fluid by the amniotic membrane. **A.** Original AxioScan image. **B.** Schematic representation of fetal anatomy overlaid on the original image..... 190

**Figure 4-7:** ACLP/AEBP1 labelling with DAB detection kit of in-amnio paraffin embedded fetus, sagittal cross-section through the umbilicus, imaged with Zeiss AxioScan Z1 slide scanner with 40x objective. This shows significant background staining of the 13.5 dpc phenotypically normal (**A**) and AWD fetuses (**B**). There is absent staining in both the 18.5 dpc phenotypically normal (**C**) and AWD (**D**) fetuses. Key: AM – amniotic membrane, PH – physiological hernia, AWD – abdominal wall defect. .... 192

**Figure 4-8:** TGF $\beta$  labelling with DAB detection kit of in-amnio paraffin embedded fetus, sagittal cross-section through the umbilicus, imaged with Zeiss AxioScan Z1 slide scanner with 40x objective. This shows significant background staining of cross-sections. **A.** 13.5 dpc phenotypically normal fetus. **B.** 13.5 dpc AWD fetus. **C.** 18.5 dpc phenotypically normal fetus. **D.** 18.5 dpc AWD fetus. Key: AM – amniotic membrane, PH – physiological hernia, AWD – abdominal wall defect. .... 193

**Figure 4-9:** Whole mount 18.5 dpc ileal specimens stained for ICC with anti-CD117, images acquired using confocal microscopy, 40x objective, maximum intensity project of z-stack images. **A.** Untreated control. **B.** Untreated AWD. **C.** IL-8 injected control. **D.** IL-8 injected AWD. .... 201

**Figure 4-10:** Whole mount 18.5 dpc ileal specimens stained for enteric neurons with anti-PGP9.5, images acquired by confocal microscopy, 40x objective, maximum intensity project of z-stack images. **A.** Untreated control. **B.** Untreated AWD. **C.** IL-8 injected control. **D.** IL-8 injected AWD..... 203

**Figure 4-11:** Representative spatiotemporal maps from each experimental group. **A and B.** Untreated control. **C and D.** Untreated AWD. **E and F.** IL-8 injected AWD. **A, B and D.** Black diagonal lines represent contraction complexes travelling in the oral to anal direction..... 205

**Figure 4-12:** Contraction strength, represented as proportion of bowel achieving a given maximum percentage change from the mean diameter. **A.** Data from all experiments. **B.** Mean from each experimental group. **C.** Mean area underneath the curve for each experimental group..... 206

**Figure 4-13:** Fast Fourier transform (FFT) analysis of the selected 3 most contractile vertical slices per bowel segment. Representative vertical slice selections and corresponding FFT output for untreated control (**A and B**), untreated AWD (**C and D**) and IL-8 injected AWD (**E and F**). Comparison of dominant number of contractions per minute between groups. Brackets show significant comparison (one-way ANOVA)..... 208

**Figure 4-14:** Fast Fourier transform (FFT) analysis for all 0.022mm incremental vertical slices for all segments of bowel. **A.** Untreated control. **B.** Untreated AWD. **C.** IL-8 injected AWD. **D.** Mean from each experimental group. .... 209

**Figure 4-15:** Comparison of schematic representations of a 13.5 dpc phenotypically normal fetus exhibiting physiological herniation (**A**) with a 13.5 dpc AWD fetus (**B**). If adherence of the amniotic membrane to the umbilical blood vessels had occurred forming a normal umbilical cord in the AWD fetus (**B**) then it would have the same anatomical appearance as the phenotypically normal fetus, which exhibits physiological herniation (**A**). .... 211

**Figure 4-16:** Analysis optimisation using MATLAB software. **A.** Bowel edge detection performed by light thresholding showing reducing light intensity in the oral to anal direction and the presence of a bubble artefact. Gut appears in yellow, pink line marks ileal edge, green line marks centre point of bowel. **B.** Spatiotemporal map of change in bowel diameter in absolute millimetres showing decreasing bowel diameter from the oral to anal direction (normal bowel anatomy) and bubble artefact (black arrow). **C.** Spatiotemporal map of change in bowel diameter as a percentage

change from the mean diameter providing uniform analysis of contraction depth along the length of the bowel. Black arrow indicates bubble artefact. .... 220

**Figure 5-1:** Images taken with; (1) 5x and (2) 40x objective. Image (3) is an enlarged section of 40x objective image. **A.** Immunohistochemistry. ICC stained with CD117 and DAB detection kit (dark brown staining), nuclei stained with Eosin counterstain (purple). **B.** Immunofluorescence. Composite images showing triple staining for ICC with anti-CD117 (green), enteric neurons with anti-HuC/D (red) and nuclei with DAPI (blue). Key: LM – longitudinal muscle, CM – circular muscle, MP – myenteric plexus, ICC – interstitial cells of Cajal. .... 224

**Figure 5-2:** Composite images showing triple staining of ICC (green), enteric neurons (red) and nuclei (blue), images taken with 40x objective. **A and B.** Control small bowel images. **C and D.** Gastroschisis small bowel images. Key: LM – longitudinal muscle, CM – circular muscle, MP – myenteric plexus, arrows indicating example ICC adjacent to ganglia. .... 225

**Figure 5-3:** Correlation between ICC numbers (**A**) and enteric neuron numbers (**B**) between control and gastroschisis small bowel. .... 226

**Figure 5-4:** Linear regression analysis comparing ICC (**A and B**) and neuron (**C and D**) numbers with age at time of bowel resection, including all bowel resection specimens. **A and C.** Including the outlier (indicated by the blue circles). **B and D.** Excluding the outlier. .... 227

**Figure 5-5:** Relationship between gastroschisis ICC (**A**) and neuron (**B**) numbers with time to full enteral feeds (ENT). .... 229

**Figure 5-6:** Composite images from 2 different meconium ileus small bowel specimens, showing triple staining of ICC (green), enteric neurons (red) and nuclei (blue), images taken with 40x objective. Key: LM – longitudinal muscle, CM – circular muscle, MP – myenteric plexus, arrows indicating example ICC adjacent to ganglia. .... 230

**Figure 6-1:** Comparison of **A.** entire wall thickness, **B.** entire muscle thickness, **C.** longitudinal muscle thickness **D.** circular muscle thickness, **E.** serosal thickness and **F.** villus to crypt ratio between the control and gastroschisis groups. All comparisons reached statistical significance. .... 241

**Figure 6-2:** Comparison of **A.** longitudinal muscle number of cells, **B.** longitudinal muscle thickness of cells, **C.** circular muscle number of cells and **D.** circular muscle thickness of cells. \*Comparison that reached statistical significance. .... 242

**Figure 6-3:** Representative H&E images of **A.** control and **B.** gastroschisis bowel. Bowel sections imaged using Zeiss AxioScan Z1 slide scanner using 40x objective and analysed with Zeiss ZEN lite imaging software. Key: S – serosa, LM – longitudinal muscle, CM – circular muscle, Sub – submucosa, V – villi. Images showing scale bar indicating 500µm. Control bowel (**A**) shows very mild serosal inflammatory infiltrate. Gastroschisis bowel (**B**) shows serosal fibrosis, loose connective tissue and chronic inflammatory infiltrate. .... 244

**Figure 6-4:** Linear regression analysis comparing entire bowel wall and age at time of bowel resection. **A.** Control group ( $p=0.06$ ,  $R^2=0.27$ ). **B.** Gastroschisis group  $p=0.003$ ,  $R^2=0.4$ . Linear regression analysis comparing entire muscle thickness and age at time of bowel resection. **C.** Control group  $p=0.7$ ,  $R^2=0.007$ . **D.** Gastroschisis group ( $p=0.006$ ,  $R^2=0.35$ ). .... 245

**Figure 6-5:** Linear regression comparing gastroschisis (**A**) entire bowel wall thickness ( $p=0.01$ ,  $R^2=0.5$ ), (**B**) entire muscle layer thickness ( $p=0.08$ ,  $R^2=0.3$ ) and (**C**) serosal thickness ( $p=0.6$ ,  $R^2=0.34$ ) with time to full enteral feeds (ENT). Bowel Wall Architecture. .... 246

**Figure 6-6:** Comparison of **A.** longitudinal muscle area, **B.** circular muscle area, **C.**  $\alpha$ -SMA longitudinal muscle % positive staining and **D.**  $\alpha$ -SMA circular muscle % positive staining. \*Comparison that reached statistical significance. .... 249

**Figure 6-7:** Images showing  $\alpha$ -smooth muscle actin ( $\alpha$ -SMA) staining, taken with 40x objective. **A and C:** control small bowel centred on **A.** longitudinal muscle, **C.** circular muscle. **B and D:** Gastroschisis small bowel centred on **B.** longitudinal muscle, **D.** circular muscle. Key: LM – longitudinal muscle, CM – circular muscle, MP – myenteric plexus..... 250

**Figure 6-8:** Images showing picosirius red (PS) staining, taken with 40x objective. **A, C, E and G:** control small bowel centred on **A.** serosa, **C.** longitudinal muscle, **E.** circular muscle and **G.** submucosa. **B, D, F and H:** Gastroschisis small bowel centred on **B.** serosa, **D.** longitudinal muscle, **F.** circular muscle and **H.** submucosa. Key: LM – longitudinal muscle, CM – circular muscle..... 252

**Figure 6-9:** Images showing transforming growth factor-beta 3 (TGF- $\beta$ 3) staining, centred on longitudinal muscle, taken with 40x objective. **A.** Control small bowel. **B.** Gastroschisis small bowel. Both images showing significant background staining.255

**Figure 7-1:** Study population and demographics ..... 268



<b>Figure 7-2:</b> Effect of gestational age at birth on; <b>A.</b> ENT and <b>B.</b> LOS. Linear regression of log transformed ENT or LOS data with 95% confidence interval (dotted lines) of best fit line. Vertical lines highlight 34 and 37 weeks GA.....	271
<b>Figure 7-3:</b> Cox regression of effect of gestational age category on: <b>A.</b> ENT and <b>B.</b> LOS. ....	274
<b>Figure 7-4:</b> Cox regression analysis of effect of maternal antenatal corticosteroids on <b>A.</b> ENT and <b>B.</b> LOS and effect of gastroschisis complexity on <b>C.</b> ENT and <b>D.</b> LOS. ....	282
<b>Figure 8-1:</b> Relationship of measured intra-abdominal bowel dilatation (IABD) and extra-abdominal bowel dilatation (EABD) with simple and complex gastroschisis. Hosrizontal line at median. ....	297

## Table of Tables

Table 1-1: Specimens collected within the control and gastroschisis study groups. .	74
<b>Table 1-2:</b> Breakdown of gastroschisis patient recruitment at University College London Hospital and King’s College Hospital fetal medicine centres. ....	75
<b>Table 1-3:</b> Summary of bowel wall morphology findings within animal gastroschisis models. GS = gastroschisis, AF = amniotic fluid. ....	85
<b>Table 1-4:</b> Summary of ICC findings within animal gastroschisis models. GS = gastroschisis, IHC = immunohistochemistry. ....	87
<b>Table 1-5:</b> Summary of teratogens that result in gastroschisis like defects including dosage, incidence and concomitant defects. ....	99
<b>Table 1-6:</b> Timing of in-utero abdominal wall defect creation, fetal collection and duration of full term for each type of surgical animal model of gastroschisis.....	100
<b>Table 1-7:</b> Summary of reported genetic mouse models that exhibit a gastroschisis like defect. ....	103
<b>Table 2-1:</b> Primers used for genotyping. ....	111
<b>Table 2-2:</b> PCR reagents and volumes for genotyping. ....	111
<b>Table 2-3:</b> PCR temperature cycle settings .....	112
<b>Table 2-4:</b> Breakdown of tissue staining performed on the sectioned human small bowel tissue. ....	131
<b>Table 2-5:</b> Blocking solutions for cross-sectioned tissue immunofluorescence. ....	137
<b>Table 2-6:</b> Primary antibodies for cross-sectioned tissue immunofluorescence. ....	137
<b>Table 2-7:</b> Secondary antibodies for cross-sectioned tissue immunofluorescence. ....	138
<b>Table 2-8:</b> Primary antibodies for whole mount immunofluorescence. ....	139
<b>Table 2-9:</b> Secondary antibodies for whole mount immunofluorescence. ....	139
<b>Table 2-10:</b> Primary antibodies for immunohistochemistry staining.....	147
<b>Table 2-11:</b> Bowel wall layers imaged by stain. ....	148
<b>Table 3-1:</b> Gross, phenotype-genotype characterisation of the floxed <i>Scrib</i> ( <i>Scrib<sup>fl</sup></i> ) mouse model. ....	164
<b>Table 4-1:</b> Comparison of bowel wall measurements (mean $\pm$ SEM) between untreated control and untreated AWD bowel. ....	195
<b>Table 4-2:</b> Comparisons of bowel length, weight and weight per unit length (mean $\pm$ SEM) between experimental groups. Comparisons made between: untreated control	

versus untreated AWD, untreated AWD versus IL-8 injected AWD and untreated control versus IL-8 injected control. \*Indicates p-values that reached significance. .... 196

**Table 4-3:** Comparisons of bowel wall layer measurements (mean  $\pm$  SEM) between untreated AWD and IL-8 injected AWD groups. \*Indicates p-values that reached significance. .... 197

**Table 4-4:** Comparisons of bowel wall layer measurements (mean  $\pm$  SEM) between untreated control and IL-8 injected control groups. \*Indicates p-values that reached significance. .... 198

**Table 4-5:** Comparisons of the number of ICC (mean  $\pm$  SEM) per high powered field of view ( $45\text{nm}^2$ ) between experimental groups. Comparisons made between: untreated control versus untreated AWD, untreated AWD versus IL-8 injected AWD and untreated control versus IL-8 injected control. \*Indicates p-values that reached significance. .... 200

**Table 4-6:** Comparisons of the number of enteric neurons (mean  $\pm$  SEM) per high powered field of view ( $45\text{nm}^2$ ) between experimental groups. Comparisons made between: untreated control versus untreated AWD, untreated AWD versus IL-8 injected AWD and untreated control versus IL-8 injected control. .... 202

**Table 5-1:** Pathology resulting in small bowel resection in the control and gastroschisis groups. .... 223

**Table 5-2:** Multiple regression analysis of ICC and neuron numbers taking into account age at time of bowel resection and diagnosis of gastroschisis, including all bowel resection specimens. .... 228

**Table 5-3:** Degree, distribution and type of inflammation present in resected bowel sections included in Zani-Ruttenstock et al. study. .... 233

**Table 6-1:** Pathology resulting in small bowel resection in the control and gastroschisis groups. \*Indicates the pathologies that are different to those infants included in the analysis of ICC and enteric neurons in human gut tissue. .... 238

**Table 6-2:** Comparison of bowel wall measurements between control and gastroschisis small bowel. Entire wall layer thickness measurement includes all bowel wall layers from the serosa to submucosa. Entire muscle layer thickness measurement includes the circular and longitudinal muscle layers. \*Indicates p-values that reached significance. .... 240

<b>Table 6-3:</b> Number and thickness of muscle cells within the longitudinal and circular muscle layers of control and gastroschisis small bowel specimens. *Indicates p-values that reached significance.....	242
<b>Table 6-4:</b> Muscle area and percentage (%) of positive $\alpha$ -smooth muscle actin ( $\alpha$ -SMA) staining within the longitudinal and circular muscle layers of control and gastroschisis small bowel specimens. *Indicates p-values that reached significance. ....	248
<b>Table 6-5:</b> Serosal and submucosal layer area and percentage (%) of positive picosirius red (PS) staining in all bowel wall layers of control and gastroschisis small bowel specimens. *Indicates p-values that reached significance.....	251
<b>Table 6-6:</b> Total number of nuclei per area and the percentage (%) of proliferating nuclei within the longitudinal and circular muscle layers of control and gastroschisis small bowel specimens.....	254
<b>Table 6-7:</b> Percentage (%) of positive transforming growth factor-beta 3 (TGF- $\beta$ 3) staining within all bowel wall layers of control and gastroschisis small bowel specimens. ....	255
<b>Table 7-1:</b> Impact of antenatal corticosteroids on bowel and intestinal function in animal surgical models of gastroschisis. ....	265
<b>Table 7-2:</b> Reasons for early delivery and documented triggers of spontaneous delivery in infants born at <37 weeks GA. ....	269
<b>Table 7-3:</b> Effect of gestational age at birth and birth weight on ENT and LOS (linear regression of log transformed ENT or LOS data). ....	270
<b>Table 7-4:</b> Univariate analysis of postnatal outcomes using Mann-Whitney (median [range]) and *Fisher's exact test. ....	272
<b>Table 7-5:</b> The effect of gestational age at birth and complexity of gastroschisis on ENT and LOS. Cox regression adjusted for complexity and gestational age and censored for death, not achieving full feeds and not being discharged from hospital. Data for gestational age at birth is per week earlier birth. HR = hazard ratio, CI = confidence interval. ....	273
<b>Table 7-6:</b> Comparison of postnatal outcomes between those infants with and without bowel inflammation/serosal peel using Mann-Whitney (median [range]).	276
<b>Table 7-7:</b> Gastroschisis antenatal maternal corticosteroid study population and demographics. ....	277

<b>Table 7-8:</b> Gastroschisis complexity, corticosteroid administration and postnatal outcomes. *>1 pathology in 9 complex patients. Univariate analysis was **Mann-Whitney (median [range]) and Fisher’s exact tests.....	279
<b>Table 7-9:</b> The effect of antenatal maternal corticosteroids, complexity of gastroschisis and gestational age at birth on ENT and LOS. Cox regression adjusted for complex gastroschisis, birth GA, source hospital and antenatal corticosteroid administration and censored for death, not achieving full feeds and not being discharged from hospital as appropriate. Data for gestational age at birth is per week later birth. HR = hazard ratio, CI = confidence interval. ....	281
<b>Table 7-10:</b> Summary of literature investigating effect of timing of delivery on gastroschisis infant outcomes. *Indicates studies supporting elective preterm delivery. GA=gestational age.....	289
<b>Table 8-1:</b> Presence of intra-abdominal bowel dilatation (IABD), extra-abdominal bowel dilatation (EABD) and both IABD/EABD (combined) throughout pregnancy by gastroschisis complexity group. Positive predictive value and negative predictive value are for complex gastroschisis. ....	296
<b>Table 8-2:</b> Size of measured intra-abdominal bowel dilatation (IABD) and extra-abdominal bowel dilatation (EABD) for both simple and complex gastroschisis...	298
<b>Table 8-3:</b> Comparison of complex patients and the diameter of bowel dilatation between the planned early delivery for intra-abdominal bowel dilatation (IABD) versus no early delivery for IABD. ....	299
<b>Table 8-4:</b> Summary of studies investigating the association of antenatally detected intra-abdominal bowel dilation (IABD) and extra-abdominal bowel dilatation (EABD) with complex gastroschisis and surrogate infant outcomes (ENT and LOS). ....	304
<b>Table 9-1:</b> Summary of the previously held dogmas within the gastroschisis literature of bowel wall changes that may be the cause of GRID compared to the findings presented in this thesis .....	309
<b>Table 9-2:</b> Summary of the previously held dogmas within the gastroschisis literature of timing of delivery, antenatal corticosteroid administration and predictive value of antenatally detected bowel dilatation compared to the findings presented in this thesis.....	312

**Table 9-3:** Summary of the previously held dogmas within the gastroschisis literature of genetic gastroschisis mouse models compared to the findings presented in this thesis..... 313

## Acknowledgements

I am extremely grateful to Simon Eaton whose support, advice, guidance and friendship made this work possible. To Alan Burns whose laboratory guidance, editorial feedback, scientific knowledge and technical assistance provided the backbone for my laboratory work. In addition, I would like to thank Agostino Pierro who started as my primary supervisor and gave me this invaluable opportunity to undertake these studies both within University College London and Toronto.

There are a number of individuals with whom I have collaborated in undertaking this work and I would like to thank them for their generosity, support, time and ideas; P Charlesworth, A Copp, J Curry, M Davenport, P De Coppi, M Ghionzoli, P James, M Lythgoe, D Moulding, K Nicolaides, F Norris, S Pereira, T Roberts, G Ryan, D Savery, N Sebire, P Shah, A Virasami. In particular I would like to thank; Anna David who enabled the animal and clinical aspects of this research and provided excellent guidance and mentorship. Connor Mccann, who trained me in multiple laboratory techniques. Alison Hart whose mathematical background and extensive MATLAB knowledge made the motility studies analysis possible. Thomas Roberts and Mark Lythgoe whose time and expertise made the in-amnio micro-MRI possible.

Additional thanks to all my lab friends and colleagues who made repetitive laboratory protocols enjoyable and my office mates in particular Rashmi Singh, Haris Achilleos and Alessandro Borghi for their listening ears, laughter and gossip.

Finally, a large proportion of this thesis was written whilst on maternity leave and I would like to thank my husband Gary who has listened (or at least pretended to listen) to my trials and tribulations, provided advice and support, sacrificed holidays and weekends to enable me to complete this thesis even taking a week off work to provide 'Daddy Day Care'. To my beautiful daughter Zoe who was born two weeks late giving me an extra period of baby free write up time, on occasions napped for an extended period of time to allow me to work and every day provides me with the motivation to succeed. To my neighbour Ailsa and my in-laws Tricia and Peter who entertained Zoe once a week whilst I typed. Without any of these people, well ok if I hadn't of had Zoe things may have been easier, I would not have finished this thesis.

## Abbreviations

<b>Abbreviation</b>	<b>Description</b>
<b>11<math>\beta</math>-HSD2</b>	11- $\beta$ -hydroxysteroid dehydrogenase isozyme 2
<b><math>\alpha</math>-SMA</b>	Alpha smooth muscle actin
<b>ACLP</b>	Aortic carboxypeptidase-like protein
<b>AEBP1</b>	Adipocyte enhancer binding protein 1
<b>AWD</b>	Abdominal wall defect
<b>BMP1</b>	Bone morphogenetic protein 1
<b>CGA</b>	Corrected gestational age
<b>CI</b>	Confidence interval
<b>CIPO</b>	Chronic idiopathic intestinal pseudo-obstruction
<b>DAPI</b>	4',6-diamidino-2-phenylindole
<b>DAB</b>	3,3'-diaminobenzidine
<b>dpc</b>	Days post coitum
<b>EABD</b>	Extra-abdominal bowel dilatation
<b>ENT</b>	Time to full enteral feeds
<b>FFT</b>	Fast Fourier transform
<b>GA</b>	Gestational age
<b>GOSH</b>	Great Ormond Street Hospital
<b>GRID</b>	Gastroschisis-related intestinal dysfunction
<b>H&amp;E</b>	Haematoxylin and eosin
<b>IABD</b>	Intra-abdominal bowel dilatation
<b>ICC</b>	Interstitial cells of Cajal
<b>ICH</b>	Institute of Child Health
<b>IL-8</b>	Interleukin-8
<b>KCH</b>	King's College Hospital
<b>LMP</b>	Last menstrual period



<b>LOS</b>	Length of hospital stay
<b>micro-MRI</b>	Micro-magnetic resonance imaging
<b>MMC</b>	Migrating motor complex
<b>MSH</b>	Mount Sinai Hospital
<b>NGT</b>	Nasogastric tube
<b>NICU</b>	Neonatal Intensive Care Unit
<b>NPV</b>	Negative predictive value
<b>NTD</b>	Neural tube defect
<b>PBS</b>	Phosphate buffered saline
<b>PBT</b>	Phosphate buffered 1% Triton X-100 solution
<b>PCR</b>	Polymerase chain reaction
<b>PFA</b>	Paraformaldehyde
<b>PN</b>	Parenteral nutrition
<b>PPV</b>	Positive predictive value
<b>PS</b>	Picrosirius red
<b>RCT</b>	Randomised controlled trial
<b><i>Scrib</i><sup>fl</sup></b>	Floxed <i>Scrib</i> allele
<b>SEM</b>	Standard error of mean
<b>TUJ1</b>	Neuronal class III $\beta$ -tubulin
<b>TGF-<math>\beta</math>3</b>	Transforming growth factor-beta 3
<b>UCL</b>	University College London
<b>UCLH</b>	University College London Hospital
<b>WT</b>	Wildtype

## Definitions

<b>Term</b>	<b>Definition</b>
<b>Neonate</b>	An infant under 28 days of age
<b>Complex gastroschisis</b>	Infants with compromised (ischaemic or necrotic bowel), non-continuous (atresia) or narrowed (stenotic) bowel.
<b>Developmental age</b>	Pregnancy duration calculated from time of fertilisation.
<b>First trimester</b>	Denotes the time in pregnancy from 1 week gestational age through to 12 weeks gestational age.
<b>Gestational age</b>	Pregnancy duration calculated from the last menstrual period.
<b>Intra-amniotic fetus</b>	Mouse fetus with the uterine muscle removed but intact amniotic membranes and placenta.
<b>Length of hospital stay</b>	Time from birth to discharge from hospital
<b>Second trimester</b>	Denotes the time in pregnancy from 13 weeks gestational age through to 27 weeks gestational age.
<b>Simple gastroschisis</b>	Infants who have otherwise healthy, intact, continuous bowel (includes patients with bowel inflammation).
<b>Third trimester</b>	Denotes the time in pregnancy from 28 weeks gestational age through to birth.
<b>Time to full enteral feeds</b>	Time taken from birth to achieve full enteral feeds

# **Chapter 1: Introduction**

## **1.1 Overview**

The work in this thesis concerns gastroschisis which is a congenital abdominal wall defect that results in significant intestinal dysfunction at birth requiring prolonged duration of parenteral nutrition and hospital stay. In order to fully consider this condition it is important to introduce the normal structure and function of the gut, fetal development, clinical aspects of gastroschisis, current understanding of gastroschisis-related intestinal dysfunction and animal models of gastroschisis.

## **1.2 Normal Function and Structure of the Gut**

### **1.2.1 Functions of the Gut**

The alimentary tract (mouth, pharynx, oesophagus, stomach, jejunum, ileum, colon, rectum and anus) plus the connected accessory secretory organs (salivary glands, liver, gall bladder and pancreas) performs multiple coordinated functions in order to achieve nutritional absorption, which is essential for survival. Coordinated action of voluntary and smooth muscle of the palate and pharynx is required to achieve a safe swallow and ingestion of macromolecules. Appropriate stimulation of secretory cells and accessory secretory organs releases digestive enzymes, acid and bile into the gastrointestinal lumen. Digestion requires effective mixing and propulsion (gut peristalsis) of the secretory products and ingested luminal contents in order to enable breakdown of the ingested macromolecules. Absorption of the resultant micromolecules, electrolytes and water is achieved primarily by the jejunum and ileum but also partly by the colon at an extensive brush boarder providing a large surface area for absorption. The undigested or non-absorbable luminal contents are then eliminated from the body by defaecation. Dysregulation of any of the four essential functions (motility, secretion, digestion and absorption) prevents enteral autonomy and requires supportive approaches to ensure appropriate nutritional intake (Vander et al., 2001).

Additionally, the gut houses an extensive microbiome of more than 100 trillion microorganisms, which is important for digestion, intestinal motility, intestinal development, digestion, synthesis of vitamins, defence against infection, immune modulation, brain development and behaviour (Slattery et al., 2016, Lynch and Pedersen, 2016). The gut microbiome differs greatly between individuals that begins to be seeded in-utero and continues to develop during infancy and childhood (Romano-Keeler and Weitkamp, 2015, Tamburini et al., 2016). A steady state is thought to be achieved during adolescence, which persists throughout adult life until a decline in stability and function of the microbiome occurs in older age (Hollister et al., 2015). The composition of the microbiome is thought to be influenced by several factors including the environment, diet (including type of feed from birth), genetics, mode of delivery, age, medical treatments and early microbial exposure (Consortium [Human Microbiome Project Consortium], 2012). Pathological imbalance of the microbiome (dysbiosis) can occur at any stage of life and may be the cause or an effect of several pathologies (DeGruttola et al., 2016). Dysbiosis has been related to an increasing number of intestinal and extra-intestinal diseases including; inflammatory bowel disease, irritable bowel syndrome, obesity, diabetes mellitus, neuropsychological conditions and allergies (Jandhyala et al., 2015).

### **1.2.2 Structure of the Gastrointestinal Tract Wall**

The gastrointestinal tract is a hollow tube which has a similar wall architecture from the mid oesophagus to the anus and is composed of four layers from the luminal surface outwards; mucosa, submucosa, muscularis externa and serosa (Figure 1-1) (Vander et al., 2001).

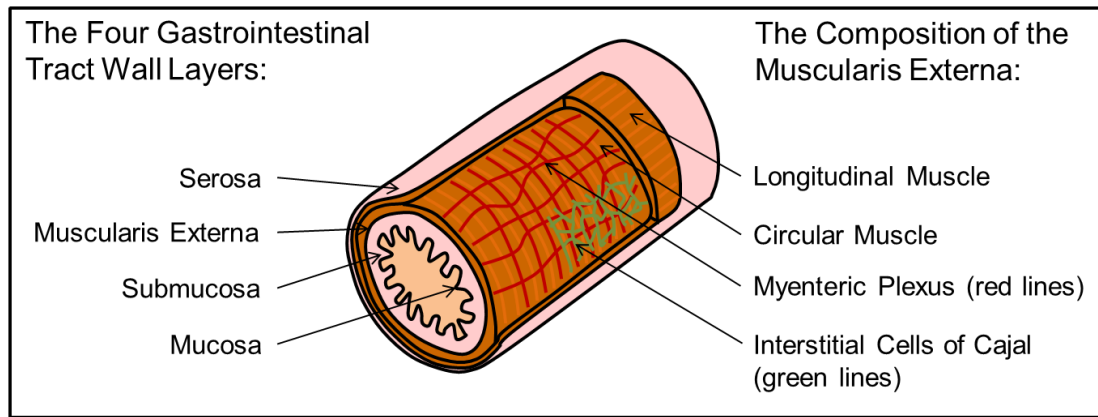


**Figure 1-1:** General structure of the gastrointestinal tract. Showing (from luminal surface outwards) the convoluted mucosal surface, submucosa, muscularis externa composed of the inner circular smooth muscle and outer longitudinal smooth muscle between which is the myenteric plexus and interstitial cells of Cajal and finally the outermost layer is the serosa.

The inner mucosal layer provides the interface between the luminal contents and entry into the body and is composed of three layers, namely the epithelium, lamina propria and muscularis mucosa. The simple columnar epithelium contains exocrine (secretory) and endocrine (hormone producing) cells, below which is the lamina propria that is composed of connective tissue allowing passage of blood vessels, nerves and lymphatic ducts. Separating the mucosa from the underlying tissues is a thin layer of muscle called the muscularis mucosa, which provides structural support to the mucosa. The mucosal surface of the small intestine (jejunum and ileum) is highly specialised for absorption with finger like projections (villi) extending into the lumen. The surface membrane of the simple columnar epithelial cells exhibit a brush border with further small projections called microvilli (Figure 1-2). The combination of villi and microvilli results in an increase in surface area of approximately 600-fold over a flat tube. The centre of each intestinal villus contains a blind ending lymphatic vessel (lacteal) for absorption of fat and a blood capillary network for absorption of water soluble nutrients (Figure 1-2). Finally, the villus crypts located between the base of adjacent villi contain stem cells that provide continual replacement of epithelial cells resulting in sloughing of disintegrated cells into the gut lumen (Figure 1-2) (Vander et al., 2001).

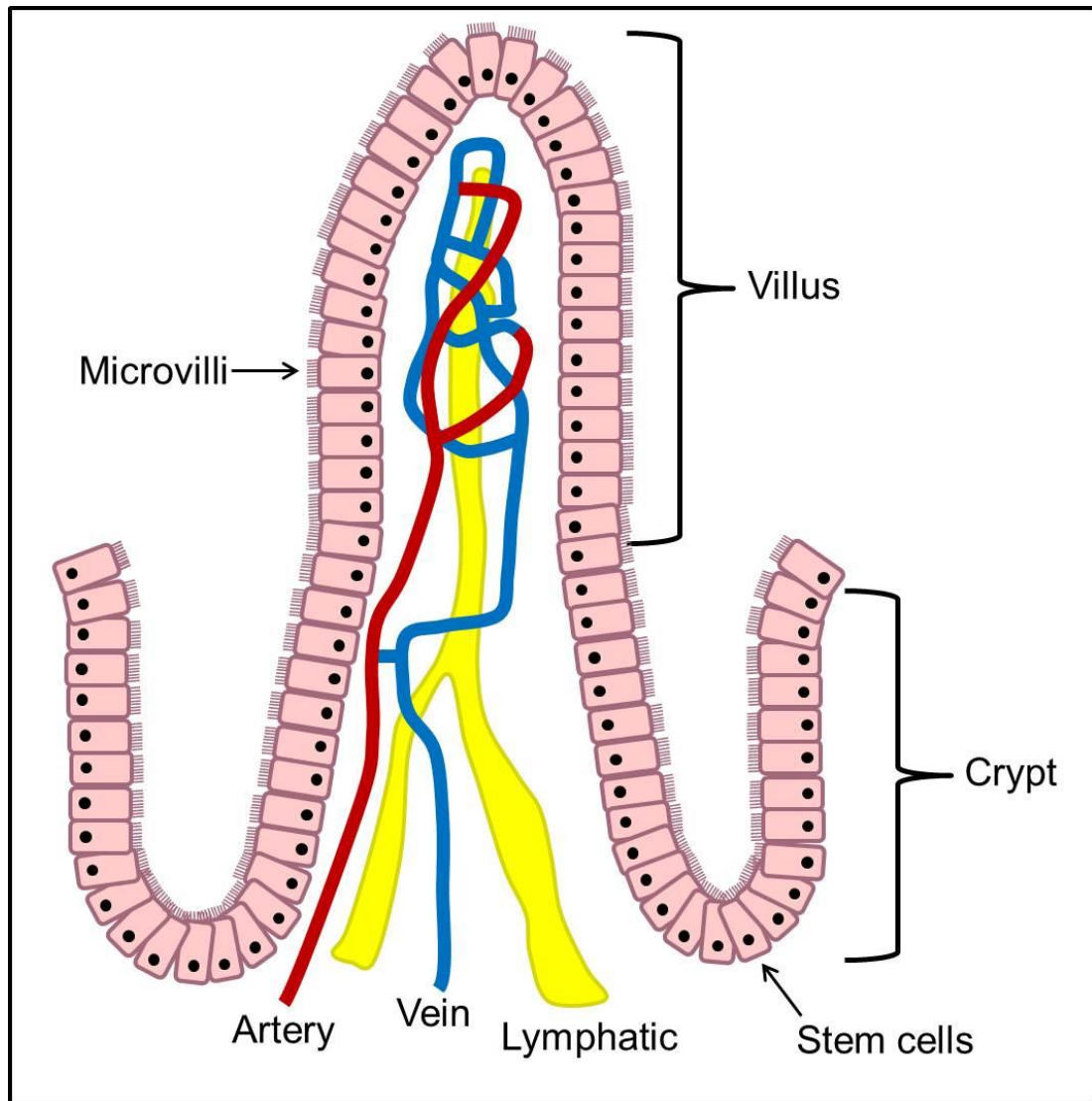


**Figure 1-2:** Structure of jejunal and ileal villi, demonstrating simple columnar epithelia with microvilli brush border, villus crypts and a central blind ending lymphatic vessel (lacteal) and blood capillary network.

The submucosa is a second layer of connective tissue containing nerves, blood vessels and lymphatics, which supply the mucosa and muscularis externa. The muscularis externa is composed of two distinct layers of smooth muscle; the inner circular and outer longitudinal muscle (Figure 1-1). Contraction of the inner circular layer results in narrowing of the lumen whilst the outer longitudinal layer produces shortening of the gut tube. In combination, the contraction of these two muscle layers provides the mixing and propulsion required for digestion and transit of the intestinal content in a rostrocaudal direction. In between the circular and longitudinal smooth muscle layers is the extensive myenteric plexus (Figure 1-1) composed of the enteric neurons and glial cells, which are closely associated with the interstitial cells of Cajal

(ICC, the pacemaker of the gut). The outermost layer of the gut tube is the serosa composed of loose connective tissue and coated in mucous preventing friction between the intestinal loops during peristalsis. The extracellular matrix, produced by myofibroblasts and other mesenchymal cells, is present within all connective tissue layers of the bowel wall and provides physical support to the tissue layers and transmits information to and from cells in the form of chemical messengers, which regulate cell growth, migration and differentiation thus helping to maintain tissue homeostasis especially in response to injury (Bonnans et al., 2014). Finally, the majority of the gastrointestinal tract is suspended from the posterior abdominal wall by a sheet of connective tissue called the mesentery through which the large intestinal blood vessels and lymphatics supply the gastrointestinal tract (Vander et al., 2001).

### **1.2.3 Gut Motility**

To achieve normal motility patterns the gut relies on the close interaction of the muscularis externa, enteric neurons and ICC (Bornstein et al., 2004). On ingestion of food boluses (postprandial), gut motility involves gastric peristalsis and intestinal segmentation to facilitate digestion and absorption of nutrients. Whilst in between meals (interdigestive), a cyclical, recurring motility pattern known as the migrating motor complex (MMC) ensures clearance of debris, secretions and microbes (Deloose et al., 2012).

Ingestion of a food bolus stimulates the receptive relaxation of the stomach increasing the capacity of the stomach from 50ml to 1.5L enabling acceptance of the bolus with little increase in gastric pressure. Gastric peristaltic waves ensue originating from the gastric body and travelling towards the pyloric sphincter, which is initially closed enabling mixing of gastric contents. Relaxation of the pyloric sphincter expels the contents (chyme) into the duodenum. Segmentation occurs throughout the small intestine with little apparent net distal movement and involves contraction of the circular smooth muscle producing division and movement of the chyme in both oral and anal directions ensuring mixing and maximal absorption of luminal contents (Husebye, 1999).

Following completion of nutritional absorption, segmentation stops and the cyclical MCC motility pattern takes over, which is regulated by gut hormones, the parasympathetic and enteric nervous system. The MMC was first reported in 1969 and described by the author as the interdigestive “housekeeper” of the small bowel (Szurszewski, 1969). Since the original description of the MMC, extensive research has been conducted in order to understand the physiological role and pathophysiological significance of this intestinal motility pattern, which remains incompletely understood (Husebye, 1999, Deloose et al., 2012). The MMC occurs during fasting and is composed of 4 phases; phase I is a state of inactivity or quiescence, phase II involves random contractions, phase III sudden bursts of contractions with maximal amplitude and duration, and phase IV rapid decrease in contractions. The MMC is a recurrent event that moves from the stomach to the terminal ileum over a period of 2 hours. Distension of the stomach results in termination of the MMC in the stomach and upper small bowel whilst presence of nutrients within the small intestine terminates MMC patterns throughout the entire bowel (Code and Marlett, 1975).

#### **1.2.4 Intestinal Smooth Muscle**

The muscle layers that make up the muscularis externa are not truly circular or longitudinal but helical. Individual smooth muscle cells are interconnected by gap junctions providing electrical coupling resulting in depolarisation within one muscle area spreading outwards to adjacent sections. Electrical coupling enables coordinated contraction of an entire ring of circular muscle rather than small patches ensuring effective mixing and propulsion of luminal contents (Vander et al., 2001). The muscularis externa has two actions; (1) prolonged tonic contractions to maintain the three dimensional shape of the gastrointestinal tract against intraluminal forces created by food boluses and (2) short lasting muscle contractions creating force generation. In combination these actions enable maintenance of the intraluminal volume capacity and propulsion of contents along the gut (Bitar, 2003).



### **1.2.5 Enteric Nervous System**

The enteric nervous system comprises neurons and glial cells (neuronal supporting cells) that form a large interconnecting network of cells along the entire bowel length. There are two large nerve plexuses: the myenteric plexus, which is located between the layers of the muscularis externa and the submucosal plexus (Figure 1-3), which is located in the submucosal connective tissue. There are also scattered neurons within the mucosa. The enteric nervous system supplies the smooth muscle and exocrine glands creating an autonomous nervous system controlling and regulating gut motility, secretions, vascular tone and hormone release throughout the gut. A stimulus at one part of the bowel is transmitted both cranially and caudally along the enteric nervous system, thus stimulus of the upper small intestine may also result in an effect in the stomach and lower intestinal tract. Motility is largely controlled by the myenteric plexus but in humans the submucosal plexus is also thought to be involved (Burns et al., 2009). Additionally, branches of the parasympathetic and sympathetic autonomic nervous system synapse with the enteric nervous system through which the central nervous system can also modulate motility and secretory function of the gastrointestinal tract (Browning and Travagli, 2014). The enteric nervous system contains cholinergic and adrenergic neurons as well as noncholinergic and nonadrenergic neurons that release neurotransmitters including nitric oxide, several neuropeptides and adenosine triphosphate (ATP) (Burns et al., 2009, Vander et al., 2001).

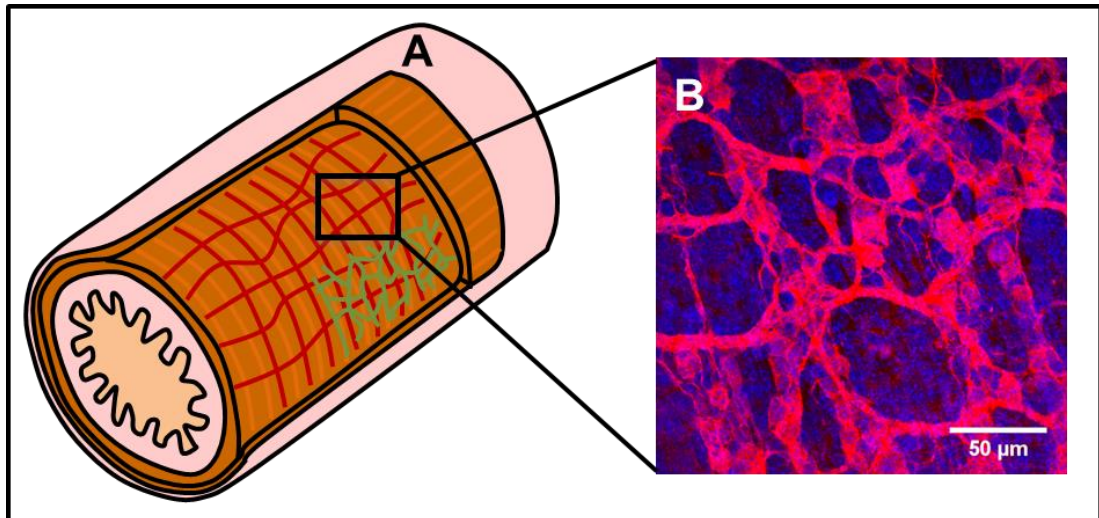


**Figure 1-3:** **A.** Schematic of ileum. **B.** Immuofluorescence image of the myenteric plexus (red) and nuclei (blue) showing the interconnecting network of enteric neurons and glial cells.

### 1.2.6 Interstitial Cells of Cajal

The interstitial cells of Cajal (ICC) are the pacemaker cells of the gut and are an integral part of the motor function of the bowel. They initiate and propagate electrical slow waves, which regulate gut peristalsis and mediate neurotransmission between the enteric neurons and smooth muscle of the bowel (Burns, 2007). ICC are found throughout the entire gastrointestinal tract in several distinct populations with different functional roles (Komuro, 2006, Burns et al., 1997). The most essential populations are the branching ICC networks associated with the myenteric plexus, which generates spontaneous slow rhythmical pacemaker activity (Hirst et al., 2006), and the spindle shaped ICC located intramuscularly that propagate electrical waveforms throughout the muscle (Huizinga and Chen, 2014).

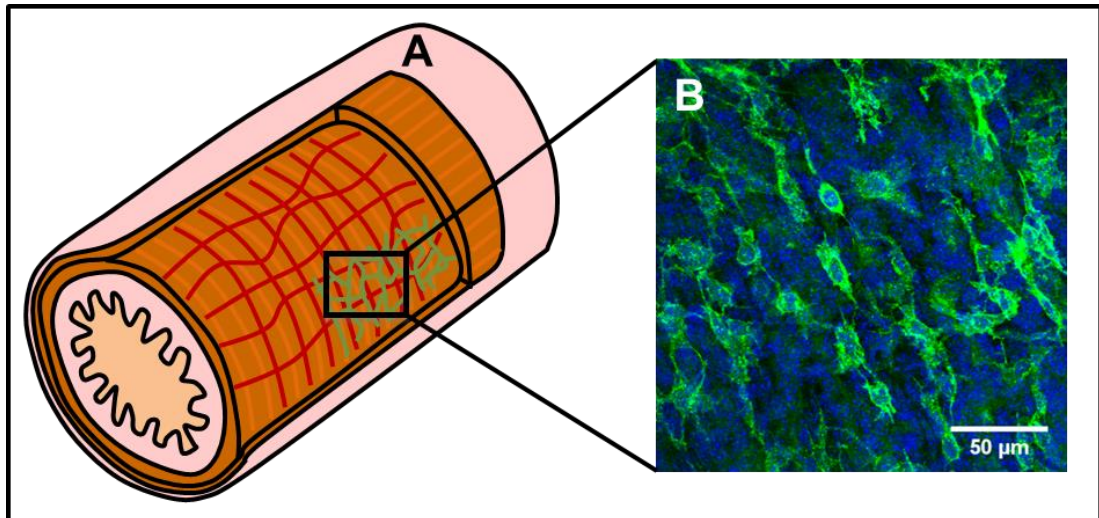


**Figure 1-4:** **A.** Schematic of ileum. **B.** Immuofluorescence image of the ICC (green) network at the level of the myenteric plexus and nuclei (blue) showing the branching network of ICC.

ICC were first described by Ramón y Cajal in 1911 (Thuneberg, 1999) and many years later were identified by crude histochemical techniques. The advent of electron microscopy in the 1960s revealed the ultrastructure of these cells (Rogers and Burnstock, 1966), which were found to have gap junctions with smooth muscle cells and close associations with nerve terminals consistent with Ramón y Cajal's original functional hypothesis. However, the histochemical techniques lacked cell specificity and electron microscopy is time consuming and labour intensive. So it wasn't until the 1990s when ICC were discovered to express the protooncogene *c-kit* (Maeda et al., 1992) that ICC could easily and robustly be studied.

*C-Kit* encodes a transmembrane receptor tyrosine that can be manipulated through blockade or genetic mutation and is specifically labelled by anti-Kit antibodies making ICC readily manipulatable and detectable. Physiological studies have identified that binding of membrane-bound stem cell factor to the extracellular Kit receptor is required for activation of the intracellular tyrosine kinase domain (Ward et al., 1995, Mikkelsen et al., 1998). Blockade with an anti-Kit antibody or disruption of Kit function by mutation of the Dominant white spotting (W) locus in animal models results in ICC loss, electrical quiescence and loss of bowel motility (Maeda et al., 1992). These findings highlight Kit to be an essential pathway in both function

and maintenance of ICC and therefore a useful histochemical marker for studying ICC development, function and pathology.

### **1.3 Overview of Human Embryological and Fetal Development**

#### **1.3.1 Overview of the Embryonic and Fetal Period**

The human embryonic period refers to the first 8 weeks of development from the time of fertilisation and has been described in 23 developmental stages (Carnegie stages) based on the Carnegie Collection of human embryos (O'Rahilly, 1979). The Carnegie stages are based purely on morphological features and are not dependent on size or age of the embryo (O'Rahilly, 1979). During the embryonic period the three germ layers form (ectoderm, mesoderm and endoderm) from epiblasts (gastrulation) followed by establishment of all the organ systems. The embryonic period of development is very rapid resulting in 90% of all adult structures being identifiable by the end of this period. Hence, the pregnancy is at its most vulnerable from teratogenic influences during these first 8 weeks of development due to extensive cell divisions, cell migration and cell differentiation, which can result in congenital malformations. The remainder of the pregnancy is designated the fetal period during which the organs differentiate, grow and become functional (organogenesis) (Sadler, 2004).

#### **1.3.2 Terminology of Pregnancy**

Clinically, the term gestational age (GA) is used to indicate the pregnancy duration as calculated from the time of the last menstrual period (LMP) and although this normally occurs 2 weeks before the start of ovulation, it is a time point that most women can remember and serves as a guide to the time of fertilisation. The term developmental age indicates pregnancy duration based on calculations from the time of fertilisation i.e. approximately 2 weeks less than the GA and is the term used by embryologists and developmental biologists. Pregnancy is divided into 3 trimesters; the first trimester spans from 1 week GA through to 12 weeks GA, the second from 13 weeks GA to 27 weeks GA and the third from 28 weeks GA to birth. The approximate due date is calculated as 40 weeks from the date of the LMP therefore

the actual length of pregnancy is 38 weeks from fertilisation. However, a pregnancy is considered to have reached full term from 37 weeks GA onwards. Neonates born at less than 37 weeks GA are considered premature.

### **1.3.3 The Placenta, Fetal Membranes, Umbilical Cord, and Amniotic Fluid**

The placenta develops from the blastocysts at the time of implantation into the maternal endometrium and provides a high surface area for transfer of substances between the maternal and fetal blood. The placenta provides gas exchange, waste removal, nutrition, immune and endocrine support and a source of stem cells for the developing fetus. The embryo's initial nutrition source is the yolk sac until the umbilical cord is formed by week 5 of development when the placenta takes over this function.

The entire fetus is surrounded by 2 membranes, namely the chorionic and amniotic membrane. The chorionic membrane lines the placenta (chorion frondosum) and uterine wall (chorion leave). The avascular amniotic membrane arises as a single sheet of cells covering the dorsal surface of the embryo and gradually enlarges to surround the embryo. Initially the two membranes are separated by the exocoelomic cavity, which is a fluid-filled space containing an ultra-filtrate of the maternal serum and also proteins from the placenta and secondary yolk sac thus aiding the exchange of predominantly proteins between mother and fetus (Jauniaux and Gulbis, 2000). By the end of the first trimester the exocoelomic cavity is obliterated due to the expansion of the amniotic cavity, which becomes the only significant collection of extrafetal fluid. Following obliteration of the exocoelomic cavity the chorionic and amniotic membranes come into direct contact forming the chorioamniotic membrane. At this point the chorionic and amniotic membranes are slightly adherent but can be easily separated due to a spongy layer between the membranes. The chorioamniotic membrane has dynamic viscoelastic properties providing resilience to rupture and fetal protection (Creasy et al., 2009, Winn and Hobbins, 2000).

The umbilical cord is the vascular connection between the placenta and fetus, which develops from the yolk sac and allantois. The cord consists of 3 blood vessels (2 arteries and 1 vein), which are surrounded by Wharton's jelly and the amniotic

membrane. The umbilical cord blood vessels originate from the placenta at their point of exit from the placenta. The amniotic membrane diverges from the chorioamniotic membrane bilayer and adheres to the umbilical vessels for their entire length. The umbilical cord terminates by inserting centrally on the ventral abdominal wall. The umbilical vein continues as the ductus venosus, the umbilical arteries insert onto the internal iliac arteries and the amniotic membrane becomes continuous with the abdominal wall ectoderm (Bargy and Beaudoin, 2014).

The composition of amniotic fluid alters throughout pregnancy. Before keratinisation of the fetal skin at 25 weeks GA, the amniotic fluid composition is similar to fetal plasma and serves as an extension of the extracellular compartment. After keratinisation the composition and volume of amniotic fluid is determined by fetal urine, secretion of oral and airway fluids, swallowing and chorioamniotic membrane absorption (Gilbert and Brace, 1993). Thus in the third trimester of pregnancy there is an increase in urea and creatinine and a reduction in sodium, chloride and osmolality (Underwood et al., 2005). In addition, evidence suggests that fetal defecation is a normal physiological fetal phenomenon occurring sporadically in the second trimester and relatively frequently in the third (Ramon y Cajal and Martinez, 2003, Ciftci et al., 1996) thus introducing bile, enteric enzymes and interleukin-8 (IL-8) into the amniotic fluid.

## **1.4 Development of the Gastrointestinal Tract and Abdominal Wall**

### **1.4.1 General Development of the Gastrointestinal Tract**

The primitive gut tube comprising the mucosa, mucosal glands and submucosal glands develops from the endoderm lining of the yolk sac secondary to cephalocaudal and lateral folding of the embryo. During embryo folding the stiff axial structures results in the embryo curving ventrally and the endodermal-lined yolk cavity ballooning anteriorly creating a three dimensional embryo and the primitive gut tube. The mesenteries that suspend the gastrointestinal tract from the body cavity are derived from the mesoderm, which wraps around the endodermal gut tube giving rise to the structures of the outer gut wall (lamina propria, muscularis mucosa, submucosal connective tissue and blood vessels, muscularis externa, ICC,

and serosa). Finally, the ectoderm gives rise to the neural crest, from which the enteric nervous system is derived.

Initially the gastrointestinal tract develops as a hollow tube but during the 5th week of development the gut wall undergoes multiple proliferations resulting in complete blockage of the lumen (solid stage) by week 6 of development. This tissue over the course of the next 2 weeks gradually degenerates and reforms a hollow gut tube by the end of week 8 of development. This process is called recanalization.

The entire gut tube extends the length of the embryo and from four weeks developmental age three distinct gut segments are apparent (foregut, midgut and hindgut) each with a defined blood supply (Figure 1-5). The foregut is supplied by the coeliac artery and includes the oesophagus, stomach, upper duodenum, liver, gall bladder, bile ducts, trachea and lungs. The midgut is supplied by the superior mesenteric artery and includes the lower duodenum, jejunum, ileum, caecum, appendix, ascending colon and proximal two thirds of the transverse colon. The hindgut is supplied by the inferior mesenteric artery and includes the distal third of the transverse colon, descending colon, sigmoid colon, rectum, upper anal canal, urogenital sinus. The midgut develops from lateral embryonic folding, which 'pinches off' a segment of the yolk sac and the two compartments remain temporarily connected via the vitelline duct.

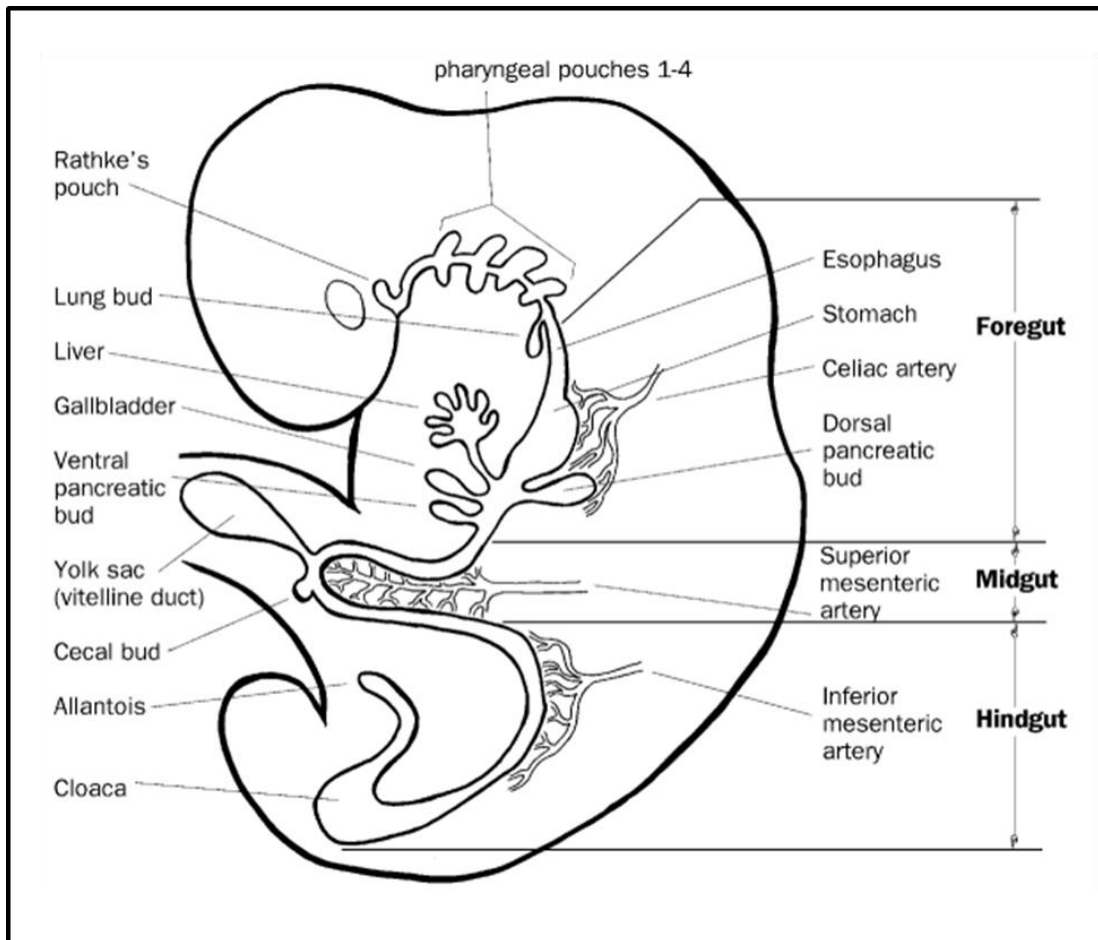


**Figure 1-5:** Primitive digestive tract showing the developing foregut, midgut and hindgut with the respective arterial supply and the vitelline duct, which temporarily contacts the gut tube to the yolk sac (Gest, 2002).

During organogenesis the individual gut structures (e.g. oesophagus, stomach, ileum, etc.) develop from the gut tube. Structural identity of the gastrointestinal tract occurs secondary to the reciprocal interaction between the endoderm and mesoderm whereby regionalisation of the endoderm is determined by the overlying mesoderm. *HOX* genes are expressed along the length of the gut mesoderm, which are induced as a result of *sonic hedgehog* expression by the endoderm. Once the mesoderm *HOX* code is expressed it instructs the endoderm to form the appropriate regional structural component of the gastrointestinal tract (Sadler, 2004).



### **1.4.2 Ventral Abdominal Wall Closure and Development of the Midgut Intestinal Loops**

The closure of the abdominal wall and the development of the intestinal loops are inextricably linked (Sadler, 2010). Ventral abdominal wall closure begins during gastrulation from the mesodermal folds at week 3 of development. At this time the umbilical ring is represented by the circumference of the flat embryo. During week 4 of development the thorax and abdomen come to be positioned ventrally following cephalocaudal and lateral folding of the embryo. Abdominal closure occurs following migration of the cephalic, caudal and two lateral mesodermal folds, which converge centrally forming the umbilical ring (Brewer and Williams, 2004a).

The midgut undergoes rapid elongation during the 6th week of development forming a primary intestinal loop (Figure 1-6A). This coincides with the expansion of the liver and the abdominal cavity becomes temporarily too small to contain the intestinal loops. As such, the intestinal loops project through the open umbilical ring into the base of the umbilical cord known as physiological herniation. During physiological herniation the intestinal loops rotate approximately 90° anticlockwise around the axis of the superior mesenteric artery and the intestine continues to elongate forming numerous jejunal and ileal coiled loops (Figure 1-6B). The intestinal loops begin to return to the abdominal cavity and rotate a further 180° (Figure 1-6C). The jejunum returns to the abdomen first and lies on the left side (Figure 1-6D) with later returning loops lying more on the right (Figure 1-6E). The caecal bud initially returns and lies in the right upper quadrant and later descends into the right iliac fossa placing the ascending colon on the right side of the abdomen (Figure 1-6D and E). The factors involved in the return of the intestinal loops to the abdominal cavity are not fully understood but may be linked to reduced liver growth and expansion of the abdominal cavity (Sadler, 2004). Resolution of the physiological hernia occurs at around week 10 of development (12 weeks GA) resulting in final closure of the abdominal wall (Sadler, 2010). Additionally, by the 10th week of development the vitelline duct completely obliterates breaking the connection between the midgut and yolk sac.

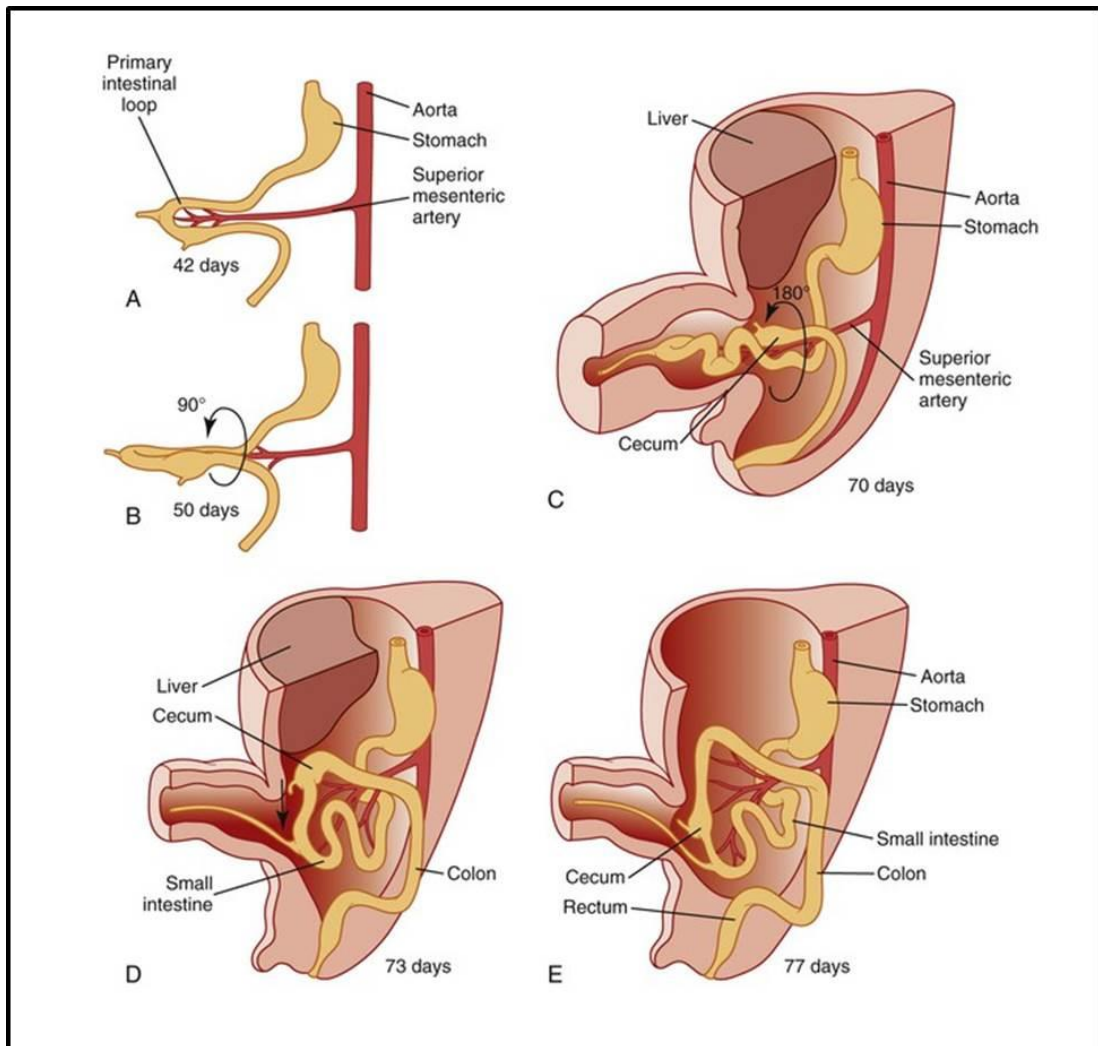


**Figure 1-6:** Physiological herniation and development of the midgut. A. Rapid elongation of the primary intestinal loop during the 6<sup>th</sup> week of development. B. Rotation of the bowel during physiological herniation. C. Return and rotation of the intestinal loops into the abdominal cavity. D. Initial returning loops lie on the left side of the abdomen. E. Later returning loops come to lie on the right side of the abdomen and the caecal bud comes to lie in the right iliac fossa. Physiological herniation resolves around 10<sup>th</sup> week of development (Larsen, 1997).

The initial primary abdominal wall closure is composed of a thin epithelial membrane. Proliferation of myoblasts from the myotome enables secondary structures to form including the four muscle pairs (rectus abdominis, external oblique, internal oblique and transversus abdominis), fascia and skin (Nichol et al., 2012). The umbilical ring forms the transition zone between the ectoderm of the ventral abdominal wall and the amniotic membrane that surrounds the umbilical vessels (Bargy and Beaudoin, 2014). Although the gross structural development of the ventral abdominal wall is known, little is understood regarding the mechanisms

underpinning cell signalling and migration and therefore the causes of abdominal wall defects are not fully understood (Sadler, 2004).

### **1.4.3 Neuromuscular Development of the Gut**

The gastrointestinal enteric neurons and smooth muscle are both functionally and developmentally coordinated. The gut is populated by the enteric neurons by cell migration in an oral to anal cell direction, whilst the smooth muscle has a gradient of maturation along the gut again in an oral to anal direction. In contrast, the ICC do not appear to develop in a migratory fashion. The enteric neurons develop from the neural crest, which is a transient population of cells appearing between the ectoderm and dorsal neural tube during early embryo development. The migrating neural crest-derived precursors of the enteric nervous system are seen within the midgut by week 5 of development and the entire gut is colonized by week 7 of development (Wallace and Burns, 2005). Initially the migrating cells form the myenteric plexus and then migrate centripetally to form the submucosal plexus 2-3 days after establishment of the myenteric plexus. The gastrointestinal smooth muscle develops from the mesoderm and appears, as identified by smooth muscle actin antibody staining, in the oesophagus by week 8 of development and the hindgut by week 11 of development. The smooth muscle layers are well defined throughout the gut by week 14 of development. The ICC are also derived from the mesoderm and appear in the muscularis externa of the midgut during weeks 7-9 of development and are more distinct by week 11 of development (Burns et al., 2009, Wallace and Burns, 2005). The ICC associated with the myenteric ganglia are the first of the ICC populations to develop and become a continuous network throughout the entire gut by week 17 of development. By week 14 of development the gut has a relatively mature appearance in terms of the presence of defined muscle layers, enteric neurons and myenteric ICC, although the remaining ICC populations continue to develop throughout fetal life and into the newborn period. The intramuscular ICC appear by 36 weeks gestational age and the deep muscular plexus appears during the early neonatal period. This continued development of ICC during fetal life could explain why functional recordings of premature neonates show immature ileal motility (Fausone-Pellegrini et al., 2007).

## **1.5 Human Congenital Anomalies**

### **1.5.1 Overview of Congenital Anomalies**

Congenital anomalies develop in-utero before birth and are also known as congenital defects or malformations. The term encompasses: (1) Structural defects, which result from disruption of body wall folding or organogenesis during the embryonic or fetal stage of development creating anatomical abnormalities of structures such as the heart, liver, abdominal wall, spinal cord, etc. Frequently the cause of these defects is unknown; (2) Functional anomalies are conditions that impact on organ or system function and are often genetically inherited including metabolic (glycogen storage disease, Lesch-Nyhan syndrome) and haematological disorders (Sickle cell, thalassaemia); (3) Chromosomal anomalies, including chromosomal duplication (Down's, Patau's and Edward's syndromes), chromosomal deletion (Turner's) and missing, extra or irregular portions of chromosomal DNA (Wolf-Hirschhorn syndrome, Charcot-Marie-Tooth disease type 1A).

Improvements in antenatal ultrasound and developments of new diagnostic techniques have enabled many congenital anomalies to be detected during the antenatal period. Early detection enables appropriate antenatal counselling, monitoring and clinical management, delivery planning and arrangements for postnatal management or equally the option for termination. However, other congenital anomalies may not be detectable until birth or if symptoms or signs of the condition are not evident at birth then later in life (childhood or adulthood).

In the UK two antenatal ultrasound scans are performed routinely. A first trimester dating/screening ultrasound scan at 11 to 14 weeks GA, which determines the gestational age of the pregnancy and the risk of chromosomal anomalies such as Down's syndrome. Additionally, it is possible to detect abdominal wall defects at this stage. A second trimester anomaly ultrasound scan at 18 to 20 weeks GA is performed to systematically review the structural development of the fetus in order to detect the presence of any sonographically evident structural defects. A significant number of structural anomalies can be detected at this stage including abdominal wall defects, heart defects, spina bifida, cleft lip and palate and congenital

diaphragmatic hernia (Todros et al., 2001). Further monitoring scans are performed if the fetus is found to have a structural defect.

Screening for chromosomal anomalies (Down's syndrome, Patau's and Edwards) is performed at the 12 to 13 weeks GA dating/screening scan. Those with a high risk of such conditions are offered the opportunity to undergo chorionic villus sampling (a sample of chorionic villus is removed from the placenta under ultrasound guidance) between the 11<sup>th</sup> and 14<sup>th</sup> weeks GA or amniocentesis (a sample of amniotic fluid is removed under ultrasound guidance) between the 15<sup>th</sup> to 20<sup>th</sup> weeks GA to confirm the fetal chromosomal and genetic profile (Alfirevic et al., 2003). However, both these procedures are invasive and carry risks to the pregnancy (Akolekar et al., 2015, Alfirevic et al., 2003). As such, a new technique has been developed to detect 'cell-free fetal DNA' from a maternal blood sample. This non-invasive test can detect fetal DNA circulating within the maternal blood and determine the fetal chromosome (including sex) and genetic profile from 10 weeks GA onwards (Barrett et al., 2011).

The aetiology of many structural defects remains unknown but common causes and risk factors include genetic or chromosomal factors, parental consanguinity, maternal infections, maternal nutritional status, environmental factors (such as chemicals, recreational drugs, medications, pesticides and radiation), young maternal age and low socioeconomic status (Brent, 2004, Hobbs et al., 2014, Vrijheid et al., 2000). Preventative measures in the peri-conception period have reduced the incidence of certain structural conditions such as spina bifida (Burren et al., 2008, Williams et al., 2015) and advances in modern medicine have significantly reduced infant morbidity and mortality from many congenital anomalies in developed countries. However, worldwide birth anomalies remain a leading cause of infant death and it is estimated that 276 000 neonates (infants under 28 days of age) die each year (WHO, 2014).

### **1.5.2 Congenital Ventral Abdominal Wall Defects**

Congenital ventral abdominal wall defects are structural anomalies that involve failed closure of the ventral body wall. The most common abdominal wall defects are gastroschisis (4.4/10,000 live births) (Kilby, 2006) and exomphalos (2.5/10,000 live births) (Weber et al., 2002) but also includes other rare conditions namely bladder

exstrophy (1:30,000-50,000 live births) (Ben-Chaim et al., 1996) and body stalk anomaly (0.4 to 3.2:100,000 live births and universally fatal) (Bugge, 2012). The pathogenesis of abdominal wall defects remains controversial. Exomphalos is largely considered to develop secondary to failed return of the bowel following physiological herniation (Sadler, 2010) and body stalk anomaly is thought to be due to either an early rupture of the amnion and direct mechanical pressure on the developing fetus (Paul et al., 2001) or a germinal disk abnormality preventing body wall folding (Lockwood et al., 1986). However, there are multiple hypotheses for the pathogenesis of both gastroschisis and bladder exstrophy with no overarching consensus (Sadler, 2010, K et al., 2015).

Gastroschisis (Figure 1-7A) exhibits a relatively small paraumbilical, full thickness defect (approximately 1 to 2cm wide) that usually lies to the right of the umbilicus (Sadler, 2010) through which most of the bowel and occasionally other organs herniate. The bowel has no covering membrane and therefore lies in direct contact with the amniotic fluid. Frequently at birth the bowel appears thickened and inflamed and 10-15% of gastroschisis infants also have concomitant intestinal pathologies (Carnaghan et al., 2014, Bradnock et al., 2011) including atresia, stenosis, perforation and necrosis. However, concomitant extra-abdominal malformations or chromosomal abnormalities are rare.

In contrast, exomphalos (Figure 1-7B) exhibits a ventral abdominal wall defect disrupting the umbilical ring ranging in severity from minor (<5 cm) to major (>5 cm) (Carnaghan et al., 2009, Groves et al., 2006). The abdominal viscera including bowel and frequently liver herniates into the base of the umbilical cord. The viscera are characteristically contained within a membranous sac composed of the amniotic membrane at the base of the umbilical cord, which protects the viscera from the amniotic fluid. Exomphalos is commonly associated with extra-abdominal anomalies including structural defects of the heart, diaphragm and limbs, pulmonary hypoplasia and metabolic and chromosomal disorders. However, at birth the bowel function is normal and exomphalos is rarely associated with concomitant intestinal pathology (Vachharajani et al., 2009, Carnaghan et al., 2009). Finally, exomphalos also rarely occurs as part of a syndrome called pentalogy of Cantrell exhibiting 5 key features;

exomphalos, cleft sternum, ectopia cordis (externalised heart), diaphragmatic hernia (anterior diaphragmatic deficiency) and cardiac defects.

A body stalk anomaly is also known as limb-body wall complex involving malformation of the abdomen, thorax and usually limbs. This complex, lethal condition involves varying degrees of failed ventral wall closure, which may be located centrally or to one side of the torso and can result in externalisation of both thoracic and abdominal viscera into an amnioperitoneal membrane. During in-utero development a proportion of the fetus lies outside of the amniotic cavity within the exocoelomic cavity, there is incomplete fusion of the amnion to the chorion and a short or absent umbilical cord. Finally other structural defects include limb deformities, scoliosis (curvature of the spine) and malformations of the anorectal canal and genitourinary tract (Bugge, 2012).

Bladder exstrophy (Figure 1-7C) involves failed closure of the inferior ventral abdominal wall and splitting of the anterior bladder wall and urethra resulting in an exposed bladder plate. Classically exstrophy exhibits a low lying umbilicus, diastasis of the pubic symphysis, abnormal genitalia and anorectal malformation. Males exhibit severe epispadias and in females a bifid clitoris and vaginal ectopia (K et al., 2015).

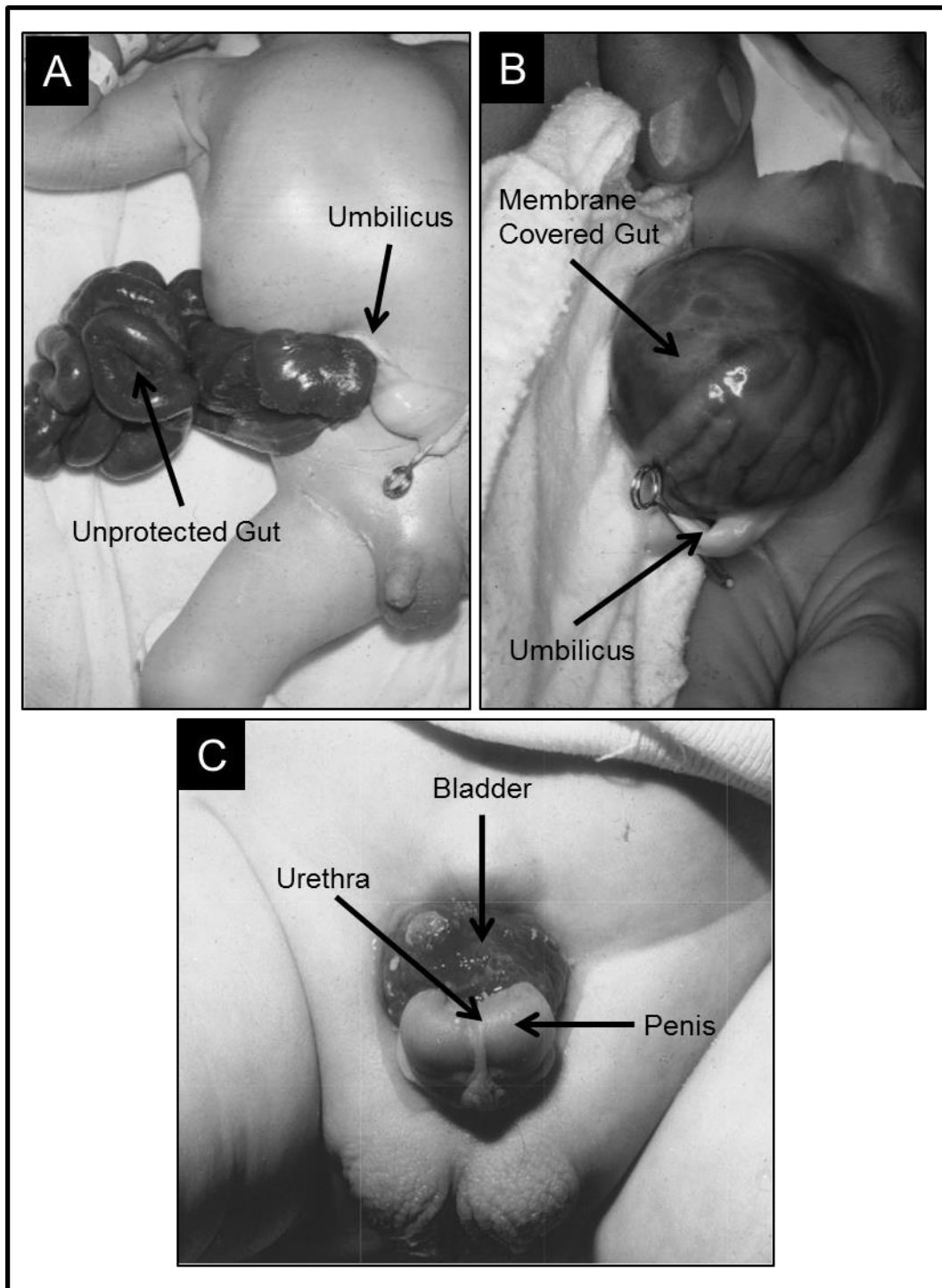


**Figure 1-7:** Types of survivable congenital ventral abdominal wall defects. **A.** Gastroschisis showing a ventral abdominal wall defect to the right of the umbilicus and externalised gut without a covering membrane. **B.** Exomphalos showing a large central abdominal wall defect with gut herniating into the base of the umbilical cord providing a protective membrane. **C.** Bladder exstrophy showing a lower midline central abdominal wall defect exposing the bladder plate and associated epispadias (Coran et al., 2012).



### **1.5.3 Congenital Gastrointestinal Defects**

The majority of congenital gastrointestinal defects involve disruption of luminal continuity including atresia (complete occlusion of the lumen, Figure 1-8A), stenosis (narrowing of the lumen, Figure 1-8B) and perforation. Atresia and stenosis of the jejunum, ileum and colon are thought to occur secondary to an in-utero vascular accident such as external bowel wall compression or a vasoconstrictive/thromboembolic event resulting in bowel necrosis and tissue resorption (atresia) or scarring (stenosis) (Koga et al., 1975, Louw and Barnard, 1955). This is in contrast to duodenal atresias, which are thought to develop secondary to failed recanalisation of the primitive gut tube (Sadler, 2004). Isolated intestinal perforation (Figure 1-8C) can occur due to a focal attenuation of the muscularis externa, which may be caused by focal outer bowel wall necrosis (Lai et al., 2014, Izraeli et al., 1992).

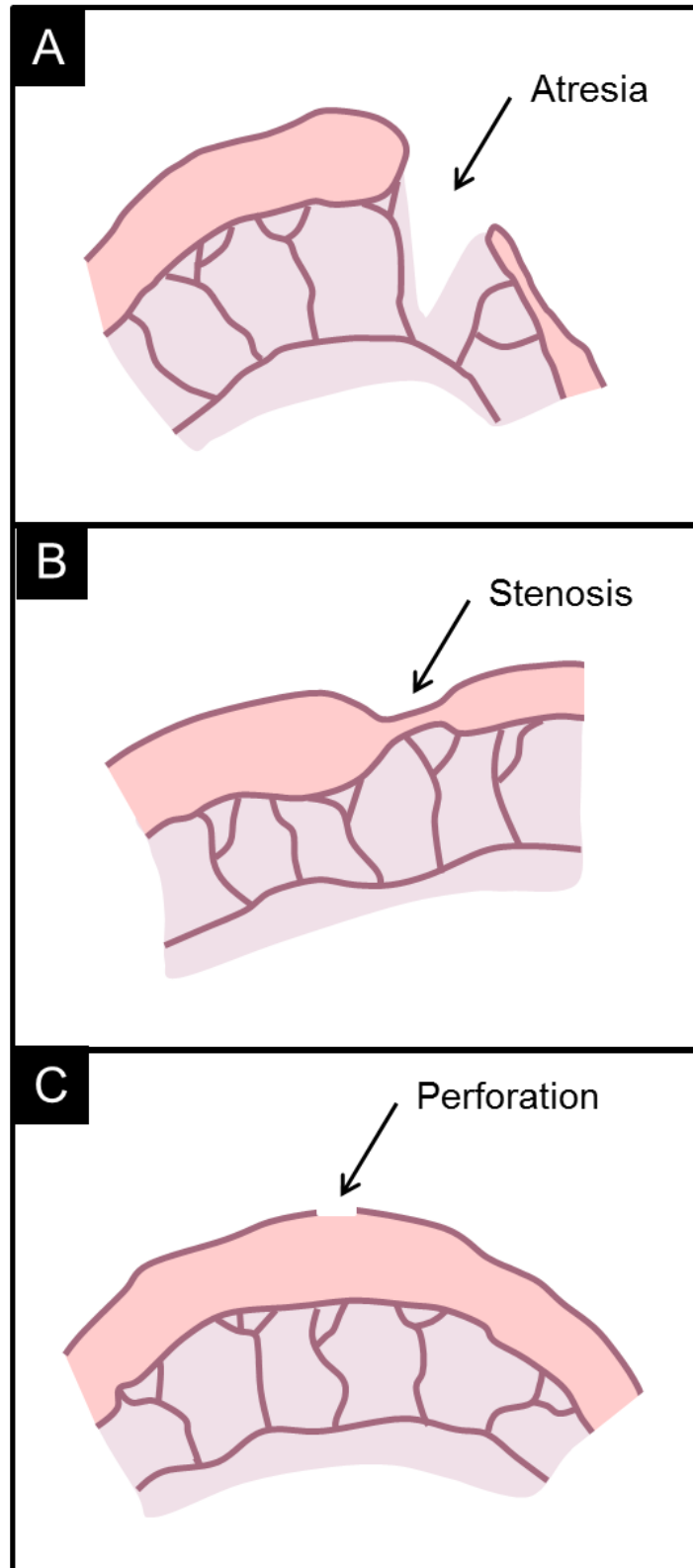


**Figure 1-8:** Schematic representation of gastrointestinal pathologies. **A.** Atresia depicting blind ending proximal and distal bowel. **B.** Stenosis depicting narrowed bowel lumen. **C.** Perforation depicting a hole in the bowel wall.

Other congenital defects include duplication cysts, Meckel's diverticulum, intestinal malrotation, intestinal aganglionosis and anorectal malformations. Duplication cysts form following incomplete recanalization of the primitive gut tube resulting in parallel intestinal lumens, which can result in stenosis and obstruction of the primary gastrointestinal lumen. Meckel's diverticulum results from incomplete resorption of the vitelline duct during fetal development and ranges in size from a patent duct between the midgut and umbilicus to a fibrous cord connecting the midgut to the umbilicus. Intestinal malrotation or non-rotation is abnormal rotation and fixation of the bowel during organogenesis of the midgut. The condition includes a narrow mesenteric attachment to the posterior abdominal wall around which the gut can twist resulting in a midgut volvulus causing bowel necrosis secondary to mesenteric vessel obstruction. Intestinal aganglionosis, also known as Hirschsprung's disease, results from failure of the enteric neural crest cells to migrate from mouth to anus during fetal development. The length of the aganglionosis varies from being a short 1cm segment affecting the rectum to a long segment affecting the entire colon and occasionally the terminal ileum. In all instances the aganglionosis is continuous with no skip lesions. Anorectal malformations encompass a broad spectrum of anomalies in which the distal hindgut fails to develop a normal anal opening within the centre of the anal sphincter complex. Frequently there is an imperforate anus and the intestine terminates with a fistulous connection to the perineum or genitourinary tract. Severity of these defects ranges from a mildly displaced anal opening with an excellent functional prognosis to imperforate anus associated with deficient sphincter and pelvis musculature, genitourinary defects and also spinal anomalies resulting in poor functional outcome (Davenport and Pierro, 2009).

## **1.6 Gastroschisis**

### **1.6.1 Overview and Characteristic Features**

Gastroschisis is a relatively small paraumbilical ventral abdominal wall defect that typically lies to the right (in 95% of cases) of the umbilical cord (Sadler, 2010, Hombalkar et al., 2015). The umbilical cord forms normally consisting of 3 blood vessels (2 arteries and 1 vein) covered by Wharton's jelly and the amniotic membrane (Bargy and Beaudoin, 2014). The full thickness gastroschisis abdominal

wall defect is positioned between the umbilical cord insertion and the right lateral ventral wall fold disrupting the continuation of the amniotic membrane with the abdominal wall ectoderm at this point. As such, the externalised abdominal contents lie free floating within the amniotic cavity without a covering membrane placing the viscera in direct contact with the amniotic fluid. The eviscerated organs usually include most of the small and large bowel but can also include stomach, spleen, bladder, gonads, uterus and very rarely the liver (McClellan et al., 2011, Mousty et al., 2012). Frequently at birth the bowel appears thickened, inflamed and matted, which is thought to be due to the abnormal exposure of the serosal surface to the irritant amniotic fluid or constriction at a tight abdominal wall defect (Langer et al., 1989). Figure 1-9 and Figure 1-10 schematically depicts the gastroschisis defect.

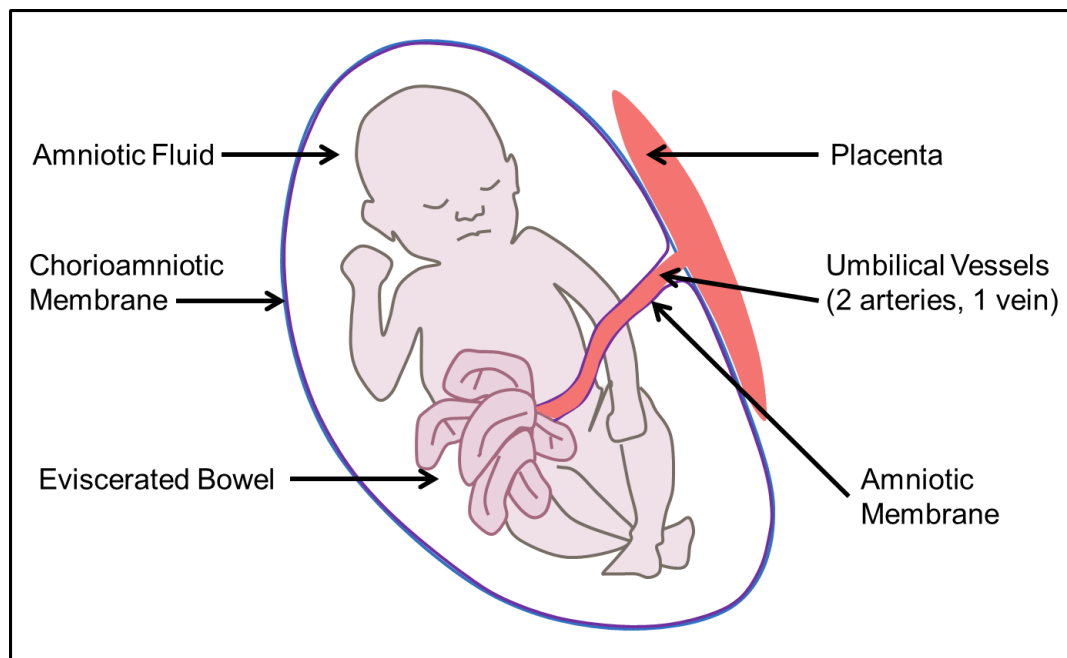


**Figure 1-9:** Schematic illustration of an in-utero gastroschisis fetus.

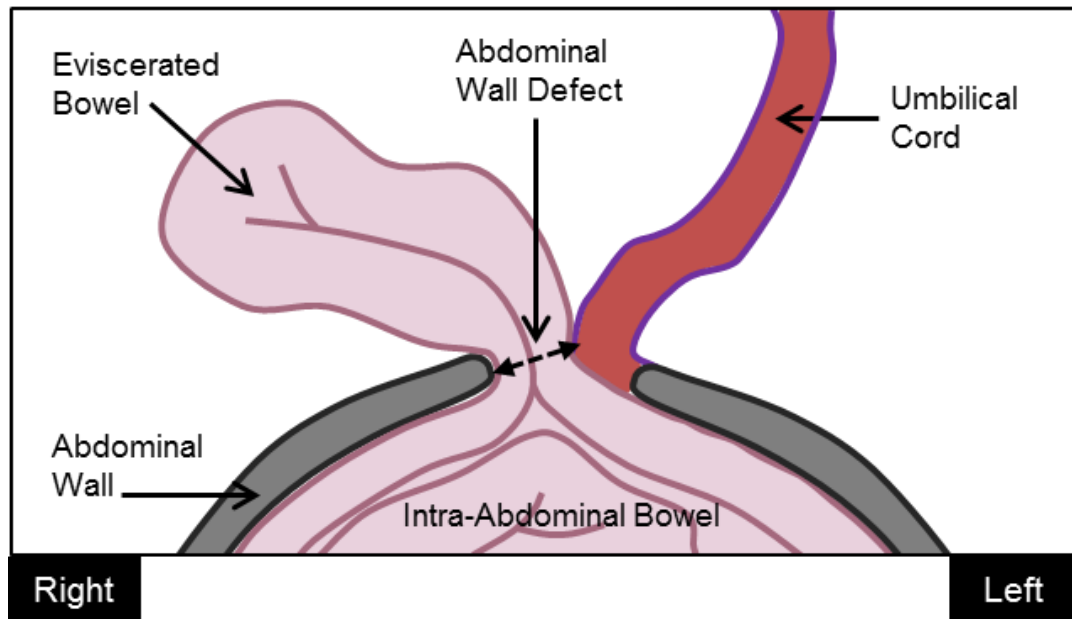


**Figure 1-10:** Schematic illustration of the gastroschisis abdominal wall defect in transverse section.

### 1.6.2 Concomitant Congenital Defects

Gastroschisis is not usually associated with any extra-abdominal congenital malformations, chromosomal or genetic defects. However, concomitant congenital intestinal pathologies occur in 10-15% of gastroschisis infants (Carnaghan et al., 2014, Bradnock et al., 2011, Bergholz et al., 2014) including atresia, stenosis, perforation and necrosis. It is thought these pathologies develop secondary to disruption of the mesenteric vascular supply (Louw and Barnard, 1955) either due to an intrinsic vasoconstrictive/thromboembolic event (Hoyme et al., 1990) or external compression at a tight abdominal wall defect (Carnaghan et al., 2009, Houben et al., 2009). The terms simple and complex gastroschisis are used to delineate between those infants who do and do not have concomitant intestinal pathologies. Simple gastroschisis refers to infants who have otherwise healthy, intact, continuous bowel (includes patients with bowel inflammation), whilst complex gastroschisis refers to patients with compromised (ischaemic or necrotic), non-continuous (atresia or perforated bowel) or narrowed (stenotic) bowel and is associated with higher morbidity and mortality rates (Mousty et al., 2012). In all cases of gastroschisis the bowel is malrotated due to the failed return of the bowel to the abdominal cavity during fetal development. However, individuals affected by gastroschisis are not at

risk of volvulus following corrective surgery due to the significant amount of serosal inflammation and bowel matting present at birth, which prevents free movement of the intestinal loops and therefore rotation around a narrow mesenteric pedicle. Finally, gastroschisis is associated with undescended testes, which occurs in approximately 30-40% of boys with gastroschisis of which 50% will descend spontaneously and the remainder require orchidopexy (Yardley et al., 2012, Lawson and de La Hunt, 2001, Hill and Durham, 2011).

### **1.6.3 Pathogenesis**

The pathogenesis of gastroschisis remains controversial and the point during embryogenesis at which gastroschisis develops is unknown. The earliest routine antenatal ultrasound for pregnant women occurs at 11 to 14 weeks GA when gastroschisis is easily detectable. However, studies have reported gastroschisis to be present concomitantly with physiological herniation (Byrne and Feldkamp, 2008, Tibboel et al., 1986), which would suggest the defect may develop prior to physiological herniation, which develops from 8 weeks GA and resolves by 12 weeks gestation (Sadler and Feldkamp, 2008). Several developmental theories have been suggested (Sadler, 2010) including: (i) regression of the right umbilical vein causing abnormal apoptosis (deVries, 1980); (ii) disruption of the omphalomesenteric artery resulting in necrosis at the umbilical cord insertion (Hoyme et al., 1981); (iii) failure of the ventral lateral folds to fuse in the midline (Duhamel, 1963) secondary to delayed right sided abdominal wall closure (Miller, 1982); (iv) failure of the umbilical cord to attach to the umbilical ring (Rittler et al., 2013); (v) damage and subsequent rupture of the amniotic membrane at the base of the umbilical cord (Shaw, 1975, Bargy and Beaudoin, 2014), and (vi) escape of the yolk sac (Stevenson et al., 2009).

The vascular theories were suggested due to the high association of gastroschisis with concomitant intestinal pathologies (atresia, stenosis, perforation and necrosis). However, the vascular theories suggested are not supported embryologically or anatomically. Firstly, the right umbilical vein transports blood from the placenta to the fetus and does not supply the anterior body wall (Sadler and Rasmussen, 2010). Secondly, the omphalomesenteric artery supplies the yolk sac not the abdominal

wall. Therefore disruption to either of these vessels would be unlikely to cause abnormal apoptosis or necrosis of the abdominal wall. Finally, the abdominal wall is supplied by intersegmental arteries arising from the aorta that anastomose extensively providing a rich blood supply to the abdominal wall (Moore and Dalley, 1999).

Hence, an embryological cause is more likely. Research in chick embryos has shown asymmetry in cell proliferation of the lateral ventral folds with the right side lagging behind the left (Miller, 1982). Additionally, a human embryo study describes the amniotic membrane covering the right side of the umbilical cord base to be thinner than the left and suggests rupture of this thin area during physiological herniation causes gastroschisis (Bargy and Beaudoin, 2014). Hence, the gastroschisis defect may result from failed right lateral fold development, failed umbilical cord insertion or a combination of the two.

#### **1.6.4 Aetiology, Incidence and Risk Factors**

Failed abdominal wall closure in gastroschisis is unlikely to have a single gene aetiology as the defect largely occurs in isolation and is very rarely associated with any defined genetic conditions. Additionally, unlike other congenital abnormalities the incidence of gastroschisis has almost doubled in the UK from 2.5/10,000 live births in 1994 to 4.4/10,000 in 2004 (Kilby, 2006). This increased incidence is not an isolated phenomena to the UK but has also been observed worldwide (Reid et al., 2003, Kirby et al., 2013, Loane et al., 2011, Suita et al., 2000) with marked regional variation (Castilla et al., 2008, Root et al., 2009) and race specific differences (Castilla et al., 2008, Tan et al., 2008) suggesting an environmental contribution is likely. Attention has fallen on a number of factors known to be associated with an increased risk of gastroschisis; namely poor maternal diet, low socioeconomic status, unemployment and maternal smoking (Feldkamp et al., 2011, Lam and Torfs, 2006, Rasmussen and Frias, 2008). To date the strongest epidemiological factor found to be associated with an increased risk of gastroschisis is young maternal age (Gill et al., 2012, Rankin et al., 1999, Tan et al., 1996). Recent studies have also revealed a possible association between maternal peri-conceptual folic acid supplementation and the risk of developing gastroschisis. One study found that omission of maternal

peri-conceptual folic acid supplementation was associated with an increased risk of gastroschisis (David et al., 2014) and another showed that increased duration of peri-conceptual folic acid reduced the risk of gastroschisis (Paranjothy et al., 2012). Drug abuse was hypothesised to be a risk factor due to its vasoactive effects and possible links with intestinal atresia (Hoyme et al., 1990) but a study that performed analysis of hair taken from women with gastroschisis pregnancies has shown that neither smoking nor recreational drug use were significantly associated with gastroschisis incidence after adjusting for maternal age (David et al., 2014).

### **1.6.5 Mortality**

In 1943 the first successful primary surgical gastroschisis closure (full reduction of the abdominal viscera and closure of the abdominal wall defect at the time of birth) was described by Watkins (Watkins, 1943). Prior to this gastroschisis was universally fatal. Although primary abdominal wall closure was possible the mortality rate remained significant and was reported to be as high as 90%. The main causes of death were; (i) failure to achieve primary abdominal wall closure due to viscerio-abdominal disproportion in which the abdominal compartment is too small to accommodate the externalised viscera preventing abdominal closure; (ii) respiratory insufficiencies and abdominal compartment syndrome due to high abdominal pressures secondary to a tight abdominal wall closure or (iii) prolonged gastroschisis-related intestinal dysfunction preventing enteral feeding resulting in malnutrition and death. However, in the late 1960s the mortality rate dramatically dropped for two reasons: (1) the development of a surgical procedure to achieve stage reduction of the externalised viscera into the abdomen followed by abdominal wall closure (Schuster, 1967) and (2) the advent of safe total parenteral nutrition enabling the provision of nutritional requirements intravenously until the infant can achieve full enteral autonomy (Dudrick and Palesty, 2011). Over the past 4 decades the outcome for gastroschisis infants in high-income countries has significantly improved and the mortality rate is currently reported to be between 3-10% of live born gastroschisis neonates (Bradnock et al., 2011, McClellan et al., 2011, Kassa and Lilja, 2011, Skarsgard et al., 2008). Deaths in high-income countries are associated with complex gastroschisis (particularly bowel necrosis), prolonged hospitalisation and long-term parenteral nutrition (PN) resulting in sepsis, liver failure or inability to gain central



venous access for the provision of PN (Erdogan et al., 2012, Bradnock et al., 2011, Rodrigues et al., 2006). However, it is also important to note that low income countries continue to experience high mortality rates of >90% due to the lack of prenatal diagnosis, tertiary centre care and provision of PN (Wesonga et al., 2016).

### **1.6.6 Morbidity**

The focus for gastroschisis clinical management and research in high-income countries has now shifted from reducing mortality to improving infant morbidity. The most frequent gastroschisis-related morbidity is that of intestinal dysfunction resulting in a significant delay in attainment of full enteral feeding and enteral autonomy. A UK national one-year cohort study reported the median time to full enteral feeds in simple gastroschisis was 24 days (range 3->365) (Bradnock et al., 2011) whilst infants with complex gastroschisis it was 47 days (range 30->365) and 50% of gastroschisis infants are categorised as having type 2 intestinal failure requiring >28 days of PN (Bradnock et al., 2011). As such, infants with gastroschisis require prolonged periods of PN, which carries significant risks (van Manen et al., 2013) of sepsis secondary to central line infection (Roberts and Gollow, 1990, Gray et al., 1994), cholestatic liver dysfunction (Jolin-Dahel et al., 2013) and growth restriction. A retrospective study revealed neonates with an abdominal wall defect (gastroschisis or exomphalos) lost on average 0.07 ( $p<0.0001$ ) weight Z-scores per week of PN and 0.08 ( $p<0.001$ ) head circumference Z-scores per week of PN (Carnaghan et al., 2012) (Appendix 2). Protracted hospital stays also carry risks of hospital acquired infections (Sekar, 2010), prevents parental bonding due to separation from the family and places an increased burden on neonatal cots. Additionally, the rising incidence of gastroschisis between 1996 to 2005 increased the cost to the NHS by approximately £11.4 million (Keys et al., 2008).

Otherwise gastroschisis infants rarely exhibit concomitant abnormalities or pathologies and due to the small abdominal wall defect generally do not exhibit signs of pulmonary hypoplasia unlike exomphalos in which a strong association has been shown between increasing exomphalos defect size and severity of pulmonary hypoplasia. A study investigating lung development in a rabbit surgical gastroschisis

model showed no demonstrable effects on lung growth or maturation in the gastroschisis group compared to controls (Biard et al., 2004).

Infants with complex gastroschisis experience the highest level of morbidity. Those who lose significant lengths of bowel for reasons including; (1) in-utero closed gastroschisis (vanishing gastroschisis) resulting in loss of all the externalised bowel prior to birth (Dennison, 2016), (2) bowel necrosis requiring extensive bowel resection or (3) multiple intestinal atresias resulting in significant bowel loss, may never achieve full enteral autonomy and require life-long PN and in some cases a small bowel transplant.

### **1.6.7 Clinical Management of Gastroschisis**

The clinical management of gastroschisis is divided into antenatal and postnatal. Although the treatment principles are universal, antenatal and postnatal management protocols vary between centres. Antenatally the emphasis is on diagnosis, fetal monitoring, identifying fetal distress, counselling and optimising timing and location of delivery. Fetal interventional strategies have been trialled to improve postnatal outcomes for gastroschisis infants but none are used routinely and are covered in section 1.8 Clinical Therapeutic Strategies Trialled in Humans to Improve GRID. Immediate postnatal management addresses cardiorespiratory stabilisation, fluid resuscitation, care of externalised abdominal viscera, gastric decompression and safe transfer to a neonatal intensive care unit (NICU) with paediatric surgical cover. The aims for ongoing care are to return the externalised viscera to the abdomen, close the abdominal wall defect and provide nutritional support until autonomous enteral feeding is achieved.

#### ***1.6.7.1 Antenatal Management of Gastroschisis***

##### ***1.6.7.1.1 Antenatal Diagnosis and Monitoring***

Gastroschisis is usually diagnosed during the 11 to 14 week antenatal dating scan when the bowel loops are seen floating in the amniotic fluid. Elevated levels of alpha fetoprotein in maternal serum are also frequently found during the second trimester

(routinely performed to screen for open spina bifida and trisomy 21) and raises suspicion for gastroschisis (Palomaki et al., 1988, Saller et al., 1994). Following detection of a gastroschisis defect the pregnant woman is referred to a tertiary fetal medicine centre. Gastroschisis fetuses are serially monitored by antenatal ultrasound due to the relatively high risk of intrauterine fetal death (South et al., 2013, Meyer et al., 2015). Usually monitoring occurs at 4-weekly intervals until 30 weeks GA, 2-weekly intervals between 30 and 34 weeks and once weekly after 34 weeks GA. However, there is no formal consensus on antenatal monitoring strategies between fetal medicine centres mainly due to a paucity of evidence associating antenatal sonographic findings with fetal/infant outcomes and in turn management of gastroschisis (Overton et al., 2012, Amin et al., 2018).

Generally ultrasound monitoring encompasses potential causes of intrauterine fetal death including cardiovascular compromise, umbilical cord compression, oligohydramnios, mesenteric vasculature compromise, intrauterine growth restriction and bowel compromise (South et al., 2013). As such, fetal monitoring usually includes; (1) fetal biophysical profile, which entails sonographic assessment of fetal movement, tone, breathing and amniotic fluid index (to detect oligohydramnios and polyhydramnios) and cardiotocography to assess fetal heart rate (nonstress test), (2) fetal growth given gastroschisis neonates are frequently small for GA, (3) umbilical and mesenteric Doppler's, (4) bowel thickness, diameter and appearance and (5) stomach position and diameter (Lepigeon et al., 2014). Oligohydramnios complicates 25% of gastroschisis pregnancies (Towers and Carr, 2008) and on rare occasions of severe oligohydramnios in the preterm period intrapartum amnioinfusion with warmed saline has been performed (Dommergues et al., 1996, Sapin et al., 2000). The aim of the procedure is to restore the amniotic fluid volume, prolonging pregnancy and reduce the risk of bowel damage, umbilical vessel compression, pulmonary hypoplasia and fetal death. Early induction of labour or emergency caesarean section is frequently performed if there is evidence of fetal distress which includes a concerning biophysical profile, severe intrauterine growth restriction (IUGR), poor umbilical or mesenteric Doppler's, an abnormal fetal heart rate trace, severe oligohydramnios or occasionally due to marked bowel dilatation raising concerns of significant and potentially life threatening bowel compromise (Baud et al., 2013, Carnaghan et al., 2016, Carnaghan et al., 2014, Lepigeon et al., 2014).

However, it is important to note that sonographic findings have limitations. IUGR is generally over-estimated in gastroschisis as antenatal estimates of birth weight rely upon ultrasound measurements of fetal abdominal circumference which in gastroschisis fetuses is difficult to measure and frequently inaccurate because of the externalised abdominal viscera (Mirza et al., 2015, Payne et al., 2011). Studies measuring pulsatility and systolic/diastolic ratio in the superior mesenteric artery and its branches and the umbilical artery show no differences in Doppler findings between good and poor infant outcome groups (Abuhamad et al., 1997, Stuber et al., 2016). However, the literature suggests that the presence and degree of bowel dilatation may be predictive of complex gastroschisis (Huh et al., 2010, Houben et al., 2009, Ghionzoli et al., 2012, Nick et al., 2006) and is investigated further in Chapter 9.

Amniotic fluid is known to be pro-inflammatory with elevated neutrophils, mononuclear cells, interleukin-8, interleukin-6, total protein and ferritin levels (Morrison et al., 1998, Burc et al., 2004, Guibourdenche et al., 2006). However, amniocentesis is not routinely performed as currently no specific amniotic fluid biomarker has been robustly identified to inform antenatal management of fetal/infant outcomes and gastroschisis is not usually associated with genetic or chromosomal anomalies (Mastroiacovo et al., 2007, Lepigeon et al., 2014).

Finally, during the antenatal period expectant parents are counselled by a paediatric surgeon who provides information on the gastroschisis diagnosis, the antenatal and neonatal management, potential bowel complications and possible duration of admission for their baby. However, counselling cannot provide an accurate prognostic picture given the lack of antenatal ultrasound/Doppler markers or amniotic fluid biomarkers that accurately predict postnatal gastroschisis outcomes (Overcash et al., 2014).

*1.6.7.1.2 Clinical Observational Study to Determine if Amniotic Fluid, Maternal Blood or Fetal Cord Blood Biomarkers Correlate with Gastroschisis Outcomes*

In order to add to the published literature linking antenatal biomarkers with infant outcomes I performed an antenatal clinical prospective observational study over an 18 month period. The aim was to determine if an amniotic fluid, maternal blood or fetal cord blood biomarker could be identified that predicted postnatal gastroschisis outcomes. The study was designed to recruit 30 normal and 30 gastroschisis pregnancies from University College London Hospital/Great Ormond Street Hospital and King's College Hospital. In both groups the following samples were collected; amniotic fluid at time of induction of labour or caesarean section, maternal blood prior to delivery and fetal cord blood after delivery. The amniotic fluid was to be analysed using ELISA, proteomic biomarker discovery, mass spectrometry and biochemical techniques to measure inflammatory, digestive and biochemical components in amniotic fluid. The maternal and fetal cord blood was to be analysed using biochemical and flow cytometry to identify evidence of inflammation and biochemical components.

Additionally the following was performed within the gastroschisis group only; serial antenatal bowel wall thickness measurements at the time of routine antenatal ultrasound monitoring, a photograph of the externalised bowel taken at the time of delivery to document the macroscopic inflammatory appearance of the bowel, serial collection of stool postnatally to test for inflammatory proteins such as calprotectin and analyse the faecal microbiome and finally collection of prospective antenatal and postnatal clinical outcome data (Table 1-1).

	Control	Gastroschisis
Amniotic fluid	✓	✓
Maternal blood prior to delivery	✓	✓
Fetal cord blood post delivery	✓	✓
Serial measurement of bowel wall thickness by antenatal ultrasound	X	✓
Photograph of externalised bowel at time of delivery	X	✓
Serial postnatal stool collection	X	✓
Collection of clinical data	X	✓

Table 1-1: Specimens collected within the control and gastroschisis study groups.

Potential biomarkers were then to be correlated with neonatal outcomes. Time to full enteral feeds was the primary outcome measure and used as a surrogate measure for postnatal gut function. Although previous studies have examined the amniotic fluid profile in gastroschisis, there have been limited attempts to correlate with postnatal outcomes, and as such there was no data on which to base a power calculation therefore this was to be a pilot study. During the 18 month period, 22 gastroschisis patients were seen in the study hospitals fetal medicine departments (11 University College Hospital London, 11 King's College Hospital) and although 11 patients consented to the study it was only possible to collect specimens in 3 patients due to 6 spontaneous deliveries preventing sample collection, 1 patient withdrew consent and 1 fetal death at 34 weeks (Table 1-2). Unfortunately due to this low number of collected gastroschisis samples it was not possible to complete the study and the data is not further discussed in this document.

	University College London Hospital	King's College Hospital
Total number of gastroschisis pregnancies	11	11
Consent for study given	3	8
Specimens successfully collected	2	1
Early spontaneous delivery	0	6
Withdrew consent	0	1
Fetal death	1	0

**Table 1-2:** Breakdown of gastroschisis patient recruitment at University College London Hospital and King's College Hospital fetal medicine centres.

#### 1.6.7.1.3 *Timing and Mode of Delivery*

Following reports suggesting in-utero loss of fetuses with gastroschisis can occur in the late term period (>39 weeks GA) (Burge and Ade-Ajayi, 1997, Crawford et al., 1992) gastroschisis fetuses are usually planned to be delivered no later than 37 to 38 weeks GA (Baud et al., 2013, Carnaghan et al., 2014, Lepigeon et al., 2014).

Previously, the mode of delivery has been a contentious issue with fears that vaginal delivery may cause trauma or ischaemia to the externalised bowel and exposure to vaginal bacterial flora may also be detrimental to the eviscerated unprotected bowel. However, multiple studies have shown no association between mode of delivery and neonatal outcome suggesting vaginal delivery to be safe (Abdel-Latif et al., 2008, How et al., 2000, Salihu et al., 2004). Therefore gastroschisis fetuses are routinely delivered vaginally by induction of labour at 37 to 38 weeks GA unless fetal or maternal concerns necessitate earlier delivery and/or delivery by caesarean section. Routinely inducing pregnancies before the due date provides the additional benefit of controlling the location of the birth enabling delivery to occur in a tertiary centre with paediatric surgical cover preventing the need for inter-hospital transfer, which

may have a detrimental effect on neonatal outcomes (Dalton et al., 2016). However, frequently women with gastroschisis pregnancies develop spontaneous labour prior to 37 weeks GA likely due to the pro-inflammatory amniotic fluid environment (Morrison et al., 1998) associated with gastroschisis and therefore the place of delivery cannot always be controlled. At the time of induction or onset of labour the perinatal team informs the neonatologist and the paediatric surgeons of the impending birth. Delivery of a gastroschisis fetus is considered a high risk birth requiring the neonatal team to be present throughout the latter stages of labour.

### ***1.6.7.2 Neonatal and Surgical Management of Gastroschisis***

#### ***1.6.7.2.1 Immediate Postnatal Management***

Following delivery the gastroschisis neonate is assessed (as per Advance Paediatric Life Support protocols) and stabilised on the labour ward by the neonatal team. If respiratory support is required then endotracheal intubation is performed early to avoid prolonged bag-mask ventilation and prevent over distension of the stomach and bowel. A nasogastric tube (NGT) is placed and left on free drainage to aid decompression of the bowel. Inspection of the bowel is performed to identify areas of discoloration suggestive of vascular compromise to the bowel. Simple manoeuvres to straighten the bowel and remove kinking of the vascular pedicle are performed to improve the blood supply. The bowel is placed centrally on the abdomen, supported by a doughnut ring made from wet gauze and wrapped in position using non-sterile transparent cling film, which maintains the position of the bowel, reduces fluid loss, helps maintain body temperature and enables direct visualisation of the bowel. The bowel is checked regularly for signs of ischaemia and if required the cling film is repositioned to aid bowel perfusion and an urgent surgical review obtained. Venous access is obtained and blood taken for cultures and routine surgical tests (full blood count, blood group and cross-match, biochemistry, venous gas and clotting). Externalised viscera results in significant serous fluid loss and therefore fluid resuscitation is commenced in the form of bolus, maintenance and replacement fluids as per hospital policy. IV antibiotics are initiated as per local hospital policy. When stable the neonate is transferred to the NICU or transported by ambulance to another hospital with paediatric surgical cover.



### ***1.6.7.3 Surgical Management***

The surgical review is usually carried out on admission to NICU unless there are concerns regarding the vascular supply to the bowel in which case the neonate is reviewed on the labour ward. The neonate is examined to assess the vascular condition of the bowel, presence of concomitant structural intestinal pathologies, degree of bowel wall inflammation, the size of the defect ring and presence of extra-gastrointestinal malformations. This assessment identifies those neonates who require urgent surgery due to compromised vascular supply to the bowel and informs the most appropriate method for reducing the externalised viscera into the abdomen and subsequent closure of the abdominal wall defect.

Neonates with ischaemic bowel in whom perfusion fails to improve with simple bowel repositioning require urgent surgical intervention. Ischaemia can be caused by mesenteric compression at a small defect ring also known as ‘closing gastroschisis’ (Houben et al., 2009) requiring immediate widening of the defect to prevent necrosis of the bowel. The procedure is performed on NICU under local anaesthetic and involves a horizontal full thickness incision at the 9 o’clock position following which the bowel is observed for vascular improvement. If necrotic bowel is present then urgent bowel resection is required.

The method by which the abdominal viscera are routinely returned to the abdominal cavity and the abdominal wall subsequently closed is an area of controversy. Closure methods include bedside or surgical, primary or delayed closure. Surgical centres and individual surgeons usually have a preferred method of closure and initiate this within 24 hours of the neonate’s birth. Deviation from this preferred method may occur if there is evidence of concomitant intestinal pathologies requiring urgent surgery or there is significant viscerο-abdominal disproportion preventing primary closure of the abdominal wall defect (Stanger et al., 2014).

Primary closure is immediate reduction of the viscera and repair of the defect within 24 hours of birth. Primary closure is conventionally performed under general anaesthesia with the fascial (connective tissue) edges of the defect being closed using sutures or on occasions with the aid of a prosthetic patch. If reduction of the viscera

into the abdomen is not possible then a custom made silo is fashioned using silicone sheeting or a saline infusion bag and sutured to the fascial edges. Over a series of 7 to 14 days the viscera are reduced into the abdomen by decreasing the volume of the silo. Once the viscera are fully reduced secondary fascial closure of the abdominal wall is performed under general anaesthetic. Other techniques have been developed, which achieve visceral reduction and abdominal wall closure without anaesthesia. Primary closure can be performed at the cotside in selected infants with gentle manual reduction of the viscera and abdominal wall closure achieved by covering the defect with the umbilical cord securing the cord in place using Steri Strips, glue and/or Tegaderm (plastic closure). Delayed secondary closure can be achieved at the cotside using a preformed silo, which is a silicone bag with a spring-loaded opening. The externalised viscera are gently placed into the silo and the spring-loaded opening manoeuvred through the defect where it rests on the inside of the abdominal wall providing traction for the silo to be reduced in volume as previously described. Secondary closure is then performed either at the cotside with a plastic closure or under general anaesthetic with a fascial sutured closure. Studies have shown that the use of a preformed silo reduces the need for ventilation. However, the method of visceral reduction and abdominal wall closure has no impact on the infant mortality or morbidity including time to full enteral feeds (ENT) and length of hospital stay (LOS) (Charlesworth et al., 2014, Kunz et al., 2013).

#### *1.6.7.3.1 Post-Procedure Management*

Post-procedure the neonate is at risk of respiratory embarrassment, abdominal compartment syndrome and ongoing fluid loss. Abdominal wall closure (primary or secondary) under tension can result in diaphragmatic splinting and respiratory compromise requiring a period of paralysis and ventilation post procedure. Equally some neonates with small abdominal girth undergoing staged silo reduction will also require a period of paralysis to aid return of the viscera into the abdomen. All neonates require monitoring for signs of abdominal compartment syndrome, which can occur following abdominal closure or silo reduction due to reduction of externalised viscera into a small non-compliant abdomen (viscero-abdominal disproportion) resulting in increased abdominal pressure. Raised intra-abdominal pressure can compress and impede the mesenteric blood flow resulting in bowel

ischaemia and ultimately bowel necrosis (Stanger et al., 2014). Additionally, it can cause compression of other major vessels leading to renal impairment or lower limb ischaemia. Treatment involves abdominal decompression in the form of reopening a closed abdominal wall followed by application of a silo or releasing tension on a silo that is already present. Fluid management can be complex due a number of insensible fluid losses including; evaporative losses secondary to prolonged exposure of the bowel serosa during abdominal wall closure or silo application, continued third space intra-abdominal or intra-silo fluid loss post-procedure and large bilious NGT aspirates or vomiting due to post-procedure bowel ileus and gastroschisis-related intestinal dysfunction. Fluid management may be further hampered by impaired monitoring due to decreased urine output secondary to raised intra-abdominal pressure.

#### *1.6.7.3.2 Nutritional Management*

Gastroschisis-related intestinal dysfunction is a very frequent problem for gastroschisis infants and refers to prolonged intestinal dysmotility resulting in large volume bilious NGT aspirates, bilious vomiting, lack of stooling and the inability to tolerate enteral feeding. Infants require alternative nutritional and fluid support until full enteral feeding is attained, which can take weeks sometimes months to achieve. The infant's nutritional and baseline fluid requirements are met through the administration of parenteral nutrition (PN) via central venous access (usually a longline). Gastric losses in the form of NGT aspirates and vomits are replaced millilitre for millilitre with 0.9% normal saline with added potassium chloride to ensure hydration and electrolyte balance. Initially the infant is kept nil by mouth until the gastric losses become minimal and non-bile stained suggesting improved gut motility enabling small volume enteral feeds to be introduced via the NGT. Enteral feed volumes are slowly increased over several days, weeks or sometimes months. Often increasing the volume of feed results in bilious vomiting requiring the feed volume to be reduced and maintained for a few days at a lower volume before being increased again. During this period the volume of PN is titrated against the volume of enteral intake. The protocol for increasing feed volumes varies between centres and is dependent on local policies and surgeon/neonatology preference. If enteral feeding cannot be initiated within 6 weeks investigations for atresia or stenosis should be

undertaken. Careful management of the central venous access is essential to reduce the risk of infection and preserve access sites, which is particularly important for infants with prolonged gut dysmotility who may require long-term or life-long PN.

#### *1.6.7.3.3 Implications of Complex Gastroschisis*

Complex gastroschisis is associated with increased mortality and morbidity with an increased risk of; prolonged gastroschisis-related intestinal dysfunction, home PN, longer hospital stay, sepsis, short bowel syndrome and necrotizing enterocolitis (Bergholz et al., 2014). Neonates who require an extensive bowel resection for necrosis or multiple atresias are at significant risk of developing short bowel syndrome, which is a malabsorption disorder secondary to insufficient small bowel absorptive surface area. These neonates are reliant on life-long PN in order to meet their nutritional needs and may require complex surgery including a bowel transplant. The identification of reliable antenatal ultrasound markers to detect complex gastroschisis would provide a more accurate prognostic picture, guide antenatal counselling and inform antenatal and postnatal management (Overcash et al., 2014).

### **1.7 Current Understanding of Gastroschisis-Related Intestinal Dysfunction**

Gastroschisis-related intestinal dysfunction (GRID) is a temporary gut dysmotility disorder, which causes significant infant morbidity. At birth bilious vomiting and vomiting after feeds indicates a functional bowel obstruction that is hypothesised to be secondary to dysmotility affecting both peristalsis and the MMC, although, gut motility studies have never been formally investigated clinically in gastroschisis infants to confirm this hypothesis. However, with time normal feeding is eventually established in most cases of gastroschisis allowing the infant to live a normal life. Infants with complex gastroschisis are more likely to experience prolonged GRID and in some cases may never attain full enteral autonomy. The mechanism(s) underpinning GRID remain poorly understood. As such, there have been no advances in developing a therapy that will reduce the severity of GRID and in turn improve gut function. Therefore, this is an area of significant research interest and if a therapy

that improves gut function were to be developed it would considerably improve gastroschisis outcomes.

### **1.7.1 Gastroschisis versus Exomphalos: Gut Function and Anatomy**

Gastroschisis and exomphalos have important differences in postnatal intestinal function and anatomical features. Gastroschisis is associated with significant postnatal intestinal dysfunction and 10-15% of neonates are classed as complex due to concomitant bowel pathology (Carnaghan et al., 2014, Bradnock et al., 2011). Whereas exomphalos neonates usually have normal intestinal function and concomitant bowel pathology is rare (Vachharajani et al., 2009). Important anatomical differences between gastroschisis and exomphalos include; presence or absence of a protective membranous sac over the externalised viscera, the size of the abdominal wall defect and presence or absence of liver herniation. In gastroschisis the externalised bowel has no membrane coverage and lies in direct contact with the amniotic fluid, the defect is usually small approximately 1 to 2cm wide and the liver is very rarely externalised. In exomphalos the herniated bowel is contained within the amniotic membrane at the base of the umbilical cord protecting the bowel from the amniotic fluid. Additionally, the size of the exomphalos defect can range in size from a minor (<5 cm but still larger than usually seen in gastroschisis) defect with no liver herniation to a major (>5 cm) defect with extensive liver herniation (Carnaghan et al., 2009, Groves et al., 2006). Given these differences it has been hypothesised that in gastroschisis the abnormal exposure of the bowel serosal surface to amniotic fluid during fetal development (Tibboel et al., 1986) or compression/constriction of the bowel as it herniates through the tight ventral wall defect (Shah et al., 2012, Langer et al., 1989) could be the cause of GRID.

### **1.7.2 Gastroschisis Antenatal Bowel Morphological Changes and Amniotic Fluid Composition**

An observational study mapped the antenatal morphological changes of gastroschisis bowel from 26 human embryos and fetuses exhibiting gastroschisis ranging from approximately 8 weeks GA to full term. The study revealed that although the defect occurs early, progressive changes to the bowel wall only occurred after the 30th

week of gestation consisting of bowel wall inflammation and progressive fibrosis (Tibboel et al., 1986). These findings correspond with the significant changes in amniotic fluid composition that occur in the third trimester (as previously described) including increases in urea, creatinine, bile acids, enteric enzymes and IL-8 and reduction in sodium, chloride and osmolality (Underwood et al., 2005). Therefore, the development of bowel inflammation from 30 weeks gestation could be due to the accumulation of potentially noxious substance in the amniotic fluid during the third trimester to which the bowel is directly exposed.

### **1.7.3 Amniotic Fluid and Fetal Inflammatory Markers**

The morphological changes described by Tibboel et al. suggest an inflammatory process is associated with gastroschisis. Two studies have demonstrated the amniotic fluid in gastroschisis pregnancies to be in a pro-inflammatory state. The first collected amniotic fluid at the time of caesarean section from 10 pregnant women with a gastroschisis fetus and 10 pregnant women with a healthy fetus. Within the gastroschisis cohort there was an elevation in neutrophils, mononuclear cells and interleukin-8 (pro-inflammatory cytokine) compared to the healthy controls (Morrison et al., 1998). In addition, the CD15 mononuclear cell population was found to exhibit markedly elevated CD11b markers revealing these cells to be in an activated state (Morrison et al., 1998). The second study compared amniotic fluid specimens collected by amniocentesis for karyotyping between 15 and 32 weeks GA from 41 women with gastroschisis fetuses and 93 age-matched controls. This study revealed elevation of amniotic total protein, IL-6, IL-8 and ferritin levels with significantly higher amniotic fluid cell counts in gastroschisis pregnancies compared to controls (Guibourdenche et al., 2006). Finally, another study investigated the presence of systemic fetal inflammation through comparison of fetal cord blood lymphocytes collected from 21 gastroschisis pregnancies and 20 healthy controls. This study revealed gastroschisis fetal cord blood to have significantly higher numbers of effector memory CD8 and CD4 T-cells and terminally differentiated effector memory CD8 T-cells compared to controls, indicating the presence of T-cell activation (Frascoli et al., 2013). These studies suggest that inflammation could be involved in the pathophysiology of GRID.

#### 1.7.4 Bowel Wall Thickening

As described by Tibboel et al., 1986, at birth gastroschisis bowel frequently appears thickened and inflamed. Surgical animal models of gastroschisis including chick (Api et al., 2001, Olguner et al., 2006, Yu et al., 2004), rat (Correia-Pinto et al., 2002, Hakguder et al., 2011, Bittencourt et al., 2006), rabbit (Guo et al., 1995) and lamb (Srinathan et al., 1995) have demonstrated increased thickening of the bowel wall including serosal and smooth muscle layers of gastroschisis bowel compared to controls (Table 1-3). Manipulation of the amniotic fluid inflammatory environment in these surgical models has led to altering degrees of bowel wall thickening. Intra-amniotic administration of meconium, which contains numerous products from the digestive tract including IL-8 a neutrophil chemotaxin (de Beaufort et al., 1998), in chick and rat surgical gastroschisis models revealed an increase in bowel wall thickness (Api et al., 2001, Correia-Pinto et al., 2002). Dilution of meconium through induction of fetal diuresis by intra-amniotic injection of furosemide in a rat surgical gastroschisis model (Hakguder et al., 2011) showed reduction in serosal thickening. Additionally, reduction of in-utero inflammation by intra-amniotic injection of urine trypsin inhibitor (an IL-8 inhibitor) in a chick surgical model (Olguner et al., 2006) and intra-amniotic dexamethasone in chick and rabbit surgical gastroschisis models has shown a reduction in gastroschisis bowel wall thickness (Yu et al., 2004, Guo et al., 1995). These data suggest that remodelling of bowel smooth muscle and serosa resulting in bowel wall thickening may be induced by inflammation. Furthermore, increased levels of transforming growth factor-beta 3 (TGF- $\beta$ 3), which is known to cause organ dysfunction through alterations in smooth muscle, have been found in human gastroschisis gut compared to controls (Moore-Olufemi et al., 2015) and may be a mediator of gastroschisis bowel wall thickening.

Study	Animal	Surgical or Genetic	In-Utero Intervention	Tissue Type, Timing of Collection	Bowel Wall Layers Assessed	Number per Group	Blinded	GS Bowel Wall Compared to Controls
Api et al., 2001	Chick	Surgical (created at 5 dpc)	-GS + varying concentrations of meconium suspensions (1:200, 1:400, 1:600, 1:800) injected into AF	-Random small intestine -Eviscerated bowel in GS -18 dpc	-Serosa -Measured histologically	-10 control -10 GS for all meconium concentration groups	Yes	-GS + 1:200 and 1:400 meconium groups: serosal thickening -GS + 1:600 and 1:800 meconium groups: serosa same as controls
Olguner et al., 2006	Chick	Surgical (created at 5 dpc)	-GS + 1:400 meconium suspension and varying concentrations of urinary trypsin inhibitor (UTI, 50, 100 and 200 U/ml) injected into AF	-Random small intestine -Eviscerated bowel in GS -18 dpc	-Serosa -Measured histologically	-10 control -10 GS for all meconium + UTI concentration groups	Yes	-GS + meconium + 50 U/ml UTI: Increased serosal thickening compared to controls -GS + meconium + 100 U/ml and 200 U/ml UTI groups: serosa same as controls
Yu et al., 2004	Chick	Surgical (created at 15 dpc)	-GS + saline or dexamethasone injected into the AF	-Random small intestine -Eviscerated and non-eviscerated bowel in GS -19 dpc	-Entire bowel wall and all bowel wall layers -Visual histological comparison	-15 sham -20 GS -17 GS + saline -17 GS + dexamethasone	No	-GS and GS + saline groups: entire bowel wall and all bowel wall layers thickened compared to controls -GS + dexamethasone: entire bowel wall and all bowel wall layers less thickened compared to GS and saline groups
Correia-Pinto et al., 2002	Rat	Surgical (created at 18.5 dpc)	-GS + Anal ligation (to reduce AF meconium) -GS + colon perforation (to increase AF meconium)	-Random small intestine -Eviscerated bowel in GS -21.5 dpc	-Entire bowel wall -Visual histological comparison	-11 control (sham) -10 GS -7 GS + anal ligation -9 GS + colon perf	Yes	-GS: bowel wall thickened compared to controls -GS + colonic perforation: bowel wall thickened more so than GS alone -GS + anal ligation: no bowel wall thickening compared to controls



Study	Animal	Surgical or Genetic	In-Utero Intervention	Tissue Type, Timing of Collection	Bowel Wall Layers Assessed	Number per Group	Blinded	GS Bowel Wall Compared to Controls
Hakguder et al., 2011	Rat	Surgical (created at 18.5 dpc)	-GS + intra-amniotic furosemide injection	-Random small intestine -Eviscerated bowel in GS -21.5 dpc	-Serosa -Measured histologically	-4 control -5 sham -6 GS -6 GS + furosemide	Yes	-GS: serosal thickness significantly thicker than control and sham groups -GS + furosemide: serosal thickness significantly lower than GS group
Bittencourt et al., 2006	Rat	Surgical (created at 18.5 dpc)	-GS + sterile water or dexamethasone maternal intraperitoneal injection	-Distal jejunum or proximal ileum -Eviscerated bowel in GS -21.5 dpc	-Entire bowel wall and all bowel wall layers -Measured histologically	-45 control -45 sham -20 GS + sterile water -20 GS + dexamethasone	Yes	-GS + water: entire bowel wall and all layers (submucosa, smooth muscle and serosa) thickened compared to controls -GS + dexamethasone: Bowel wall layers thickened as above no reduction in thickness secondary to dexamethasone
Guo et al., 1995	Rabbit	Surgical (created at 24 dpc)	-GS + dexamethasone maternal intraperitoneal injection	-Distal small intestine -Eviscerated bowel in GS -31 dpc	-Entire bowel wall and all bowel wall layers -Visual histological comparison	-10 GS -10 GS + dexamethasone		-GS: bowel wall oedema, thickened smooth muscle and submucosa, villus blunting, -GS + dexamethasone: Reduction in oedema, thinner smooth muscle and submucosa, preservation of villous architecture compared to GS only group
Srinathan et al., 1995	Lambs	Surgical (created at 80 dpc)	-GS + bowel constriction to mimic relative size of abdominal wall defect present in humans	-Random small intestine -Eviscerated bowel in GS -100 and 135 dpc	-Smooth muscle thickness, cell number, cell size and cell proliferation -Submucosal thickness -Quantitative assessment of cell numbers -Bowel measured histologically	-2 control (sham) at 100 dpc -2 control (sham) at 135 dpc -2 GS + constriction at 100dpc -2 GS + constriction at 135 dpc	Yes	-GS at 100dpc: increased smooth muscle cell numbers (hyperplasia) -GS at 135 dpc: same number of smooth muscle cells as control. Significant thickening of circular and longitudinal muscle layers (hypertrophy)

**Table 1-3:** Summary of bowel wall morphology findings within animal gastroschisis models. GS = gastroschisis, AF = amniotic fluid.

### **1.7.5 Deficiency of the Interstitial Cells of Cajal**

Investigations in animal gastroschisis models and resected human gut specimens have also implicated deficiency of the bowel wall interstitial cells of Cajal (ICC) as the cause of GRID, which could form the target for an antenatal therapy.

Animal studies in chick (Vargun et al., 2007), rat (Auber et al., 2013, Midrio et al., 2004), and lamb (Krebs et al., 2014) surgical gastroschisis models and also the aortic carboxypeptidase-like protein (ACLP) knockout genetic gastroschisis mouse model (Danzer et al., 2010) have suggested architecturally immature and reduced number of bowel wall ICC are present in gastroschisis (Table 1-4). Additionally, two studies (Auber et al., 2013, Danzer et al., 2010) compared both eviscerated and non-eviscerated gastroschisis fetal bowel with control fetal bowel. Both studies reported the eviscerated small bowel to exhibit architecturally immature and reduced number of ICC compared to controls, whilst the non-eviscerated bowel exhibited the same architecture and ICC numbers as that of controls. Suggesting ICC development is only impaired in the eviscerated bowel of gastroschisis.

Study	Animal	Surgical or Genetic	In-Utero Intervention	Tissue Type, Timing of Collection	ICC Identification Method	Number per Group	Blinded	Quantification Method	GS ICC Architecture and Numbers Compared to Controls
Vargun et al., 2007	Chick	Surgical (created at 13 dpc)	-GS + Amniotic exchange -GS + Bicarbonate infusion	-Random small intestine -Eviscerated bowel in GS -18 dpc	-Cross sectioned tissue -IHC Anti-CD117	-10 control -8 GS -9 exchange -8 bicarb	Yes	-Architecture: qualitative description -Cell numbers: counted per field of view, randomly orientated tissue	Normal architecture all groups ICC number: -GS group: reduced -GS + bicarb: reduced -GS + exchange: same as controls
Midrio et al., 2004	Rat	Surgical (created at 18.5 dpc)	None	-Random small intestine -Eviscerated bowel in GS -18.5 dpc (control only) -21.5 dpc	-Cross sectioned tissue -IHC Anti-CD117 -Transmission electron microscopy	-10 control (18.5 dpc) -5 Sham (21.5 dpc) -10 GS (21.5 dpc)	No	-Architecture: qualitative description -Cell numbers: qualitative description	GS: ICC architecturally immature and similar to that of control bowel at 18.5 dpc GS: ICC numbers reduced
Auber et al., 2013	Rat	Surgical (created at 18 dpc)	None	-Random small intestine -Eviscerated and non-eviscerated bowel in GS -22 dpc	-Cross sectioned tissue -IHC Anti-CD117	-9 control -22 Sham -11 GS	Yes	-Architecture: qualitative description -Cell numbers: Semi-quantitative scoring, randomly orientated tissue	Eviscerated GS: ICC architecturally immature and reduced in number Non-eviscerated GS: ICC normal architecture and number
Krebs et al., 2014	Sheep	Surgical (created at 77 dpc)	-GS + partial bowel coverage -GS + full bowel coverage	-Random small intestine -Eviscerated bowel in GS -135 dpc	-Cross sectioned tissue -IHC Anti-CD117	-3 control -11 GS -5 GS partial coverage -2 GS full coverage	Yes	-Architecture: not done -Cell numbers: Semi-quantitative scoring, randomly orientated tissue	ICC number: -GS: reduced -GS + partial coverage: reduced -GS + complete coverage: normal
Danzer et al., 2010	Mouse	Genetic (ACLP)	None	-Random small intestine -Eviscerated and non-eviscerated bowel in GS -18.5 dpc	-Cross sectioned tissue -IHC Anti-CD117	-6 control -6 GS	Yes	-Architecture: qualitative description -Cell numbers: Semi-quantitative scoring, randomly orientated tissue	Eviscerated GS: ICC architecturally immature and reduced in number Non-eviscerated GS: ICC normal

**Table 1-4:** Summary of ICC findings within animal gastroschisis models. GS = gastroschisis, IHC = immunohistochemistry.

Fetal interventions to try and improve ICC development have been trialled in animal models (Table 1-4). Vargun et al., 2007 investigated whether fetal intervention with amnio-allantoic exchange or bicarbonate infusion in a chick surgical gastroschisis model would improve ICC development. The aim of amnio-allantoic exchange was to remove and replace the potentially noxious amniotic fluid and the bicarbonate infusion to buffer the amniotic fluid preventing the normal function of any enzymes that may be present in the amniotic fluid from intestinal waste products. This study showed there was still a significant reduction in ICC numbers in the bicarbonate infusion group compared to controls but no significant difference in ICC numbers in the amnio-allantoic exchange group compared to controls. Suggesting amnio-allantoic exchange lessens the noxious effect of amniotic fluid on the exposed bowel improving ICC development. Also, Krebs et al., 2014 attempted to cover the externalised bowel in-utero in surgically created gastroschisis lamb fetuses in order to protect the bowel from amniotic fluid exposure. The procedure achieved full coverage in 2 gastroschisis lambs and partial coverage in 5 gastroschisis lambs. However, none of the coverings remained in place until the end of pregnancy due to dislocation during late pregnancy. Even so the paper reported in the full coverage group the number of ICC to be the same as controls. However, there was a reduction in ICC numbers compared to controls in the partial coverage group. These results suggest that direct exposure of the bowel wall to amniotic fluid may be the cause of ICC deficiency but given the small numbers in each group little more can be interrupted from the results.

It is important to note that all these animal studies have methodological limitations. The studies used tissue from randomly selected sections of small intestine (eviscerated small intestine in gastroschisis fetuses), which therefore may include a mixture of jejunum and ileum and may not be directly comparable. Cross-sectioned bowel was used in all the studies but given the small stature of the experimental animals used the bowel was equally very small and on assessment of the published images of the cross-sectioned tissue it is very difficult to identify ICC cell bodies or discern the ICC branching architecture. Therefore based on these images it appears difficult to accurately assess ICC architecture or robustly quantify cell numbers using this tissue preparation method. All but one paper performed either semi-quantitative (e.g. cell grading system of sparse: 0-2 cells, few: 3-7 cells, moderate: 8-12 cells and

many: >12 cells (Danzer et al., 2010)) or qualitative (e.g. cell grading system of 1 for mature, 2 for moderately mature and 3 for very mature (Auber et al., 2013)) methods for quantifying ICC (which could result in bias) instead of a robust quantitative method. Also, the field of views used to quantify cells from were randomly oriented thereby including a varying area of bowel wall within each image. Due to these limitations the results of these studies need to be interpreted with caution

Within the human literature there are 2 published studies investigating ICC development in gastroschisis infants. The first study (Midrio et al., 2008) qualitatively analysed ICC at two time points in a single case of human gastroschisis. The first was at birth following bowel resection and stoma formation for bowel necrosis and the second at one month of age when partial enteral feeding was tolerated enabling stoma closure. At birth the ICC were described to be decreased in number and immature. However, at one month the ICC were observed to have formed groups and many were differentiated (Midrio et al., 2008) implying ICC numbers and function recovered over time. Finally, during the experimental period of this PhD thesis a larger human archival gastroschisis gut study was published (Zani-Ruttenstock et al., 2015). Bowel specimens were analysed using a quantitative method from 12 gastroschisis patients that had stoma formation (time point 1) and then stoma reversal (time point 2). ICC numbers were compared against non-gastroschisis infants who had stoma formation for necrotising enterocolitis, ileal atresia and malrotation/volvulus. The authors showed that there was no difference in ICC numbers between gastroschisis and controls at time point 1 but there were significantly more ICC in the control group at time point 2. Concluding within the gastroschisis group, that there was no ICC improvement or recovery during the study period and ICC modulation may be beneficial in the treatment of GRID.

These studies also have limitations, which are; inclusion of resection margins with severely inflamed abnormal tissue due to inclusion of conditions such as necrotising enterocolitis or stoma reversal which could adversely affect ICC numbers giving spurious results, quantification from randomly orientated fields of view thereby including a varying area of bowel wall within each image and in the first study a qualitative ICC assessment with no comparison to control bowel.

Finally, anti-CD117 (antibody to the c-Kit receptor tyrosine kinase present on ICC) was used in all the studies and is the most commonly used marker for ICC histological assessment. However, this only provides evidence of the presence of c-Kit receptor tyrosine kinase and the absence or fluctuations in staining doesn't prove absence of the cell. The most robust way of analysing the presence and architecture of ICC is by electron microscopy (Tamada and Kiyama, 2015), which although provides highly detailed images is an expensive, time consuming and difficult method of microscopy and is infrequently used. One of the above animal studies (Midrio et al., 2004) also used electron microscopy for the qualitative assessment of ICC in eviscerated gastroschisis bowel. This study reported that in the less-damaged gastroschisis bowel loops some cells with features that resembled ICC were identified on electron microscopy but in the more damaged gastroschisis bowel loops no cells with features of ICC could be recognised confirming ICC deficiency may be the cause of GRID.

#### **1.7.6 ICC Plasticity and Response to Inflammation**

Studies have shown ICC to exhibit inherent plasticity resulting in phenotypic change and loss of function under certain unfavourable conditions. For example, in one study (Torihashi et al., 1999) blockade of Kit receptors resulted in ICC loss which was not accounted for by apoptosis assays but analysis with electron microscopy revealed remaining ICC had developed features of smooth-muscle cells.

Additionally, loss of ICC have been reported in inflammatory bowel conditions including inflammatory bowel disease and necrotising enterocolitis (Burns, 2007) suggesting ICC phenotypic change occurs secondary to inflammation. Furthermore, another study has shown that ICC regenerate following removal of unfavourable conditions. This study induced gut inflammation in adult mice with *Trichinella spiralis* which led to damaged ICC processes between cells and desynchronous electrical activity at 1–15 days post infection. However, after 60 days and resolution of gut inflammation the ICC architecture and electrical signals returned to normal (Der et al., 2000). This research shows that bowel inflammation can result in phenotypic change of ICC and loss of function and this could be the mechanism underpinning GRID and a potential antenatal therapeutic target.

## **1.8 Clinical Therapeutic Strategies Trialled in Humans to Improve GRID**

### **1.8.1 Amnioexchange**

Amnioexchange was proposed as a method for diluting and removing potentially harmful biochemical and inflammatory products from the third trimester amniotic fluid of gastroschisis pregnancies. Animal experiments have reported potentially beneficial effects on bowel wall development following amnioexchange. In chick (Vargun et al., 2007, Sencan et al., 2002, Aktug et al., 1998a, Aktug et al., 1998b) and rabbit (Ashrafi et al., 2008) surgical gastroschisis models, improvements in the appearance of macroscopic intestinal damage (peal, matting and adhesions between bowel loops), microscopic bowel wall thickness and ICC numbers have been reported. Whilst dilution of the amniotic fluid through diuresis stimulated by furosemide in a rat surgical model of gastroschisis has also shown reduced serosal thickness (Hakguder et al., 2011).

In humans amnioexchange involves the removal of amniotic fluid by amniocentesis and replacement of the fluid with warm normal saline on a weekly or twice weekly basis during the third trimester. Studies have reported mixed results with some showing a benefit in neonatal outcomes including shorter time to full enteral feeds and length of hospital stay (Luton et al., 1999, Luton et al., 2003) and others showing no improvement in neonatal outcomes or change in the biochemical or inflammatory status of the amniotic fluid (Midrio et al., 2007). This is likely due to the rapid 24 hour turnover of amniotic fluid (Underwood et al., 2005). A randomised controlled trial investigating the effect of amnioexchange was undertaken in France. The preliminary results were reported at the 11<sup>th</sup> World Congress in Fetal Medicine, 2012, which concluded that so far the results showed no clinical improvement with amnioexchange and the procedure may be associated with an increased risk of stillbirth (Khalil, 2012). The study was later stopped prior to completion due to clinically significant iatrogenic complications including infections and increased rate of intra-uterine death. However, the final outcome results of the study are yet to be published.

A similar procedure called amnioinfusion has also been suggested, whereby warmed saline is instilled via amniocentesis to increase the amniotic fluid volume and reduce the concentration of potentially noxious substances. However, animal research investigating infusion of saline or sterile water has shown no improvement in bowel wall development (Bittencourt et al., 2006, Yu et al., 2004). Additionally, in the general population clinical studies have been performed to investigate the use of serial amnioinfusion in cases of preterm premature rupture of membranes with severe oligohydramnios but safety and efficacy data for this intervention is still lacking (Van Teeffelen et al., 2013). As such, amnioinfusion is not performed routinely in gastroschisis pregnancies and is only performed on rare occasions in the presence of preterm severe oligohydramnios in an attempt to prevent fetal distress and death (Sapin et al., 2000, Dommergues et al., 1996).

### **1.8.2 Early Delivery**

Planned early delivery of gastroschisis fetuses aims to reduce the duration of bowel exposure to the potentially deleterious third trimester amniotic fluid and in turn reduce the degree of gut inflammation and therefore severity of GRID. Currently, many centres electively deliver gastroschisis fetuses at 37 to 38 weeks GA due to concerns relating to unexpected fetal death in later gestation (Burge and Ade-Ajayi, 1997, Crawford et al., 1992, David et al., 2008). However, some surgeons suggest that delivery at less than 37 weeks and even as early as 34 weeks GA would improve gut function after birth. A number of studies, the majority of which contain small numbers of patients, present conflicting evidence both for (Gelas et al., 2008, Moir et al., 2004) and against (Charlesworth et al., 2007, Logghe et al., 2005) delivery at less than 37 weeks GA. Given the inconclusive nature of the data standard practice continues to be delivery at 37 to 38 weeks GA in most centres.

### **1.8.3 Fetoscopic Surgery**

Fetal surgery was developed for defects that cause secondary, progressive damage to the fetus resulting in severe morbidity or death. The aim of intervention was to ultimately improve infant outcomes and prevent fetal demise (Laberge, 1986). Three main types of intervention exist: (1) percutaneous fetal therapy involves placing a



needle or catheter in-utero and performing a procedure under sonographic/endoscopic guidance, (2) fetoscopic surgery is similar to other forms of minimally invasive surgery such as laparoscopic or thoracoscopic surgery and utilises small incisions, trocars, specially designed instruments and direct visualisation using a fetoscope and additional guidance from ultrasound, and (3) open fetal surgery whereby hysterotomy is performed, the fetus is exteriorised and operated on directly.

Fetal surgery is becoming more common place for conditions such as severe congenital diaphragmatic hernia (Van der Veecken et al., 2018) and myelomeningocele (Adzick et al., 2011, Moldenhauer and Adzick, 2017). In the case of diaphragmatic hernia severe lung hypoplasia can lead to significant postnatal morbidity and mortality due to severe lung hypoplasia. The aim of fetal surgery is not to repair the primary diaphragmatic defect (initial attempts to do this by open fetal surgery led to suboptimal outcomes (Harrison et al., 1990)) but to improve lung development. As such fetal endoluminal tracheal occlusion (FETO) was developed secondary to lessons learned from tracheal atresia whereby the fetus develops larger than normal lungs due to the accumulation of lung secretions causing lung stretch and in turn increased lung proliferation. FETO is performed by a percutaneous technique under sonographic and endoscopic guidance in which a latex balloon is endoscopically positioned in the trachea and inflated. Prior to birth the balloon is removed (plug-unplug sequence) to enable balanced development of both type I and type II pneumocytes. Clinically the procedure is offered routinely to right-sided defects and an International randomised control trial is ongoing to assess the benefit of FETO in severe and moderate left sided defects (Van der Veecken et al., 2018).

Invasive fetal intervention for gastroschisis (other than amnioexchange) has not been performed clinically in humans but has been trialled in fetal lambs with surgically created gastroschisis. Attempts to achieve safe fetoscopic primary repair of the abdominal wall defect in fetal lambs was found not to be possible due to visceroperitoneal disproportion preventing safe return of the externalised viscera into the abdominal cavity (Bergholz et al., 2012, Kohl et al., 2009). As such, similar to fetal intervention for congenital diaphragmatic hernia where the aim is to improve lung development, fetal interventions in gastroschisis that aim to improve gut

development are potentially more appropriate. Two fetoscopic techniques that have been trialled in fetal lambs include defect widening (Kohl et al., 2009) and coverage of the externalised viscera. Defect widening is based on the hypothesis that bowel compression at a tight abdominal wall defect is the cause of GRID and severe bowel compression could lead to necrosis and bowel loss. The aim of decompression is to improve gut development and in turn postnatal gut function in the less severe cases and bowel salvage in the most severe cases. Although the procedure has been shown to be technically possible (Kohl et al., 2009) it has not been used clinically due to the lack of evidence supporting extrinsic bowel compression as the cause of GRID or robust sonographic antenatal markers to detect fetuses that may benefit from this procedure for example those with impending bowel necrosis secondary to a closing gastroschisis defect. Coverage of the externalised viscera is based on the hypothesis that exposure of the bowel to amniotic fluid causes GRID and therefore protecting the eviscerated bowel would improve bowel development. Studies have shown it is possible fetoscopically to cover the bowel with a synthetic or biological sheet to protect the bowel from the potentially noxious amniotic fluid (Roelofs et al., 2013, Krebs et al., 2014) but safety and efficacy of the procedure have yet to be proven and therefore it has not been performed clinically in humans.

#### **1.8.4 Postnatal Prokinetics**

It had been postulated that postnatal prokinetics could stimulate bowel function. As such, a double blind randomised controlled trial was conducted to investigate whether enteral erythromycin (a smooth muscle motilin receptor agonist, which induces intense intestinal motor activity similar to phase III migrating motor complexes) would reduce the time to achieve ENT. However, the trial showed no improvement in postnatal outcomes and concluded that GRID was likely secondary to gastrointestinal damage that was not amenable to stimulus by a prokinetic (Curry et al., 2004). These findings suggest that an antenatal therapeutic approach to improve GRID may be more beneficial.

## **1.9 Animal Models**

### **1.9.1 Overview of Animal Research**

Animal models are used to mimic human pathology in order to enable a better understanding of the aetiology, pathophysiology and outcomes of such conditions. Animal models enable researchers to perform experiments that are not possible in humans and may yield essential information, which could be used to prevent or improve therapeutic options for the investigated pathology. Additionally, they enable new therapeutic strategies to be tested before use in human trials. In order to fully understand the pathophysiological mechanisms underlying GRID and to enable investigation of new therapies to improve postnatal gut function the use of a gastroschisis animal model is essential.

The Animals (Scientific Procedures) Act 1986 is in place to regulate the use of animals for research in the UK. The Act applies to any research that could cause pain, suffering, distress or lasting harm to an animal. It ensures that research is performed in a humane and safe way with as minimal suffering as possible to the animal. The Act stipulates that in order for results to be relevant to the human disease it is essential to refine the animal model to ensure that the induced condition most closely resembles the human condition with respect to structural and functional characteristics (Klocke et al., 2007). Poorly designed animal models can lead to misleading data resulting in inaccurate physiological assumptions or theories (Chu et al., 2002, Klocke et al., 2007). Furthermore, extrapolation of such data to humans can be misleading (Casals et al., 2011). Several gastroschisis animal models have been described but none have been accepted as the definitive model that most reliably mimics the features of the human disease.

### **1.9.2 Types of Animal Models**

Rodent models are frequently used in medical research because they share many biological similarities to humans and develop disease over the span of days or weeks rather than months or years. Additionally, they have short gestational periods and large litter sizes which are invaluable for researching congenitally acquired diseases.

Other commonly used animals include zebrafish, chicks, hamsters, guinea pigs, rabbits and sheep and very rarely dogs and primates.

There are four types of animal model: induced, spontaneous, negative and orphan. Induced models are experimentally created. Spontaneous models involve animals that naturally develop a condition similar to human pathology. Negative models involve specific conditions that inhibit growth or a reaction to specific stimulus as a mechanism to understand physiology. Orphan models are pathologies that occur naturally in animals but have not been identified in humans (Casals et al., 2011). A gastroschisis animal model falls into the category of an induced model as gastroschisis is not known to occur naturally in animals such as chick, mouse, rat, rabbit and sheep, which are the most frequently utilised animals for basic science research.

### **1.9.3 Induced Models of Human Pathology**

Induced models are usually created by surgical creation, genetic manipulation or chemical induction.

#### ***1.9.3.1 Surgical Animal Models***

Surgically created models involve a surgical procedure to induce a human pathology in an animal. In cardiovascular or ischaemic disease this frequently involves the constriction of blood vessels, which can be achieved by a variety of methods including banding, ligation or blockage (Casals et al., 2011, Klocke et al., 2007, Louw and Barnard, 1955). In the case of structural malformations, such as gastroschisis, this involves the surgical creation of an abdominal wall defect that mimics the human condition at an appropriate time point in the animals' life cycle (Langer et al., 1989).

#### ***1.9.3.2 Genetically Modified Animal Models***

Genetic manipulation of animals involves adding, changing or removing targeted DNA sequences. Mice are most widely used for this application as advancements in genomic techniques have made manipulation of the murine genome relatively simple

enabling creation of phenotypes that are analogous to human pathology. The International Mouse Knockout Consortium aims to manipulate all protein-encoding genes in mouse embryonic stem cells using gene trapping and gene targeting techniques (Collins et al., 2007). As a result, some conditions now have known target genes, for example, investigations into the molecular mechanisms of craniorachischisis are focussed around *loop-tail* and *circletail* (Murdoch, 2003) gene manipulation. Whilst other conditions, such as gastroschisis, have no known genetic cause/link and rely upon incidental phenotype recognition during genetic model creation for other reasons (Murdoch, 2003, Layne et al., 2001).

### ***1.9.3.3 Chemically Induced Animal Models***

Chemical induction involves delivering a substance to an animal by ingestion or injection or removing a substance from an animals' diet in order to mimic the human condition. This manipulation may involve either wild type or genetically modified animals. For example, to create coronary atherosclerosis wild type rats are fed a high fat/cholesterol diet (Wilson and Hartroft, 1970) whilst dietary folate restriction to pregnant dams induces neural tube defects (NTD) in *plotch* embryos (Burren et al., 2008). Gastroschisis like defects can be created in animal fetuses with the use of several teratogens ( Table 1-5) (Van Dorp et al., 2010, McBride et al., 1982, Sukra et al., 1976, Fisher and Sawyer, 1980, Padmanabhan, 1998, Szabo et al., 1978, Gutova et al., 1971, Beauchemin et al., 1984, Samarawickrama and Webb, 1981, Hoffman and Moore, 1979, Singh, 2003, Yan and Hales, 2006, Pampfer and Streffer, 1988, Quemelo et al., 2007). However the incidence of gastroschisis like defects in these models is low and is frequently associated with significant concomitant malformations that could confound results. As such, chemically induced gastroschisis mutants will not be further discussed here.

Study	Teratogen	Animal	Incidence of Gastroschisis Like Defect	Concomitant Defects
McBride et al., 1982	Scopolamine hydrobromide (100µg, Tx96 h)	Chick	21/62 (34%)	-Exencephaly -Reduction deformities of the limbs -Microphthalmia -Buphthalmia
	Scopolamine hydrobromide (200µg, Tx96 h)		36/46 (78%)	
Sukra et al., 1976	Selenium and mercury	Chick	Not specified	-Webbed, fused, and curled toes -Cracked, crooked, and shortened beaks -Liver malformations -Renal malformations
Fisher and Sawyer, 1980	Triamcinolone acetone	Chick	Not specified	-Reduced body weight -Encephalocele -Micrognathia, -Curled toes, and club feathers -Reduced haematopoiesis
Padmanabhan 1998	Retinoic acid (200mg/kg)	Mouse	Not specified	-Tail agenesis -Caudal vertebral defects -Spina bifida occulta/aperta -Imperforate anus -Rectovesicle or rectourethral fistula -Renal malformations -Cryptorchidism -Limb malformations -Craniofacial malformations
Szabo et al., 1978	SK&F 36,914 (4–8 mg/kg, TxD6–18)	Rabbit	2/72 (2.8%)	-Acephaly -Neural tube defects
	SK&F D-39162 (0.5–3 mg/kg, TxD6–18)		1/256 (0.4%)	-Hydrocephalus, -Cleft palate
	SK&F D-39162 (4–8 mg/kg, TxD6–18)		2/57 (3.5%)	-Umbilical hernia -Diaphragmatic hernia
	SK&F D-39162 (16–32 mg/kg, TxD6–18)		1/20 (5%)	-Amelia-phocomelia -Brachy-ectrodactyly
	Gold sodium thiomalate (1–2.5 mg/kg, TxD6–18)		1/89 (1.1%)	-Tail anomalies -Fused/absent ribs and vertebrae
	Gold sodium thiomalate (20–45 mg/kg, TxD6–18)		2/95 (2.1%)	-Lung anomalies -Cardiovascular anomalies
Gutova et al., 1971	6-azauridine (12 mg/kg, TxD6–12)	Rat	4/69 (5.8%)	-Encephalocele -Malformations of the extremities
Beauchemin et al., 1984	Alcohol (0.03ml/g of 25% alcohol, TxD10)	Rat	4/51 (7.8%)	- Adactyly -Wrinkled skin, -Umbilical hernias -Interatrial-septal defect

Study	Teratogen	Animal	Incidence of Gastroschisis Like Defect	Concomitant Defects
Samarawickrama and Webb, 1981	Cadmium	Rat	Not specified	-Renal damage -Hydrocephalus -Eye defects -Umbilical hernia
Hoffman, 1979	Mercury (3µg, Tx72 h)	Duck	2.6%	Low dose: -Minor skeletal aberrations -Incomplete ossification  Higher doses: -Micromelia -Eye defects -Brain defects
	Mercury (9µg, Tx72 h)		2.9%	
	Mercury (27µg, Tx72 h)		14.0%	
	Mercury (90µg, Tx72 h)		5.1%	
Singh, 2003	Carbon monoxide and protein-zinc deficiency	Mouse	Not specified	-Growth restriction -Skeletal malformation
Yan and Hales, 2006	Hydroxyurea and glutathione deficiency (400 mg/kg, TxD9)	Mouse	1/113 (0.9%)	-Curly tail -Hind limb malformations -Hydrocephaly -Exencephaly -Open eye -Spina bifida
	Hydroxyurea and glutathione deficiency (600 mg/kg, TxD9)		4/61 (6.6%)	
Pampfer and Streffer, 1988	Neutron-irradiation (12cGy)	Mouse	4/245 (1.6%)	-Exomphalos -Anencephalies -Skeletal malformations -Growth restriction
	Neutron-irradiation (25cGy)		8/160 (5.0%)	
	Neutron-irradiation (50cGy)		17/220 (7.7%)	
	Neutron-irradiation (75cGy)		25/119 (21.0%)	
	X-irradiation (25cGy)		3/133 (2.3%)	
	X-irradiation (50cGy)		6/197 (3.0%)	
	X-irradiation (100cGy)		9/147 (6.1%)	
	X-irradiation (200cGy)		29/178 (16.3%)	
Quemelo et al., 2007	Retinoic acid (70mg/kg, TxD7)	Mouse	2/31 (6.4%)	-Exencephaly -Neural tube defects -Exomphalos -Lower limb alterations -Tail agenesis/alteration -Imperforated anus
	Retinoic acid (70mg/kg, TxD8)		3/55 (5.4%)	

**Table 1-5:** Summary of teratogens that result in gastroschisis like defects including dosage, incidence and concomitant defects.

## 1.9.4 Animal Models of Gastroschisis

### 1.9.4.1 Surgical Animal Models of Gastroschisis

The creation of an animal surgical model of gastroschisis involves creation of an abdominal wall defect in the in-utero fetus and exteriorisation of the fetal bowel. The method has been described in chick, rat, rabbit and sheep (Vargun et al., 2007, Auber et al., 2013, Hakguder et al., 2011, Oyachi et al., 2004, Krebs et al., 2014, Bergholz et al., 2012). Table 1-6 outlines the approximate timing of abdominal defect creation, fetal collection and full term for each animal model. In all animals the procedure is technically difficult, increases suffering to the pregnant dam and places the pregnancy at risk of abortion.

Animal Model	Defect Creation (days post coitum)	Fetal Collection (days post coitum)	Full Term (days post coitum)
Chick	Between 5 and 15	18	21
Rat	18.5	21.5 or 22	22
Rabbit	24	Between 29 and 31	31
Lamb	77	135	152

**Table 1-6:** Timing of in-utero abdominal wall defect creation, fetal collection and duration of full term for each type of surgical animal model of gastroschisis.

### 1.9.4.2 Genetic Mouse Models of Gastroschisis

Genetic mouse models of abdominal wall defects are ideal given the short gestation, large litter sizes and that the process of abdominal wall closure is very similar to that of human development. In the mouse, primary abdominal wall closure starts at 8.5 days post coitum (dpc) during which the left and right lateral plate mesoderm, which are composed of a thin epithelial membrane, elongate laterally and come to meet in



the ventral midline. In the midline the umbilical ring is thought to be formed of the same four mesodermal folds as previously described for human abdominal wall closure namely the cephalic, caudal and 2 lateral mesodermal folds (Brewer and Williams, 2004b). Centrally the umbilicus acts as the transition zone between the ventral wall ectoderm and the amniotic membrane, which are continuous with each other as seen in human development (Bargy and Beaudoin, 2014). At 10.5 dpc the relatively wide umbilical ring permits the herniation of the rapidly elongating midgut creating a physiological hernia. From 12 dpc, during the period of physiological herniation, the process of secondary abdominal wall closure occurs whereby myoblasts migrate from the myotome into the primary epithelial abdominal wall (Nichol et al., 2012). This process gives rise to the development of the secondary abdominal wall structures including keratinised epithelia, muscle and connective tissue. At 16.5 dpc the herniated bowel returns to the abdominal cavity and secondary closure is completed through closure of the umbilical ring (Kaufman and Bard, 1999).

Other similarities between mouse and humans includes the development of the bowel wall neuromusculature and the extra-fetal fluid cavities. Mouse bowel neuromuscular development like humans involves anal to oral migration of both the enteric nerves (fully populated by 14.5 dpc) (Kapur et al., 1992) and smooth muscle (complete by 18 dpc) (Torihashi et al., 1997), whilst the myenteric ICC are developed prior to birth by 18 dpc with continued development of other ICC populations after birth (Torihashi et al., 1997). Mouse extra-fetal fluid cavities like humans comprise an amniotic fluid cavity (located between the fetus and the amniotic membrane) and an exocoelomic fluid cavity (located between the amniotic membrane and visceral yolk sac) (Renfree et al., 1975, Pereira et al., 2011) both of which are similar in composition to humans but the amniotic fluid volume shows some differences. The mouse amniotic fluid composition is modulated by fetal urine, meconium, secretions of oral and airway fluids, swallowing and amniotic membrane absorption and over the course of gestation the potassium, chloride and lactate levels increase and the sodium, calcium and glucose levels decrease (Cheung and Brace, 2005). Whilst the composition of mouse exocoelomic fluid is determined by exchange of substances from the overlying visceral yolk sac serving as the principle site for materno-fetal protein exchange (Jauniaux and Gulbis, 2000). The volume of the mouse amniotic

fluid rises from mid gestation (11 dpc) to peak at 16 dpc (50% of the embryo weight) but then, unlike humans, sharply declines after this point and by 18 dpc only weighs 10% of the embryo weight (Renfree et al., 1975, Cheung and Brace, 2005).

In the literature four genetic models have been described as exhibiting a gastroschisis like defect (Table 1-7) - the Scribble mutant mouse model (Murdoch, 2003), the aortic carboxypeptidase-like protein (ACLP) knockout mouse (Layne et al., 2001, Danzer et al., 2010), *Alx-4* mutant mouse (Qu et al., 1997) and *Bmp1* mutant mouse (Suzuki et al., 1996). However, the *Alx-4* mutant mouse was later described to be exomphalos (Matsumaru et al., 2011) and the *Bmp1* mutant mouse is reported to exhibit failed folding of the amniotic membrane around the umbilical vessels (Suzuki et al., 1996) resulting in the externalised bowel lying in the exocoelomic cavity rather than the amniotic fluid cavity and is therefore not a true gastroschisis defect.

Study	Name of Model	Genotype of Mutants	Protein Effected	Impact on Protein	Protein Normal Function	Described Abdominal Wall Defect (AWD)	Other Expressed Phenotypes	Other Comments
Murdoch et al., 2003	<i>Circletail</i>	-Homozygote - <i>Crc/Crc</i> - Mutated target allele	Scribble	Premature termination of Scribble protein and therefore loss of function Knocked out	-Signalling protein -Cell membrane protein -Involved in epithelial cell migration, polarity and proliferation	Gastroschisis	- <i>Craniorachischisis</i> (severe neural tube defect)	
Layne et al., 2001 and Dauner et al., 2010	<i>ACLP</i> knockout	-Homozygote - <i>ACLP<sup>-/-</sup></i> -Gene deletion	Aortic carboxypeptidase-like protein (ACLP)		-Signalling protein -Secreted during development into the extracellular matrix of connective tissues -Acts as a binding protein, facilitating cell aggregation/adhesion and cell-cell recognition	Gastroschisis	-Deficient wound healing, dermal fibroblasts exhibit reduced proliferative capacity	
Qu et al., 1997	<i>Alx4</i> mutant	-Homozygote - <i>Alx-4<sup>mlg<sup>w</sup></sup>/ Alx-4<sup>mlg<sup>w</sup></sup></i> - Mutated target allele	<i>Alx-4</i>	Protein abnormal structure preventing DNA binding during transcription	-Transcription factor -Intracellular protein -Controls the activity of genes that regulate cell proliferation, differentiation, migration and survival	Gastroschisis	-Preaxial polydactyly -Decreased size of skull parietal plate	Later AWD reclassified as exomphalos by Matsumaru et al., 2011
Suzuki et al.,	<i>Bmp1</i> mutant	-Homozygote - <i>Bmp1<sup>ml</sup>/ Bmp1<sup>ml</sup></i> - Mutated target allele	Bone Morphogenetic Protein 1 (Bmp1)	Protein lacks the active site, which is an <i>astacin</i> -like protease domain	-Activates procollagen -Extracellular matrix protein -Forms cross links to stabilise collagen and elastin -Enhances the activity of TGFβ growth factors	Gastroschisis like defect	-Reduced ossification of skull bones -Abnormal folding of the amniotic membrane with failed adherence to the umbilical vessels therefore abnormal umbilical cord	Externalised bowel lies in <i>exocoelomic</i> fluid not amniotic fluid.

**Table 1-7:** Summary of reported genetic mouse models that exhibit a gastroschisis like defect.

### **1.9.5 Surgical Versus Genetic Gastroschisis Animal Models**

Surgical models of gastroschisis require the pregnant dam and the fetuses to undergo a technically difficult (in the case of small animals) invasive surgical procedure in order to create an abdominal wall defect similar to gastroschisis. This procedure increases the risks of fetal loss and the level of animal suffering. Given the amniotic fluid is replaced with saline during the procedure the potentially deleterious amniotic fluid components causing bowel dysmotility are removed. However, the natural turnover of amniotic fluid is 24 hours and therefore the effect of replacing the amniotic fluid is likely to be short lived. Additionally, the surgical procedure will create confounding inflammatory changes, which could impact on the bowel development. In small animal gastroschisis surgical models the time between defect creation and collection of the fetuses is short reducing the duration of bowel exposure to amniotic fluid and the time available to experimentally manipulate the amniotic fluid environment. As such, large animal surgical models are the most advantageous. However, large animals are costly, have long gestations and small litter sizes increasing the number of dams required to complete experiments and are therefore not ideal for this type of research.

In comparison, genetic mouse gastroschisis models exhibit an abdominal wall defect that occurs early in pregnancy similar to humans providing a more representative model of the effects of amniotic fluid exposure without the development of confounding inflammation caused by surgical defect formation. There are no known or anticipated negative effects for heterozygote mice or pregnant dams thus reducing the level of suffering. Additionally, mice have short gestations, similar sequence of abdominal wall closure to humans and large litter sizes reducing the number of dams required to complete the experiments. To prevent suffering of affected pups pregnancies are prevented from reaching full term.

### **1.10 Summary**

Gastroschisis-related intestinal dysfunction is a significant issue affecting most infants with gastroschisis. Although the pathophysiology of GRID is not fully understood, there are significant data within the literature to suggest that deficiency

and immaturity of bowel wall ICC (the pacemaker of the gut) secondary to inflammation during fetal life is the cause of GRID. Given the evidence for ICC plasticity in response to inflammation, the transient nature of GRID could be explained by the gradual postnatal resolution of bowel wall inflammation and resultant maturation and increase in bowel wall ICC. Therapeutic options antenatally and postnatally have been trialled but no improvements in postnatal intestinal function have been achieved to date.

### **1.11 Hypotheses**

Gastroschisis-related intestinal dysfunction is secondary to deficient, immature bowel wall ICC caused by bowel inflammation and amelioration of inflammation antenatally will improve gut function.

### **1.12 Thesis Aims**

The underlying aims of the work contributing to this thesis are centred on addressing the pathophysiology of GRID with a primary line of investigation focussing on ICC development in gastroschisis from which further research could develop an antenatal therapy to improve intestinal function before birth for gastroschisis infants. The aims of this work are to determine:

1. The morphology of gastroschisis bowel wall including ICC, enteric neurons and bowel wall architecture
2. The impact of inflammatory modulation on gastroschisis bowel wall ICC and bowel contractility
3. The impact of clinical antenatal interventions on infant outcomes.

### **1.13 Outline of Work to be undertaken**

In order to address these aims a number of studies have been designed utilising a variety of resources including genetic mouse gastroschisis models, human pathological gut tissue and retrospective analysis of clinical data.

### **1.13.1 Gastroschisis Bowel Wall Morphology**

Quantitative morphological analysis of bowel wall ICC, enteric neurons and architecture will be performed using immunofluorescence and histological techniques utilising a genetic mouse gastroschisis model and human pathological gut tissue. Gastroschisis bowel will be compared to bowel from controls.

### **1.13.2 Impact of Inflammatory Modulation on Gastroschisis Bowel Wall Morphology and Bowel Contractility**

Intra-amniotic injections of the pro-inflammatory mediator IL-8 will be performed in the genetic mouse gastroschisis model following which quantitative morphological analysis of the bowel wall ICC, enteric neurons and architecture will be undertaken. In addition, bowel contractility of untreated and injected fetal mice will be analysed within an organ bath.

### **1.13.3 Impact of Simple Clinical Antenatal Measures on Clinical Outcomes**

Retrospective clinical data from three paediatric surgical centres will be collected to determine whether early delivery of gastroschisis fetuses or the administration of maternal antenatal corticosteroids could improve infant morbidity and if antenatally detected bowel dilatation could be used to predict infant outcomes.

## **Chapter 2: Materials and Methods**

### **2.1 Animal Models General Methods**

#### **2.1.1 Ethics Statement**

All animal experimental protocols were approved by the University College London (UCL) Biological Services Ethical Review Committee and granted Home Office approval under the UK Animals (Scientific Procedures) Act 1986 (PPL 70 7408 - Prenatal therapy with stem cells and gene transfer).

#### **2.1.2 Selected Animal Models**

Genetic rodent models were considered to be the most refined animal model for this application whilst reducing the number of animals required and the level of suffering induced. The similar mouse abdominal wall closure time sequence and ICC/enteric neuron development compared to humans makes genetic mouse models of gastroschisis ideal for this research. The Scribble knockout mouse model and the ACLP knockout mouse model were used in this thesis.

#### **2.1.3 Model Source and Creation of Null Fetuses**

##### ***2.1.3.1 Scribble Knockout Mouse Model***

A *Scrib<sup>fl</sup>* mutant mouse colony was already housed in the UCL Biological Services. The *Scrib<sup>fl</sup>* allele was originally a kind gift from Dr Patrick Humbert, Peter MacCullum Cancer Centre, Melbourne. Null alleles (*Scrib<sup>-/-</sup>*) were created by matings between *Scrib<sup>fl/fl</sup>* homozygotes with mice expressing the ubiquitously expressed  $\beta$ actin-Cre. Timed matings between adult heterozygotes (*Scrib<sup>fl/+</sup>*) generated *Scrib* knockout fetuses (*Scrib<sup>-/-</sup>*).

### **2.1.3.2 *ACLP Knockout Model***

Two male and two female heterozygote ( $ACLP^{+/-}$ ) mice with a mixed C57BL/6J-129Sv background were a kind gift from Matthew Layne, School of Medicine Biochemistry, Boston University. Rederivation was performed at University College London using C57BL/6J female mice to avoid prolonged quarantine of imported mice. Colony expansion was achieved through mating of rederived heterozygote female mice with C57BL/6J wild type males. Timed matings between adult heterozygotes ( $ACLP^{+/-}$ ) generated ACLP knockout fetuses ( $ACLP^{-/-}$ ).

## **2.1.4 *Animal Husbandry***

### **2.1.4.1 *Housing of Mouse Colonies***

The mouse colonies were housed in the UCL Biological Services. The Scribble knockout mouse colony was housed in open cages throughout the duration of the experiments. However, the ACLP mouse colony was housed from September 2012 in open cages but moved to individually ventilated cages in June 2014 following a laboratory wide change in caging system. The bedding material used was 3R's premium white bedding/Litaspen B8/20 sawdust bedding material. The laboratory was kept at a temperature of 19-23 degrees with a 12 hour light dark cycle with graded transition between light settings. Harlan 2018 feed and tap water were replenished daily.

### **2.1.4.2 *Pinworm treatment***

The animal facility developed a laboratory wide infestation of pinworm. As a consequence, all mice were treated for 9 weeks (September 2014 to December 2014) with a Fenbendazole diet and rooms were deep cleaned with Neopresidan 2% and fumigated. ACLP knockout mouse model experiments were stopped for the duration of the treatment period to prevent results being compromised by unknown fetal drug side effects. Experimental data from animals prior to September 2014 have been used because pinworm is transmitted by the faecal-oral route and cannot cross the placenta therefore mouse fetuses are thought to be unaffected by the infestation.



#### **2.1.4.3 *Breeding Pairs***

Six adult (mice >8 weeks old) breeding pairs were maintained at all times crossing wild type females with heterozygote males. Breeding females were exchanged after 6 pregnancies or if litter sizes decreased. Breeding males were exchanged when they reached >18 months of age or fertility dropped. Pups from breeding pair litters were genotyped. To maintain a sustainable colony a minimum of 6 wild type females and 3 heterozygote males were kept to enable replacement of breeding pairs when required. For time matings, 6 stud heterozygote males and all heterozygote females were maintained in the colony. All other pups were euthanized to ensure an affordable colony.

#### **2.1.4.4 *Timed Mating***

Timed matings between adult heterozygote females and stud heterozygote males generated null (homozygote knockout) fetuses. Timed matings were paired at 6pm and vaginal plugs checked by 10am the following morning. The morning on which a vaginal plug was detected was designated 0.5 dpc.

#### **2.1.4.5 *Fetal Collection***

Pups born with an abdominal wall defect (AWD) die postnatally and therefore to prevent suffering of affected pups fetuses were collected by 18.5 dpc at the latest. Pregnant dams were euthanized by cervical dislocation and fetuses collected in-utero by maternal hysterectomy. Fetuses were transported in the intact uterus to the dissecting room in 1x phosphate buffered saline (PBS).

### **2.1.5 *Genotyping***

#### **2.1.5.1 *Tissue for Genotyping***

Genotyping was performed by polymerase chain reaction (PCR). Ear biopsies were taken from pups generated from breeding pairs for the purpose of identification and DNA extraction for genotyping. Tail biopsies were taken from fetuses generated

from time matings and used for DNA extraction for genotyping. All biopsies were stored dry at -20°C prior to DNA extraction.

#### **2.1.5.2 DNA extraction**

DNA extraction was performed on approximately 3mm segments of tissue. The tissue was added to 75µl of 25mM sodium hydroxide containing 0.2mM ethylene diamine tetraacetic acid disodium (EDTA Na<sub>2</sub>) at pH 12 and heated to 95°C for 10 minutes. The mixture was allowed to cool to room temperature followed by addition of 75µl of 40mM Tris hydrochloride at pH 5. At this point the DNA extraction mixture could be stored at -80°C for PCR genotyping at a later date or used immediately for genotyping by PCR

#### **2.1.5.3 Genotyping by PCR**

PCR genotyping was performed with HotStarTaq Master Mix® (Qiagen). Two separate reactions were set up for identification of wildtype ([WT], *Scrib* and *ACLP*) and knockout (*Scrib*<sup>fllox-neo</sup> and *ACLP*) DNA sequences. The primers used were as outlined in Table 2-1. The WT reaction included common forward and WT reverse primers. The knockout reaction included common forward and mutant reverse primers. The PCR reagents and volumes were as outlined in Table 2-2. A DNA extraction sample from a known heterozygote was used as a positive control. RNase-free water was used instead of DNA to create a negative control. The PCR programmes used were as outlined in Table 2-3 following which samples were stored at 4°C until gel electrophoresis was performed.

Primer Type	Primer Sequence
<i>Scrib</i> common forward	5' GGACTCAGACCCTCTTTCGT '3
<i>Scrib</i> WT reverse	5' GCCATGGTGGCAGAGGTTGG 3'
<i>Scrib</i> mutant rev	5' CTTCCATTTGTCACGTCCTGC 3'
<i>ACLP</i> Common forward	5' CAATATGGCACGAGCAGAG '3
<i>ACLP</i> WT reverse	5' GAGGCAAGCGAGGAGGTA 3'
<i>ACLP</i> mutant reverse	5' TCTTGACGAGTTCTTCTGAG 3'

**Table 2-1:** Primers used for genotyping.

Reagent	Volume ( $\mu$ l)
HotStarTaq Master Mix®	12.5
forward primer (0.1 $\mu$ g/ $\mu$ l common)	0.375
reverse primer (0.1 $\mu$ g/ $\mu$ l WT or mutant)	0.375
RNase-free water	10.25
DNA extraction mixture	2

**Table 2-2:** PCR reagents and volumes for genotyping.

Temperature and duration	Number of Cycles
<b>Scribble Mouse Model</b>	
94°C, 5 minutes	1
94°C , 1 minute 56°C, 1 minute 30 seconds 72 °C, 1 minute 30 seconds	35
72°C, 10 minutes	1
<b>ACLP Mouse Model</b>	
94°C, 5 minutes 58°C, 30 seconds 68°C, 45 seconds	3
94°C, 30 seconds 58°C, 30 seconds 68 °C, 45 seconds	32
68°C, 7 minutes	1

**Table 2-3:** PCR temperature cycle settings

#### **2.1.5.4 Gel Electrophoresis**

The electrophoresis gel was made from 1.5% agarose in 100mls of 1x TAE (mixture of Tris base, acetic acid and EDTA) buffer, which was heated in a microwave for 2 minutes until the agarose dissolved. 8µl of ethidium bromide was added to the mixture and the gel left to set for 30 minutes. A mix of 2µl of loading dye and 12µl of DNA sample were loaded into the wells. Each line of wells contained a positive control and TrackIt™ DNA ladder (Thermo Fisher Scientific) for identification of positive bands.

### 2.1.5.5 Electrophoresis Bands

#### 2.1.5.5.1 Scribble Knockout Mouse Model

The *Scrib* (WT) allele fragment size was 286 bp and *Scrib*<sup>lox-neo</sup> (knockout) allele fragment size was 512 bp (Figure 2-1).

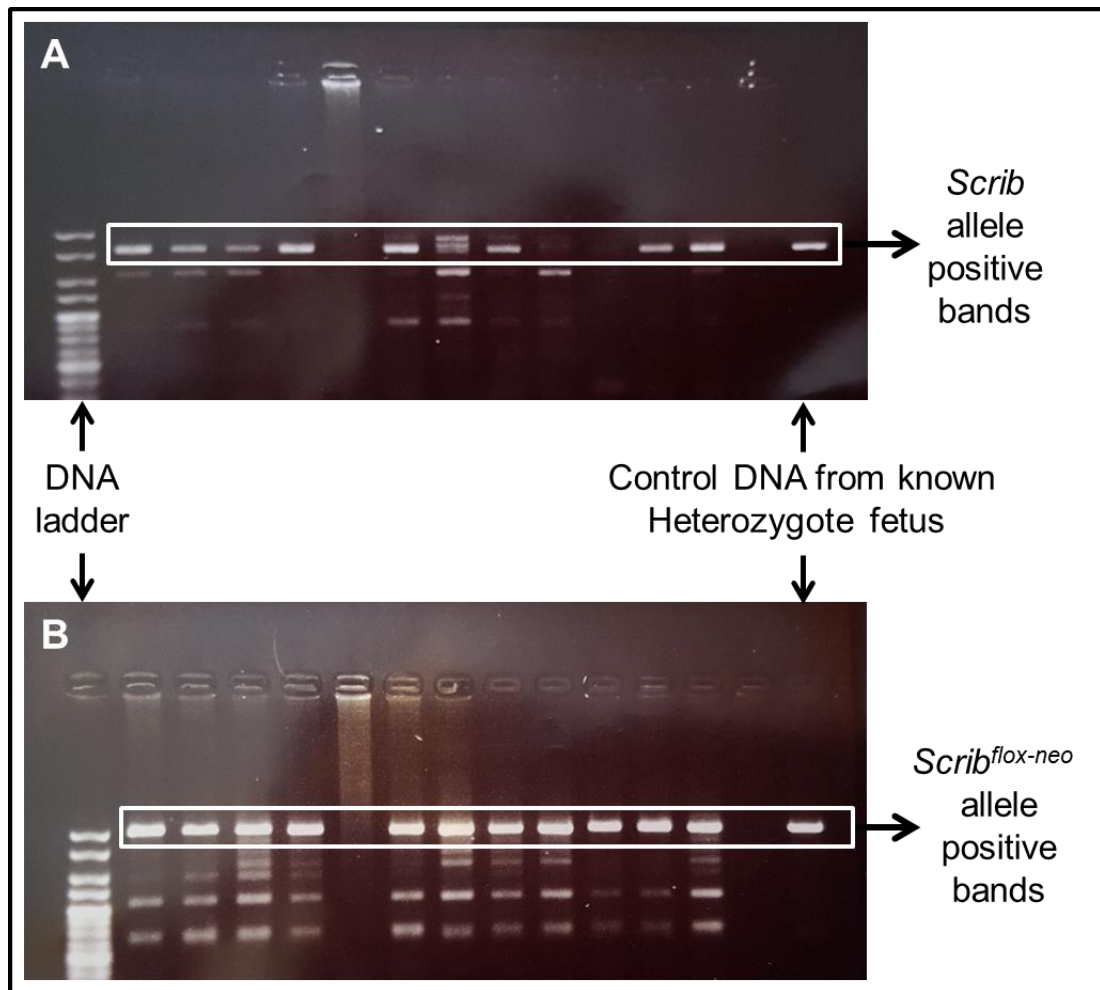


**Figure 2-1:** *Scrib* and *scrib*<sup>lox-neo</sup> allele gel electrophoresis, including DNA ladder and control DNA from a known heterozygote fetus. **A.** Gel electrophoresis for *Scrib* (WT) allele, box highlights positive allele bands. **B.** Gel electrophoresis for *scrib*<sup>lox-neo</sup> (knockout) allele, box highlights positive allele bands.

### 2.1.5.5.2 *ACL*P knockout Mouse Model

The *ACL*P (WT) allele fragment size was 381 bp and *ACL*P<sup>-</sup> (knockout) allele fragment size was 475 bp (Figure 2-2).

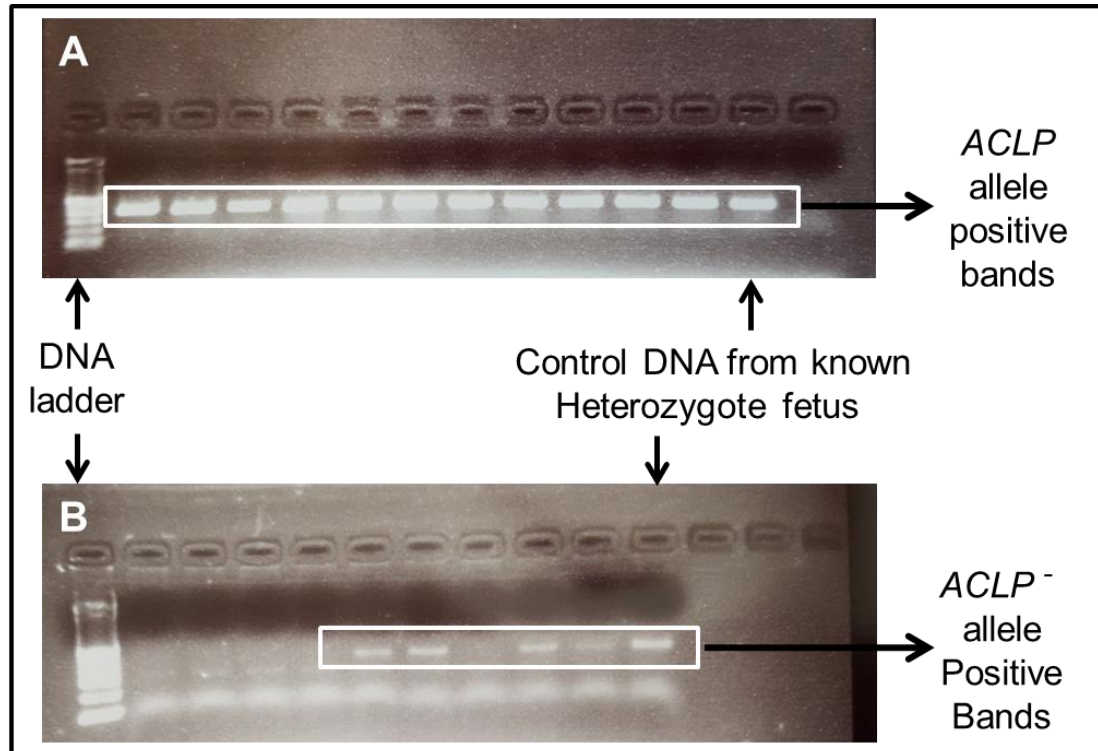


**Figure 2-2:** *ACL*P and *ACL*P<sup>-</sup> allele gel electrophoresis, including DNA ladder and control DNA from a known heterozygote fetus. **A.** Gel electrophoresis for *ACL*P (WT) allele, box highlights positive allele bands. **B.** Gel electrophoresis for *ACL*P<sup>-</sup> (knockout) allele, box highlights positive allele bands.

## 2.1.6 Abdominal Wall Defect Phenotyping

### 2.1.6.1 Fetal Preparation

Phenotypically normal and AWD fetuses were collected at varying time points. The intact uterus was dissected in 1x PBS under a dissecting stereo microscope (Zeiss SV6, USA). The uterine muscle was carefully removed leaving the amniotic membranes and placenta intact for each fetus. Visualisation and gross identification of phenotypically normal and mutant fetuses was performed through the relatively translucent intact amniotic membranes. Phenotypically normal and AWD fetuses were imaged under the Zeiss SV6 microscope.

### ***2.1.6.2 Microdissection and Imaging***

The anatomy of the abdominal wall in relation to the amniotic membranes and umbilical cord of both phenotypically normal and AWD fetuses was assessed by careful opening and dissection of the amniotic membranes with as little disruption as possible to the umbilical/AWD region. The fetuses were then euthanized by cervical dislocation and the anatomy of the abdominal wall including the insertion of the amniotic membrane and umbilical cord examined under the Zeiss SV6 microscope and imaged with a Leica DC500 camera.

The amniotic membranes in mice are extremely delicate and difficult to dissect without causing damage to the important anatomical relations between the fine fetal membranes and the AWD and externalised abdominal viscera. Therefore, two techniques were developed in order to visualise the fetal anatomy in-amnio without disruption to the delicate fetal membranes. These techniques were in-amnio micro-magnetic resonance imaging (micro-MRI) and in-amnio paraffin embedded cross-sections as described below.

### ***2.1.6.3 In-Amnio Fetal Micro-MRI***

Phenotypically normal and AWD fetuses with intact amniotic membranes and placenta (intra-amniotic fetuses) were fixed in 4% paraformaldehyde (PFA) for 1 hour and then embedded in 1% agarose gel in individual 50ml centrifuge tubes to prevent amniotic membrane rupture. The embedded fetuses were stored at 4°C and imaging performed within 24 hours of fixation.

During preliminary development of this technique it was found that smaller 15ml centrifuge tubes were too narrow resulting in amniotic membrane rupture. Additionally, attempts to inject gadolinium-based MRI contrast agent to enhance the distinction of the amniotic fluid compartment resulted in rupture of the amniotic membrane.

Embryos were scanned, performed by Thomas A Roberts, UCL Centre for Advanced Biomedical Imaging, using a 9.4T VNMRS system (Agilent Technologies, Inc.,

Santa Clara, CA, USA) with a 33mm volume coil (RAPID Biomedical GmbH, Germany). T2-weighted, high-resolution (256<sup>3</sup> pixels with a 25.6<sup>3</sup> mm field of view; resolution of 100 µm/pixel) micro-MR images were acquired using a 3D fast spin echo sequence with repetition time of 1500ms. Images were converted and reconstructed using Analyse 7.5 data format using ImageJ (NIH, USA) and images generated using Amira 5.4 (Visage Imaging, Inc., Berlin, Germany). Across the image being compared the contrast levels were windowed equally. Imaging was performed by Roberts, Norris, et al (Roberts et al., 2014).

#### ***2.1.6.4 In-Amnio Paraffin Embedded Cross-Sections***

##### *2.1.6.4.1 Paraffin Embedding*

Phenotypically normal and AWD fetuses were fixed in 10% formalin in amnio at room temperature for 48 hours, dehydrated in increasing concentrations of ethanol (70% ethanol one wash for 30 seconds, 95% ethanol one wash for 30 seconds and 100% ethanol 2 washes for 30 seconds), cleared in xylene (2 washes of 5 minutes duration) and then paraffin embedded using the automated Sakura Tissue-Tek TEC FFPE embedding station. Full penetration of the paraffin through the larger 18.5 dpc fetuses was achieved by creating tiny needle punctures in the amniotic membrane with a 33G needle. Puncturing the amniotic membrane in the region adjacent to the fetal spine enabled full penetration of the paraffin without causing disruption to the amniotic membrane associated with the umbilical/AWD region. Serial 3µm sagittal sections were cut through the umbilical/AWD region.

##### *2.1.6.4.2 Dewaxing and Rehydration of Paraffin Embedded Cross-Sections*

Sections were allowed to dry overnight at 37°C and then transferred to a 60°C oven for 1 hour. Sections were dewaxed in xylene (2 washes of 5 minutes duration), rehydrated in decreasing concentrations of alcohol (100% ethanol 2 washes for 5 minutes, 95% ethanol one wash for 5 minutes and 70% ethanol one wash for 5 minutes) and washed in distilled water for 1 minute. Slides were then ready for either Haematoxylin and Eosin (H&E) staining or epitope retrieval in preparation for immunostaining.



#### *2.1.6.4.3 Antigen Retrieval*

Paraffin embedding can result in masking of epitopes due to cross-linking of amino acids. Antigen retrieval was therefore performed to reverse epitope masking and enable reliable epitope-antibody binding.

Sections were washed in 1x PBS for 10 minutes, placed in a citrate/EDTA (pH 6) buffer and heated in a pressure cooker to a temperature of 125°C. Slides were washed in 1x PBS and allowed to cool prior to immunostaining.

#### *2.1.6.4.4 H&E Staining*

Sections were stained with H&E for histological analysis. Slides were soaked in Mayer's Hematoxylin solution for 5 minutes, washed 3 times in distilled water (1 minute each wash), placed in 95% ethanol for 1 minute and then soaked in Eosin solution for 1 minute 30 seconds.

#### *2.1.6.4.5 ACLP/AEBP1 and TGF $\beta$ Labelling*

To determine the expression and distribution of ACLP protein within AWD fetuses cross-sections were labelled for ACLP/AEBP1. Additionally, there is evidence to suggest that ACLP interacts with TGF $\beta$  signalling and affects collagen expression (Tumelty et al., 2014), which can lead to disruption of collagen fibrils located at the level of the amniotic membrane (Suzuki et al., 1996). Cross-sections were therefore also labelled for TGF $\beta$ .

In-amnio paraffin embedded cross-sections were single labelled for ACLP and TGF $\beta$  on a Leica Bond-Max autostainer using anti-ACLP/AEBP1 (Santa Cruz Biotechnology, polyclonal IgG raised in rabbit, concentration 1:100) or anti-TGF $\beta$  (abcam, polyclonal IgG, raised in rabbit, concentration 1:200) respectively with a 3,3'-diaminobenzidine (DAB) detection kit.

#### *2.1.6.4.6 Dehydration and Mounting of Stained Paraffin Embedded Cross-Sections*

Stained sections were then dehydrated in increasing concentrations of ethanol (70% ethanol one wash for 30 seconds, 95% ethanol one wash for 30 seconds and 100% ethanol 2 washes for 30 seconds), cleared in xylene (2 washes of 5 minutes duration) and coverslip mounted with Permount™ mounting media (Fisher Scientific). Slides were then stored at room temperature.

#### *2.1.6.4.7 Imaging of In-amnio Paraffin Embedded Cross-Sections*

Slides were imaged with 40x objective using Zeiss AxioScan Z1 slide scanner, which digitally captures large sample areas creating a virtual image of entire slides through digital stitching of multiple high-resolution tiles. It was therefore possible to create a digital high powered microscopy image of an entire in-amnio fetus enabling detailed examination of the fetal anatomy. Images were viewed using Zeiss ZEN lite imaging software. Differences in ACLP and TGFβ labelling were visually compared.

### **2.1.7 Experimental Groups**

#### *2.1.7.1 Scribble Knockout Mouse Model Experiments*

Gut was analysed from two experimental groups; (1) phenotypically normal fetuses and (2) AWD fetuses. No fetal intervention groups were included in this study.

#### *2.1.7.2 ACLP Knockout Mouse Model Experiments*

Gut was analysed from four experimental groups; (1) untreated phenotypically normal fetuses, (2) untreated AWD fetuses, (3) phenotypically normal fetuses who received intra-amniotic IL-8 injection at 16.5 dpc and (4) AWD fetuses who received intra-amniotic IL-8 injection at 16.5 dpc.

### **2.1.8 Intra-Amniotic Injections**

In order to potentiate the inflammatory environment of the fluid surrounding the externalised gut, intra-amniotic injections of IL-8, which induces neutrophil chemotaxis (Bickel, 1993), diluted in 1x PBS were performed.

#### ***2.1.8.1 Timing of injections***

Injections were performed at 16.5 dpc following resolution of physiological herniation and fetuses were collected as previously stated at 18.5 dpc for ileal studies.

#### ***2.1.8.2 Procedure***

The procedure was performed using loupes with a 2.8 magnification, by a sterile technique including sterile drapes, instruments, IL-8 and PBS. Pregnant dams were anaesthetised using inhalational isoflurane and transferred to the operating table. Inhalation anaesthesia was maintained via a nose cone. The dam was laid supine on a warming mat and the legs taped. Veet sensitive hair removal cream was applied to the abdominal wall and left for approximately 5 minutes and removed with a swab. Chlorhexidine was used to prepare the abdominal skin. A midline laparotomy was performed and each horn of the uterus externalised. To prevent drying of uterine tissues, approximately 0.5ml of 1x PBS was applied to the uterine surface. 20µl of IL-8 solution was injected using a 33G needle into the fluid compartment surrounding the externalised gut of each mutant fetus and the intra-amniotic cavity of each phenotypically normal fetus. Following injection, the uterus was returned to the abdominal cavity and approximately 0.5ml of 1x PBS instilled into the abdominal cavity. Closure was performed with 5/0 VICRYL RAPIDE™ using a continuous suture to close the peritoneum and interrupted sutures with a buried knot to close the skin. Subcutaneous marcaine local anaesthetic was given for pain relief. Animals were housed individually, recovered overnight in a warming cage and returned to their normal environment the next day.

### **2.1.8.3 *IL-8 Dose-Finding Study***

The presence of uterine inflammation can lead to pre-term labour and early delivery of fetuses. Therefore varying concentrations of intra-amniotic injected recombinant IL-8/CXCL8 (PeproTech, biological range for neutrophil chemotaxis 0.025µg/ml and 0.15µg/ml) were trialled using WT pregnant dams at 16.5 dpc. Concentrations of 0.025µg/ml, 0.05µg/ml, 0.075µg/ml, 0.1µg/ml, 0.125µg/ml and 0.15µg/ml were tested. Preterm delivery occurred following injection of IL-8 at a concentration of 0.125µg/ml and 0.15µg/ml. IL-8 concentration of 0.075µg/ml was therefore used for intra-amniotic injection during the ACLP experiments to induce inflammation without inducing preterm labour.

### **2.1.9 Gut Tissue Gross Dissection, Handling and Specimen Numbers**

#### ***2.1.9.1 Harvest Timing, Number and Coding of Gut Specimens***

The gut from the gastroesophageal junction to the ileocaecal valve was removed from 10 fetuses from each experimental group at 18.5 dpc. Ileal lengths of the excised gut were used for immunofluorescence (1.5cm ileal length taken 1cm from the ileocaecal valve, eviscerated in AWD group) and haematoxylin and eosin (H&E) staining (1cm ileal length taken 2.5cm from the ileocaecal valve). All fetuses were pseudonymised and all specimens labelled with the relevant code blinding the investigator to the origin of the tissue for the remainder of the experiment.

Additional internal control bowel samples that could have been included in the study were; (1) non-eviscerated bowel from AWD fetuses (e.g. duodenum or colon) and (2) corresponding section of bowel from phenotypically normal fetuses. These groups were not included due to limitations of time and prioritising the inclusion of motility studies.

### ***2.1.9.2 Gut Length and Weight***

The excised gut was placed in a pre-weighed 1.5ml centrifuge tube containing 1x PBS and weighed. The gut weight (g) was calculated (gut weight = total weight – known tube weight).

The gut was then placed in a dissecting dish (10cm petri dish with SYLGARD® 184 silicone elastomer covering the base) containing 1x PBS. The gut was straightened by cutting the mesentery between gut loops, pinned along the mesentery avoiding placing pins into the gut tissue and the length measured (cm), trying not to stretch the gut. The weight per unit length (g/cm) was subsequently calculated (weight ÷ length).

### **2.1.10 Gut Motility Studies**

In order to determine whether differences in ICC numbers resulted in a change in gut function, motility studies were performed to compare contractility between ACLP mouse model groups.

#### ***2.1.10.1 Gut Preparation***

Fetal dissection was performed in oxygenated physiological Ringer's solution. The gut from gastroesophageal junction to ileocaecal valve was removed from five fetuses in each ACLP mouse model experimental group. The gut was straightened and the mesentery removed. The tissue was then transferred to an organ bath containing physiological Ringer's solution, heated to a temperature of 37°C with bubbled oxygen and a pin placed in the stomach, which was positioned to the right of the organ bath and the terminal ileum, which was positioned to the left of the organ bath. The gut was allowed to equilibrate for 30 minutes to enable restoration of normal bowel contractility before imaging of the ileum was commenced.

#### ***2.1.10.2 Motility Imaging***

The bubbled oxygen was turned off 5 minutes prior to imaging and remained off for the duration of the recording to prevent rippling of the Ringer's solution and

movement artefact of the bowel. Additionally, oxygenation of the organ bath created air bubbles therefore any bubbles adherent or overlying the gut wall were dislodged prior to imaging. Still images of the ileum were taken every 0.5 seconds for 60 seconds. The camera lens zoom and distance of the gut from the lens was the same for all recordings. The camera recorded a horizontally inverted, black and white image of the gut resulting in the oral end of the gut positioned to the left of the image, the anal end to the right of the image with the gut appearing white (Figure 2-3A). The lighting in the room was kept consistent for all recordings. A reference image was taken of graph paper with 1mm increments in order to calculate the number of pixels per unit area and detect any distortion from the camera lens (Figure 2-3B).

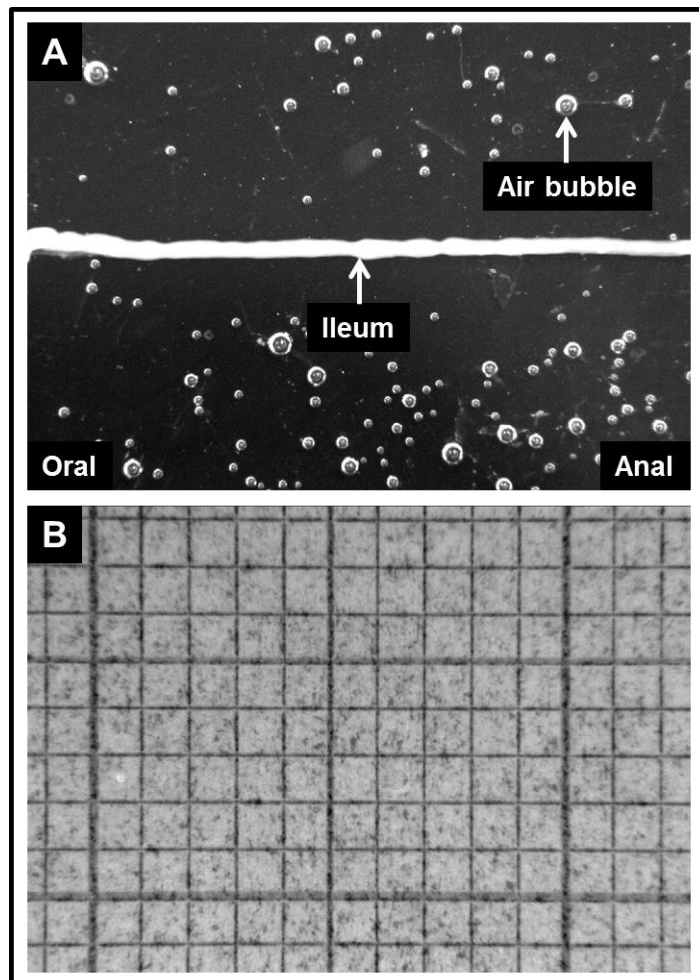


**Figure 2-3:** Gut motility recording. **A.** One frame taken from a 60 second recording of ileal motility. The ileum appears white in this black and white image. Also evident are numerous air bubbles generated from oxygenation of the organ bath. **B.** Reference image of graph paper with 1mm increments.

### ***2.1.10.3 Gut Edge Detection and Spatiotemporal Mapping***

A MATLAB algorithm, created by Dr Alison Hart (affiliation: independent) was used to analyse the ileal recordings. Firstly, the image was vertically inverted and the gut edge detected based on changes in light intensity between the white gut and black background and the centre point of the bowel calculated (Figure 2-4B). Following edge detection, vertical slice analysis at each pixel incremental point (pixel width 0.22mm) along the length of the bowel was used to calculate diameter changes. This enabled changes in the mean gut diameter at each vertical slice to be calculated over time (Figure 2-4C) creating spatiotemporal maps. Measurement of ileal diameter change provided a surrogate marker for strength of gut contractions.

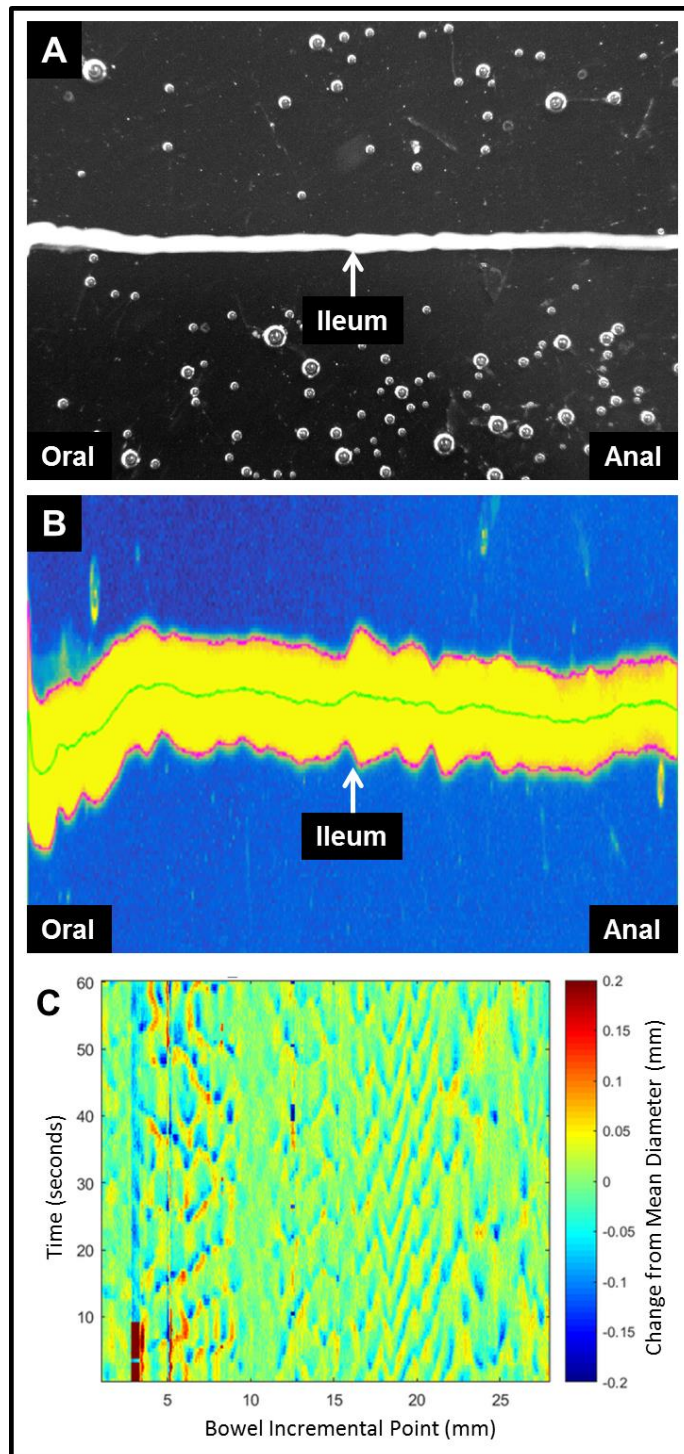


**Figure 2-4:** Ileal edge detection using MATLAB software. **A.** Original frame from ileal recording. **B.** Vertically inverted light intensity image created in MATLAB. Ileum appears yellow, the pink line indicates the ileal edge and the green line is the centre point of the bowel. **C.** Graph representing change from mean diameter (mm) against vertical slice bowel incremental point (mm) with time (seconds).



#### ***2.1.10.4 Frequency of Gut Contractions***

For each vertical slice the change in bowel diameter was converted into a plot showing change from mean diameter against time (Figure 2-5A). This data was used to generate a fast Fourier transform (FFT), which breaks each signal into sine waves with an amplitude, frequency and phase. The sine wave with the largest amplitude was used to determine the dominant frequency of contraction at each bowel incremental point (Figure 2-5B). Frequency was then converted into contractions per minute (Figure 2-5C).

#### ***2.1.10.5 Statistical Analysis of Gut Motility***

Mean values for each experiment were calculated and graphically plotted for contraction strength and dominant frequency of contractions. These graphs and spatiotemporal maps were qualitatively assessed and described. Additionally, the data points were used to compare absolute numbers and the area under the curve using ANOVA.

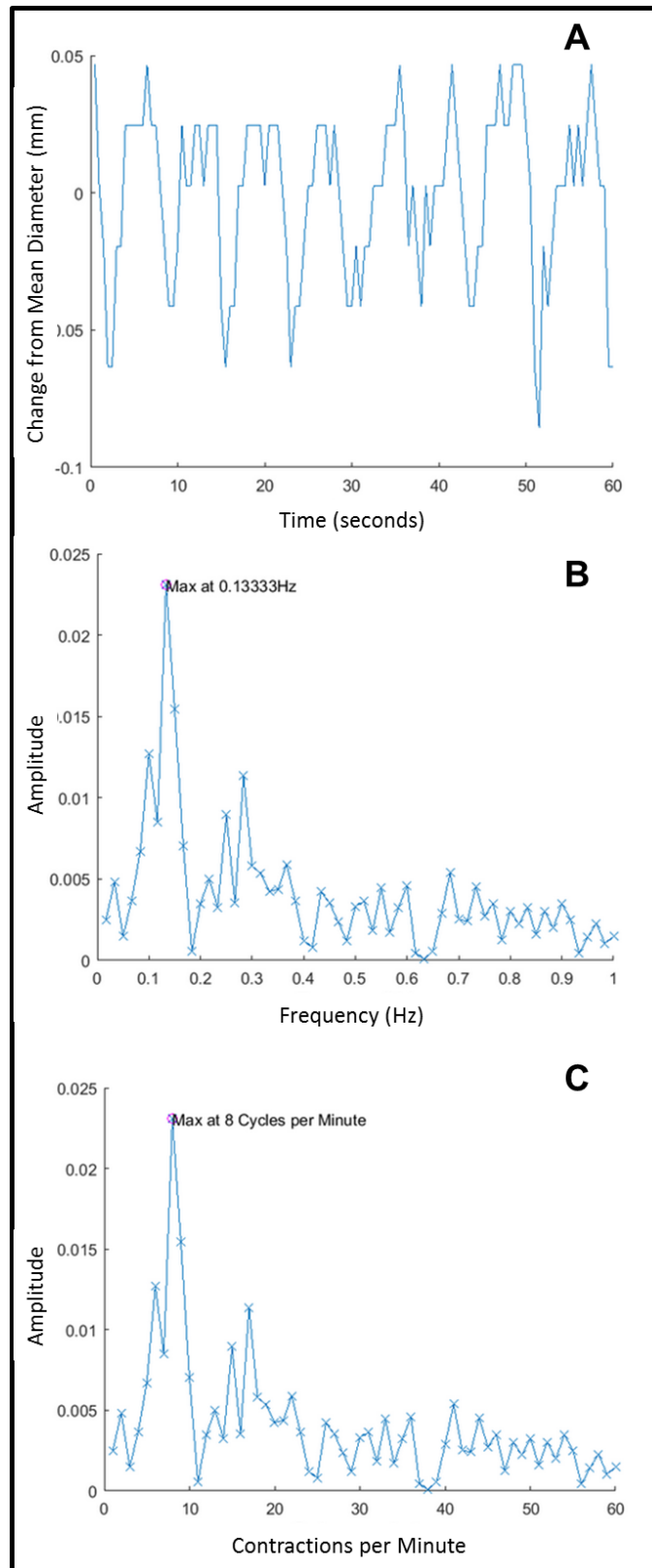


**Figure 2-5:** analysis of frequency of gut contractions using MATLAB software. **A.** Change in ileal diameter over time for one vertical slice analysis. **B.** Fast Fourier transform (FFT) highlighting the most dominant frequency of contraction. **C.** FFT converted from frequency to contractions per minute.

## **2.2 Archived Human Gut Tissue General Methods**

### **2.2.1 Ethics Statement**

Studies involving archived human gut tissue were approved by the London – City Road and Hampstead NHS Research Ethics Committee (reference number 11/LO/1030). This allowed for archived human gut tissue stored pre 2006 and those stored under the Human Tissue Act to be used for research purposes without the need for patient consent.

### **2.2.2 Sample Selection Criteria**

Small bowel tissue processed and paraffin embedded in either a longitudinal or transverse orientation by the GOSH pathology department and stored pre 2006 or under the Human Tissue Act were included. All identified tissue was reviewed by Professor Neil Sebire, Professor of Paediatric and Developmental Pathology, Great Ormond Street Hospital and only specimens with grossly normal resection margins (Figure 2-6A) were selected. Small bowel tissue with grossly abnormal resection margins (Figure 2-6B) were excluded due to gross destruction of tissue architecture. This enabled comparison of architecturally similar tissue only.

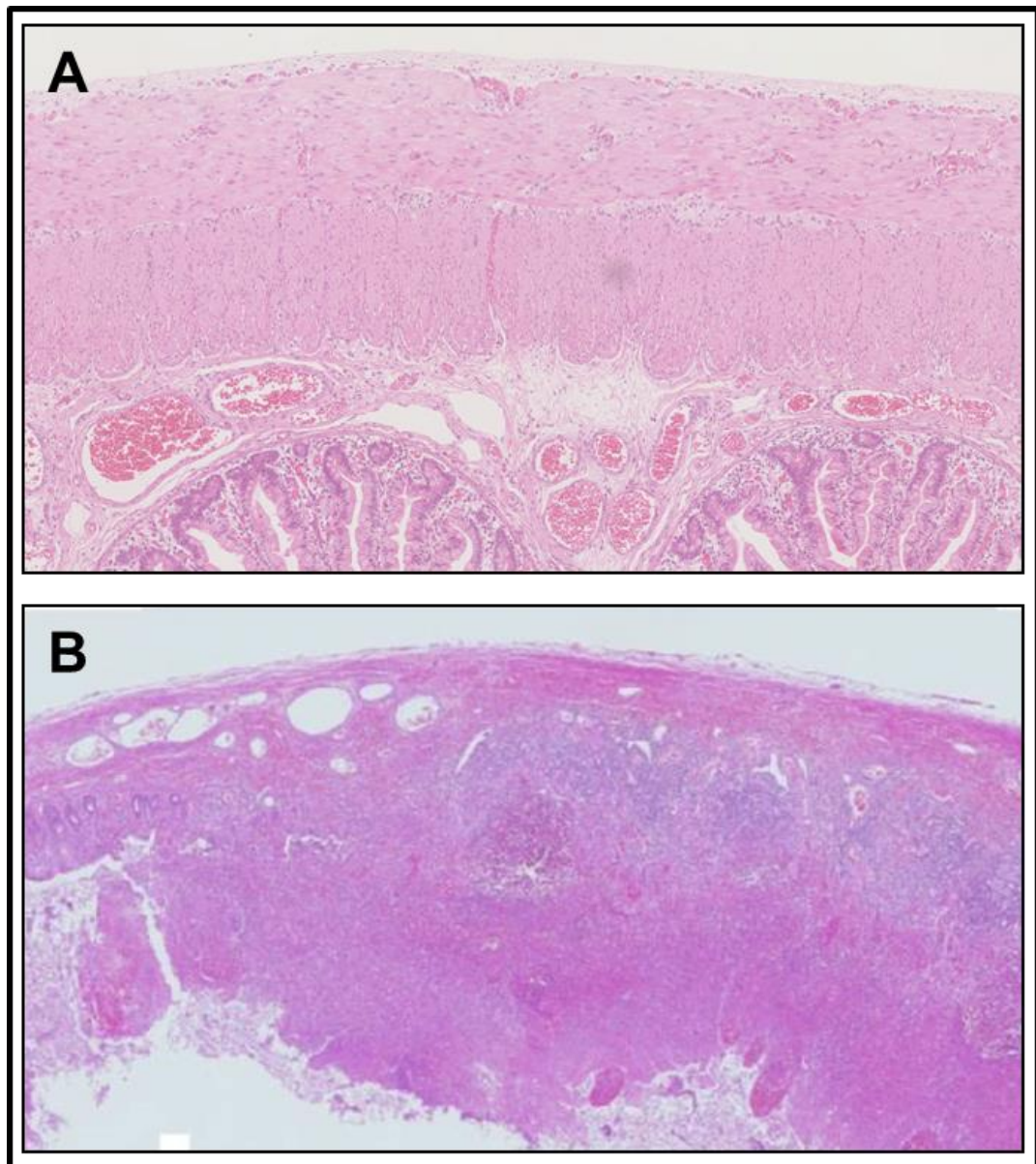


**Figure 2-6:** Sample selection criteria. **A.** Inclusion of grossly normal resection margins. **B.** Exclusion of grossly abnormal resection margins.

### 2.2.3 Specific Inclusion and Exclusion Criteria

Bowel is not resected from simple gastroschisis or otherwise healthy infants unless there is concomitant intestinal pathology. As such, it is not possible to obtain samples from otherwise healthy gastroschisis infants or completely normal controls.

Therefore, specific conditions have been included and excluded from the studies to prevent results being impacted by other pathologies.

### ***2.2.3.1 Inclusion Criteria for ICC and Enteric Neuron Analysis***

The control group included small bowel specimens resected from otherwise healthy infants for intussusception, strangulated hernia, volvulus, Meckel's diverticulum, isolated perforation and stenosis. The gastroschisis study group included small bowel specimens that were resected from gastroschisis infants due to ischaemia, necrosis, anastomotic stricture, stenosis, perforation and persistently dysmotile bowel. Due to poor labelling at the time of surgery the resected tissue was generally labelled as 'small bowel' and therefore it was not possible to distinguish between ileal and jejunal tissue.

### ***2.2.3.2 Exclusion Criteria for ICC and Enteric Neuron Analysis***

Tissue resected from gastroschisis or otherwise healthy infants for a concomitant condition that in the literature has been reported to have low ICC, including atresia (Tander et al., 2010, Midrio et al., 2010) and meconium ileus (Toyosaka et al., 1994, Yoo et al., 2002) were excluded. Tissue resected for conditions known to cause bowel wall inflammation were also excluded to prevent results being influenced by inflammation from a different pathological sequence. As such, necrotising enterocolitis, which causes significant bowel wall inflammation, and stoma reversal tissue, which is known to exhibit chronic inflammatory changes, were excluded. Finally, post-mortem bowel specimens were also excluded because the gastrointestinal tract autodigests rapidly following death.

### ***2.2.3.3 Inclusion Criteria for Bowel Wall Morphological Analysis***

In addition to the inclusion criteria for ICC and enteric neuron analysis, in order to increase numbers within the morphological study, small bowel resected from gastroschisis and otherwise healthy infants for atresia and meconium ileus were also included as there is no evidence that these conditions cause gross morphological changes.

#### **2.2.3.4 Exclusion Criteria for Bowel Wall Morphological Analysis**

Inflammation and necrosis causes significant disruption to the normal architecture of the bowel wall and therefore post-mortem bowel specimens and bowel resected for necrotising enterocolitis and stoma closure were excluded.

#### **2.2.4 Specimen Identification**

Specimens were identified through interrogation of the GOSH pathology electronic database. All H&E sections relating to the identified specimens were reviewed under a microscope with a Consultant Histopathologist and any abnormal resections were identified and excluded.

#### **2.2.5 Specimen Pseudonymisation**

All samples were given a unique identifier ensuring confidentiality. The code for the pseudonymisation was kept on a password protected NHS computer by the histopathology pathology department and the investigator blinded preventing potential researcher bias.

#### **2.2.6 Clinical Data Collection**

Clinical data was collected on the year of birth, GA at delivery, age at bowel resection, reason for bowel resection, concomitant gastrointestinal pathology (atresia, stenosis, necrosis, perforation, volvulus and necrotizing enterocolitis), ENT and LOS.

#### **2.2.7 Specimen Sectioning**

Twenty two 3µm sections were cut from each specimen block. Table 2-4 delineates how these 22 sections were utilised during this study.

Number of Sections	Tissue Staining	Purpose
5	Triple stain: Anti-CD117, anti-HuC/D and DAPI (immunofluorescence)	Quantify ICC and enteric neurons
5	H&E	Morphological assessment of the bowel wall
3	Alpha smooth muscle actin (immunohistochemistry)	Quantify smooth muscle
3	Picrosirius red	Quantify collagen
3	Ki67 (immunohistochemistry)	Quantify proliferating nuclei
3	TGF $\beta$ 3 (immunohistochemistry)	Quantify inflammation

**Table 2-4:** Breakdown of tissue staining performed on the sectioned human small bowel tissue.

## 2.3 ICC and Enteric Neuron Quantification (Animal and Human Tissue)

### 2.3.1 Outcome Measures

The primary outcome measure was ICC density. The secondary outcome measure was enteric neuron density. For the archived human gut study, an additional secondary outcome measure was ENT defined as the time taken from birth to achieve ENT as described in the hospital charts.

### **2.3.2 ICC and Enteric Neuron Quantification Method Selection**

In the literature several quantitative methods for ICC and enteric neuron quantification have been described including; flow cytometry to quantify CD117 positive ICC from fresh bowel tissue (Chen et al., 2014), image software processing of high powered fields of view to calculate the area of positive staining (Wang et al., 2009, Bernardini et al., 2012) and manual counting of cell bodies from high powered fields of view (Bernardini et al., 2012). However, all previous gastroschisis animal studies (Vargun et al., 2007, Auber et al., 2013, Midrio et al., 2004, Krebs et al., 2014, Danzer et al., 2010) and the only published human data at the time of starting this thesis research (Midrio et al., 2008) have utilised semi-quantitative (e.g. cell grading system of sparse: 0-2 cells, few: 3-7 cells, moderate: 8-12 cells and many: >12 cells (Danzer et al., 2010)), qualitative (e.g. cell grading system of 1 for mature, 2 for moderately mature and 3 for very mature (Auber et al., 2013)) or descriptive (Midrio et al., 2008) methods for quantifying ICC and enteric neuron numbers. All off these semi-quantitative methods have limitations and are not suitable for robust quantification comparisons between groups.

For the purposes of this study manual cell counting from high powered fields of view was selected for the quantification of ICC and enteric neurons in both animal and human tissue in order to provide method uniformity across the study. A cell was defined as an area of positive staining containing a nucleus as previously described in the literature (Swaminathan and Kapur, 2010). Image software analysis to calculate the percentage area of positive staining was not used as background staining may impact on the detection of true positive staining resulting in misleading results.

### **2.3.3 Animal Gut Tissue Preparation for Immunofluorescence**

Both transverse cross-sectioned and whole mount ileal tissue preparations were tested to determine which was the most appropriate for accurate quantification of ICC and enteric neurons. For both gut preparation techniques immunofluorescence was performed on 1.5cm ileal lengths taken 1cm from the ileocaecal valve.



### ***2.3.3.1 Transverse Cross-Sectioned Ileal Tissue***

The luminal contents of the ileum were washed out using 1x PBS. The whole ileal tube was then fixed in 4% PFA for 30 mins at room temperature and 60 minutes at 4°C, followed by 6 washes (20 minutes per wash) in 1x PBS at room temperature and placed in 30% glucose solution overnight at 4°C. The ileum was cut into 0.5cm sections, stood vertically in OCT wells and stored at -80°C. Five transverse cross-sections (4µm) were cut using a cryostat. OCT medium was aspirated off the slide, the tissue fixed with 4% PFA and washed twice with 0.1% Triton X-100 in 1x PBS (PBT). The immunofluorescence protocol was then started on the same day.

### ***2.3.3.2 Whole Mount Ileal Tissue***

During the Scribble knockout model experiments, whole mount ileal tissue was prepared by removing the mucosa from the underlying muscularis propria leaving the muscle layers and serosa intact. However, fetal mouse ileum at 18.5 dpc is very fragile with a diameter of approximately 1 – 2mm resulting in specimens being damaged and therefore discarded. Therefore, a second technique was developed during the ACLP knockout experiments in which immunostaining was performed on lengths of intact ileum reducing specimen loss and simplifying tissue processing.

#### ***2.3.3.2.1 Whole Mount Tissue: Muscle Layer Only***

In a dissecting dish containing 1x PBS, the ileum was pinned along the mesentery avoiding placing pins in the ileal tissue. Micro spring scissors were used to cut the ileum longitudinally along the mesenteric border opening the ileal tube. The ileum was additionally pinned along the anti-mesenteric border under tension to flatten the tissue. Dumont micro forceps were used to delicately strip the mucosa from the underlying muscularis propria through application of mesenteric counter traction and grasping of the mucosal folds. Specimens were fixed using 4% PFA for 20 minutes and washed 6 times (20 minutes per wash) in 1x PBS at room temperature. The immunofluorescence protocol was then started on the same day.

#### 2.3.3.2.2 *Whole Mount Tissue: Intact Gut Tube*

In a dissecting dish containing 1x PBS, the ileum was pinned along the mesentery avoiding placing pins in the ileal tissue. Specimens were fixed using 4% PFA for 20 minutes and washed 6 times (20 minutes per wash) in 1x PBS at room temperature. The immunofluorescence protocol was then started on the same day.

#### 2.3.4 **Human Gut Tissue Preparation for Immunofluorescence**

Immunofluorescence was performed on 5 sections per paraffin embedded specimen, which were cut a distance of 12µm apart (every fourth slide cut) to reduce the possibility of quantifying the same cell more than once. The paraffin sections were dewaxed, rehydrated and antigen retrieval performed as previously described in the animal models general methods section. The immunofluorescence protocol was then started on the same day.

#### 2.3.5 **Immunofluorescence Protocols**

Ileal tissue was triple labelled for ICC, enteric neurons and nuclei. The appropriate primary and secondary antibody concentrations were worked up using adult mouse gut tissue or human control gut tissue by testing 5 concentrations (e.g. 1:100, 1:250, 1:500, 1:750 and 1:1000) based around the manufacture's recommended range. During experiments adult gut from the euthanized dam and control human gut tissue was used as a positive and negative control. For the negative control the same immunofluorescence protocol was followed but the primary antibodies were omitted.

##### 2.3.5.1 *Interstitial Cells of Cajal*

ICC express the protooncogene *c-kit* (Maeda et al., 1992), which encodes a transmembrane receptor tyrosine kinase that when blocked or knocked out results in ICC loss, electrical quiescence and loss of bowel motility (Maeda et al., 1992). As such, *c-kit* is an essential pathway for function and maintenance of ICC. Given this, anti-CD117/*c-kit* is the most commonly used ICC marker. However, anti-CD117 also labels mast cells, which are usually located within the bowel mucosa but have a distinctly different architecture compared to ICC (round independent mast cells

versus interconnecting, branching ICC). Although ANO1, a calcium-activated chloride channel, has been identified as a potentially more specific ICC marker (Gomez-Pinilla et al., 2009), anti-CD117 was chosen for these experiments given that mast cells are rarely located within the muscularis propria and can be easily identified and therefore excluded during manual cell counting. Anti-CD117 reliably labelled ICC when applied to cross-sectional and whole mount tissue preparation methods.

### **2.3.5.2 *Enteric Neurons***

There are multiple markers of enteric neurons. For investigations using the Scribble knockout mouse model, anti-TUJ1 was used, which is a marker of neuron-specific class III beta-tubulin and is expressed in neurons of the peripheral and central nervous system located in neuronal cell bodies and axons.

During the ACLP knockout mouse experiments, anti-HuC/D was tested in order to improve identification of enteric neuronal cell bodies. HuC/D specifically labels antigens that are present only on neuronal cell bodies. However, this antibody did not penetrate and label the enteric neurons of whole mount specimens prepared by the intact gut tube method even. Multiple alterations to the staining protocol were tried with no success including varying concentrations of anti-HuC/D primary antibody solution, incubating the tissue in separate anti-HuC/D and anti-CD117 primary antibody solutions, modifications to the blocking solution used and longer duration, varying temperatures and agitation on a shaker during tissue incubation in the anti-HuC/D primary antibody solution. Therefore this antibody was not used further for this application. Anti-TUJ1 also erratically labelled enteric neurons using the intact gut tube whole mount method. Anti-PGP9.5, which labels the cell bodies and axons of the peripheral and central nervous system, was used for the ACLP knockout mouse model experiments as it reliably labelled enteric neurons of intact gut tube whole mounts.

For human gut tissue anti-HuC/D was used, which reliably labelled the enteric neuronal cell bodies of human cross sectioned tissue and has previously been

reported as a robust means for counting all enteric neuron cell bodies in human gut tissue (Murphy et al., 2007a).

### ***2.3.5.3 Nuclei***

Nuclei were labelled using DAPI (4',6-diamidino-2-phenylindole), which is a fluorescent stain that strongly binds to AT rich regions of DNA. The fluorescent stain passes through intact cell membranes providing a robust method of nuclear staining.

### ***2.3.5.4 Immunofluorescence Staining Protocol for Cross-Sectioned Tissue***

Blocking solution (as outlined in Table 2-5) was applied for 2 hours at room temperature and then washed off using PBT. A combined primary antibody (antibodies listed in Table 2-6) diluted in blocking solution was applied for 2 hours at room temperature. This was followed by 6 washes with PBT and application for 1 hour at room temperature of a combined secondary antibody (antibodies listed in Table 2-7) diluted in blocking solution. Slides were washed with PBT, DAPI (1:1000, emission colour blue) was applied for 10 minutes at room temperature and washed a further 4 times with PBT. Slides were sealed using VECTASHIELD HardSet mounting medium and stored at 4°C.

Tissue Type	Blocking Solution Composition
Mouse tissue	0.1% Triton X-100 in 1x PBS (PBT) 1% bovine serum albumin 0.15% glycine
Human tissue	PBT 1% bovine serum albumin 0.15% glycine 10% sheep serum

**Table 2-5:** Blocking solutions for cross-sectioned tissue immunofluorescence.

Tissue Type	Target	Raised in	Dilution	Antibody Type	Supplier
Mouse	CD117	Goat	1:500	Polyclonal	R&D Systems
Mouse	TUJ1	Rabbit	1:500	Monoclonal IgG	Covance
Human	CD117	Rabbit	1:500	Polyclonal	Dako
Human	HuC/D	Mouse	1:100	Monoclonal IgG	Thermo Fisher Scientific

**Table 2-6:** Primary antibodies for cross-sectioned tissue immunofluorescence.

Tissue Type	Target	Raised in	Dilution	Colour Emission	Supplier
Mouse	Goat	Donkey	1:250	Green (488nm)	Alexa Fluor
Mouse	Rabbit	Chicken	1:250	Red (594nm)	Alexa Fluor
Human	Rabbit	Goat	1:500	Green (488nm)	Alexa Fluor
Human	Mouse	Donkey	1:250	Red (594nm)	Alexa Fluor

**Table 2-7:** Secondary antibodies for cross-sectioned tissue immunofluorescence.

#### **2.3.5.5 Immunofluorescence Staining Protocol for Whole Mount Tissue**

Ileal whole mounts were soaked in blocking solution (PBS + 1% bovine serum albumin + 1% Triton X-100) at room temperature for 2 hours. The ileum was then soaked overnight at 4°C in a combined primary antibody (antibodies listed in Table 2-8) mixture diluted in 1x PBS + 1% Triton X-100. Six washes with 1x PBS (20 minutes per wash) were performed. The ileum was then soaked for 1 hour at room temperature in a combined secondary antibody (antibodies listed in Table 2-9) mixture diluted in 1x PBS + 1% Triton X-100. This was followed by 10 minutes at room temperature in DAPI (1:1000, emission colour blue) and 6 washes of 1x PBS. Whole mounts were slide mounted flat, sealed using VECTASHIELD HardSet mounting medium and stored at 4°C.

Animal Model	Target	Raised in	Dilution	Antibody Type	Supplier
ACLP and Scribble	CD117	Goat	1:500	Polyclonal	R&D Systems
Scribble	TUJ1	Rabbit	1:500	Monoclonal IgG	Covance
ACLP	PGP9.5	Mouse	1:500	Monoclonal IgG	abcam

**Table 2-8:** Primary antibodies for whole mount immunofluorescence.

Tissue Type	Target	Raised in	Dilution	Colour Emission	Supplier
ACLP and Scribble	Goat	Donkey	1:250	Green (488nm)	Alexa Fluor
Scribble	Rabbit	Chicken	1:250	Red (594nm)	Alexa Fluor
ACLP	Mouse	Donkey	1:250	Red (594nm)	Alexa Fluor

**Table 2-9:** Secondary antibodies for whole mount immunofluorescence.

### 2.3.6 Immunofluorescence Imaging

ICC and enteric neurons at the level of the myenteric plexus were chosen for quantification as both cell populations are well developed at 18.5 dpc in mouse fetuses and at full term in human fetuses.

### 2.3.6.1 Cross-Sectioned Tissue

Images of 10 high powered fields of view at 40x objective were taken per specimen at the level of the myenteric plexus using a Zeiss Axioplan 310 fluorescence microscope. All images were taken with the myenteric plexus running in a transverse orientation across the field of view to ensure uniformity of the area quantified (Figure 2-7).

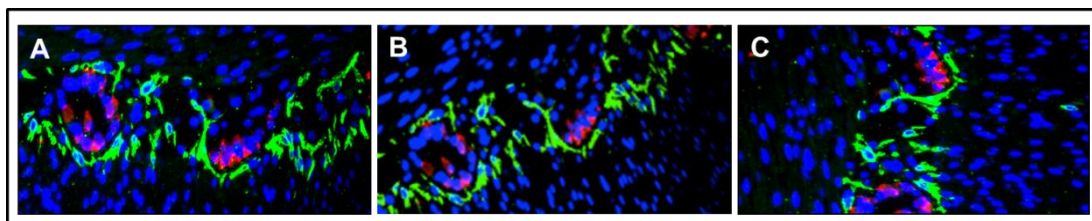


**Figure 2-7:** Random image orientation leads to differing myenteric plexus lengths and would give different counts for the same tissue region. A. Horizontal orientation. B. Diagonal orientation. C. Vertical orientation.

### 2.3.6.2 Whole Mount Tissue

Images of 10 high powered fields of view at 40x objective were taken per specimen at the level of the myenteric plexus using a Zeiss LSM 710 confocal microscope (Figure 2-8) creating z stack image sets through the entire three dimensional plexus. The confocal settings used were as follows; frame size 784x784, speed 10, averaging number 1, pinhole 1 airy unit (AU) at an interval of 0.55 $\mu$ m, imaging in 3 colour channels (488nm green, 594nm red and DAPI blue).



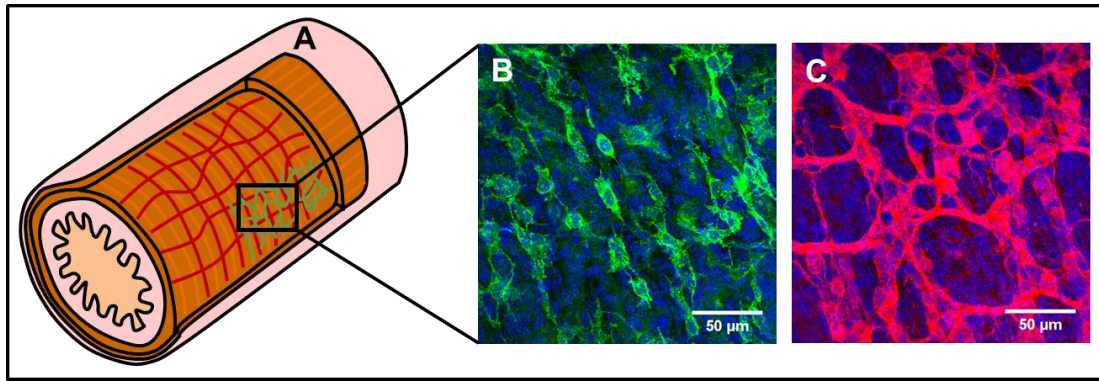


**Figure 2-8:** A. Schematic of ileum, rectangle indicating the region imaged at high power (40x objective). Maximum intensity project images of confocal z-stacks. B. Anti-CD117 green, DAPI blue. C. Anti-PGP9.5 red, DAPI blue.

### 2.3.7 ICC and Enteric Neuron Quantification

#### 2.3.7.1 Cross-Sectioned Tissue

Colour channels were combined as follows; green (ICC)/blue (nuclei, Figure 2-9) and red (enteric neurons)/blue (Figure 2-10). Images were reviewed using ImageJ (NIH, USA) software. ICC cell bodies (green staining surrounding a blue nucleus, Figure 2-9) and neuronal cell bodies (red staining surrounding a blue nucleus, Figure 2-10) were counted manually using ImageJ cell counter software. Counts were performed blinded to the tissue origin.

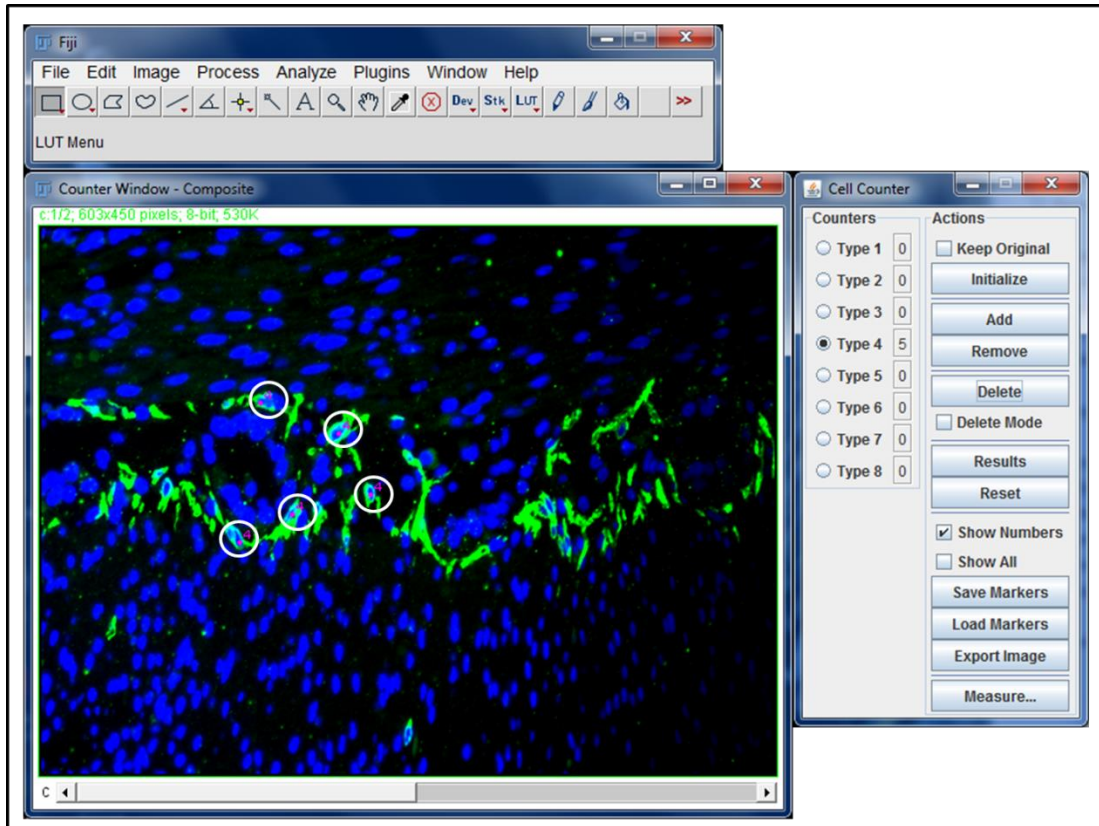


**Figure 2-9:** ImageJ anti-CD117 (ICC, green) and DAPI (nuclei, blue) combined image and ImageJ cell counter software. Magenta markers (indicated with white circles) highlighting counted ICC cell bodies.

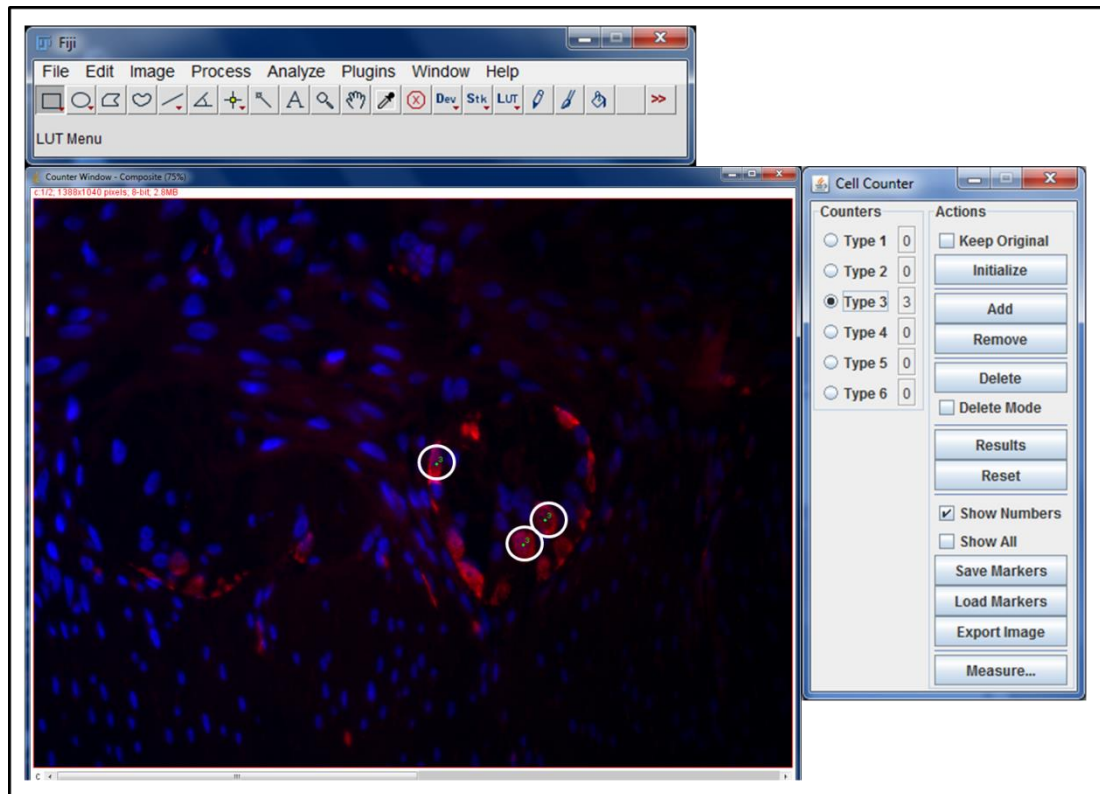


**Figure 2-10:** ImageJ anti-HuC/D (enteric neuron, red) and DAPI (nuclei, blue) combined image and ImageJ cell counter software. Green markers (indicated with white circles) highlighting counted ICC cell bodies.

### 2.3.7.2 Whole Mount Tissue

The 3 colour channels (ICC green, enteric neurons red, nuclei blue) of the confocal z stack image sets were initially separated, followed by combining of green/blue and red/blue colour channels to create maximum intensity project images for both ICC (Figure 2-11) and enteric neurons (Figure 2-12) using ImageJ software (Figure 2-4). ICC cell bodies (green staining surrounding a blue nucleus, Figure 2-11) and neuronal cell bodies (red staining surrounding a blue nucleus, Figure 2-12) were counted manually using ImageJ cell counter software.

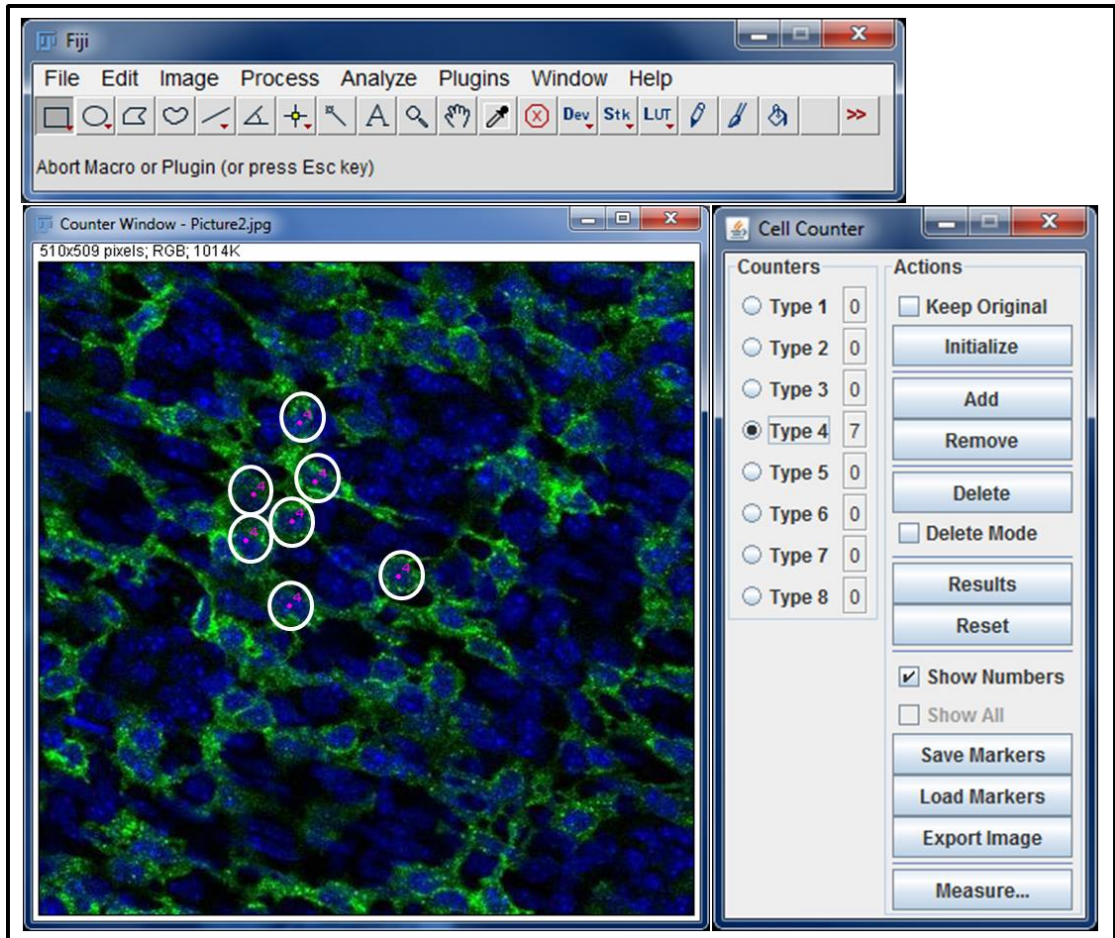


**Figure 2-11:** ImageJ ICC maximum intensity project (anti-CD117, ICC, green and DAPI, nuclei, blue) and ImageJ cell counter software. Magenta markers (indicated with white circles) highlighting counted ICC cell bodies.



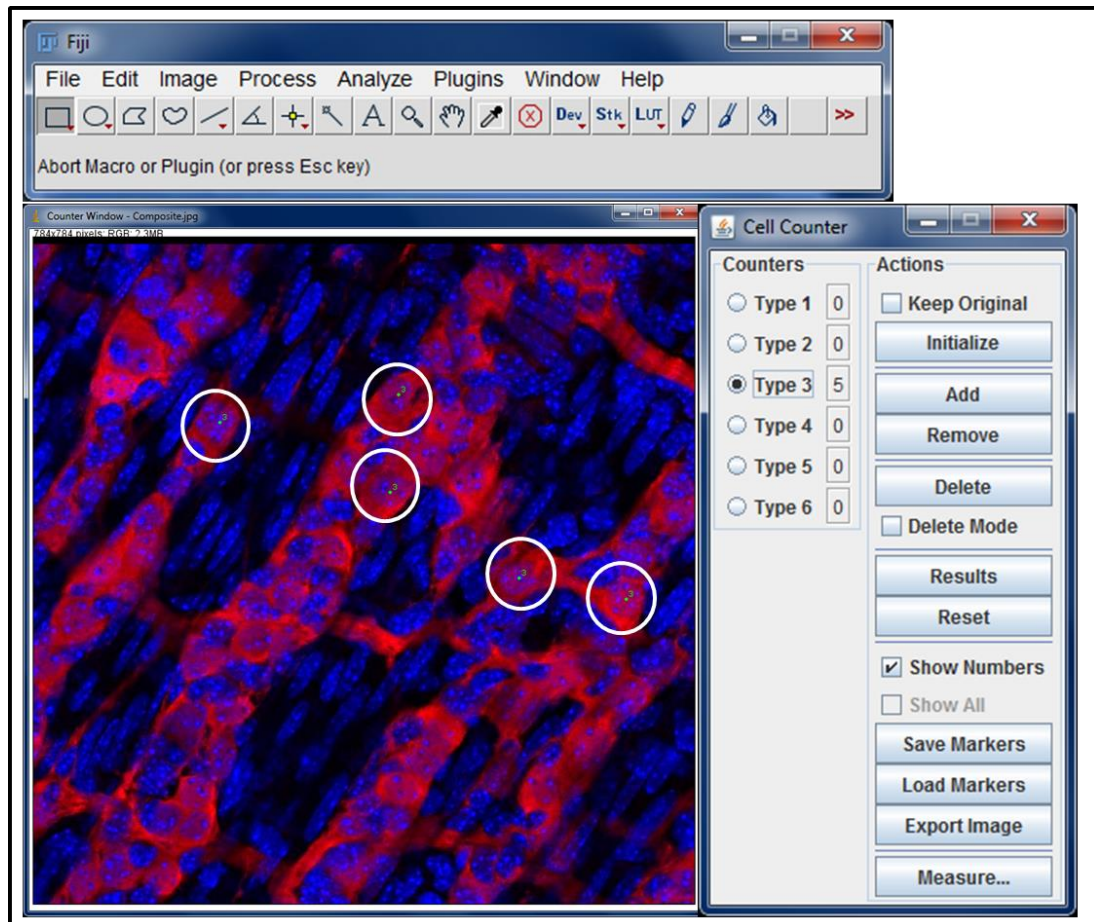


**Figure 2-12:** ImageJ enteric neuron maximum intensity project (Anti-PGP9.5, enteric neurons, red and DAPI, nuclei, blue) and ImageJ cell counter software. Green markers (indicated with white circles) highlighting counted enteric neuron cell bodies.

## 2.4 Bowel Wall Thickness and Morphology (Animal and Human Tissue)

H&E staining of paraffin embedded transversely sectioned ileum was performed in order to analyse the gross architecture of the ileum for each experimental group.

### 2.4.1 Animal Gut Tissue Preparation Morphological Studies

Paraffin embedding was performed on 1cm ileal lengths taken 2.5cm from the ileocaecal valve. The ileum was fixed in 4% PFA overnight at 4°C, cut into 0.5cm lengths. The tissue was then dehydrated, cleared in xylene and paraffin embedded (as previously described in the animal models general methods section) vertically. Five

transverse 3µm sections were cut and H&E stained as previously described in the animal models general methods section.

#### **2.4.2 Human Gut Tissue Preparation for Morphological Studies**

Five sections (3µm) were stained with H&E and 3 sections were stained for each immunohistochemical marker.

#### **2.4.3 Histology Staining Protocols**

##### ***2.4.3.1 H&E Staining Protocol***

The paraffin sections were dewaxed, rehydrated and H&E stained as previously described in the animal models general methods section.

##### ***2.4.3.2 Immunohistochemistry and Picrosirius Red Staining Protocols***

Staining for alpha smooth muscle actin ( $\alpha$ -SMA), collagen (picrosirius red [PS]) and proliferating nuclei (Ki67) was performed on human gut tissue to determine whether increased myopathy, fibrosis or cell proliferation (respectively) was present in gastroschisis bowel compared to controls. Additionally, sections were stained for TGF $\beta$ 3 as a marker of inflammatory and morphogenic triggers in gastroschisis bowel wall compared to controls. Three sections were stained for each marker.

Paraffin sections were dewaxed as previously described in the animal models general methods section. Antigen retrieval was not required for these markers.

Alpha-SMA, Ki67 and TGF $\beta$ 3 staining was performed (one stain per section) using the automated Leica BondMax system using the antibodies listed in Table 2-10 with a DAB detection kit and Eosin counterstain.

For PS staining, slides were placed in picrosirius red for one hour.

Sections were rehydrated and mounted following staining as previously described in the animal models general methods section.

Target	Raised in	Dilution	Antibody Type	Supplier
$\alpha$ -SMA	Mouse	Ready to use preparation	Monoclonal IgG	Leica
Ki67	Mouse	Ready to use preparation	Monoclonal IgG	Leica
TGF $\beta$ 3	Rabbit	1:100	Polyclonal	abcam

**Table 2-10:** Primary antibodies for immunohistochemistry staining

#### 2.4.4 Histology Imaging

##### 2.4.4.1 *Imaging of H&E Cross-Sections*

The H&E ileal transverse cross-sections were imaged using the Zeiss AxioScan Z1 slide scanner at 40x objective creating a virtual image of the entire cross-section.

##### 2.4.4.2 *Imaging of Immunohistochemistry Cross-sections*

Bright field images of 10 high powered fields of view at 40x objective on a Zeiss Axioplan 310 microscope were taken. Bowel wall layers were imaged as outlined in Table 2-11. All images were taken with the bowel wall running in a transverse orientation across the field of view to ensure uniformity of the area quantified

Immunohistochemistry Stain	Bowel Wall Layer Imaged
$\alpha$ -SMA	Longitudinal muscle Circular muscle
Ki67	Longitudinal muscle Circular muscle
TGF $\beta$ 3	Longitudinal muscle Circular muscle Submucosa Epithelium
PS	Serosa Longitudinal muscle Circular muscle Submucosa

**Table 2-11:** Bowel wall layers imaged by stain.

## 2.4.5 Morphological Bowel Wall Analysis

### 2.4.5.1 Bowel Wall Measurements and Muscle Fibre Quantification

Bowel wall measurements ( $\mu\text{m}$ ) were taken at the thinnest point in the section to remove bias from oblique sectioning using the measurement tool in the Zeiss ZEN lite imaging software. Layers measured in mouse bowel include; entire outer wall, submucosa and muscle layer thickness, villus length (longest villus in the section) and crypt depth (Figure 2-13). Layers measured in the human bowel include; entire outer wall, submucosa, circular muscle, longitudinal muscle and serosal thickness, villus height (longest villi in the section) and crypt depth (Figure 2-14). The villus to crypt ratio (villus height/crypt depth) was calculated for both the animal and human measurements. Additionally, the number of circular and longitudinal muscle fibres



that bisected the measurement line were counted and the muscle fibre thickness calculated (muscle layer thickness [ $\mu\text{m}$ ]/number of muscle fibres = muscle fibre thickness [ $\mu\text{m}$ ]). For each specimen, a total of 10 of each measurement were made.

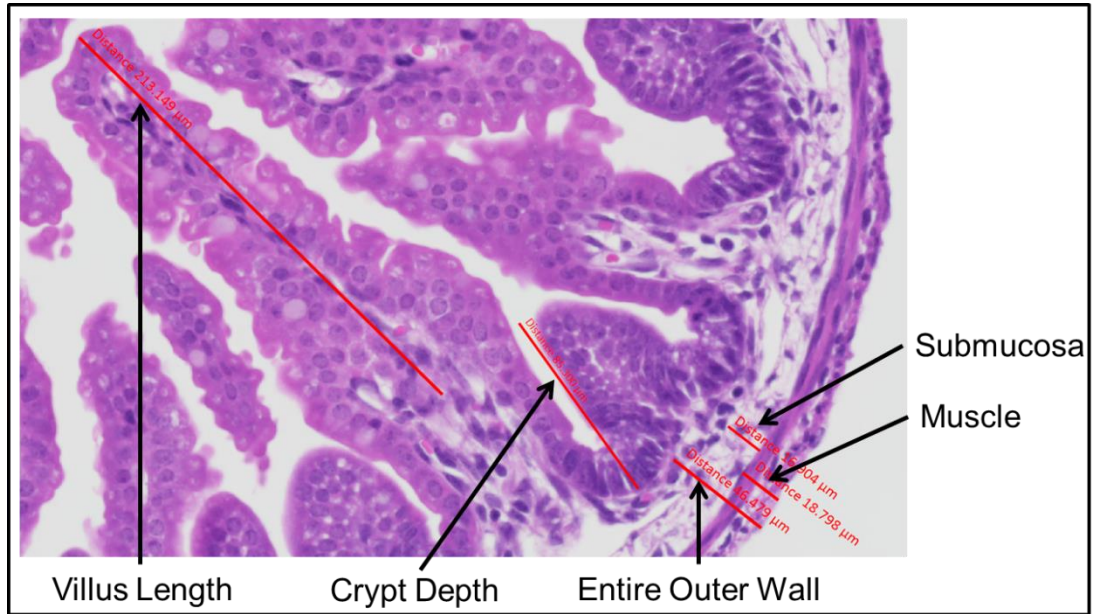


**Figure 2-13:** Mouse bowel wall measurements performed using Zeiss ZEN lite imaging software.

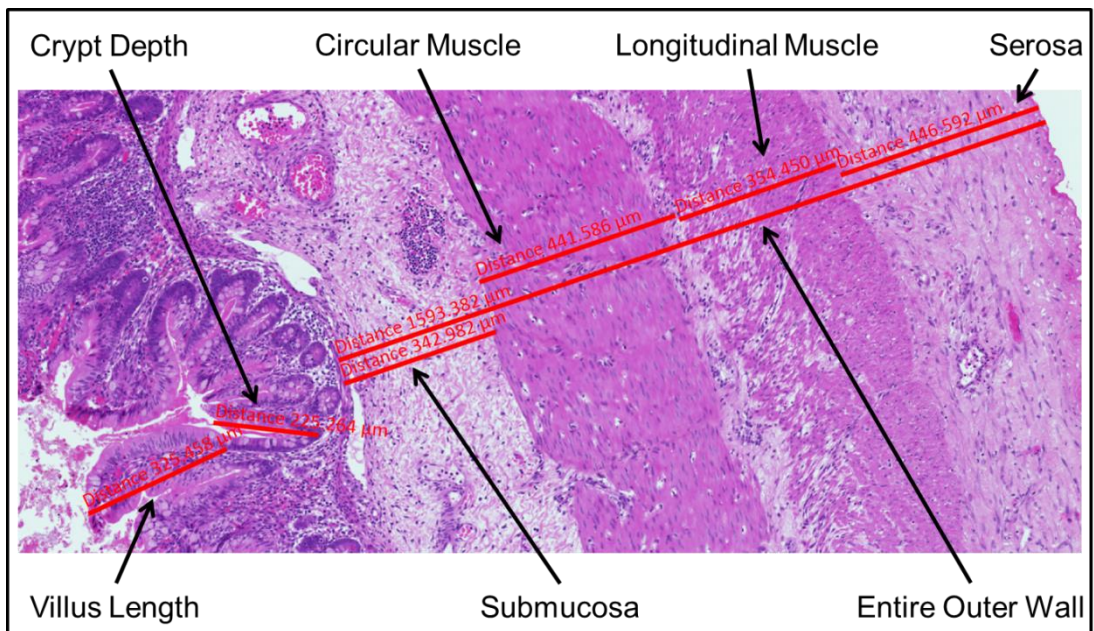
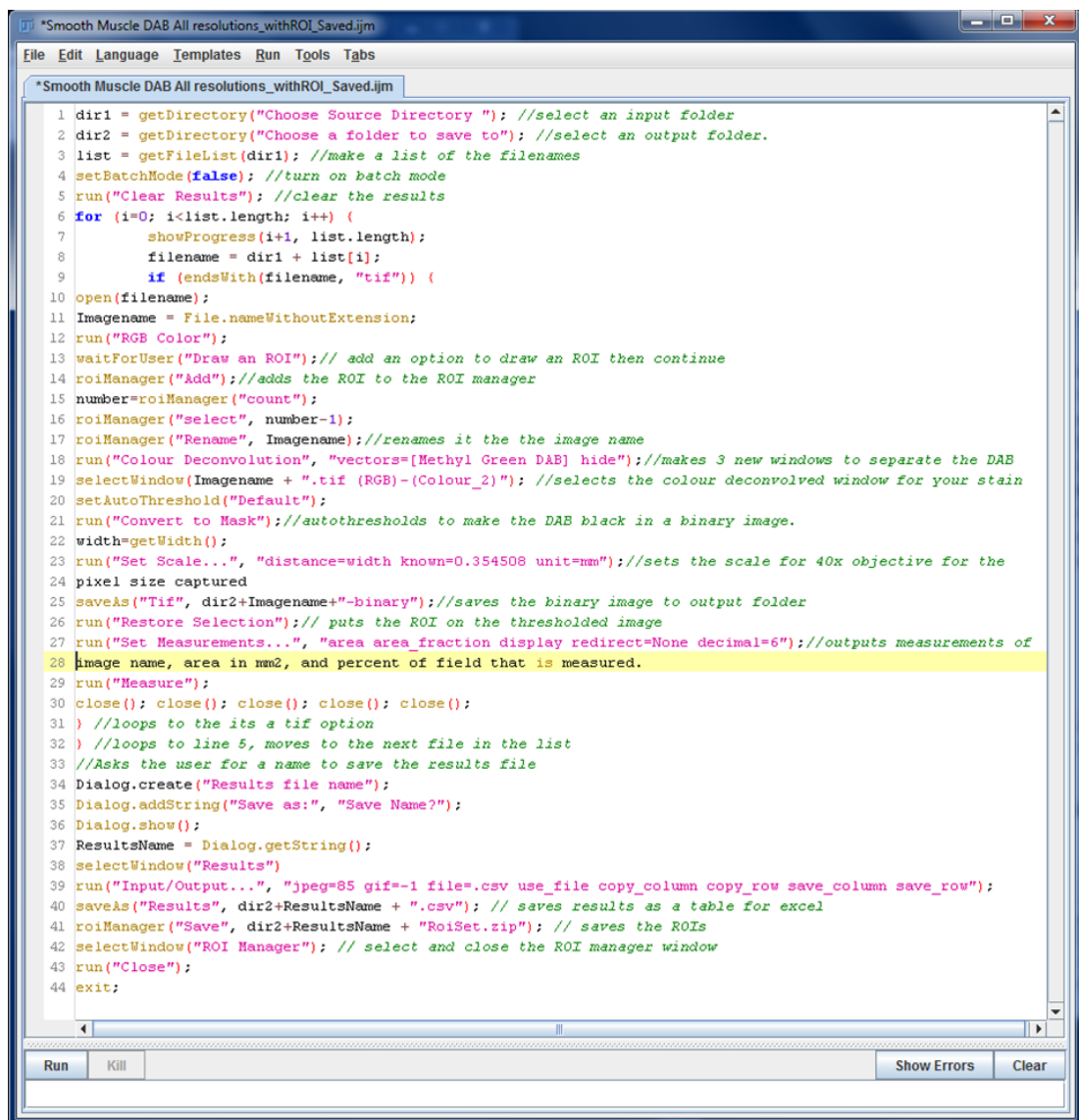


**Figure 2-14:** Human bowel wall measurements performed using Zeiss ZEN lite imaging software.

### 2.4.5.2 $\alpha$ -SMA, PS and TGF $\beta$ 3 quantification

The total area (mm<sup>2</sup>) of the region of interest ([ROI] i.e. the area filled by the bowel layer e.g. serosa, circular muscle, etc, in the imaged 40x field of view) and the percentage area of positive  $\alpha$ -SMA, TGF $\beta$ 3 and PS within the ROI were quantified using ImageJ software. Due to the large number of images requiring quantification a macro was written (with the support from Dr Dale Moulding, ICH Imaging Facility Manager) for each stain in order to enable where possible batch analysis of each group of 10 images taken per specimen for each bowel wall layer (Figure 2-15).



```
*Smooth Muscle DAB All resolutions_withROI_Saved.ijm
File Edit Language Templates Run Tools Tabs
*Smooth Muscle DAB All resolutions_withROI_Saved.ijm
1 dir1 = getDirectory("Choose Source Directory "); //select an input folder
2 dir2 = getDirectory("Choose a folder to save to"); //select an output folder.
3 list = getFileList(dir1); //make a list of the filenames
4 setBatchMode(false); //turn on batch mode
5 run("Clear Results"); //clear the results
6 for (i=0; i<list.length; i++) {
7     showProgress(i+1, list.length);
8     filename = dir1 + list[i];
9     if (endsWith(filename, ".tif")) {
10 open(filename);
11 Imagename = File.nameWithoutExtension;
12 run("RGB Color");
13 waitForUser("Draw an ROI");// add an option to draw an ROI then continue
14 roiManager("Add");//adds the ROI to the ROI manager
15 number=roiManager("count");
16 roiManager("select", number-1);
17 roiManager("Rename", Imagename);//renames it the the image name
18 run("Colour Deconvolution", "vectors=[Methyl Green DAB] hide");//makes 3 new windows to separate the DAB
19 selectWindow(Imagename + ".tif (RGB)-(Colour_2)"); //selects the colour deconvolved window for your stain
20 setAutoThreshold("Default");
21 run("Convert to Mask");//autothresholds to make the DAB black in a binary image.
22 width=getWidth();
23 run("Set Scale...", "distance=width known=0.354508 unit=mm");//sets the scale for 40x objective for the
24 pixel size captured
25 saveAs("Tif", dir2+Imagename+"-binary");//saves the binary image to output folder
26 run("Restore Selection");// puts the ROI on the thresholded image
27 run("Set Measurements...", "area area fraction display redirect=None decimal=6");//outputs measurements of
28 image name, area in mm2, and percent of field that is measured.
29 run("Measure");
30 close(); close(); close(); close();
31 } //loops to the its a tif option
32 } //loops to line 5, moves to the next file in the list
33 //Asks the user for a name to save the results file
34 Dialog.create("Results file name");
35 Dialog.addString("Save as:", "Save Name?");
36 Dialog.show();
37 ResultsName = Dialog.getString();
38 selectWindow("Results")
39 run("Input/Output...", "jpeg=85 gif=-1 file=.csv use_file copy_column copy_row save_column save_row");
40 saveAs("Results", dir2+ResultsName + ".csv"); // saves results as a table for excel
41 roiManager("Save", dir2+ResultsName + "RoiSet.zip"); // saves the ROIs
42 selectWindow("ROI Manager"); // select and close the ROI manager window
43 run("Close");
44 exit;
```

Figure 2-15:  $\alpha$ -SMA quantification macro written for ImageJ software.

#### 2.4.5.2.1 *$\alpha$ -SMA Quantification Macro*

The macro was opened in ImageJ and run generating a prompt for the investigator to select a folder containing 10 images. All images were automatically converted into RGB colour. A second prompt enabled the investigator to select the ROI by hand for each image. Colour deconvolution using the methyl green DAB vector and automatic colour thresholding of the resultant brown colour image was performed to select only positive areas of DAB staining and the image converted into a binary image. The measurement scale was set automatically based on the known pixels per mm for that image. The total ROI area ( $\text{mm}^2$ ) and the percentage area of positive staining within the ROI were measured. An output file with the measurements was then created and saved (Figure 2-16).

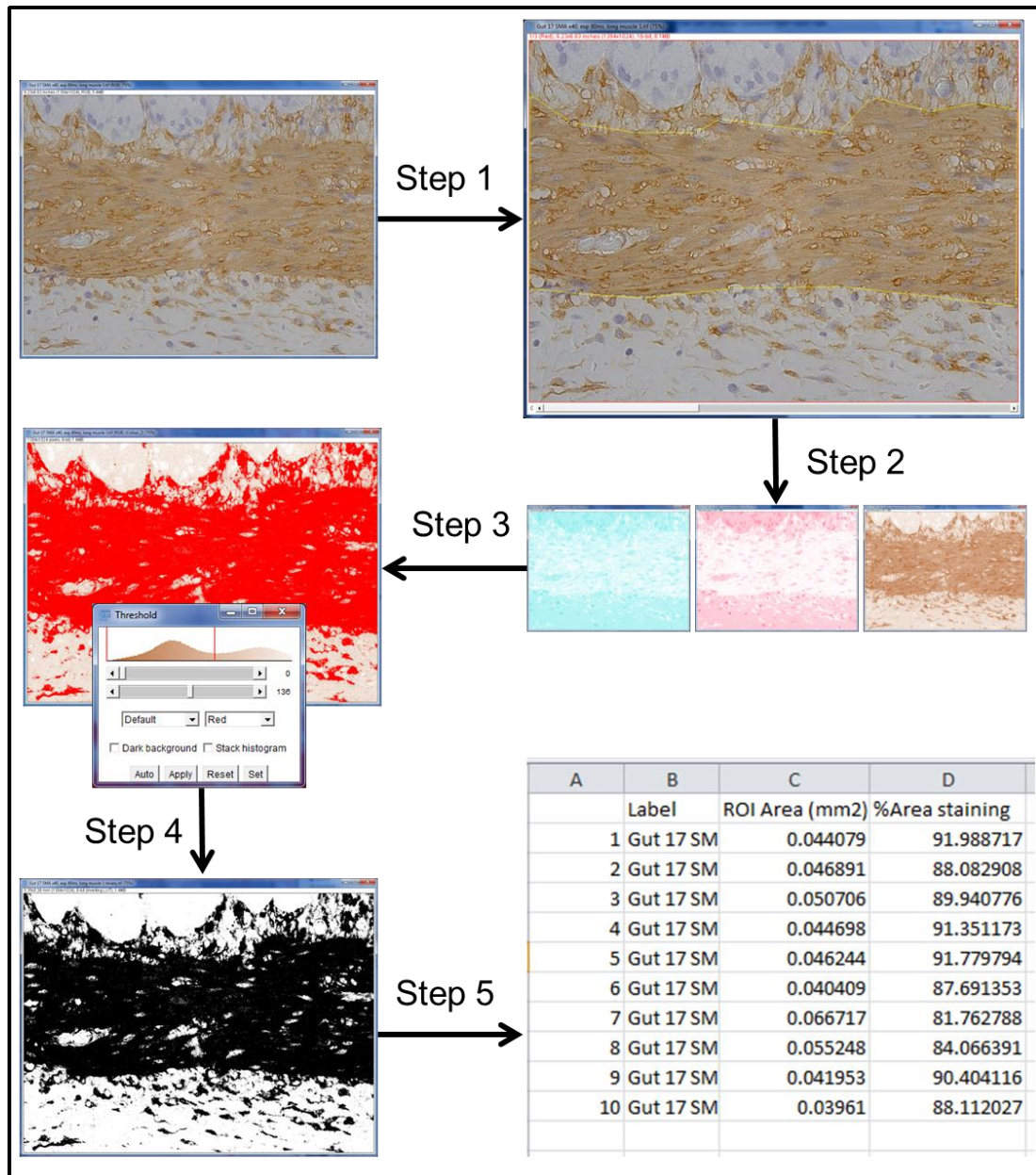


**Figure 2-16:** Quantification protocol for  $\alpha$ -SMA. **Step 1:** Convert image to RGB and draw region of interest (bounded by the yellow line). **Step 2:** Colour deconvolution using methyl green DAB vector. **Step 3:** Automated colour thresholding of resultant brown colour image. **Step 4:** Convert to a binary image. **Step 5:** Data output.

#### 2.4.5.2.2 PS Quantification Macro

The same macro was used as described for  $\alpha$ -SMA. However, in order to accurately select for the pink staining of PS a manually created vector of [r1]=19.86824 [g1]=71.61538 [b1]=58.39616 was used for colour deconvolution instead of the methyl green DAB vector.



### 2.4.5.2.3 TGF $\beta$ 3 Quantification Macro

The same macro as described for  $\alpha$ -SMA was used. However, the TGF $\beta$ 3 staining was associated with a high level of background preventing the automatic colour threshold tool from accurately separating positive TGF $\beta$ 3 staining from background. As such, another prompt was added to enable the investigator to perform manual colour thresholding for each image (Figure 2-17).

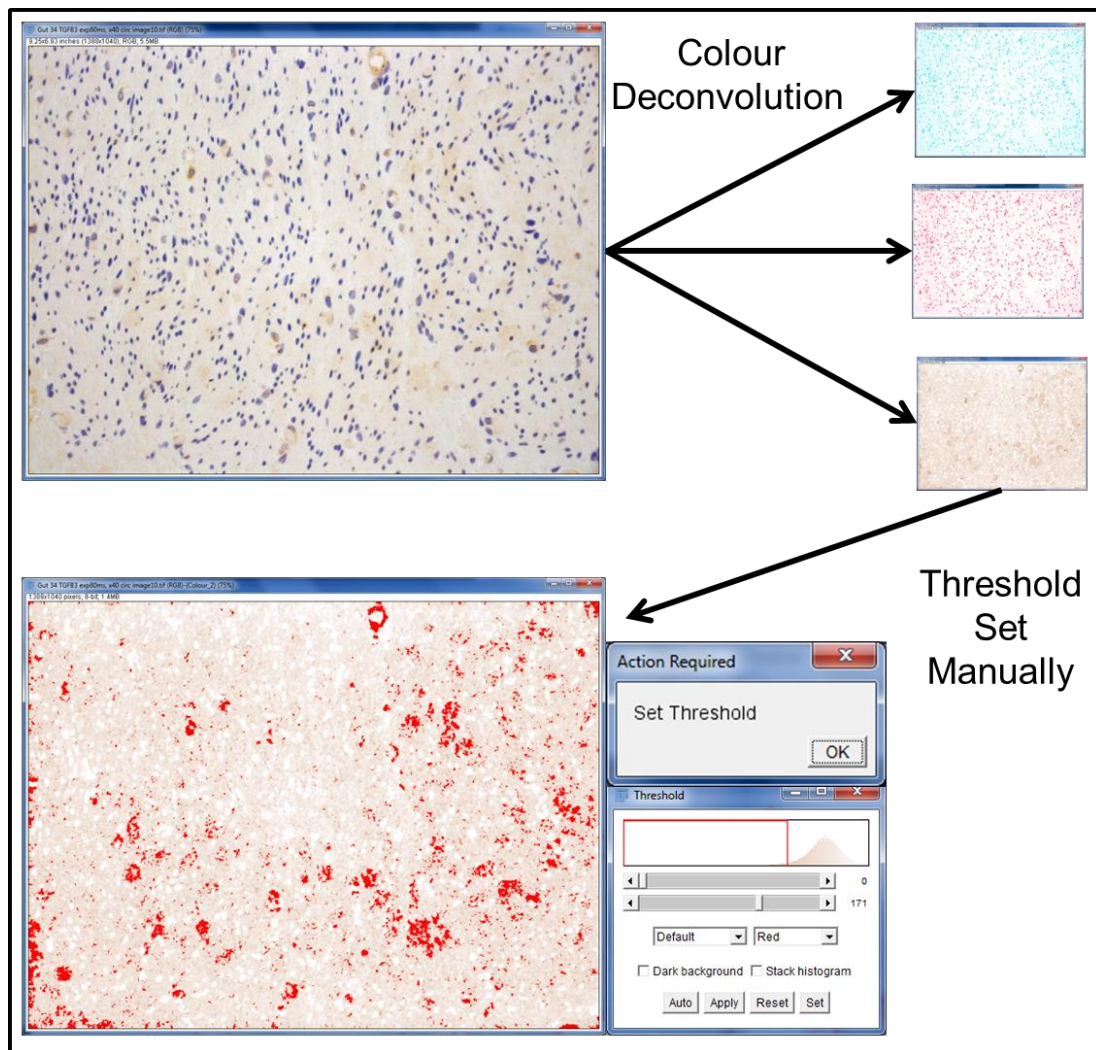


**Figure 2-17:** Manual colour thresholding following colour deconvolution for TGF $\beta$ 3 quantification.

### ***2.4.5.3 Ki67 Quantification***

The number of Ki67 positive nuclei and the total number of nuclei (ki67 positive nuclei + counter stained nuclei) were quantified using the aid of a macro.

The macro opened one image at a time and converted the image into RGB colour and applied Gaussian blur. A prompt enabled the investigator to select the ROI by hand. The measurement scale was set automatically based on the known pixels per mm for that image and the total ROI area (mm<sup>2</sup>) was measured. The find maxima tool was opened and a second prompt enabled manual adjustment of the maxima settings in order to detect as accurately as possible all nuclei within the ROI. Maxima detected nuclei were then quantified automatically and an output file generated. Ki67 positive cells were counted by hand using the cell counting software (Figure 2-18).

The proliferation index (proliferation index = ki67 positive nuclei ÷ total number of cells x 100) and the number of cells per unit area were then calculated for each image.

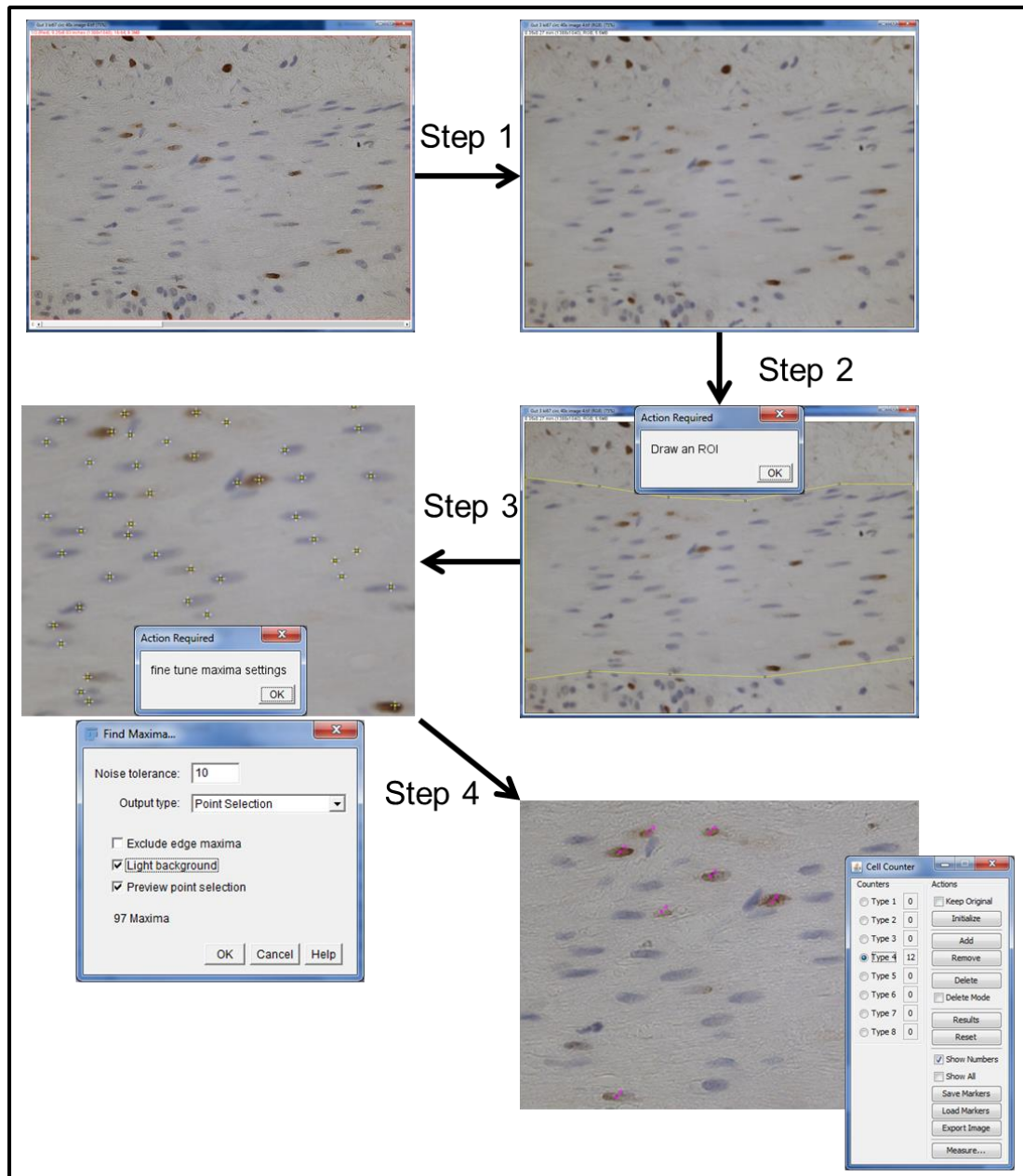


**Figure 2-18:** Quantification protocol for Ki67. **Step 1:** Convert image into RGB and apply Gaussian blur. **Step 2:** Draw ROI (bounded by the yellow line). **Step 3:** Adjust maxima settings to detect all nuclei within ROI (imaged zoomed in). **Step 4:** Manually count Ki67 positively stained nuclei (magenta marker) with cell counting software (image zoomed in).

#### 2.4.6 Statistical Analysis ICC, Enteric Neurons and Morphological Data

A mean value for all measurements was calculated for each specimen. Data were compared using Student T-test (for normally distributed data), Mann-Whitney (for non-normally distributed data) or ANOVA (for multiple group analysis) as appropriate using GraphPad Prism version 6 software. Additionally, for the human

studies, linear regression and Spearman correlation were performed using SPSS version 22. A p-value of <0.05 was considered significant.

## **2.5 Clinical Retrospective Multicentre Cohort Studies**

The incidence of gastroschisis is 4.4/10,000 live births (Kilby, 2006) and therefore falls into the category of a rare disease (defined by the European Union as a condition that affects less than 5/10,000 of the general population, [http://ec.europa.eu/health/rare\\_diseases/policy/index\\_en.htm](http://ec.europa.eu/health/rare_diseases/policy/index_en.htm)). As such, the number of cases seen by one centre per year is low. The previously published gastroschisis national cohort study (Bradnock et al., 2011) studied 393 infants from 27 UK centres over an 18 month period equating to approximately 10 infants per centre per year. Given the low number of cases seen by each individual centre retrospective data were collected from multiple centres initially including two London centres. However, due to the low number of gastroschisis infants that had received maternal antenatal corticosteroids and in order to improve the validity of results with an international approach this study was expanded to also include a Canadian centre. The collected data were used to analyse the impact of timing of delivery and administration of maternal antenatal corticosteroids on infant outcomes.

### **2.5.1 Institutional Approval**

Appropriate institutional approvals were obtained to collect antenatal and neonatal data by retrospective patient note review without the need for patient consent. Ethical approval was obtained from Mount Sinai Hospital, Toronto (Research Ethics Board application number 14-0231-C, including agreement for transfer of non-identifiable patient data for analysis at the UCL, Institute of Child Health, London, UK) and Hospital for Sick Children, Toronto (Research Ethics Board approval number 1000032644, including agreement for transfer of non-identifiable patient data for analysis at the UCL, Institute of Child Health, London, UK). In the UK centres (University College London Hospital, Great Ormond Street Hospital for Children and King's College Hospital), the study was approved as audits and waived the need for ethical approval.



## **2.5.2 Inclusion Criteria**

All infants with gastroschisis managed between January 1992 and July 2014 at the following linked fetal and paediatric surgical centres were included in the retrospective cohort study; (1) Fetal Medicine Unit, University College London Hospital (UCLH) and the Paediatric Surgery Department at Great Ormond Street Hospital for Children (GOSH), London, UK, (2) Fetal Medicine Unit and Paediatric Surgery Department at King's College Hospital (KCH), London, UK and (3) Fetal Medicine Unit at Mount Sinai Hospital (MSH) and the Division of General and Thoracic Surgery at The Hospital for Sick Children, University of Toronto, Canada. Due to the limited numbers of patients and varying study designs of previously published studies there was no robust data on which to base a power calculation therefore all gastroschisis infants were included in the study.

The individual retrospective clinical studies included the following specific paediatric surgery centres:

### ***2.5.2.1 Timing of Delivery and Impact on Gastroschisis Infant Outcomes Study***

1. Fetal Medicine Unit, UCLH and the Paediatric Surgery Department at GOSH
2. Fetal Medicine Unit and Paediatric Surgery Department at KCH.
3. Fetal Medicine Unit at MSH and the Division of General and Thoracic Surgery at The Hospital for Sick Children.

### ***2.5.2.2 Maternal Antenatal Corticosteroid Administration and Impact on Gastroschisis Infant Outcomes Study***

1. Fetal Medicine Unit, UCLH and the Paediatric Surgery Department at GOSH
2. Fetal Medicine Unit and Paediatric Surgery Department at KCH.
3. Fetal Medicine Unit at MSH and the Division of General and Thoracic Surgery at The Hospital for Sick Children.

### ***2.5.2.3 Predicting Infant Outcomes with Antenatal Bowel Dilatation Study***

1. Fetal Medicine Unit, UCLH and the Paediatric Surgery Department at GOSH

2. Fetal Medicine Unit and Paediatric Surgery Department at KCH.

### **2.5.3 Exclusion Criteria**

Any fetus or infant who received the main portion of their antenatal or postnatal treatment in a centre outside of the study centres were excluded from the study due to variations in management approaches between centres.

### **2.5.4 Patient Management**

Patients managed during the retrospective study period were referred to the study hospitals from obstetric centres at local hospitals following diagnosis of gastroschisis either at the time of the 12 week GA dating ultrasound scan or 20 week GA anomaly ultrasound scan. Patients were then assessed in the tertiary centres at four weekly intervals up until 30 weeks and then 1-2 weekly thereafter until delivery. Pregnancies were monitored for fetal growth, bowel dilatation, oligohydramnios and signs of fetal distress.

All centres had a policy of elective vaginal delivery by induction of labour at 37-38 weeks GA. Caesarean section delivery was only performed if there were other obstetric concerns e.g. breech position, maternal concerns, failure to progress, fetal distress, etc. Vaginal delivery by induction of labour was performed prior to 37-38 weeks GA if fetal assessment showed evidence of significant intra-uterine growth restriction, presence of marked intra-abdominal bowel dilatation, non-reassuring fetal heart rate or umbilical Doppler, reduced fetal movements or if there were maternal health concerns. Delivery prior to 37-38 weeks GA also occurred if labour onset was spontaneous.

Maternal antenatal corticosteroids had been given for fetal lung maturation if preterm labour occurred or was threatened to occur at  $\leq 34^{+6}$  weeks GA or delivery was performed by caesarean section at  $\leq 38^{+6}$  weeks (the latter in UK centres only) (Gynaecologists, Oct 2010, Crane et al., 2003). Antenatal corticosteroid treatment involved maternal intra-muscular injection of either 12mg betamethasone, two doses, 24 hours apart or 6mg dexamethasone, four doses, 12 hours apart. An incomplete or

modified antenatal corticosteroid treatment regimen was given to women in whom labour progression was quick or emergency caesarean section was required resulting in delivery before completion of the course.

Following delivery, gastroschisis neonates were immediately stabilised within the NICU located at the birth centre and then transferred when safe to the linked paediatric surgical centre for definitive management. Gastroschisis neonatal management varied between centres, including surgical closure method (primary closure versus silo staged closure) and feeding regime, due to the differing departmental policies and individual surgeon preference.

### **2.5.5 Identification of Patients**

Patients were identified through interrogation of hospital databases and linked fetal and neonatal data were obtained from computerized and handwritten patient notes at the respective hospitals.

### **2.5.6 Data Collection**

Data was collected retrospectively from review of maternal and infant case notes.

Antenatal data collection included GA at time of ultrasound, concomitant fetal abnormalities, presence or absence of antenatal intra-abdominal bowel dilation or extra-abdominal bowel dilatation and size (mm) of the dilatation if it was documented, labour onset, mode of delivery, indication for premature delivery (if applicable), GA at delivery, year of birth, birth weight and timing, dosage and reason for maternal antenatal corticosteroid administration. GA was calculated as a continuous variable with incomplete weeks gestation calculated as a decimal (e.g.  $34^{+5} = 34.7$ ).

Postnatal data collection included appearance of bowel at birth, concomitant intestinal pathology (atresia, stenosis, necrosis, perforation, volvulus and necrotizing enterocolitis), time to start enteral feeds, ENT, LOS, episodes of sepsis and death.

### **2.5.7 Outcome Measures**

The primary outcome measure was ENT defined as the time taken from birth to achieve full enteral feeds as described in the hospital charts. The secondary outcome measures included: LOS defined as time from birth to discharge from hospital; and development of sepsis defined as isolation of pathogenic organism detected on blood culture.

### **2.5.8 Confidentiality**

Collected data was entered into an Excel spreadsheet created for each of the fetal/paediatric surgical study centres and all patients given a unique identifier. Personal identifying data including name and date of birth were omitted from the datasheet. The code for the pseudonymisation was kept on a password protected hospital computer (data safe haven) in each centre as per Toronto Research Ethics Board and London audit guidelines.

### **2.5.9 Statistical Analysis**

Statistical analysis was performed using SPSS version 22 and GraphPad Prism version 6 software. Data is presented as median [range] and a p-value of <0.05 was considered significant.

#### ***2.5.9.1 Timing of Delivery and Impact on Gastroschisis Infant Outcomes Study***

Log-transformed data were used to perform linear regression analysis of ENT and LOS across the entire cohort and those born at  $\geq 34$  weeks GA. Infants were also divided in two groups; (1) those born 34 and 36<sup>+6</sup> weeks GA and (2) those born at or after 37 weeks GA. Fisher's exact test and Mann-Whitney was used to compare the two groups. Outcomes were compared with and without taking into account corrected GA. Cox regression analysis was also used, adjusting for complexity and GA and censoring for those infants who failed to achieve the 'event' including; failure to achieve ENT, not being discharged from hospital and death as appropriate.

### ***2.5.9.2 Maternal Antenatal Corticosteroid Administration and Impact on Gastroschisis Infant Outcomes Study***

Cox regression analysis was primarily used enabling analysis of time to event data whilst adjusting for confounders by multi-variable analysis. Potential confounders were identified and adjusted for including; complex gastroschisis, birth GA, source hospital and antenatal corticosteroid administration. Censoring was performed for those infants who failed to achieve ENT, or infants who were discharged on home PN, transfer to another hospital on PN, discharge home following transfer to another hospital, babies who were not discharged from hospital or death. Additionally, Mann-Whitney and Fisher's exact test were used as appropriate.

### ***2.5.9.3 Predicting Infant Outcomes with Antenatal Bowel Dilatation Analysis***

Data were analyzed using Mann-Whitney tests or t-tests as appropriate, positive and negative predictive values were used for proportion data and log-transformed data was used to perform linear regression analysis of ENT and LOS.

## **Chapter 3: Phenotypic and ICC Characterisation in the Scribble Knockout Mouse Model of an Abdominal Wall defect**

### **3.1 Introduction**

Gastroschisis was previously reported to be exhibited by a Scribble mutant mouse model (*Circletail*), which was initially developed to investigate the neural tube defect (NTD) craniorachischisis (Murdoch, 2003). This model has a frame shift in the *Scrib* allele resulting in early termination of the Scribble protein. Since then the Scribble mutant mouse model has been further developed through creation of a floxed *Scrib* (*Scrib<sup>fl</sup>*) allele, whereby the *Scrib* allele is flanked between two *lox P* sites, allowing for gene excision at the *lox P* sites with the use of Cre recombinase (Nagy, 2000). The floxed allele has enabled conditional *Scrib* gene targeting allowing *Scrib* function to be analysed in various biological systems (Hartleben et al., 2012, Pearson et al., 2011). Scribble null fetuses generated by the *Scrib<sup>fl</sup>* allele have been reported to express morphological features that mirror the *Circletail* mutant model including gastroschisis and craniorachischisis (Hartleben et al., 2012, Pearson et al., 2011). For the purposes of this research the *Scrib<sup>fl</sup>* allele was used to create a Scribble knockout mouse model to induce the gastroschisis AWD.

The aims of this part of the study were to; (i) accurately delineate the AWD anatomy that results from Scribble loss of function and (ii) compare bowel wall ICC development of phenotypically normal fetuses with AWD fetuses.

### **3.2 Results**

#### **3.2.1 Gross Characterisation of Scribble Knockout Fetuses**

During the experimental period a total of 127 fetuses were collected, 78 at 18.5 dpc and 49 at 17.5 dpc, of which 112 (88%) were phenotypically normal (i.e. no NTD or AWD) and 15 (12%) expressed an AWD phenotype. Of those that expressed an

AWD phenotype; 5 occurred in isolation and 10 with a concomitant extensive NTD. None of the fetuses collected exhibited an isolated NTD (Figure 3-1).

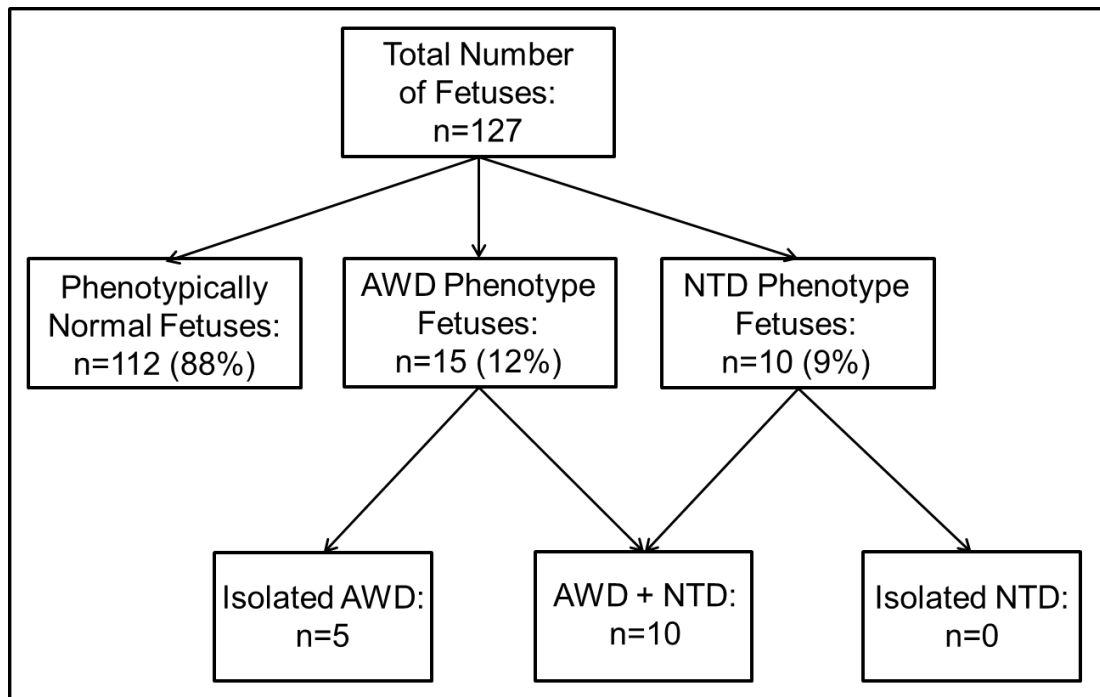


**Figure 3-1:** Gross phenotypic characterisation of the floxed *Scrib* (*Scrib<sup>fl</sup>*) mouse model.

Genotyping was performed on 58 randomly fetuses revealing 12 (21%) wild types (*Scrib<sup>fl/fl</sup>*), 20 (34%) heterozygotes (*Scrib<sup>fl/-</sup>*) and 26 (45%) homozygote knockouts (*Scrib<sup>-/-</sup>*). These ratios do not appear to fall into the expected Mendelian ratios of 25% WT, 50% heterozygotes and 25% knockouts. However, the numbers are too small to reliably determine whether this is a significant deviation from the expected distribution. All wild type fetuses were phenotypically normal. Nineteen heterozygotes were phenotypically normal and 1 expressed a large AWD with concomitant NTD. Twenty homozygote knockouts were phenotypically normal and 6 were phenotypically abnormal of these 4 exhibited an isolated AWD (3 with a large AWD and 1 with a small AWD) and 2 exhibited a large AWD with concomitant NTD (Table 3-1). Hence, the penetrance of an AWD in *Scrib* null mice was 23% and NTD was 8%.

Genotype	Total in Group	Phenotypically Normal	Isolated AWD	AWD + NTD
Wild Type ( <i>Scrib<sup>fl/fl</sup></i> )	12 (21%)	12	0	0
Heterozygote ( <i>Scrib<sup>fl/-</sup></i> )	20 (34%)	19	0	1
Homozygote ( <i>Scrib<sup>-/-</sup></i> )	26 (45%)	20	4	2

**Table 3-1:** Gross, phenotype-genotype characterisation of the floxed *Scrib* (*Scrib<sup>fl</sup>*) mouse model.

### 3.2.2 Abdominal Wall Defect Phenotype

#### 3.2.2.1 Timing of Abdominal Wall Phenotyping

Phenotyping of fetuses was performed at 17.5 dpc (after resolution of physiological herniation). This time point was chosen due to the larger amniotic fluid volume present compared to 18.5 dpc fetuses, which aided microdissection (n=6 control and n=6 AWD fetuses) reducing damage to fine membranous structures associated with the externalized abdominal viscera and abdominal wall defect. Additionally, the larger amniotic fluid volume aided visualization of fine intra-amniotic structures following in-amnio micro-MRI (n=2 control and n=3 AWD fetuses).

#### 3.2.2.2 Visualisation of Intra-Amniotic Fetuses

Examination of fetuses through intact amniotic membranes revealed three abdominal wall phenotypes; phenotypically normal, small AWD and large AWD.

Phenotypically normal fetuses (Figure 3-2A) exhibited no structural defects and were positioned with the four limbs tightly folded in front of the torso. Viewing these fetuses from the side revealed complete closure of the abdominal wall and a centrally inserted umbilical cord. Fetuses with a small AWD (Figure 3-2B) exhibited a



discrete, central abdominal wall defect through which the abdominal viscera (including liver and bowel) herniated into a membranous sac, which was continuous with the umbilical cord, consistent with an exomphalos. The limbs were splayed laterally to accommodate the centrally herniated viscera. Fetuses with a large AWD (Figure 3-2C) exhibited complete failure of the abdominal wall to form and the externalised abdominal viscera (including liver and bowel) appeared to be free floating within the amniotic cavity. However, there also appeared to be a membranous structure compartmentalising the intra-amniotic cavity. The limbs were also splayed laterally. Additionally, AWD fetuses (small or large) with a concomitant NTD (Figure 3-2B) exhibited exposed neural tissue from the cranium to sacrum.

The amniotic fluid was clear and non-blood stained in all phenotypically normal and isolated small and large AWD fetuses. However, the amniotic fluid was blood stained in fetuses with a concomitant NTD. The placenta appeared grossly normal in all fetuses.

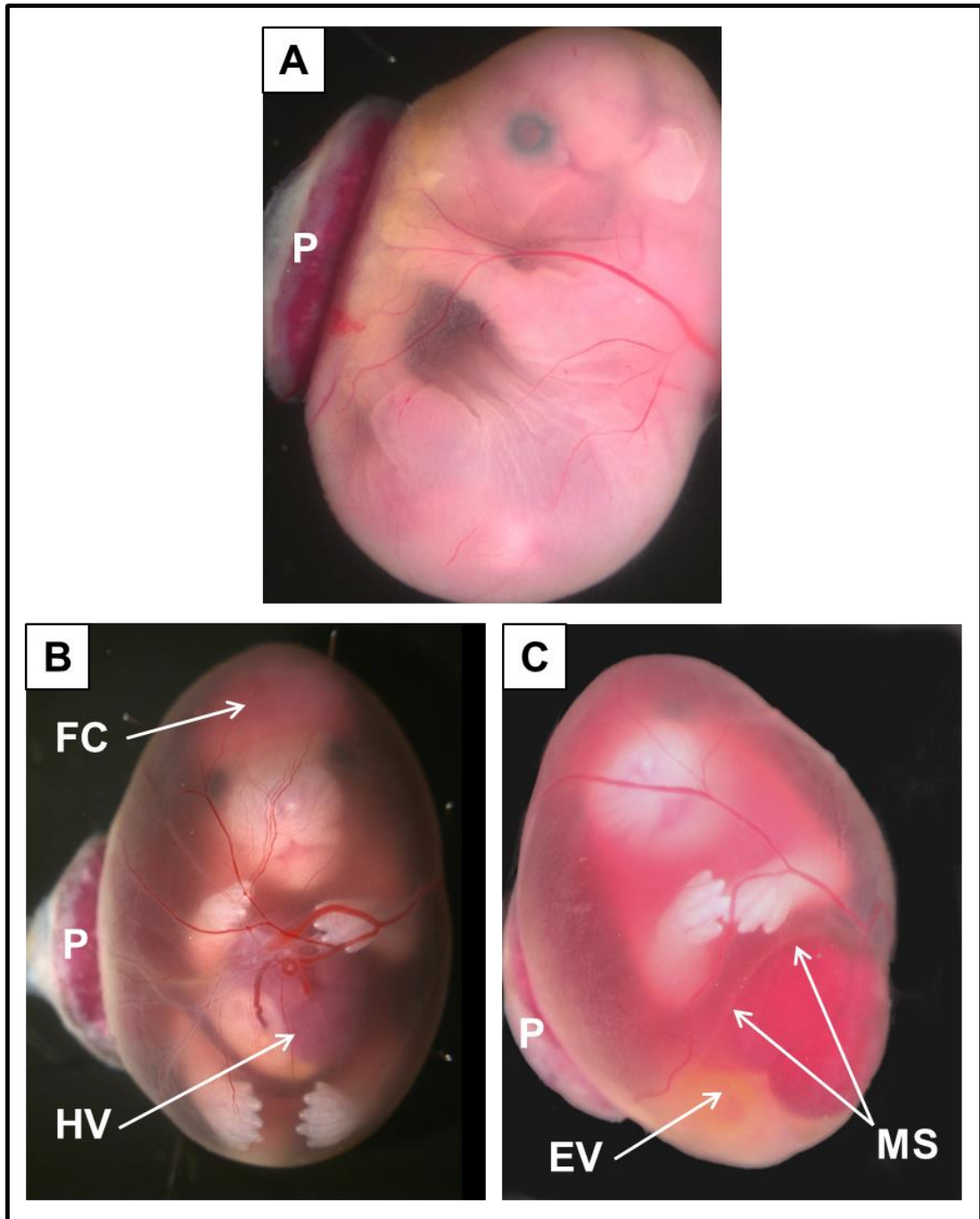


**Figure 3-2:** Intra-amniotic fetuses including intact placenta (P) at 17.5 dpc, 0.8x objective. **A.** Phenotypically normal fetus. **B.** Fetus with small AWD. The herniated viscera (HV) is contained within a membrane sac. Also evident in this image is failed closure (FC) of the cranium and blood stained amniotic fluid. **C.** Fetus with large AWD. Externalised viscera (EV) appear to be free floating. There is evidence of an intra-amniotic membrane structure (MS) compartmentalising the intra-amniotic cavity. This fetus additionally had a concomitant NTD (not visible on this image due to orientation) and blood stained amniotic fluid.

### **3.2.2.3 *Microdissection***

The presence of three anatomically distinct abdominal wall phenotypes was confirmed following microdissection. Phenotypically normal fetuses as previously described exhibited complete ventral abdominal wall closure. The umbilical cord was found to be structurally normal (3 blood vessels contained within a membrane) originating from a grossly normal placenta and inserting centrally on the abdominal wall (Figure 3-3A).

The small AWD was characteristic of exomphalos (total n=3; 18.5 dpc n=1, 17.5 dpc n=2) with disruption and failed closure of the umbilical ring resulting in a central abdominal wall defect. The herniated abdominal viscera (including bowel and liver) were contained within a membranous sac that was continuous with the umbilical cord. The umbilical cord was otherwise structurally normal as described above originating from a grossly normal placenta (Figure 3-3B).

The large AWD was confirmed to comprise of a complete failure of the ventral abdominal wall to develop (total n=12, 18.5 dpc n=8, 17.5 dpc n=4) with no evidence of lateral ventral wall folds. The exteriorised abdominal viscera included bowel, stomach, liver and spleen. Following microdissection of the amniotic membranes a fine, ruptured membranous structure was identified that covered the externalised viscera and exhibited vascular connections to the amniotic membrane (Figure 3-3C). At 18.5 dpc it was not possible to dissect the amniotic membranes without damaging this fine membrane. The membrane may have therefore either ruptured earlier in gestation or during dissection. However, dissection at 17.5 dpc of one fetus revealed an intact fine membrane covering the herniated abdominal viscera, which was in continuity with an otherwise structurally normal umbilical cord originating from a normal placenta and therefore in keeping with a giant exomphalos (Figure 3-3D). Dissection of the amniotic membranes was easier at 17.5 dpc due to the greater volume of amniotic fluid enabling identification and protection of the fine membrane covering the externalised abdominal viscera.

The concomitant NTD was that of craniorachischisis consisting of complete failure of the neural tube to close resulting in exposure of the neural tissue from the cranium

to sacrum as previously described in the circletail mouse model (Murdoch, 2003). All AWD fetuses exhibited a curly tail but no other gross structural anomalies were identified.

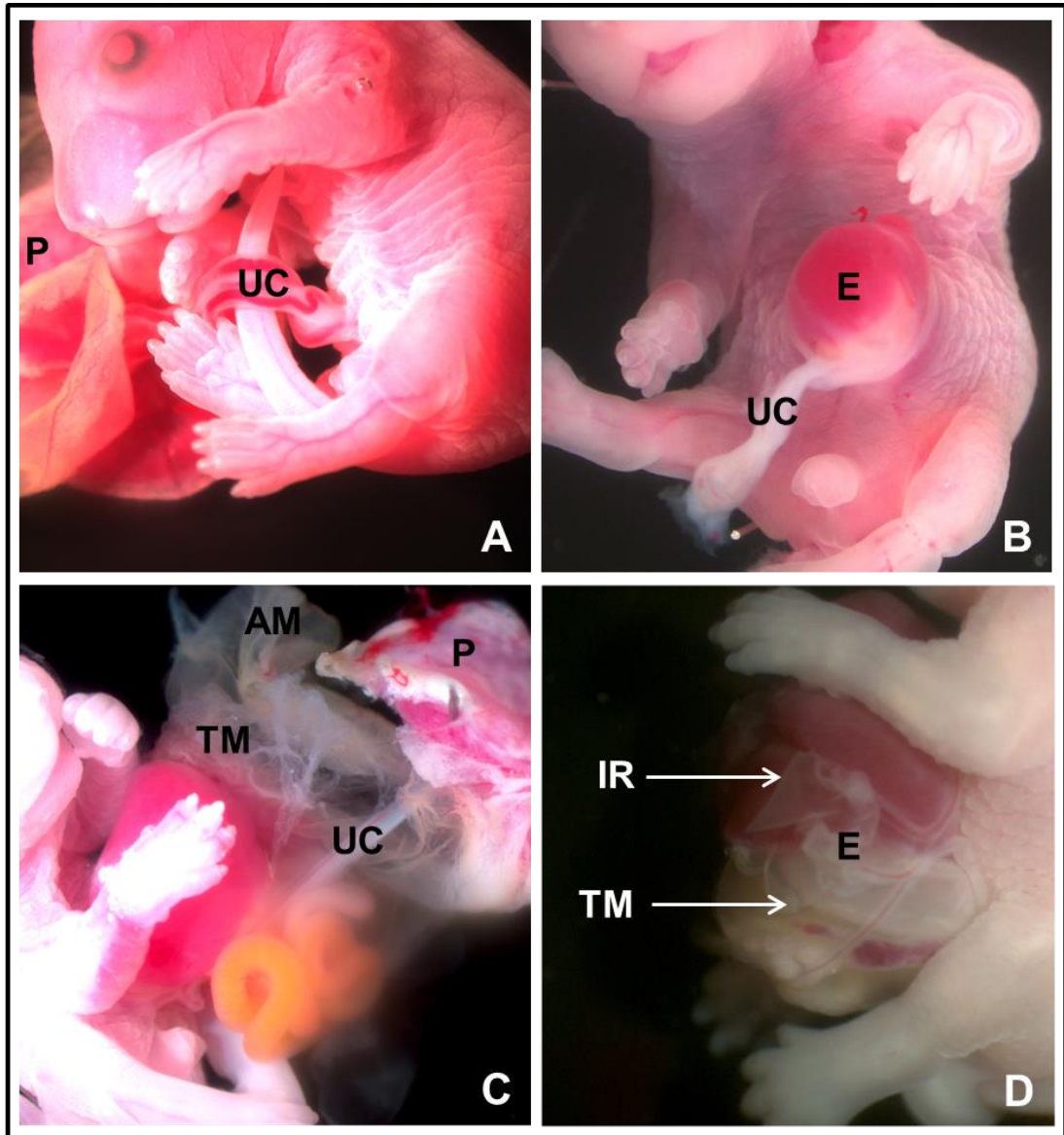


**Figure 3-3:** Scribble mutant mouse abdominal wall phenotypes at 17.5 dpc, magnification 0.8x objective. **A.** Normal phenotype with intact abdominal wall and structurally normal umbilical cord (UC) that inserts centrally on the abdominal wall. The placenta (P) also remains intact. **B.** Small AWD with membrane covered herniated liver and bowel into the base of the umbilical cord (UC) consistent with exomphalos (E). **C.** Large AWD with evisceration of liver, gut and spleen. A ruptured thin membrane (TM) is present associated with the abdominal viscera and exhibits vascular attachments to the amniotic membrane (AM). The placenta (P) and umbilical cord (UC) have been left intact. **D.** Large ventral wall defect with intact thin membrane (TM) covering herniated abdominal viscera (superior pole of the membrane was iatrogenically ruptured (IR) during dissection) consistent with exomphalos (E).

#### **3.2.2.4 *In-Amnio Fetal Micro-MRI***

Imaging of phenotypically normal fetuses (n=2) revealed complete closure of the abdominal wall and normal insertion of the umbilical cord (Figure 3-4A). One fetus with a characteristic exomphalos was imaged confirming the presence of disruption and failed abdominal wall closure at the umbilical ring with herniation of abdominal viscera. The membrane covering the herniated viscera could be tracked from the abdominal wall to the umbilical cord (Figure 3-4B). Two fetuses with complete failure of development of the ventral abdominal wall were imaged, which initially suggested the abdominal viscera to be free floating within the amniotic cavity (Figure 3-4C). However, following post-processing of the images with contrast enhancement a fine membranous structure was revealed in association with the externalised abdominal viscera, extending from the abdominal wall to the amniotic membrane (Figure 3-4D and E). These images confirm the presence of a fine membrane covering the abdominal viscera in this phenotype. However, it was not possible to determine on these images whether the membrane was intact or ruptured. Additionally, the presence of a normal umbilical cord and placenta were visualised (Figure 3-4F). Finally, the craniorachischisis defect was clearly visualised with failed closure of the neural tube from the cranium to the sacrum (Figure 3-4B and C).

Identification of intra-amniotic structures was aided by the bright contrast provided by the relatively large volume of amniotic fluid at 17.5 dpc. Imaging of the mutant fetuses revealed a higher signal intensity (Figure 3-4B and C) of the entire fetal body compared to the normal phenotype fetuses ((Figure 3-4A). This higher signal intensity likely resulted from the blood stained amniotic fluid associated with the craniorachischisis defect providing greater tissue contrast.

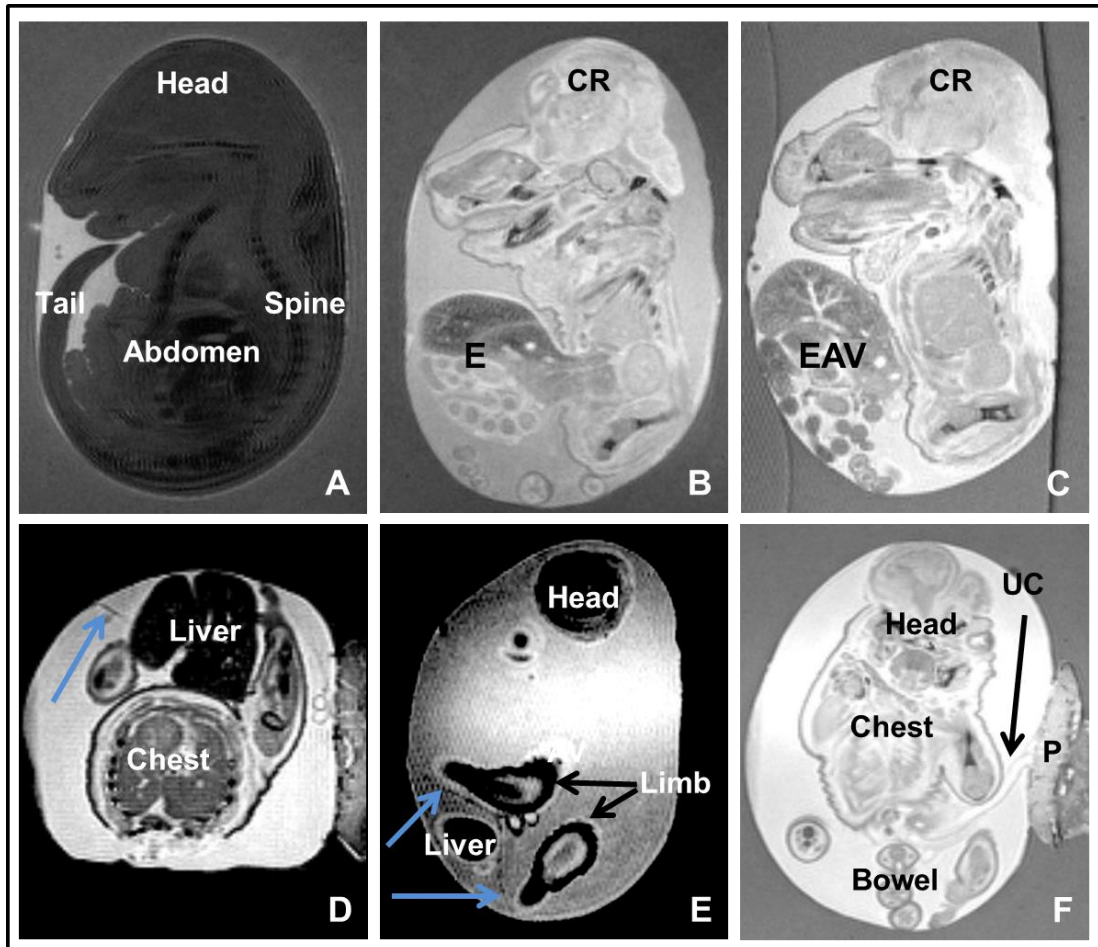


**Figure 3-4:** In-amnio micro-MRI of intra-amniotic fetuses at 17.5 dpc. **A.** Sagittal image of a phenotypically normal fetuses. **B.** Sagittal image of characteristic exomphalos (E) AWD phenotype showing herniation of abdominal viscera contained within an intact membrane. Also evident is craniorachischisis (CR) with failed neural tube closure from the cranium to sacrum. **C.** Sagittal image of the large AWD phenotype showing externalised abdominal viscera (EAV) with no discernible membrane covering. The craniorachischisis defect is also evident. **D.** Contrast enhanced axial image of the large AWD. The externalised liver is associated with a membranous structure (blue arrow). **E.** Contrast enhanced sagittal image of the large AWD. The externalised liver is associated with a membranous structure (blue arrows). **F.** Contrast enhanced coronal image of the large AWD showing the presence of a normal placental (P) and umbilical cord (UC).

### 3.2.3 Gross Bowel Morphology

To ensure uniformity of results, only tissue harvested from fetuses with the large AWD were included in this study. The bowel from AWD fetuses was observed to be shorter in length and more tortuous than controls. There was no evidence of macroscopic bowel inflammation or fibrous serosal peel in either group. There was a significant and marked difference in bowel length between control ( $7.2 \pm 0.12\text{cm}$ ,  $n=15$ ) and AWD fetuses ( $5.1 \pm 0.16\text{cm}$ ,  $n=8$ ,  $p<0.0001$ ). There was also a significant



and marked difference in bowel weight between the groups (control  $73.9 \pm 1.6\text{mg}$  versus AWD  $58.3 \pm 3.3\text{mg}$ ;  $p < 0.0001$ ). Finally, there was a small difference in weight per unit length (control  $10.3 \pm 0.9\text{mg/cm}$  versus AWD  $11.4 \pm 0.5\text{ mg/cm}$ ;  $p = 0.0453$ ), suggesting thickening of the bowel in AWD fetuses.

### 3.2.4 ICC and Enteric Neurons

#### 3.2.4.1 Immunofluorescence Staining Protocol

Immunofluorescence was performed on cross-sectioned samples and positive ICC and enteric neuron staining was achieved. However, there was also significant background staining, which made it difficult to identify ICC cell bodies or discern the ICC branching architecture (Figure 3-5B). Enteric neuron cell bodies were easier to identify but the cell architecture was poorly defined (Figure 3-5C). Therefore it was difficult to accurately quantify either cell types using this method, and quantification of ICC was only performed using whole mount tissue.

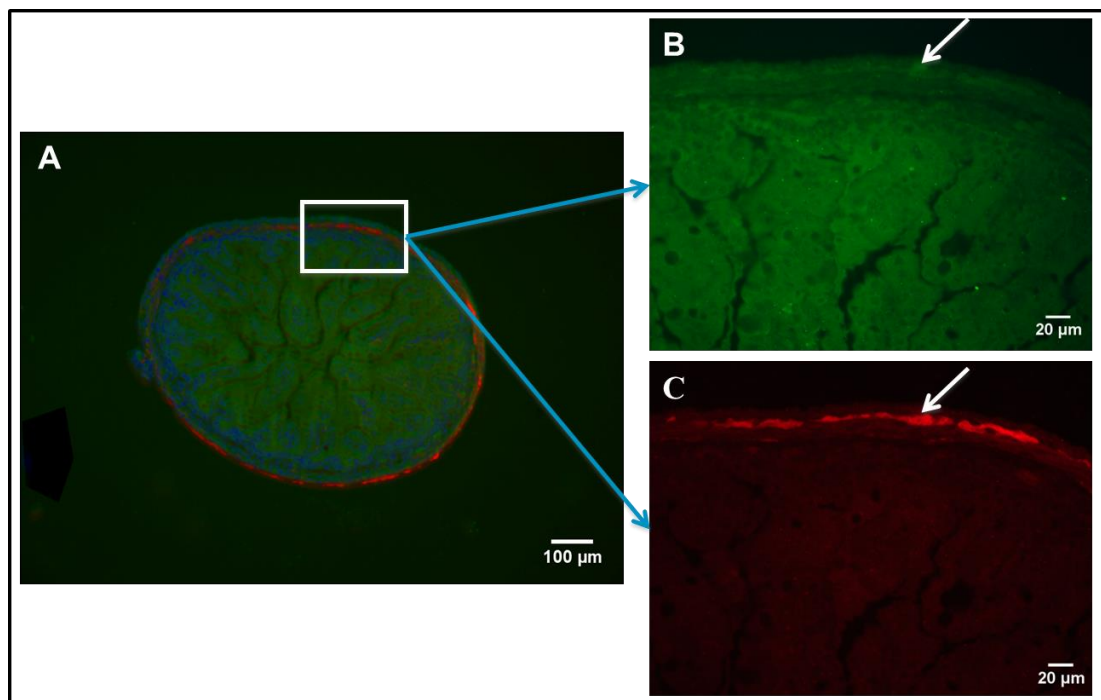


**Figure 3-5:** A. Low powered (10x objective) composite image of entire gut cross-section (anti-CD117 green, anti-TUJ1 red, DAPI blue), rectangle showing region imaged at high power. B. High powered (40x objective) image of ICC (indicated by arrow). C. High powered (40x objective) image of enteric neurons (indicated by arrow).

The preparation of whole mount, muscle only, tissue preparations was difficult. The ileum of 18.5 dpc mouse fetuses is extremely thin (approximately 1 – 2mm in diameter) and fragile resulting in tissue damage during stripping of the mucosa from the muscle layers. This resulted in tissue being discarded and of the 15 sections of ileum resected from control fetuses, 9 whole mount sections were discarded and of the 8 bowel sections from AWD fetuses, 5 were discarded. To reduce unnecessary use of animals the study was terminated before processing 10 whole mount sections in each experimental group on the grounds that the AWD expressed by Scribble knockout mice was exomphalos rather than gastroschisis and therefore not suitable for intra-amniotic injection. Hence, ICC were quantified from 6 control and 3 AWD whole mount specimens.

#### ***3.2.4.2 ICC Architecture and Numbers***

At the level of the myenteric plexus, the ICC were well developed in both control (Figure 3-6A) and AWD (Figure 3-6C) fetuses exhibiting numerous branching cytoplasmic processes that interconnected with their counterparts creating a mature plexus. As expected for this gestational stage, ICC at the level of the deep muscular plexus were not observed in either group. The number of ICC per high powered field ( $45\text{nm}^2$ ) in the control group was  $129 \pm 5$  (mean  $\pm$  SEM), range 105-146. In comparison, the number in the AWD group was  $193 \pm 37$ , range 119 - 232. Although, the number of ICC in the AWD group appear to be higher this was not statistically significant ( $p=0.38$ ) on this small number of animals.

#### ***3.2.4.3 Enteric Neuron Architecture and Numbers***

The enteric neurons at the level of the myenteric plexus appeared similar and were well developed in both control (Figure 3-6B) and AWD (Figure 3-6D) fetuses exhibiting regularly spaced cell chains lying in parallel with regular perpendicular crosslinking between chains creating a crosshatched appearance. Enteric neurons were not formally quantified during this study due to inconsistency of staining with anti-TUJ1.



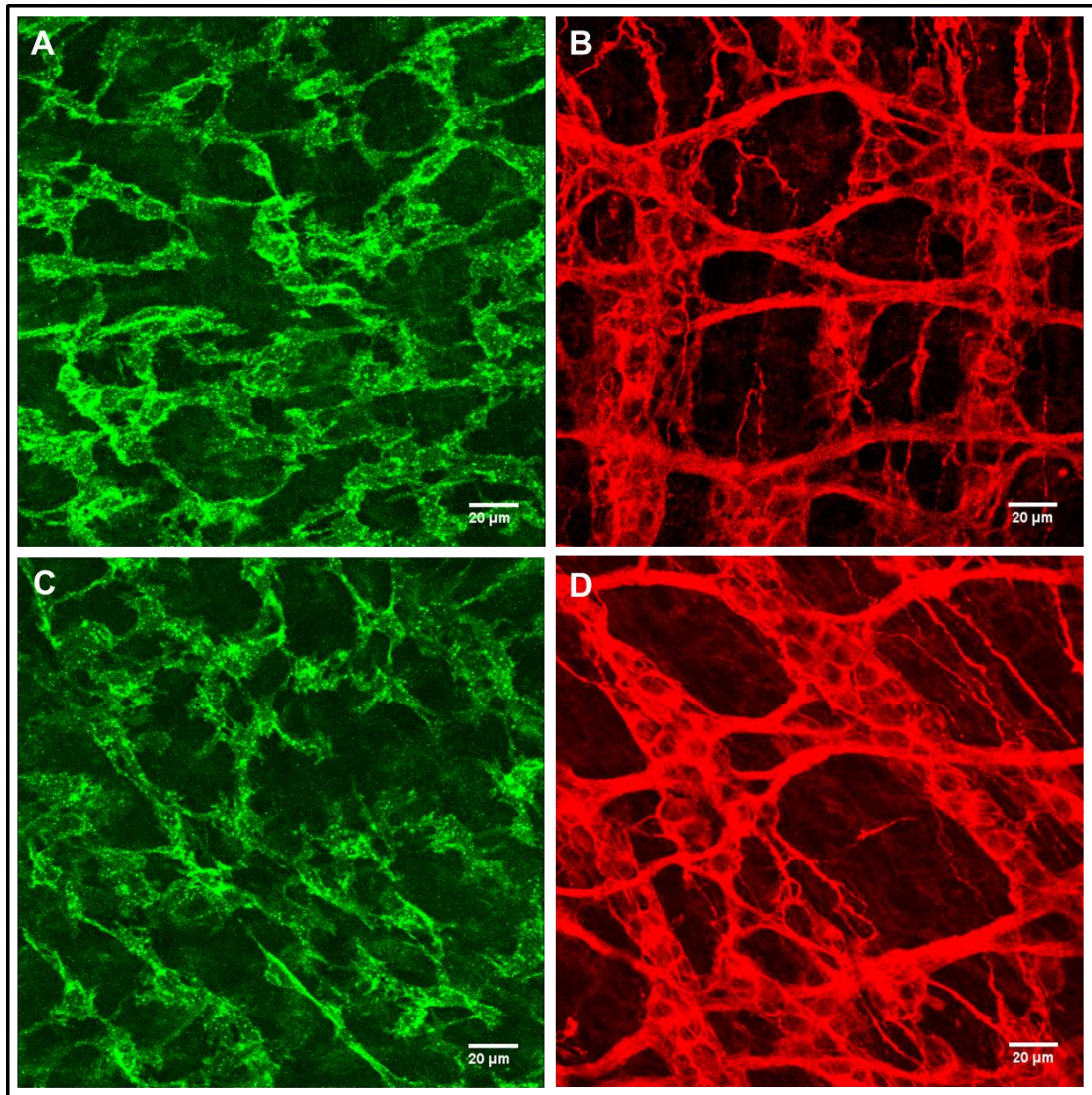


**Figure 3-6:** Whole mount 18.5 dpc ileal specimens stained for ICC with anti-CD117 (A and C) and enteric neurons with anti-TUJ1(B and D) images acquired by confocal microscopy, 40x objective, maximum intensity project of z-stack images. **A and B.** Specimen from control mouse. **C and D.** Specimen from large AWD mutant mouse.

### 3.3 Discussion

#### 3.3.1 Abdominal Wall Phenotype

##### 3.3.1.1 *Exomphalos Phenotype*

Null fetuses derived from the *Scrib*<sup>fl</sup> allele exhibit an exomphalos phenotype that varies in severity with an intact or ruptured membrane covering the herniated viscera. The least severe form of the defect phenotypically resembled exomphalos with a

well-defined membrane covering the herniated abdominal viscera. The most severe form was more ambiguous with complete failure of development of the ventral abdominal wall and evidence of a fine membrane covering the herniated abdominal viscera including bowel, stomach, liver and spleen, which may rupture intra-amniotically. The presence of this covering membrane provides evidence that this defect is consistent with a giant exomphalos rather than a large, atypical gastroschisis defect. Liver herniation is also very rare in gastroschisis and provides further evidence that this defect more closely resembles exomphalos. Additionally, the presence of a normal placenta and structurally normal umbilical cord is evidence against this AWD being a body stalk defect, which comprises an extensive AWD with an absent or extremely short umbilical cord that is frequently associated with other structural abnormalities such as failed thoracic wall closure and head, face and limb anomalies (Paul et al., 2001, Bugge, 2012)

Anatomical delineation of the giant exomphalos was possible through careful dissection under a stereo microscope enabling identification and preservation of the umbilical cord, placenta and fine membrane covering the herniated abdominal viscera. Additionally, high-resolution in-amnio micro-MRI provided a non-destructive method for visualisation and confirmation of the AWD anatomy and associated structures.

### **3.3.1.2 A Case of Mistaken Identity**

The exomphalos phenotypic description of Scribble null fetuses outlined above contradicts the previous literature. The Scribble mutant mouse AWD was originally described in the *circletail* model to be that of gastroschisis (Murdoch, 2003). Since then the AWD has continued to be described as gastroschisis in the *Scrib<sup>f1</sup>* mutant model (Hartleben et al., 2012, Pearson et al., 2011). However, none of these papers provide detailed analysis of the abdominal wall anatomy or associated structures as these studies were focused towards the investigation of craniorachischisis. A similar case of mistaken identity occurred in the phenotypic description of the *Alx-4* mutant mouse model, which was originally described as gastroschisis (Qu et al., 1997) but later reported as exomphalos (Matsumaru et al., 2011). This clearly highlights the difficulties of accurate phenotyping of AWD in genetic mouse models.

### 3.3.1.3 Importance of Accurate Phenotyping

As previously discussed, exomphalos and gastroschisis differ greatly in terms of their associated morbidities and concomitant pathologies. The primary purpose of this research was to understand the cause of GRID. However, in exomphalos, intestinal dysfunction is not usually a feature. Although GRID is hypothesised to develop due to bowel exposure to amniotic fluid, and the fine membrane covering the herniated abdominal viscera in the *Scrib<sup>fl</sup>* mouse model may rupture intra-amniotically, the timing of this rupture is unknown and may vary between fetuses. Timing of membrane rupture could only have been assessed if it was possible to serially assess the continuity of the covering membrane prenatally *in vivo*. This may have been possible using micro-ultrasound fetal mouse imaging (Foster et al., 2002, Foster et al., 2011, Liu et al., 2017), which would have enabled serial *in-vivo* fetal imaging of AWD fetuses and possible assessment of membrane architecture but this imaging modality was not available during the experimental period so could not be investigated at this time. As such, the *Scrib<sup>fl</sup>* model does not reliably mimic the impact of prolonged amniotic fluid exposure on bowel development and function. Therefore it is an inappropriate model for the investigation of GRID and could result in misleading research data.

However, the *Scrib<sup>fl</sup>* model would be potentially useful for the investigation of exomphalos related pulmonary hypoplasia, which is one of the most significant causes of morbidity and mortality in patients with exomphalos. A strong association has been shown between exomphalos defect size and severity of pulmonary hypoplasia with major/giant exomphalos defects exhibiting the most severe hypoplasia (Vachharajani et al., 2009, Argyle, 1989). The *Scrib<sup>fl</sup>* mutant mouse model may be advantageous for the investigation of exomphalos related pulmonary hypoplasia given the model exhibits both moderate and giant defect sizes. As such, it would be possible to directly compare lung development between normal controls and differing sizes of exomphalos defect. Characterisation of macroscopic and microscopic lung development alongside development of an in-utero therapy to improve lung function would be possible with the *Scrib<sup>fl</sup>* model.

#### **3.3.1.4 Concomitant Pathology and Penetrance**

The majority of fetuses with exomphalos exhibited a concomitant craniorachischisis defect (67%), which was associated with blood stained amniotic fluid. Therefore, even if the membrane covering the herniated viscera ruptured at a uniform time during gestation exposing the bowel to amniotic fluid, this model would be of limited use for the investigation of GRID due to the confounding factor of blood within the amniotic fluid, which is not a feature of gastroschisis. Even if blood staining was not a feature, the penetrance of AWD in *Scribble* null fetuses was very low (23%). As such, the *Scrib*<sup>fl</sup> model would require a large number of pregnant dams in order to fully investigate the pathophysiology of GRID and is therefore not an optimal model.

#### **3.3.2 The Use of In-Amnio Micro-MRI for Fetal Structural Phenotyping**

Cutting edge imaging technology is increasingly being used for the phenotyping of genetically manipulated mouse models of disease (Turnbull and Mori, 2007). MRI is becoming a well-established technique enabling detailed non-invasive visualisation of structures (Schneider et al., 2003) with high resolution images (Petiet et al., 2008) that can be analysed using automated computational methods (Norris et al., 2013a). To date, mouse MRI techniques have mainly involved imaging of *ex-vivo* fetuses removed from the amniotic sac (Norris et al., 2013b). Although in-utero MRI is possible the image resolution is limited and therefore can only be used for easily defined phenotypes (Nieman and Turnbull, 2010). Therefore, the in-amnio micro-MRI technique was developed specifically for this study to enable removal of the uterine wall whilst retaining the integrity of the fine membranes covering the herniated abdominal viscera prior to imaging (Roberts et al., 2014). The use of software packages such as ImageJ and Amira 5.4 enabled detailed image reconstruction and visualisation of the AWD in multiple orientations (sagittal, coronal and axial) aiding phenotyping. This technique allowed for visualisation of the AWD and associated membranous structures providing confirmation of the exomphalos phenotype. However, further MRI optimisation would be required in order to determine whether the fine covering membrane was intact or ruptured. This technique could also be used for phenotyping of other ambiguous mouse AWDs as

well as amniotic membrane, umbilical cord and placental defects where integrity of the amniotic membrane is essential for anatomical preservation.

The disadvantages of micro-MRI include long scan times, high cost and the *ex-vivo* nature of the imaging results in animal loss and inability to map the natural history of AWD formation within one fetus throughout gestation. For the purposes of this study the entire fetus was scanned resulting in a long scan duration of approximately 10 hours in order to obtain high resolution images. However, the scan duration could be shortened if site specific imaging was performed in cases where visualisation of the whole embryo is not required, which in turn would reduce the cost of performing micro-MRI.

*In-vivo* fetal Micro-ultrasound may also be a valuable tool for the phenotyping of AWDs in fetal mice. Developments in micro-ultrasound have enabled the acquisition of high resolution *in-vivo* fetal mouse images with a rapid imaging speed at a low cost (Foster et al., 2002, Foster et al., 2011, Liu et al., 2017). The ability to obtain high resolution *in-vivo* images of fetal mice would enable serial imaging of the same dam and in turn her multiple fetuses throughout gestation providing documentation of the natural history of AWD formation and associated membrane structures whilst reducing animal loss.

### **3.3.3 Bowel Development**

#### ***3.3.3.1 Gross Bowel Development***

A shorter bowel length was observed in the giant exomphalos defects compared to controls. Although mice with the giant exomphalos defect displayed no macroscopic evidence of bowel inflammation there was a slightly greater weight per unit length of bowel, which only just achieved statistical significance. This phenomenon could have been investigated further though analysis of bowel wall thickness on H&E stained cross-section bowel. The difference in giant exomphalos bowel compared to controls may represent a global failure of intra-abdominal structural development as part of the AWD formation. However, it could also represent intra-amniotic membrane rupture placing the bowel directly in contact with the amniotic fluid

resulting in the initiation of bowel wall inflammation as hypothesised to occur in gastroschisis.

### ***3.3.3.2 ICC and Enteric Neuron Development***

The small number of samples analysed in this study suggested that ICC and enteric neuron architecture at the level of the myenteric plexus was normal in giant exomphalos fetuses compared to controls. Additionally, in this small cohort the results suggested the numbers of ICC were normal in the giant exomphalos fetuses compared to controls. No further conclusions can be made due to the small number of samples analysed secondary to poor AWD penetrance, high tissue loss due to a difficult whole mount processing technique and the decision not to continue any further experiments with this mouse model on ethical grounds given the AWD expressed by the Scribble knockout mice was that of exomphalos and not gastroschisis.

### **3.3.4 ICC Quantification**

Fetal mouse bowel at 18.5 dpc has a very small diameter and is very fragile. It was not possible to accurately discern individual ICC or enteric neurons from high powered images of cross-sectioned bowel as these cells were too small within the field of view. Additionally, it was not possible to visualise the architecture of the ICC and enteric neuron networks for the same reason. Therefore cells could not be reliably counted nor the maturity of the cell networks assessed. This method for cell quantification was therefore discarded. These findings also bring into question the validity of previously reported ICC numbers in small animal gastroschisis models (Vargun et al., 2007, Danzer et al., 2010, Midrio et al., 2004, Auber et al., 2013). All such reports have relied solely on cross-sectioned tissue and semi-quantitative or qualitative quantification methods, which may have generated inaccurate and potentially misleading results due to the random presence/absence of ICC in the cross section examined. Also, not all these reports mention blinding of the investigator to the origin of the analysed tissue, which could have led to bias during quantification.

Confocal imaging of whole mount bowel preparations enabled imaging of the entire myenteric plexus, providing clear images of the interconnecting cell networks of the ICC and enteric neurons from which accurate assessment of cell maturity was possible. Individual cell bodies of both ICC and enteric neurons were easily discernible providing a robust quantification method using ImageJ cell counting software. However, whole mount, muscle only tissue preparations were difficult to process in 18.5 dpc mouse gut and therefore for later studies whole tube preparations were developed in order to improve processing efficiency and reduce tissue loss.

### **3.4 Conclusion**

The terms exomphalos and gastroschisis are being used interchangeably within the NTD literature to describe AWD in genetic mouse models without detailed assessment of the defect anatomy. Accurate characterisation of AWD is challenging but can be aided through meticulous microdissection identifying the defect location, umbilical cord insertion, umbilical ring closure and presence or absence of a membrane covering the externalised abdominal viscera. Novel imaging techniques can also greatly aid phenotyping of ambiguous structural defects in circumstances where microdissection leads to disruption of important structures making accurate phenotyping by this method difficult. This study highlights the importance of performing accurate phenotypic analysis of any structural anomaly prior to embarking on research specifically linked to the described defect. Finally, this study also highlights the importance of appropriate methods for tissue preparation, immunostaining, imaging and cell quantification in order to enable accurate qualitative quantification and architectural assessment of bowel wall ICC.

# **Chapter 4: Aortic Carboxypeptidase-Like Protein (ACLP) Knockout Mouse Model: Phenotypic Characterisation and Impact of Inflammation on ICC Development and Gut Motility**

## **4.1 Introduction**

The aortic carboxypeptidase-like protein (ACLP, also known as adipocyte enhancer binding protein 1 [AEBP1]) is a signalling protein with a discoidin I domain (Baumgartner et al., 1998) and a signal peptide amino terminus similar to metalloproteinases but missing several amino acids required for catalytic activity against standard carboxypeptidase substrates (Gomis-Ruth et al., 1999). ACLP is secreted during development into the extracellular matrix of connective tissues such as the abdominal wall, blood vessels, skeleton and dermis and acts as a binding protein, facilitating cell aggregation/adhesion and cell-cell recognition (Layne et al., 2001). The ACLP knockout mouse is reported in the literature to exhibit a gastroschisis phenotype. (Layne et al., 2001, Danzer et al., 2010).

Therefore, failed abdominal wall closure in ACLP null fetuses has been hypothesised to occur due to loss of ventral wall migratory signals (Layne et al., 2001). The AWD expressed by the ACLP knockout fetuses has been described as gastroschisis with a persistent herniation of the intestine into the amniotic fluid through an AWD located adjacent to the umbilicus (Layne et al., 2001, Danzer et al., 2010). However, this description was based on gross visualisation of the defect presumably of fetuses removed from the amnion and no detailed anatomical analysis of the AWD has been performed.

In the ACLP knockout mouse model, immunohistochemical analysis of AWD fetal cross sectional intestinal tissue shows the decrease of ICC and enteric neurons (Danzer et al., 2010) compared to controls. This suggests that abnormal development of ICC and enteric neurons in gastroschisis small bowel could be the cause of GRID. However, ICC and enteric neuron cell quantification was performed using cross-sectioned bowel with a semi-quantitative technique and no bowel motility studies were performed.



The amniotic fluid of human gastroschisis pregnancies has been shown to be pro-inflammatory with an elevation in IL-8 (pro-inflammatory cytokine) compared to healthy controls (Morrison et al., 1998) and it has been hypothesised that bowel wall exposure to IL-8 could be a trigger of GRID (de Beaufort et al., 1998, Api et al., 2001, Correia-Pinto et al., 2002, Hakguder et al., 2011, Olguner et al., 2006). However, the impact of IL-8 on ICC development in gastroschisis has not previously been investigated.

The aims of this study were to: (i) accurately delineate the AWD anatomy that results from ACLP absence; (ii) compare bowel wall ICC and enteric neuron development between experimental groups (untreated phenotypically normal, untreated AWD, intra-amniotic IL-8 injected normal and intra-amniotic IL-8 injected AWD fetuses); (iii) compare bowel motility patterns between experimental groups.

## **4.2 Results**

### **4.2.1 Gross Characterisation of ACLP Knockout Fetuses**

During the experimental period, 298 fetuses were collected, 283 at 18.5 dpc and 9 at 13.5 dpc. 215 (74%) were phenotypically normal and 77 (26%) exhibited an AWD phenotype. These ratios are as expected by Mendelian inheritance for fully penetrant phenotypes suggesting that AWD fetuses survive to full term. Mutant fetuses exhibited an isolated AWD with no other gross structural defects, such as craniorachischisis or other neural tube defects.

Genotyping was performed on 69 fetuses of which there were: 26 (38%) wild types ( $ACL P^{+/+}$ ), 21 (30%) heterozygotes ( $ACL P^{+/-}$ ) and 23 (33%) homozygote knockouts ( $ACL P^{-/-}$ ). These ratios do not fall into the expected Mendelian ratios. However, over a large population it would be expected that the ratios are similar to those anticipated by Mendelian inheritance (1:2:1). All wild type and heterozygote fetuses were phenotypically normal and therefore heterozygote fetuses were considered as normal controls. Twenty-two homozygote knockout fetuses exhibited an AWD and 1 homozygote fetus was phenotypically normal. Hence, the penetrance of AWD in ACLP knockout mice was 96%.

## **4.2.2 Abdominal Wall Defect Phenotype**

### ***4.2.2.1 Timing of Abdominal Wall Defect Phenotyping***

Microdissection of phenotypically normal and AWD fetuses was performed at 18.5 dpc prior to harvesting of gut for ileal studies. In-amnio paraffin embedded fetal cross-sections of phenotypically normal and AWD fetuses was performed at time points 13.5 dpc (during physiological herniation) and 18.5 dpc (after resolution of physiological herniation).

### ***4.2.2.2 Visualisation of Intra-Amniotic Fetuses***

Phenotyping by visualisation through intact membranes was not possible at 13.5 dpc as it was not possible to distinguish between normal physiological herniation of the bowel and evisceration of the bowel through an AWD due to the translucent nature of the membrane containing the physiologically herniated bowel. Phenotyping through intact amniotic membranes at 18.5 dpc revealed two abdominal wall phenotypes; phenotypically normal fetuses and a single type of AWD.

Phenotypically normal fetuses (Figure 4-1A) exhibited a closed abdominal wall onto which the umbilical cord centrally inserted and the limbs were tightly folded in front of the torso. Fetuses with the AWD (Figure 4-1B) exhibited externalised free floating abdominal viscera including bowel and liver, which lay in front of the abdominal wall obscuring the AWD from view. The limbs were splayed laterally to accommodate the externalised viscera. The amniotic fluid was clear and non-blood stained in both the phenotypically normal and AWD fetuses and the placenta appeared grossly normal in both phenotypes.

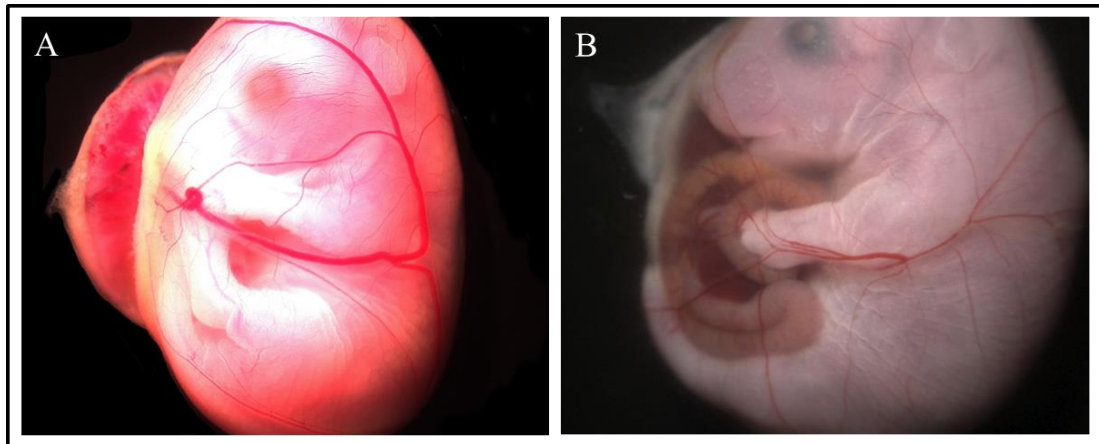


**Figure 4-1:** Intra-amniotic fetuses at 18.5 dpc, 0.6x objective. **A.** Phenotypically normal fetus. **B.** Fetus with AWD exhibiting externalised, free floating bowel and liver.

#### **4.2.2.3 Microdissection**

Microdissection at 18.5 dpc confirmed the presence of two abdominal wall phenotypes. Phenotypically normal fetuses (Figure 4-2A) were observed to have a closed ventral abdominal wall and a structurally normal umbilical cord consisting of 3 blood vessels contained within the amniotic membrane. The umbilical cord originated from a grossly normal placenta and inserted centrally on the abdominal wall. Microdissection of the AWD fetus (Figure 4-2B-D) revealed a centrally located AWD approximately 2mm in diameter permitting externalisation of the bowel, stomach, liver and spleen. There was no membrane covering the eviscerated organs, which were therefore free floating in fluid. Although the umbilical cord was of a normal length and consisted of 3 blood vessels, the blood vessels were not covered by the amniotic membrane leaving the cord uncovered. The abnormal cord entered the abdominal cavity through the left lateral edge of the ventral wall defect. Careful dissection revealed that the amniotic membrane, instead of adhering to the umbilical vessels, attached directly onto the abdominal wall defect edge maintaining continuity between the amnion and body wall ectoderm. The externalised, non-covered viscera were therefore free floating within the exocoelomic cavity, separated from the amniotic fluid by the amniotic membrane. As such, these findings suggest that ACLP knockout mice do not exhibit a true gastroschisis defect as the bowel is exposed to exocoelomic fluid rather than amniotic fluid as it would be in human gastroschisis.

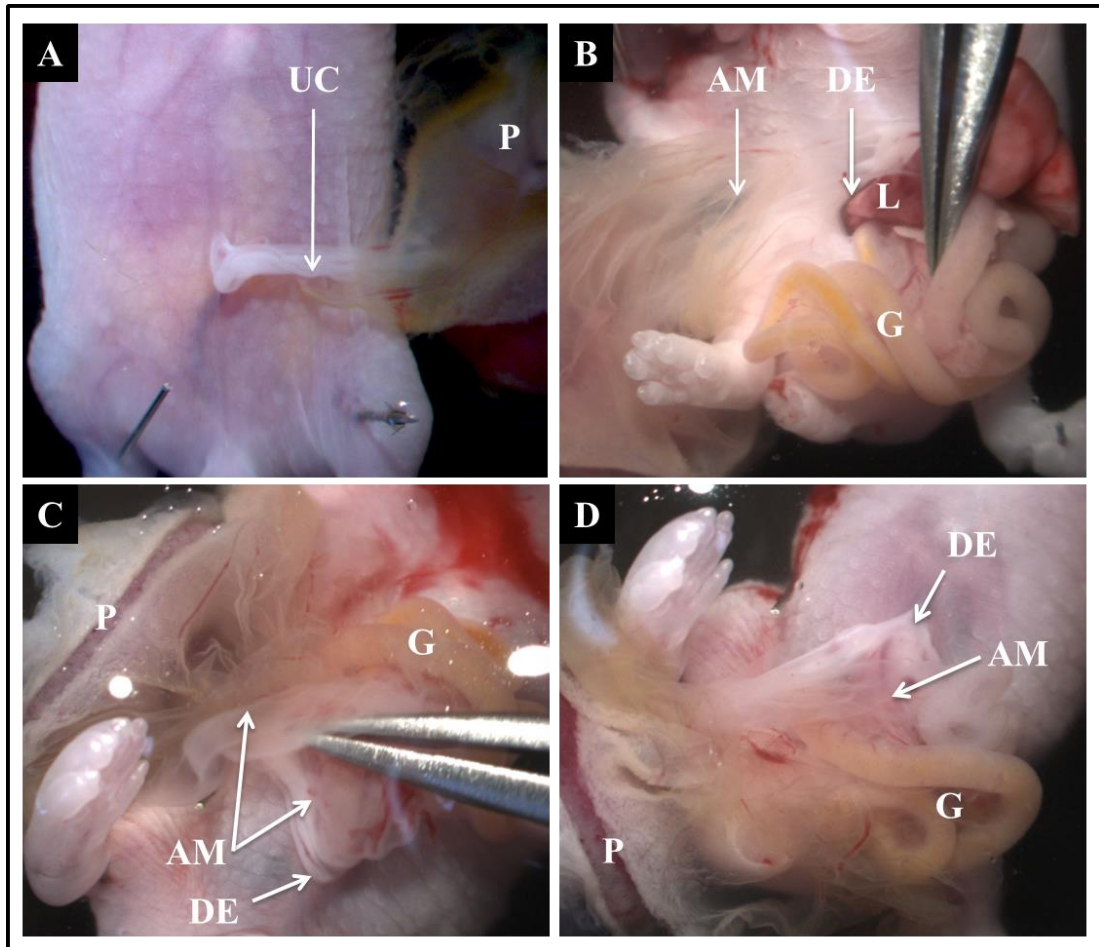


**Figure 4-2:** Microdissection images of ACLP phenotypically normal and AWD fetuses at 18.5 dpc, orientated with tail inferiorly, 0.6x objective. **A.** Phenotypically normal fetus with a structurally normal umbilical cord (UC), consisting of 3 blood vessels, covered by the amniotic membrane, which inserts centrally on a closed abdominal wall. **B-D.** AWD fetuses. The amniotic membrane (AM) attaches directly to the ventral wall defect edge (DE) and the externalised gut (G) and liver (L) are free floating within the exocoelomic cavity separated from the amniotic fluid by the amniotic membrane. **B.** Direct view of the ventral abdominal wall defect with the amniotic membrane (AM) lying flat against the abdominal wall. **C.** The amniotic membrane is displaced superiorly away from the abdominal wall to reveal the direct attachment to the inferior defect edge. **D.** The amniotic membrane is displaced inferiorly away from the abdominal wall to reveal the direct attachment to the superior defect edge. **A, C and D.** The placenta (P) was grossly normal in all fetuses.

#### 4.2.2.4 Fetal In-Amnio Paraffin Embedded Cross-Sections

In-amnio paraffin embedded H&E stained sagittal cross-sections of phenotypically normal fetuses revealed at 13.5 dpc physiological herniation and at 18.5 dpc a closed abdominal wall consistent with the normal sequence of abdominal wall formation.

Phenotypically normal fetuses at 13.5 dpc (Figure 4-3) exhibited bowel herniation through the patent umbilical ring and into the base of the umbilical cord, which provided a membrane coverage protecting the herniated bowel from the amniotic fluid consistent with physiological herniation. Tracing the entire course of the amniotic membrane showed the membrane to encircle the outer surface of the fetus and to become adherent to the umbilical blood vessels at the point of emergence from the placenta thus forming a normal umbilical cord. The amniotic membrane continued adherent to the umbilical blood vessels before separating to encase the herniated bowel and finally attaching to the abdominal wall to continue as the body wall ectoderm. The amniotic and exocoelomic cavities were fluid filled and easily distinguishable. Phenotypically normal fetuses at 13.5 dpc are schematically represented in Figure 4-3B.



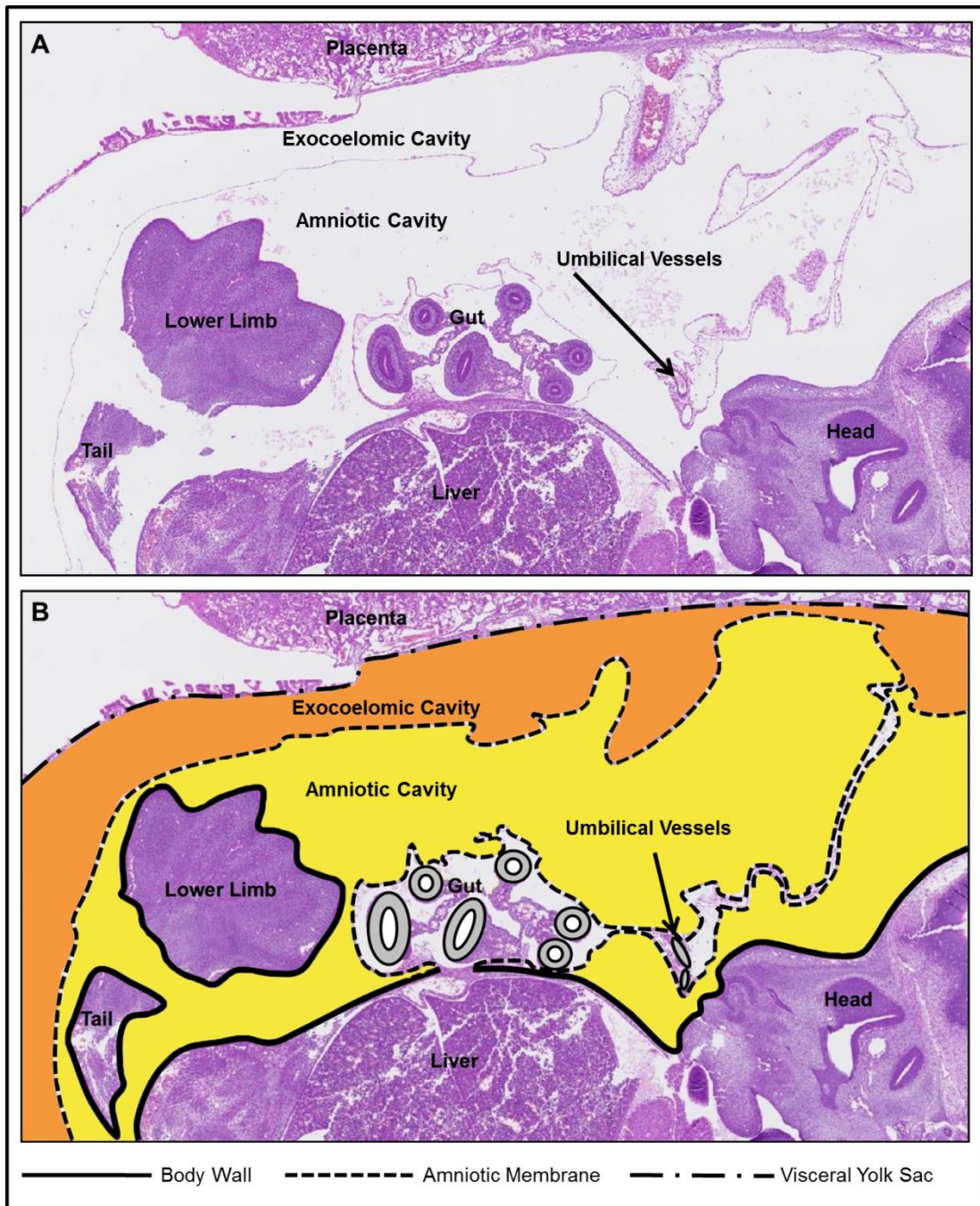


**Figure 4-3:** 13.5 dpc phenotypically normal in-amnio paraffin embedded fetus, H&E stained, sagittal cross-section through the umbilicus, imaged with Zeiss AxioScan Z1 slide scanner with 40x objective. This shows normal physiological herniation of the gut. **A.** Original AxioScan image. **B.** Schematic representation of fetal anatomy overlaid on the original image.

Cross-sections of phenotypically normal fetuses at 18.5 dpc (Figure 4-4) revealed fetuses with a closed abdominal wall and intra-abdominal viscera. The fetuses were tightly contained within the fetal membranes with little fluid present in either the amniotic or exocoelomic cavities, which is in keeping with the rapid decline in extra-

fetal fluid that is normally seen in fetal mice between 16 dpc and 18 dpc (Renfree et al., 1975) making it difficult to distinguish between the two. However, the amniotic membrane could be traced to encircle the fetus and adhere to the umbilical blood vessels. In contrast to the 13.5 dpc fetus, the amniotic membrane remained adherent to the umbilical blood vessels throughout the full length of the cord, which inserted centrally on the abdominal wall and the amniotic membrane continued as the body wall ectoderm. The anatomy is schematically represented Figure 4-4B.

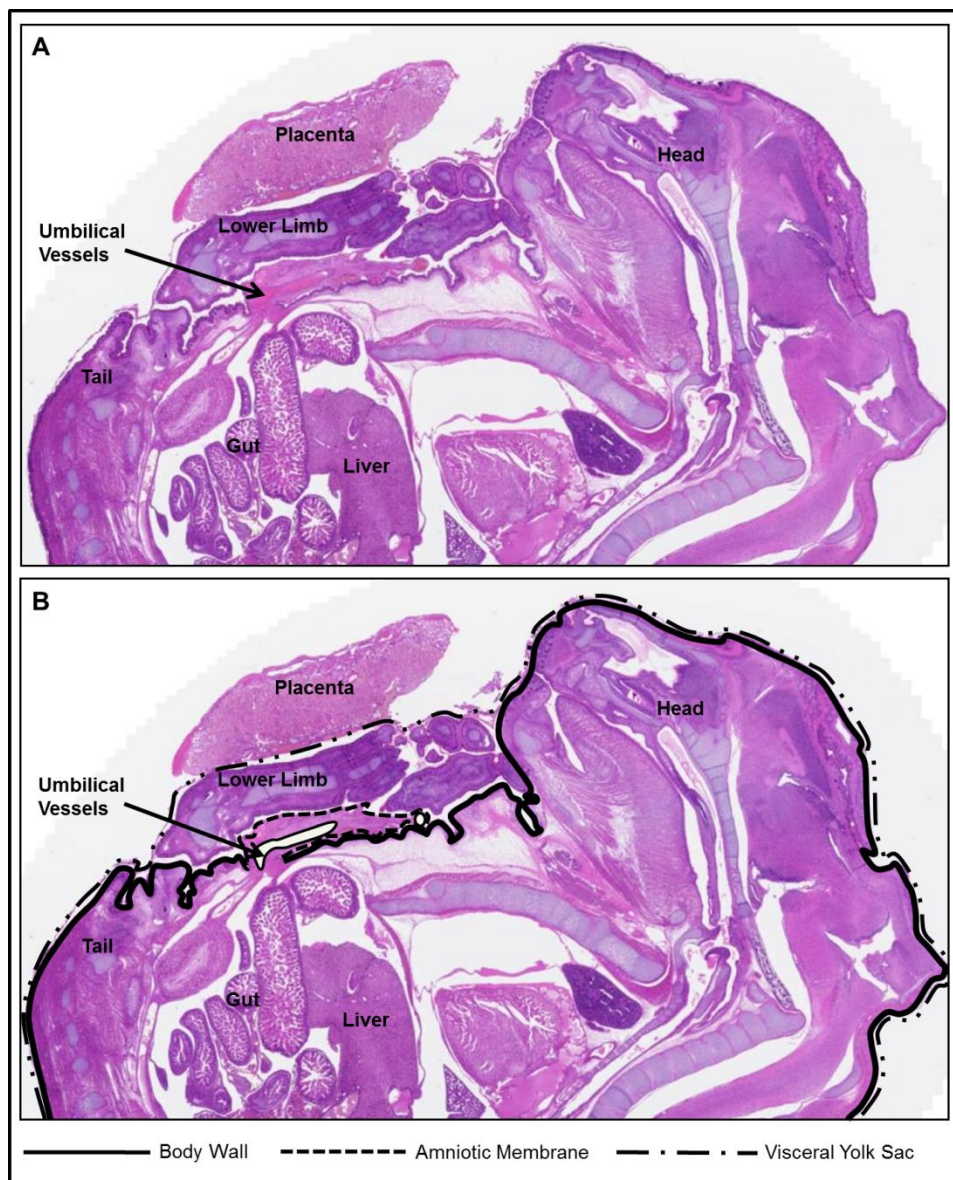


**Figure 4-4:** 18.5 dpc phenotypically normal in-amnio paraffin embedded fetus, H&E stained, sagittal cross-section through the umbilicus, imaged with Zeiss AxioScan Z1 slide scanner with 40x objective. Showing normal abdominal wall closure and a centrally inserted umbilical cord. **A.** Original AxioScan image. **B.** Schematic representation of fetal anatomy overlaid on the original image.

AWD fetuses expressed the same abdominal wall anatomy at both 13.5 (Figure 4-5) and 18.5 dpc (Figure 4-6). Fetuses exhibited a central defect through which the bowel and liver protruded without membrane coverage. The amniotic membrane was traced to encircle the fetus but failed to adhere to the umbilical blood vessels. Instead, the amniotic membrane directly attached to the abdominal wall defect edge becoming continuous with the body wall ectoderm. The gut and liver are visualised free floating within the exocoelomic cavity separated from the amniotic fluid by the amniotic membrane, confirming that ACLP knockout mice do not express a true gastroschisis defect. The amniotic and exocoelomic cavities were fluid filled at both time points and therefore easily distinguishable. AWD fetuses are schematically represented in Figure 4-5B and Figure 4-6B.

Phenotyping of AWD fetuses has shown these mutants to have a central abdominal wall defect through which bowel and liver are externalised and free floating within the exocoelomic cavity rather than the amniotic cavity as would be expected in a gastroschisis defect. The exocoelomic fluid composition is determined by the exchange of substances from the overlying visceral yolk sac serving as the principle site for the exchange of proteins between mother and fetus (Jauniaux and Gulbis, 2000), whilst the amniotic fluid composition is determined by fetal urine, meconium, secretions of oral and airway fluids and the amniotic membrane. As such, the composition of the exocoelomic fluid to which the externalised bowel of the AWD fetuses is exposed to is very different and potentially less noxious than that of the amniotic fluid, which the bowel would be exposed to if a true gastroschisis defect was present. However, phenotyping also reveals that the bowel is not contained within a membranous sac and therefore it is possible through in-utero injections to manipulate the composition of the exocoelomic fluid, which is in direct contact with the bowel.



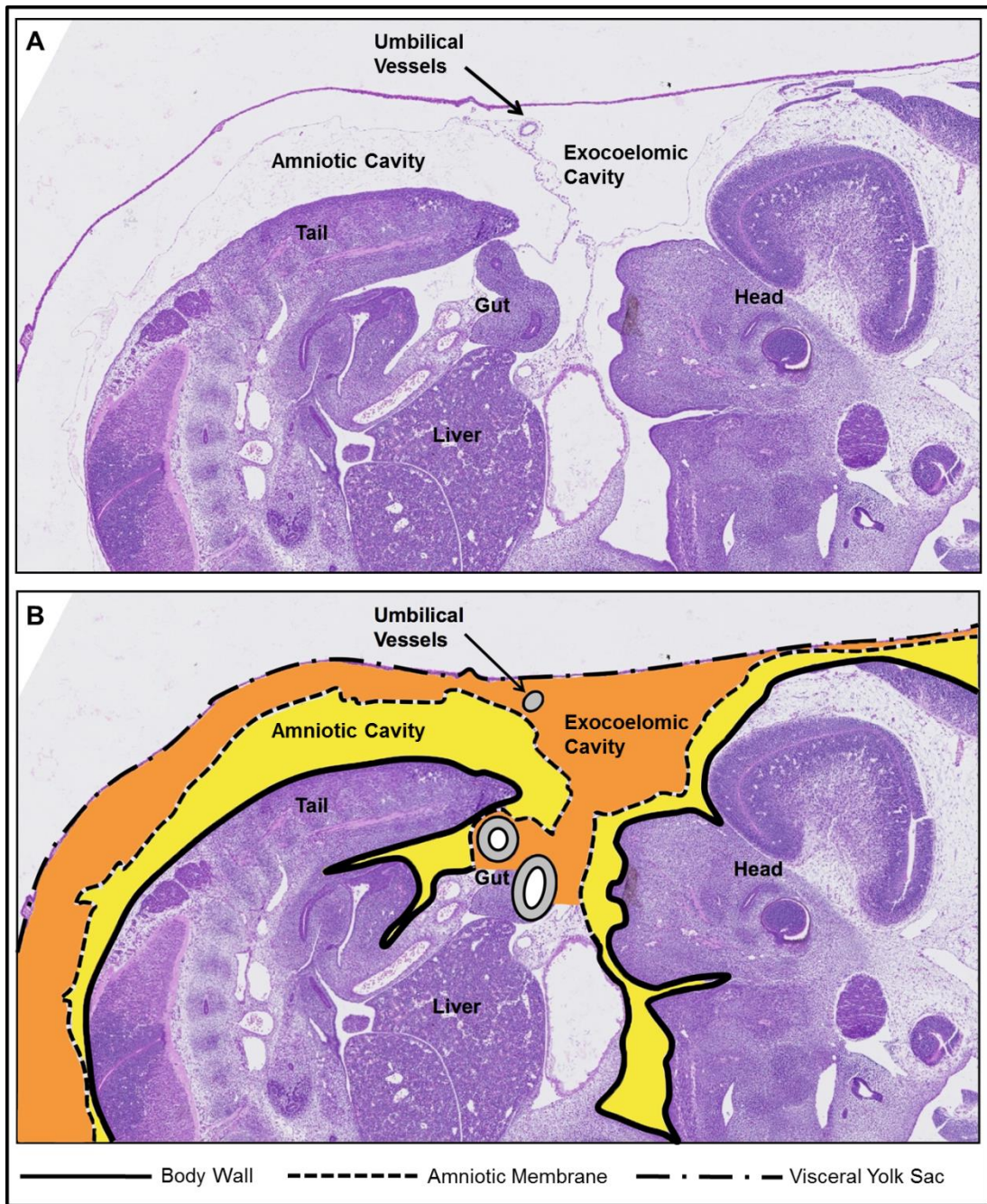


**Figure 4-5:** 13.5 dpc AWD in-amnio paraffin embedded fetus, H&E stained, sagittal cross-section through the umbilicus, imaged with Zeiss AxioScan Z1 slide scanner with 40x objective. This shows failed abdominal wall closure and failed attachment of the amniotic membrane to the umbilical cord resulting in the externalised bowel lying within the exocoelomic cavity separated from the amniotic fluid by the amniotic membrane. **A.** Original AxioScan image. **B.** Schematic representation of fetal anatomy overlaid on the original image.



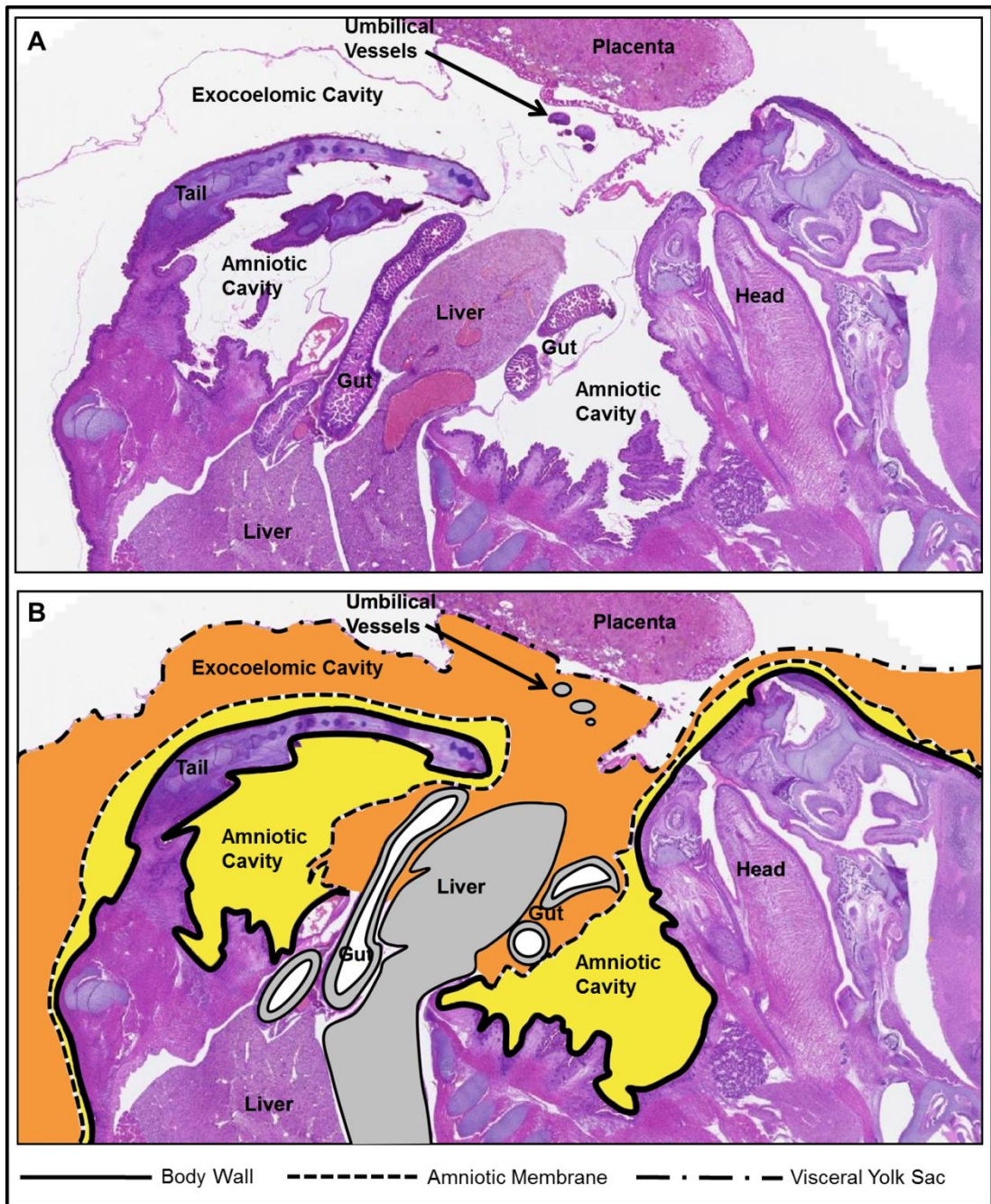


**Figure 4-6:** 18.5 dpc AWD in-amnio paraffin embedded fetus, H&E stained, sagittal cross-section through the umbilicus, imaged with Zeiss AxioScan Z1 slide scanner with 40x objective. This shows failed abdominal wall closure and failed attachment of the amniotic membrane to the umbilical cord resulting in the externalised bowel lying within the exocoelomic cavity separated from the amniotic fluid by the amniotic membrane. **A.** Original AxioScan image. **B.** Schematic representation of fetal anatomy overlaid on the original image.

#### ***4.2.2.5 Fetal Expression of ACLP and TGF $\beta$***

ACLP interacts with TGF $\beta$  signalling and affects collagen expression (Tumelty et al., 2014), which could lead to disrupted amniotic membrane collagen fibrils and be the cause of failed adherence of the amniotic membrane to the umbilical cord.

Therefore, in-amnio paraffin embedded fetuses were labelled for ACLP/AEBP1 and TGF $\beta$  with a DAB detection kit to identify possible abnormal signalling at the level of the abdominal wall and amniotic membrane. However, there was significant background staining for both the ACLP/AEBP1 (Figure 4-7) and TGF $\beta$  (Figure 4-8) labels and in the 18.5 dpc fetuses there was absent ACLP/AEBP1 (Figure 4-7C and D) staining for both phenotypically normal and AWD fetuses. Therefore, it was not possible to identify areas of positive staining from background staining and in turn assess the difference in expression of ACLP or TGF $\beta$  between the phenotypically normal and AWD fetuses. Further work would be necessary to optimise ACLP/AEBP1 and TGF $\beta$  staining in these fetuses.

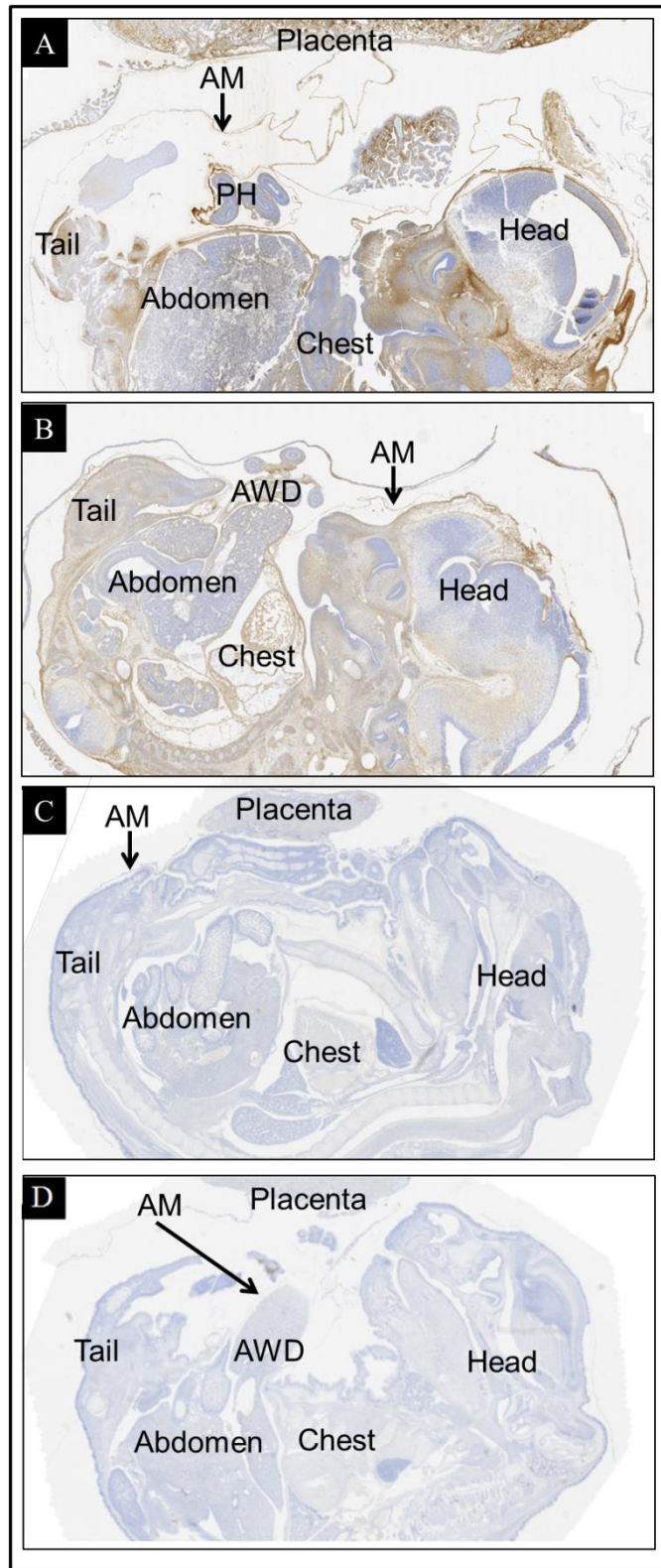


**Figure 4-7:** ACLP/AEBP1 labelling with DAB detection kit of in-amnio paraffin embedded fetus, sagittal cross-section through the umbilicus, imaged with Zeiss AxioScan Z1 slide scanner with 40x objective. This shows significant background staining of the 13.5 dpc phenotypically normal (A) and AWD fetuses (B). There is absent staining in both the 18.5 dpc phenotypically normal (C) and AWD (D) fetuses. Key: AM – amniotic membrane, PH – physiological hernia, AWD – abdominal wall defect.



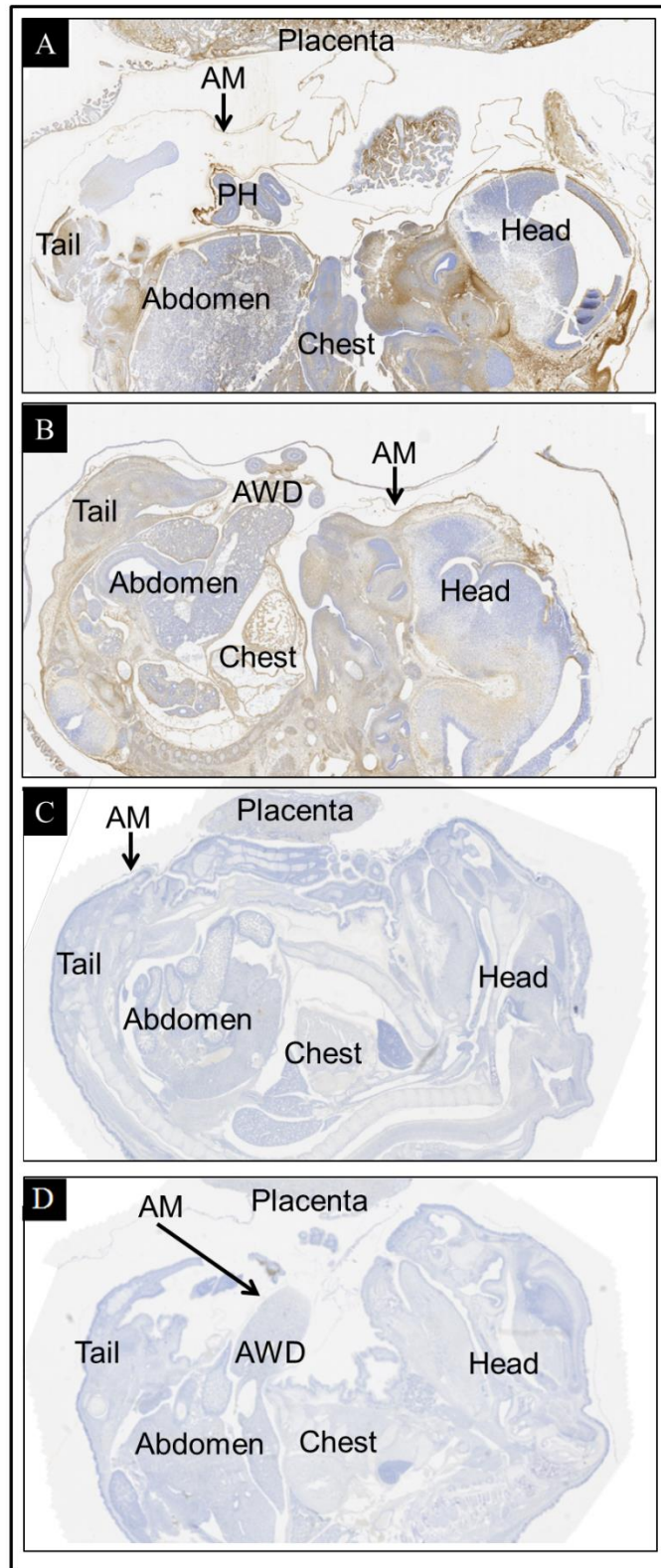


**Figure 4-8:** TGF $\beta$  labelling with DAB detection kit of in-amnio paraffin embedded fetus, sagittal cross-section through the umbilicus, imaged with Zeiss AxioScan Z1 slide scanner with 40x objective. This shows significant background staining of cross-sections. **A.** 13.5 dpc phenotypically normal fetus. **B.** 13.5 dpc AWD fetus. **C.** 18.5 dpc phenotypically normal fetus. **D.** 18.5 dpc AWD fetus. Key: AM – amniotic membrane, PH – physiological hernia, AWD – abdominal wall defect.

### **4.2.3 In-Utero IL-8 Injections**

In-utero IL-8 injections in AWD fetuses were performed into the exocoelomic fluid compartment due to the externalised bowel lying free floating within the exocoelomic cavity and not the amniotic fluid cavity. However, in the phenotypically normal (control) fetuses the exocoelomic cavity was not identifiable under direct vision and therefore in-utero IL-8 injections were performed into the amniotic cavity. Injections into the exocoelomic cavity in control fetuses may have been possible using micro-ultrasound guidance but this form of imagining was not available during the experimental period.

Comparisons of bowel wall morphology and ICC/enteric neuron numbers were made between the following experimental groups; untreated control versus untreated AWD, untreated AWD versus IL-8 injected AWD and untreated control versus IL-8 injected control.

### **4.2.4 Gross Bowel Morphology**

#### ***4.2.4.1 Pre-injection Comparison of Untreated Phenotypically Normal and Untreated AWD Fetuses***

There were no visual differences in the appearance of the bowel between either the untreated phenotypically normal (control) or untreated AWD fetuses. Bowel harvested from untreated AWD fetuses showed no evidence of inflammation or fibrous peel. There was no difference in bowel length (control  $5.9 \pm 0.1$ cm [mean  $\pm$  SEM], n=10 versus AWD  $5.7 \pm 0.2$ , n=10, p=0.26), bowel weight (control  $66.1 \pm 1.6$ mg versus AWD  $66.1 \pm 4.3$ mg, p>0.99) or weight per unit length (control  $11.2 \pm 0.3$ mg/cm versus AWD  $11.5 \pm 0.6$ mg/cm, p=0.66, Table 4-2). Although measurements of bowel wall thickness on H&E transverse cross sections showed a trend toward the untreated AWD bowel being thicker there was no significant difference in any measured parameter between the two groups (Table 4-1).

Bowel Wall Layer Measured	Untreated Control (n=10)	Untreated AWD (n=10)	p-value
Entire Wall Thickness ( $\mu\text{m}$ )	$34 \pm 1.4$	$38 \pm 1.7$	0.10
Muscle Thickness ( $\mu\text{m}$ )	$17 \pm 0.7$	$19 \pm 1.4$	0.08
Submucosa ( $\mu\text{m}$ )	$18 \pm 1.0$	$19 \pm 1.0$	0.27
Villus height ( $\mu\text{m}$ )	$190 \pm 15.4$	$194 \pm 14.2$	0.87
Crypt depth ( $\mu\text{m}$ )	$25 \pm 1.4$	$28 \pm 1.9$	0.19
Villus to Crypt ratio ( $\mu\text{m}$ )	$8 \pm 0.5$	$7 \pm 0.6$	0.11
Number of Muscle Cells	$4.7 \pm 0.12$	$5.0 \pm 0.11$	0.052
Muscle Cell Thickness ( $\mu\text{m}$ )	$3.6 \pm 0.16$	$3.8 \pm 0.10$	0.44

**Table 4-1:** Comparison of bowel wall measurements (mean  $\pm$  SEM) between untreated control and untreated AWD bowel.

#### 4.2.4.2 Statistical Comparison between Experimental Groups

Visually the serosal surface of IL-8 injected AWD bowel (n=10) compared to the other three groups appeared inflamed with more prominent blood vessels (IL-8 injected control group included n=10). On performing comparison of bowel length, weight and weight per unit length between experimental groups it showed a significant difference in bowel length between untreated AWD ( $5.7 \pm 0.2\text{cm}$ ) and IL-8 injected AWD groups ( $4.9 \pm 0.2\text{cm}$ ,  $p=0.0008$ ) but no difference between weight ( $p=0.24$ ) or weight per unit length ( $p=0.82$ ). There were no significant differences in any measurements between the untreated control and IL-8 control groups (Table 4-2).

Bowel Wall Layer Measured	Untreated Control (n=10)	Untreated AWD (n=10)	p-value
Bowel length (cm)	5.9 ± 0.1	5.7 ± 0.2	0.26
Bowel weight (mg)	66.1 ± 1.6	66.1 ± 4.3	0.99
Bowel weight per unit length (mg/cm)	11.2 ± 0.3	11.5 ± 0.6	0.66
Bowel Wall Layer Measured	Untreated AWD (n=10)	IL-8 AWD (n=10)	p-value
Bowel length (cm)	5.7 ± 0.2	4.9 ± 0.2	*0.0008
Bowel weight (mg)	66.1 ± 4.3	56.9 ± 6.2	0.24
Bowel weight per unit length (mg/cm)	11.5 ± 0.6	11.8 ± 1.3	0.82
Bowel Wall Layer Measured	Untreated Control (n=10)	IL-8 Control (n=10)	p-value
Bowel length (cm)	5.9 ± 0.1	5.6 ± 0.4	0.05
Bowel weight (mg)	66.1 ± 1.6	60.0 ± 3.3	0.11
Bowel weight per unit length (mg/cm)	11.2 ± 0.3	10.7 ± 0.5	0.40

**Table 4-2:** Comparisons of bowel length, weight and weight per unit length (mean ± SEM) between experimental groups. Comparisons made between: untreated control versus untreated AWD, untreated AWD versus IL-8 injected AWD and untreated control versus IL-8 injected control. \*Indicates p-values that reached significance.

Comparisons of bowel wall layer measurements between the untreated AWD and IL-8 injected AWD groups showed no significant differences in bowel wall thickness but evidence of crypt hyperplasia and villus blunting in the IL-8 injected AWD fetuses (Table 4-3).



Bowel Wall Layer Measured	Untreated AWD (n=10)	IL-8 AWD (n=10)	p-value
Entire Wall Thickness ( $\mu\text{m}$ )	$38 \pm 1.7$	$34 \pm 1.7$	0.07
Muscle Thickness ( $\mu\text{m}$ )	$19 \pm 1.4$	$19 \pm 1.0$	0.80
Submucosa ( $\mu\text{m}$ )	$19 \pm 1.0$	$17 \pm 2.7$	0.48
Villus height ( $\mu\text{m}$ )	$194 \pm 14.2$	$144 \pm 10.8$	*0.015
Crypt depth ( $\mu\text{m}$ )	$28 \pm 1.9$	$41 \pm 2.4$	*0.0002
Villus to Crypt ratio ( $\mu\text{m}$ )	$7 \pm 0.6$	$4.0 \pm 0.4$	*0.002
Number of Muscle Cells	$5.0 \pm 0.11$	$4.9 \pm 0.13$	0.45
Muscle Cell Thickness ( $\mu\text{m}$ )	$3.8 \pm 0.10$	$3.9 \pm 0.2$	0.71

**Table 4-3:** Comparisons of bowel wall layer measurements (mean  $\pm$  SEM) between untreated AWD and IL-8 injected AWD groups. \*Indicates p-values that reached significance.

Comparisons of bowel wall layer measurements between the untreated control and IL-8 injected control groups showed the IL-8 injected control fetuses entire bowel wall to be significantly thinner ( $30 \pm 1.3\mu\text{m}$ ) than that of the untreated controls ( $34 \pm 1.4\mu\text{m}$ ,  $p=0.04$ ). There were no other significant differences in bowel wall thickness measurements but there was evidence of crypt hyperplasia in the IL-8 injected AWD fetuses (Table 4-4).

These results therefore suggest that in-utero IL-8 injection did not cause increased bowel wall thickness in AWD or control fetuses but may have induced crypt hyperplasia and villus blunting.

Bowel Wall Layer Measured	Untreated Control (n=10)	IL-8 Control (n=10)	p-value
Entire Wall Thickness ( $\mu\text{m}$ )	$34 \pm 1.4$	$30 \pm 1.3$	*0.04
Muscle Thickness ( $\mu\text{m}$ )	$17 \pm 0.7$	$15 \pm 0.7$	0.15
Submucosa ( $\mu\text{m}$ )	$18 \pm 1.0$	$15 \pm 1.0$	0.15
Villus height ( $\mu\text{m}$ )	$190 \pm 15.4$	$166 \pm 10.1$	0.21
Crypt depth ( $\mu\text{m}$ )	$25 \pm 1.4$	$42 \pm 2.3$	* $<0.0001$
Villus to Crypt ratio ( $\mu\text{m}$ )	$8 \pm 0.5$	$4 \pm 0.5$	* $<0.0001$
Number of Muscle Cells	$4.7 \pm 0.12$	$4.3 \pm 0.1$	0.06
Muscle Cell Thickness ( $\mu\text{m}$ )	$3.6 \pm 0.16$	$3.5 \pm 0.1$	0.67

**Table 4-4:** Comparisons of bowel wall layer measurements (mean  $\pm$  SEM) between untreated control and IL-8 injected control groups. \*Indicates p-values that reached significance.

#### 4.2.5 ICC and Enteric Neurons

##### 4.2.5.1 Intact Gut Tube Whole Mount Preparation Technique

The preparation of intact gut tube, whole mount preparations was straightforward and required minimal tissue handling resulting in no tissue loss. Immunofluorescence staining was achieved reliably with anti-CD117 (ICC), anti-PGP9.5 (enteric neurons) and DAPI (nuclei). However, anti-HuC/D, which would have been the preferred option for quantification of enteric neurons did not penetrate or label the enteric neurons of intact gut tube preparations and therefore could not be used. The number of analysed whole mount specimens per experimental group was 10 untreated control, 10 untreated AWD, 9 IL-8 injected control and 11 IL-8 injected AWD.

#### ***4.2.5.2 ICC Architecture and Numbers: Comparison of Untreated Phenotypically Normal and AWD Fetuses***

The ICC at the level of the myenteric plexus were well developed in both untreated control (Figure 4-9A) and untreated AWD (Figure 4-9B) fetuses. The ICC exhibited numerous branching cytoplasmic processes, which interconnected with their counterparts creating a mature plexus. As expected for this gestational age, the myenteric ICC were the most well developed ICC population and ICC at the level of the deep muscular plexus were not observed in either group. The number of ICC per high powered field ( $45\text{nm}^2$ ) was significantly lower in the AWD group ( $80 \pm 2.1$ ) compared to the control group ( $90 \pm 2.5$ ,  $p=0.005$ ) i.e. 11% reduction in ICC number (Table 4-5).

#### ***4.2.5.3 ICC Architecture and Numbers: IL-8 Injected Groups***

The ICC at the level of the myenteric plexus in both the IL-8 injected control (Figure 4-9C) and IL-8 injected AWD (Figure 4-9D) fetuses exhibited normal cell and network architecture as described above. The numbers of ICC per high powered field ( $45\text{nm}^2$ ) appeared lower in the IL-8 injected groups (IL-8 injected AWD  $72 \pm 3.3$  and IL-8 injected control  $69 \pm 2.7$ ) than the untreated groups. However on performing comparisons of ICC numbers between experimental groups (Table 4-5) it showed no significant difference between untreated AWD and IL-8 injected AWD groups ( $p=0.08$ ) but a significant difference between untreated control and IL-8 injected control groups ( $p<0.0001$ ). These results suggest ICC numbers are affected by increased IL-8 concentrations but to a greater extent within the IL-8 injected control group than the IL-8 injected AWD group. Additional experimental animals would be necessary to examine these potential differences further and reach a definitive conclusion.

	Untreated Control (n=10)	Untreated AWD (n=10)	p-value
ICC	90 ± 2.5	80 ± 2.1	*0.005
	Untreated AWD (n=10)	IL-8 AWD (n=11)	p-value
ICC	80 ± 2.1	72 ± 3.3	0.08
	Untreated Control (n=10)	IL-8 Control (n=9)	p-value
ICC	90 ± 2.5	69 ± 2.7	*<0.0001

**Table 4-5:** Comparisons of the number of ICC (mean ± SEM) per high powered field of view (45nm<sup>2</sup>) between experimental groups. Comparisons made between: untreated control versus untreated AWD, untreated AWD versus IL-8 injected AWD and untreated control versus IL-8 injected control. \*Indicates p-values that reached significance.

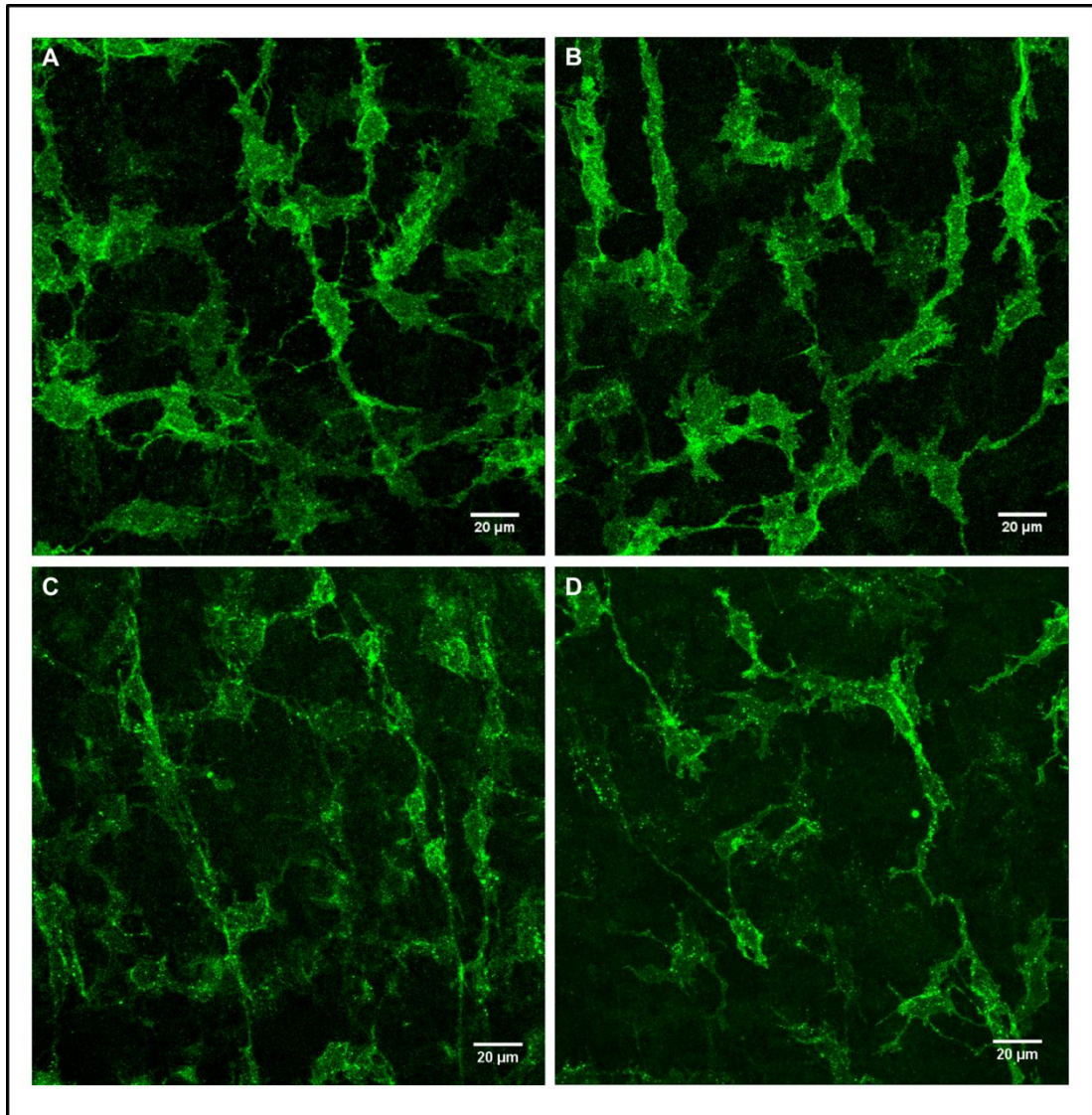


**Figure 4-9:** Whole mount 18.5 dpc ileal specimens stained for ICC with anti-CD117, images acquired using confocal microscopy, 40x objective, maximum intensity project of z-stack images. **A.** Untreated control. **B.** Untreated AWD. **C.** IL-8 injected control. **D.** IL-8 injected AWD.

#### ***4.2.5.4 Enteric Neuron Architecture and Numbers: Comparison of Untreated Phenotypically Normal and AWD Fetuses***

Enteric neurons at the level of the myenteric plexus were normally developed in both the untreated control (Figure 4-10A) and untreated AWD (Figure 4-10B) fetuses.

There were regularly spaced cell chains running parallel to each other with perpendicular crosslinking between chains giving a normal crosshatched appearance of the network. Cell quantification revealed no significant difference in the number

of enteric neurons per high powered field ( $45\text{nm}^2$ ) between the untreated control and untreated AWD fetuses (control  $85 \pm 3.5$  and AWD  $89 \pm 3.8$ ,  $p=0.46$ ).

#### 4.2.5.5 Enteric Neuron Architecture and Numbers: IL-8 Injected Groups

The enteric neurons at the level of the myenteric plexus in both the IL-8 injected control (Figure 4-10C) and the IL-8 injected AWD (Figure 4-10D) fetuses also exhibited a normal well developed architecture as described above. The numbers of enteric neurons per high powered field ( $45\text{nm}^2$ ) appeared slightly higher in the IL-8 injected groups (IL-8 injected AWD  $93 \pm 3.9$  and IL-8 injected control  $90 \pm 2.9$ ) than the untreated groups. However, on performing comparison of enteric neuron numbers between the experimental groups (Table 4-6) it showed no significant difference between untreated AWD and IL-8 injected AWD ( $p=0.47$ ) or untreated control and IL-8 injected control ( $p=0.29$ ) groups. Suggesting increased levels of inflammation did not impact on enteric neuron development.

	<b>Untreated Control (n=10)</b>	<b>Untreated AWD (n=10)</b>	<b>p-value</b>
Enteric Neurons	$85 \pm 3.5$	$89 \pm 3.8$	0.46
	<b>Untreated AWD (n=10)</b>	<b>IL-8 AWD (n=11)</b>	<b>p-value</b>
Enteric Neurons	$89 \pm 3.8$	$93 \pm 3.9$	0.47
	<b>Untreated Control (n=10)</b>	<b>IL-8 Control (n=9)</b>	<b>p-value</b>
Enteric Neurons	$85 \pm 3.5$	$90 \pm 2.9$	0.29

**Table 4-6:** Comparisons of the number of enteric neurons (mean  $\pm$  SEM) per high powered field of view ( $45\text{nm}^2$ ) between experimental groups. Comparisons made between: untreated control versus untreated AWD, untreated AWD versus IL-8 injected AWD and untreated control versus IL-8 injected control.



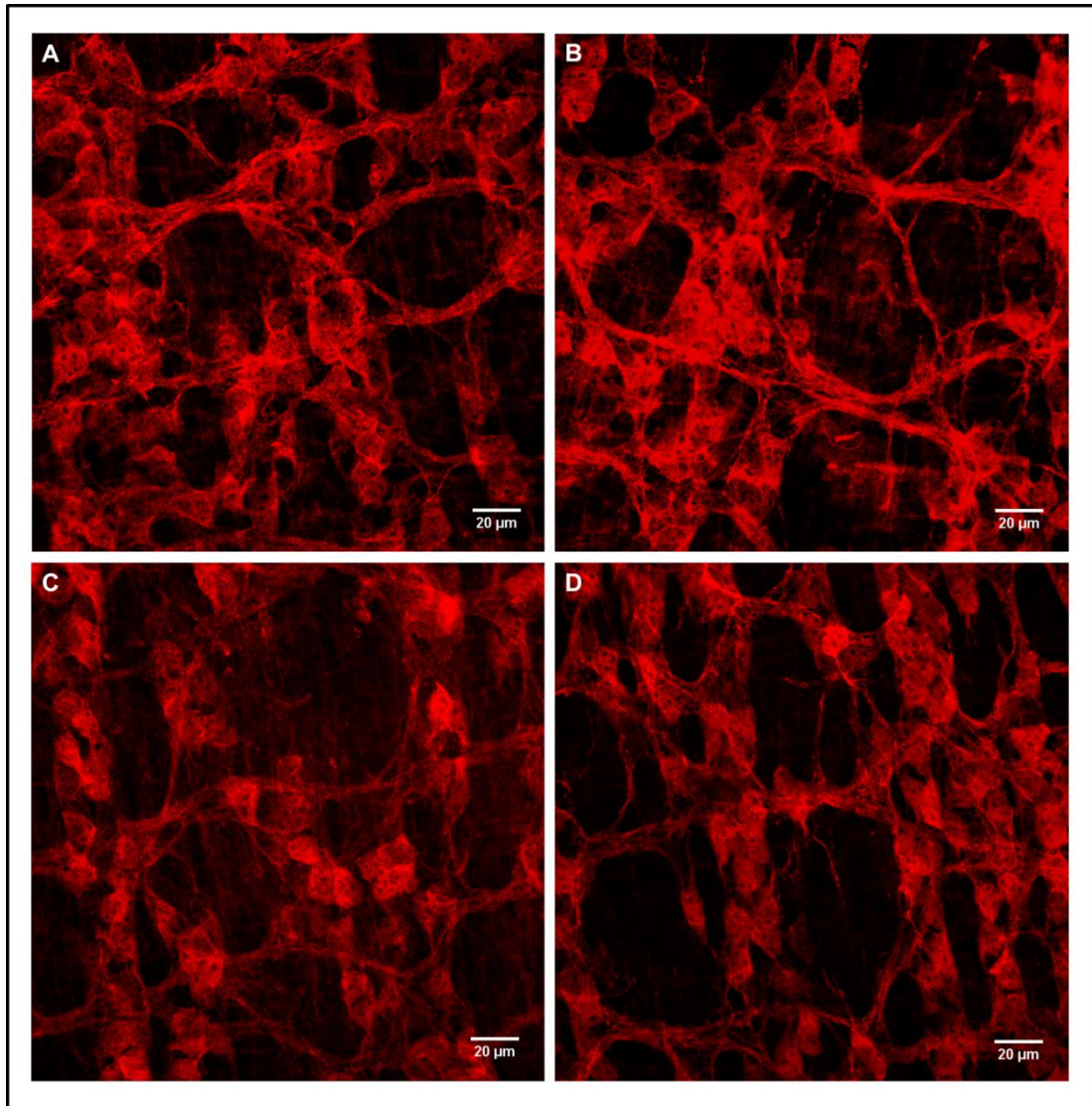


**Figure 4-10:** Whole mount 18.5 dpc ileal specimens stained for enteric neurons with anti-PGP9.5, images acquired by confocal microscopy, 40x objective, maximum intensity project of z-stack images. **A.** Untreated control. **B.** Untreated AWD. **C.** IL-8 injected control. **D.** IL-8 injected AWD.

## 4.2.6 Motility Studies

### 4.2.6.1 Experimental Groups

Recording of bowel motility and analysis of spatiotemporal maps were performed to determine whether presence of AWD or IL-8 injection affected bowel contractility. Motility studies were performed on bowel from 5 untreated control, 5 untreated AWD and 5 IL-8 injected AWD but not IL-8 injected control fetuses due interruption of the study secondary to colony infection with pinworm and subsequent treatment

regimen. However, the motility of one of the untreated control bowel segments failed to recover following dissection and transfer to the organ bath even after allowing 30 minutes for the bowel to equilibrate. Therefore this bowel segment was excluded from the analysis and only 4 untreated control bowel segments were included.

#### **4.2.6.2 *Pattern of Contractions***

Visual analysis of the spatiotemporal maps showed contractions to be present in all experimental groups. Shallow contractions considered to be ripples were present in all groups (Figure 4-11). Propagation of contractions along the bowel (contraction complexes) in both anal and oral directions was also evident in the untreated control and untreated AWD fetuses (Figure 4-11A, B and C) but not in the IL-8 injected AWD fetuses. This suggests that gut inflammation leads to rudimentary gut motility patterns.

#### **4.2.6.3 *Contraction Strength***

On visual comparison of the spatiotemporal maps, the untreated control bowel appeared to exhibit the strongest contractions followed by the untreated AWD and finally the IL-8 injected AWD bowel (Figure 4-11). To graphically visualise this data more clearly, the maximum percentage change from the mean diameter for each vertical slice was calculated. Each bowel segment was plotted on a graph depicting proportion (%) of bowel that achieved a given maximum percentage change (Figure 4-12A). The values were then averaged and displayed graphically as the mean for each experimental group (Figure 4-12B). Visually, Figure 4-12B depicts that the untreated control group achieves stronger contractions more frequently than the other groups particularly in the range of 20% to 50% maximum percentage change from the mean diameter. The IL-8 injected AWD bowel appears to achieve the weakest contractions.

To determine whether these observations reached statistical significance the area under the curve for each individual experiment was calculated and groups compared by ANOVA, which showed no statistical difference between the groups ( $p=0.14$ , Figure 4-12C). Additionally, ANOVA comparison of the proportion of bowel



achieving contractions that reached 20% ( $p=0.14$ ), 25% ( $p=0.13$ ), 30% ( $p=0.20$ ), 35% ( $p=0.21$ ), 40% ( $p=0.22$ ), 45% ( $p=0.20$ ) and 50% ( $p=0.20$ ) maximum percentage change from the mean diameter showed no significant difference. Although ANOVA analysis showed no statistical differences between the groups this could be due to the small number of experiments undertaken per group reducing the power of the comparisons.

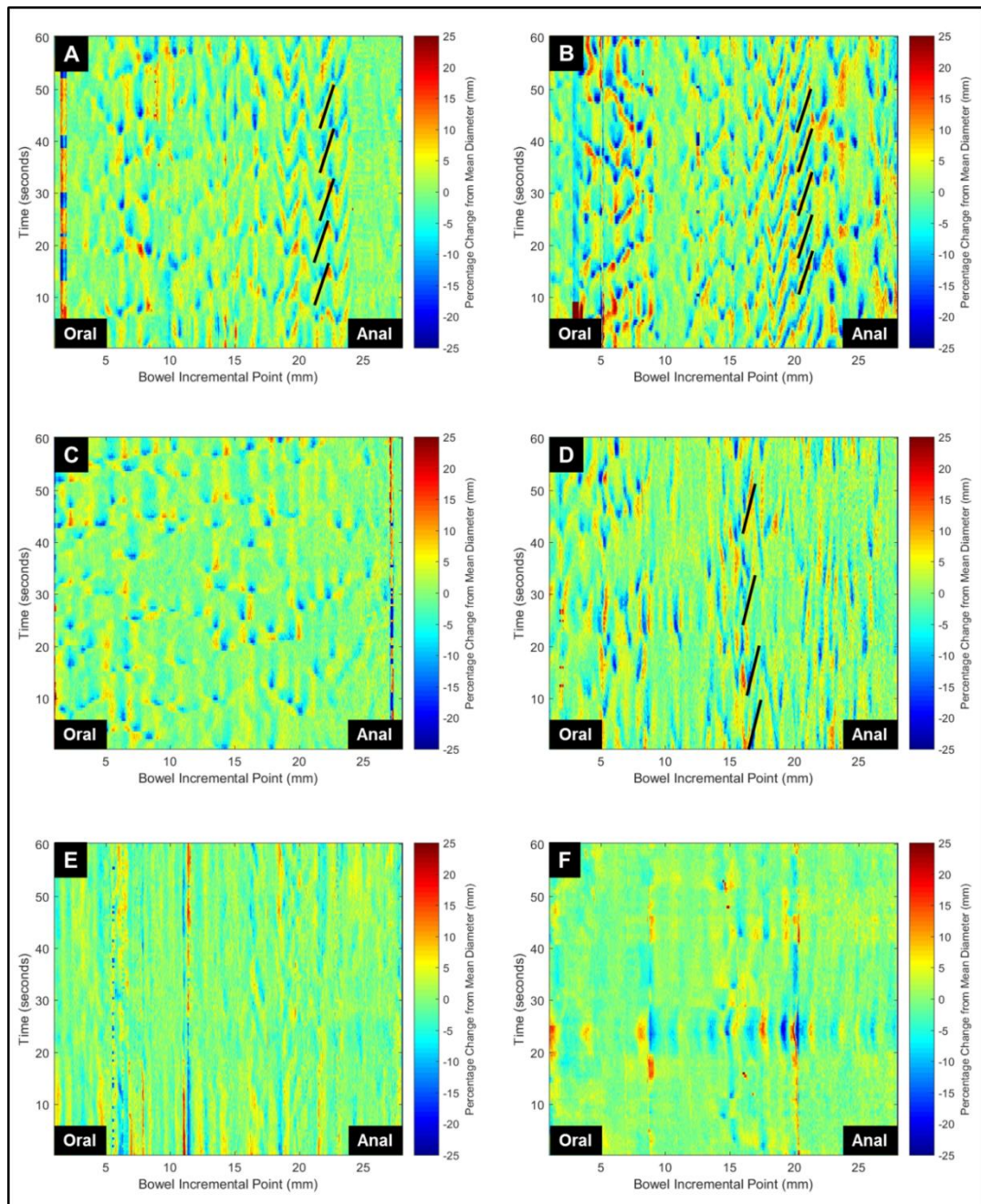


**Figure 4-11:** Representative spatiotemporal maps from each experimental group. **A and B.** Untreated control. **C and D.** Untreated AWD. **E and F.** IL-8 injected AWD. **A, B and D.** Black diagonal lines represent contraction complexes travelling in the oral to anal direction.

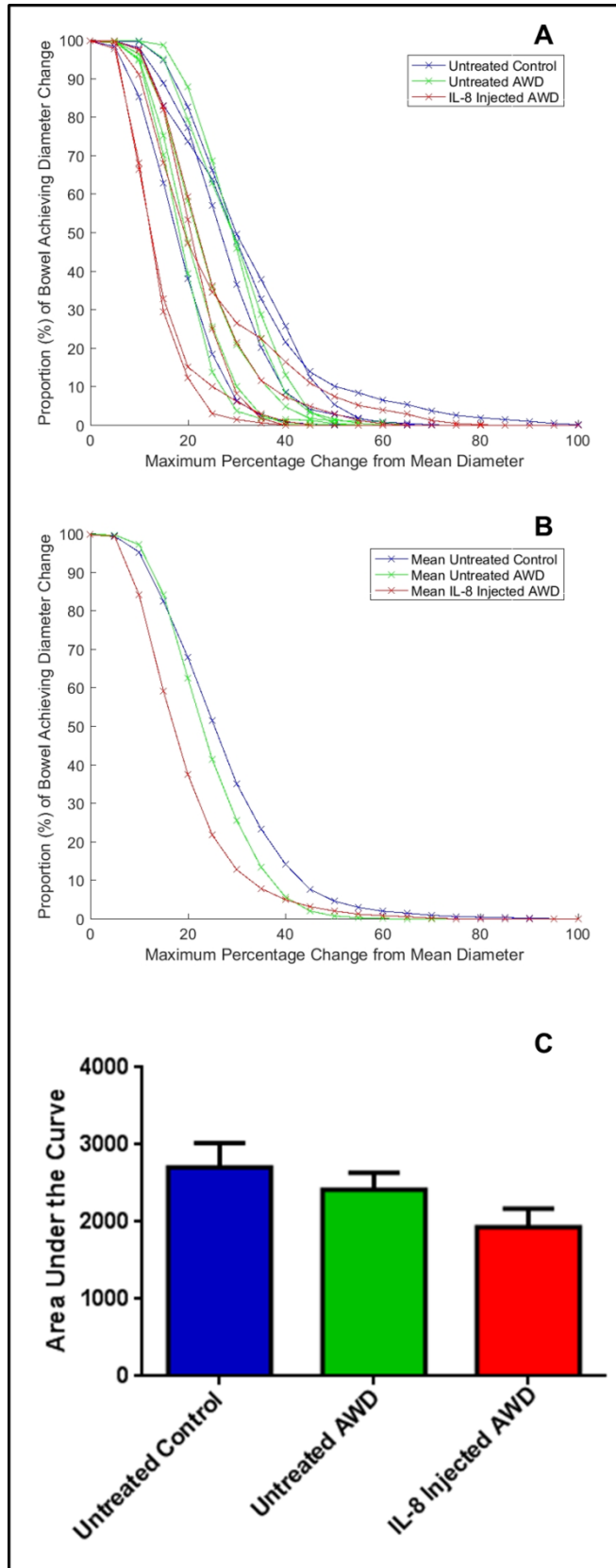


**Figure 4-12:** Contraction strength, represented as proportion of bowel achieving a given maximum percentage change from the mean diameter. **A.** Data from all experiments. **B.** Mean from each experimental group. **C.** Mean area underneath the curve for each experimental group.

#### **4.2.6.4 Frequency of Contractions**

The frequency of contractions was measured in two ways: (i) selection of the 3 most contractile vertical slices for each piece of bowel and (ii) analysis of the dominant number of contractions at all vertical slices for each piece of bowel. Figure 4-13 A, C and E shows the 3 vertical slices selected for a piece of bowel from each experimental group. The fast Fourier transform (FFT) was plotted for each selected vertical slice and the maximum amplitude taken as the dominant number of contractions per minute (Figure 4-13B, D and F). ANOVA analysis revealed a significant difference ( $p=0.009$ ) in the dominant contractions per minute between the groups. The most frequent contractions were seen in the untreated control group ( $8.9 \pm 0.8$  contractions per minute), followed by untreated AWD group ( $6.9 \pm 0.6$  contractions per minute) and lastly the IL-8 injected AWD group ( $5.7 \pm 0.6$  contractions per minute). However, multiple comparisons post test revealed the only significant difference was between the untreated control and IL-8 injected group (Figure 4-13G). Again, this is probably due to the small numbers of experiments performed.

For each piece of bowel the dominant number of contractions was calculated for all 0.022mm incremental vertical slices and plotted against the percentage of bowel contracting at each dominant frequency (Figure 4-14A – C). Any vertical slice contracting at a dominant frequency of less than 2 per minute was considered to be non-contractile and excluded from the analysis. The values were then averaged and displayed graphically as the mean for each experimental group (Figure 4-14D). Visually, Figure 4-14D depicts that the untreated control group was the most active with the commonest dominant contraction rate being 7 to 8 contractions per minute. A high proportion of the untreated AWD and IL-8 injected AWD bowel was non-contractile as evidenced by the commonest dominant contraction rate being 2 for both groups. ANOVA analysis revealed a statistically significant difference between the groups at a dominant frequency of 7 contractions per minute ( $p=0.029$ ) with multiple comparison testing revealing a significant difference between the untreated control and untreated AWD groups. However, statistical significance was not reached for any other dominant frequency rate.

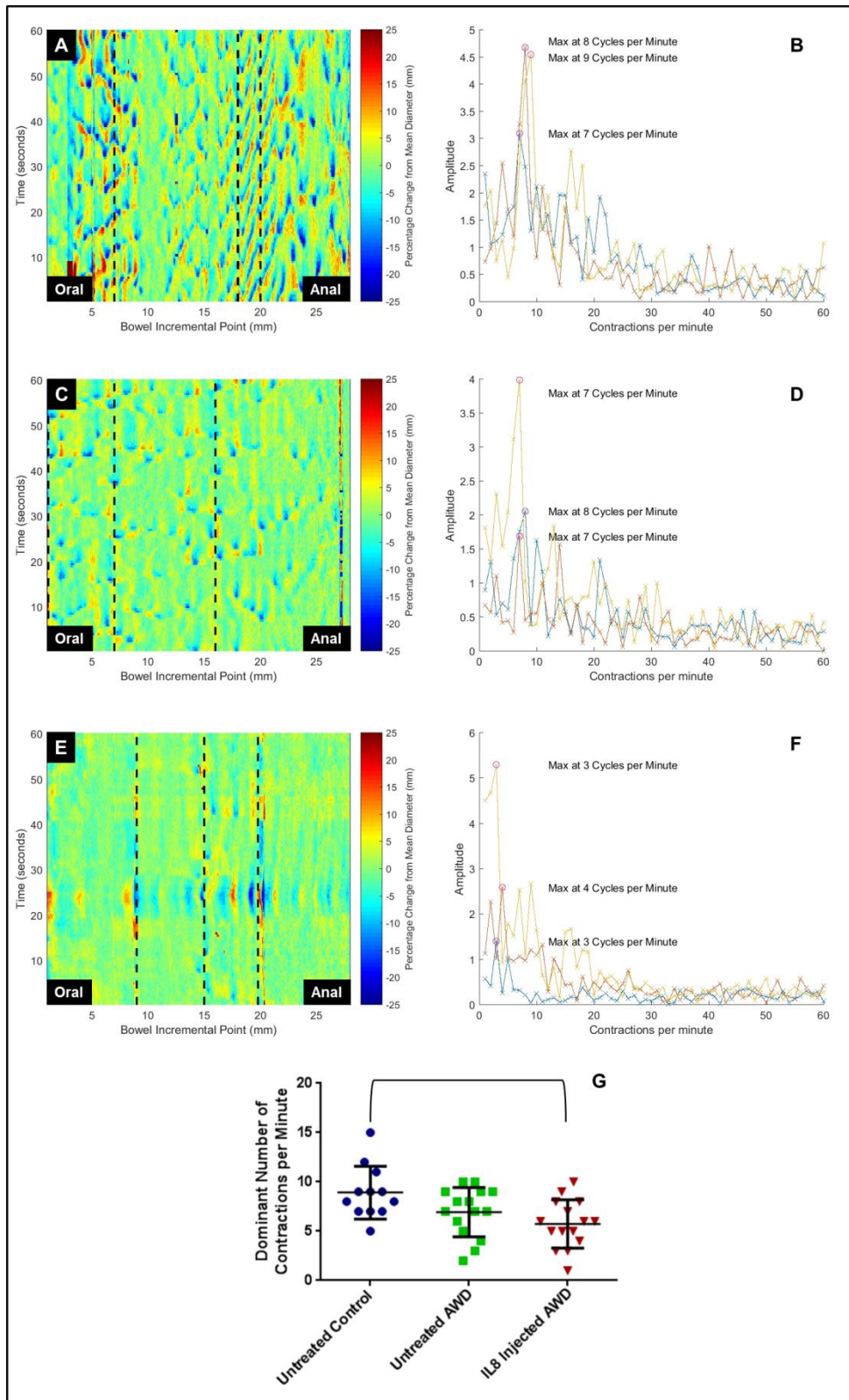


**Figure 4-13:** Fast Fourier transform (FFT) analysis of the selected 3 most contractile vertical slices per bowel segment. Representative vertical slice selections and corresponding FFT output for untreated control (**A and B**), untreated AWD (**C and D**) and IL-8 injected AWD (**E and F**). Comparison of dominant number of contractions per minute between groups. Brackets show significant comparison (one-way ANOVA).

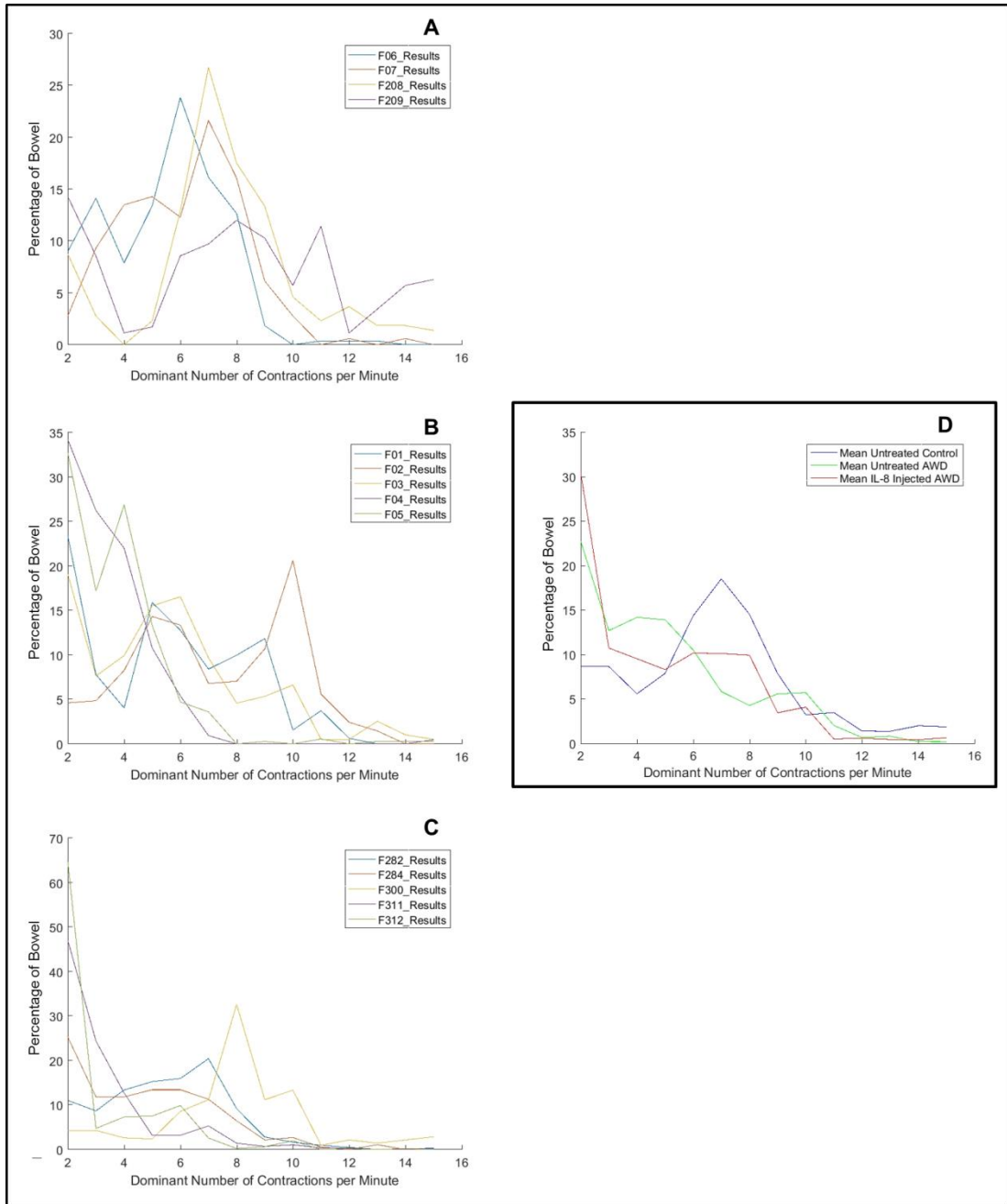


**Figure 4-14:** Fast Fourier transform (FFT) analysis for all 0.022mm incremental vertical slices for all segments of bowel. **A.** Untreated control. **B.** Untreated AWD. **C.** IL-8 injected AWD. **D.** Mean from each experimental group.



## 4.3 Discussion

### 4.3.1 Abdominal Wall Phenotype

#### 4.3.1.1 *An Unusual Exomphalos Phenotype?*

ACLP knockout fetuses exhibit failed abdominal wall closure at the umbilical ring and failed umbilical cord formation. The abdominal wall defect was centrally located and permitted the exteriorisation of abdominal viscera including bowel, stomach, liver and spleen. The amniotic membrane failed to adhere to the umbilical vessels and attached directly to the abdominal wall defect edge, resulting in the externalised viscera lying within the exocoelomic fluid. If normal umbilical cord formation had occurred in association with this centrally located AWD, then the externalised viscera would have been enclosed within the base of the umbilical cord and exhibited an exomphalos phenotype. Physiological herniation displays the same anatomical attributes as an exomphalos. Therefore direct comparison of the 13.5 dpc AWD fetal anatomy with the 13.5 dpc phenotypically normal fetuses exhibiting physiological herniation confirms failed umbilical cord formation in the ACLP mouse but illustrates that if the amniotic membrane had adhered to the umbilical vessels the AWD would be that of exomphalos (Figure 4-15). Additionally, the presence of multi-visceral herniation including the liver (as demonstrated by the ACLP knockout fetuses) is usually indicative of an exomphalos phenotype. It is unlikely this AWD is a body stalk defect due to the presence of a normal placenta (Bugge, 2012, Paul et al., 2001).

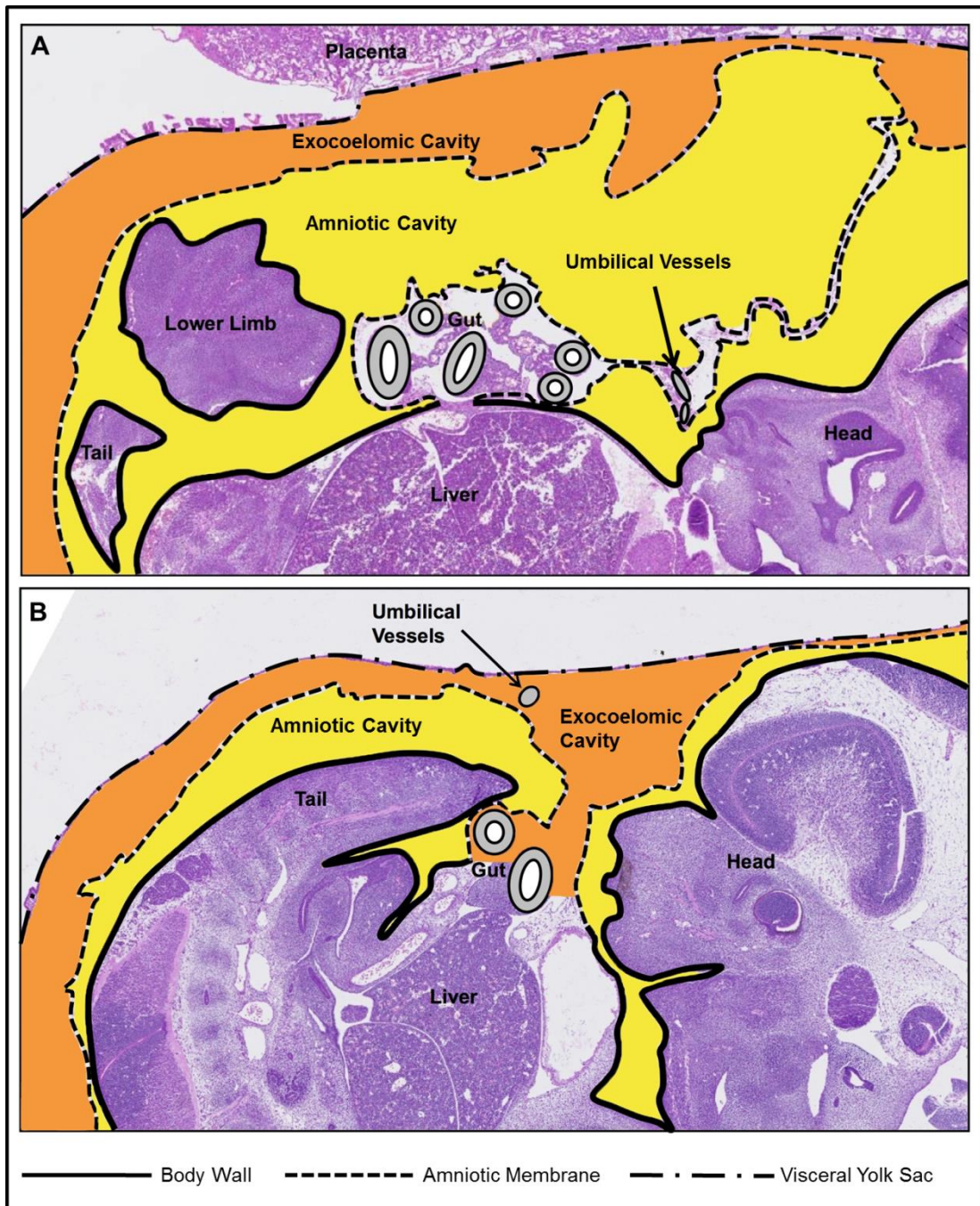


**Figure 4-15:** Comparison of schematic representations of a 13.5 dpc phenotypically normal fetus exhibiting physiological herniation (**A**) with a 13.5 dpc AWD fetus (**B**). If adherence of the amniotic membrane to the umbilical blood vessels had occurred forming a normal umbilical cord in the AWD fetus (**B**) then it would have the same anatomical appearance as the phenotypically normal fetus, which exhibits physiological herniation (**A**).

Anatomical delineation of the AWD phenotype was possible through careful dissection under a stereo microscope enabling identification and preservation of the amniotic membrane and umbilical cord. These anatomical findings were confirmed by imaging of sagittally sectioned in-amnio paraffin embedded fetuses. Paraffin

embedding of intra-amniotic fetuses enabled preservation of the visceral yolk sac and amniotic membrane. Imaging of serial sections allowed the visceral yolk sac and amniotic membranes to be traced throughout their course and the relationship of the amniotic membrane to the umbilical blood vessels and abdominal wall to be easily defined. It was therefore possible to confirm the anatomical findings described at microdissection without causing disruption to amniotic membrane, the anatomy of which was essential for accurate phenotyping of this AWD. This method of abdominal wall phenotyping provided clearer delineation of the anatomical detail than that provided by the in-amnio micro-MRI performed for the phenotyping of the Scribble knockout model (Chapter 3).

#### ***4.3.1.2 Another Case of Mistaken Identity***

Similar to the Scribble null fetuses, the above phenotypic description of the ACLP knockout fetuses contradicts the literature. The ACLP model has been described in two papers as exhibiting gastroschisis (Layne et al., 2001, Danzer et al., 2010) but neither paper performed detailed anatomical assessment of the abdominal wall defect or amniotic membrane. The abdominal wall defect of gastroschisis in humans is a full thickness defect to the right of a normally formed and inserted umbilical cord of which the covering amniotic membrane continues as the abdominal wall ectoderm. Therefore in gastroschisis, there is an abdominal wall deficiency, which also disrupts the continuity of the amniotic membrane enabling the eviscerated bowel to lie within the amniotic cavity. In the ACLP knockout mouse, there is a full thickness AWD but the amniotic membrane, although abnormal, remains intact throughout its course and separates the externalised viscera from the amniotic fluid. Hence, the externalised abdominal viscera in ACLP knockout fetuses is free floating in the exocoelomic cavity and not the amniotic fluid as would be expected for gastroschisis.

The composition of amniotic and exocoelomic fluid compartments are very different; whilst the amniotic fluid contains fetal urine, meconium and respiratory secretions (Gilbert and Brace, 1993) the exocoelomic fluid does not and the fluid composition is determined by the exchange of substances from the overlying visceral yolk sac serving as the principle site for the exchange of proteins between mother and fetus (Jauniaux and Gulbis, 2000). As such, the eviscerated bowel of the ACLP knockout



mouse is not in direct contact with the substances that are hypothesised to cause intestinal inflammation, damage and ultimately intestinal dysfunction in gastroschisis. Therefore, interpretations of experimental data using this model that infer gastroschisis pathophysiology findings must be interpreted with care. However, it is possible through in-utero injections into the exocoelomic cavity to manipulate the environment surrounding the gut and it is therefore a useful model for investigating the impact of potential amniotic fluid irritants on bowel development. The additional benefit of this model is the high penetrance of the AWD, good litter sizes (8 to 9 pups per litter) and the isolated nature of the AWD.

#### ***4.3.1.3 Failed Umbilical Cord Formation and Abdominal Wall Closure***

The anatomical relationship between the amniotic membrane, umbilical cord and AWD exhibited by the ACLP knockout mice is the same as that described in homozygous *Bone Morphogenetic Protein 1 (Bmp1)* mutant embryos (Suzuki et al., 1996). BMP1 is a metalloproteinases extracellular protein with an amino-terminus activation region, astacin-like protease domain, EGF-like motifs and protein-protein interaction domains. BMP1 is required for the activation of procollagen (Kessler et al., 1996, Li et al., 1996), is essential for the formation of cross-links to stabilise fibrous collagen and elastin (Panchenko et al., 1996) and enhances the activity of TGF $\beta$  growth factors (Hogan, 1996). Electron microscopy has revealed disrupted collagen fibrils in the amniotic membranes of *BMP1* mutant embryos consisting of thinner fibrils with barbed wire appearance surrounded by large amounts of amorphous material (Suzuki et al., 1996). Suzuki et al. hypothesised that disruption to the collagen fibrils resulted in failed folding of the amniotic membrane around the herniated bowel and the umbilical vessels at the time of physiological herniation resulting in persistence of bowel herniation and ultimately failed abdominal wall closure. The authors could not rule out that the amniotic membrane and mesodermal cells of the abdominal wall also had altered cell-cell or cell-matrix adhesion preventing adhesion of either tissue to the umbilical vessels.

It is possible that in the ACLP knockout model, failed folding and adherence of the amniotic membrane to the umbilical blood vessels was partly due to disruption of amniotic membrane collagen deposition. It has previously been shown that ACLP

promotes collagen and myofibroblast formation through the activation of TGF $\beta$  signalling (Tumelty et al., 2014). ACLP knockout fetuses exhibit reduced TGF $\beta$  activation (Tumelty et al., 2014), which could lead to disruption of collagen production as seen in the *BMP1* mutants. Although ACLP and TGF $\beta$  staining was performed on cross-sections of in-amnio paraffin embedded fetuses it was not possible to assess whether differences in expression existed between AWD and phenotypically normal fetuses due to the presence of significant background staining. Therefore, it is not possible to comment on the involvement of TGF $\beta$  in the development of the anatomical defects present in the ACLP knockout mouse. However, given ACLP is highly secreted in the extracellular matrix and acts as a signalling protein, it is likely that abnormal cell-cell migration, signalling and adherence is also implicated in the failed adherence of the amniotic membrane and mesodermal ventral wall cells to the umbilical blood vessels resulting in the AWD.

### **4.3.2 Bowel Wall Development**

#### ***4.3.2.1 Comparison of Untreated Control and Untreated AWD Fetuses***

The previously published description of bowel development in the ACLP knockout mouse model (Danzer et al., 2010) revealed the AWD fetuses to have normal bowel length, weight and wall thickness compared to controls. There was no evidence of inflammation or serosal peel, which the authors felt was due to the relatively short mouse gestational period although my results would suggest this is due to the bowel being exposed to exocoelomic fluid rather than amniotic fluid. However, they reported a reduction in ICC and enteric neuron staining of the externalised gut of AWD fetuses. The ICC were reportedly reduced by 70% in the AWD fetuses and exhibited an altered architecture with failed formation of a continuous network at the level of the myenteric plexus. This analysis was performed on cross-sections of bowel with immunohistochemistry and using a semi-quantitative scoring system.

The results presented here also confirm there was no significant difference between the bowel wall appearance or morphology of the AWD and control fetuses. However, phenotyping and quantification of ICC and enteric neurons was performed using whole mount specimens with immunofluorescence staining and in contrast to

the Danzer et al. paper both cell types were found to be architecturally normal within the AWD fetuses compared to controls. Additionally, although there was a reduction in the number of ICC in the AWD fetuses, this was only an 11% reduction as opposed to 70% reported by Danzer et al. and no difference in the numbers of enteric neurons was found between the groups. These results highlight the benefits of whole mount preparations over cross-sections providing the ability to image the entire network with confocal microscopy giving a complete and detailed picture of the cell architecture and networks and a more robust method for quantification.

The lack of bowel inflammation and the presence of normal ICC architecture may be due to the gut free floating within the exocoelomic fluid rather than the amniotic fluid providing protection from fetal urine, meconium, respiratory secretions and growth factors, which may negatively impact bowel development. Although ICC were reduced in number it is not possible to know whether this was caused by a developmental delay secondary to ACLP deficiency or exposure to exocoelomic fluid and if this would also be present in true gastroschisis.

#### ***4.3.2.2 Impact of IL-8 In-Utero Injections***

In-utero injections of IL-8, an inflammatory mediator present in meconium (de Beaufort et al., 1998), were performed to determine whether increased bowel exposure to inflammation would impact on bowel morphology or ICC and enteric neuron development. In the control fetuses, IL-8 injection was performed into the amniotic fluid cavity and therefore fetal physiological swallowing would have resulted in an increased IL-8 exposure at the mucosal surface. However in the AWD fetuses, IL-8 injection was performed into the exocoelomic cavity increasing serosal exposure to the inflammatory mediator but without increased mucosal exposure.

Increased serosal IL-8 exposure was associated with evidence of macroscopic serosal inflammation with the presence of prominent serosal blood vessels. Additionally, there was significant shortening of the bowel when compared to all other groups but there was no effect on the weight per unit length suggesting the bowel was not thickened. This was confirmed on measurement of bowel wall thickness in which increased serosal and mucosal exposure to IL-8 did not result in increased entire

bowel wall or muscle layer thickening unlike other animal studies (Api et al., 2001, Correia-Pinto et al., 2002). This could have been due to the short duration of exposure to increased IL-8 and bowel wall thickening/remodelling may require a longer time period for an effect to occur. However, there was evidence in both the IL-8 injected groups of increased hyperplasia of villus crypts suggesting mucosal development had been affected.

ICC and enteric neurons within both the IL-8 injected control and IL-8 injected AWD fetuses showed normal architecture and exhibited established cell networks. Although ICC were reduced in both groups this was more evident within the IL-8 injected control group, which was significantly reduced compared to both untreated control fetuses. However, there was no significant difference between the untreated AWD and IL-8 injected AWD fetuses. These data suggest that increased mucosal exposure to IL-8 had a greater impact on ICC development than increased serosal exposure. This suggests that GRID may result from an additive effect of both serosal and mucosal exposure to the pro-inflammatory amniotic fluid environment (Morrison et al., 1998).

#### ***4.3.2.3 Bowel Contractility and ICC Numbers***

Mouse gut motility develops prior to birth (Burns et al., 2009, Ross and Nijland, 1998) initially within the duodenum as non-neuronal mediated ripples from 13.5 dpc, neuronally/ICC mediated contraction complexes from 18.5 dpc and finally mature migrating motor complexes develop after birth (Roberts et al., 2010). The data presented here confirms the presence of contraction complexes that propagate along the bowel at 18.5 dpc within the small bowel.

There was a trend of decreasing ICC numbers with increasing fetal manipulation. The highest numbers of ICC were exhibited in the untreated control fetuses, followed by untreated AWD fetuses and the lowest number within the IL-8 injected AWD fetuses. A similar pattern was evident from the contraction data. Taking into account all variables the IL-8 injected bowel appeared to be the most dysfunctional, as evidence by: (i) the lack of contraction complexes suggesting a more rudimentary motility pattern, (ii) a lower percentage change from the mean diameter than controls

indicating shallower contractions and (iii) the highest percentage of dominant contractions occurring at a rate of 2 per minute suggesting that a large proportion of the bowel was inactive. Based on the same parameters, bowel from untreated controls showed a mature-for-stage contraction pattern, strong contractions with a high dominant frequency of contractions occurring most commonly at a rate of 7 to 8 per minute, suggesting good contractile function across the entire bowel length.

This trend is consistent with the published literature, which shows that disruption to ICC through generation of ICC knockout models (Der-Silaphet et al., 1998), blockade of ICC kit signalling (Beckett et al., 2007), or ICC disruption secondary to inflammation (Der et al., 2000) results in disorganised reduced contractility of the bowel. Although the ACLP knockout model does not exhibit gastroschisis, it shows that disruption of myenteric ICC numbers through manipulation of the inflammatory environment acting on the serosal bowel surface may result in disrupted bowel contractility and could be the cause of GRID.

### **4.3.3 Limitations of the Study**

#### ***4.3.3.1 ACLP Knockout Model***

The ACLP knockout model is not a true representation of human gastroschisis. Although bowel is free floating within fluid this was not within the amniotic fluid and therefore any reduction in ICC cannot be stated to replicate the pathology seen in gastroschisis. However, it was possible to manipulate the exocoelomic fluid environment through in-utero injection but it must also be acknowledged that it was not possible to visualise the amniotic membrane separating the exocoelomic and amniotic cavities during these injections. As such, even though IL-8 injections were performed into the space between bowel loops it cannot be guaranteed that some injections were not misdirected into the amniotic cavity instead of the exocoelomic cavity. If this was the case then some AWD fetuses would not have received an increased serosal exposure. Additionally, within the control fetuses it was not possible to identify the exocoelomic cavity under direct vision and therefore in-utero IL-8 injections were performed into the amniotic cavity therefore not generating a true comparative control. Access to a micro-ultrasound was not available during the

study period but ultrasound guidance may have enable injection into the exocoelomic cavity in control fetuses and also the amniotic cavity in AWD fetuses providing a comprehensive set of experimental and control conditions for the analysis of the effect on bowel wall development. Also, phenotypically normal fetuses were used as controls, which included both wild types and heterozygotes. The study by Layne, et al., 2001 shows through complementary DNA and messenger RNA studies in *ACLP*<sup>-/-</sup> and *ACLP*<sup>+/-</sup> fetuses that the observed phenotype in knockout fetuses is secondary to the result of the complete absence of ACLP. Also Danzer, et al., 2010 reported the intra-abdominal bowel of ACLP null fetuses to exhibit the same expression of bowel wall ICC and enteric neurons as control intestine suggesting ICC development was not effected by absence of ACLP. However, this does not completely rule out that bowel wall development in heterozygotes may be effected by partial ACLP loss and therefore could have impacted results.

Further studies that could have been done to further improve the validity of results are: (1) the inclusion of intra-abdominal bowel from AWD fetuses (e.g. duodenum or colon) and corresponding bowel from control fetuses to act as an internal control to determine whether changes in AWD bowel wall development are secondary to the AWD or as a result of ACLP deficiency and (2) to quantify inflammation in extra-fetal fluid and bowel wall.

#### ***4.3.3.2 Experimental Numbers and Treatment for Pinworm***

Statistically significant results may not have been observed for some measured parameters due to the small number of fetuses included in the study. Low numbers were partly as a result of study interruption due to a laboratory wide pinworm infection and subsequent fenbendazole treatment regimen lasting 9 weeks. The treatment resulted in reduction of fertility and small litter sizes in all mice that had received or were conceived during the pinworm treatment. To improve fertility, fresh wild type C57BL/6J female mice that had not received the fenbendazole diet were introduced into the colony. Re-establishment of the colony took 6 months from completion of the fenbendazole diet.

#### ***4.3.3.3 Motility Study Analysis Optimisation***

Bowel edge detection using MATLAB relied upon light thresholding. However, the light cast during experiments resulted in a small degree of reducing light intensity in the oral to anal direction (Figure 4-16A) resulting in an underestimation of the bowel diameter at the anal end. Therefore, a software correction within MATLAB was applied to remove this artefact. Additionally, bowel diameter naturally tapers in the oral to anal direction with the terminal ileum being visually thinner than the duodenum resulting in an apparent reduction in the contraction depth (surrogate for contraction strength) when measuring absolute bowel diameter changes in millimetres. This was apparent on spatiotemporal maps showing diameter change (mm) against bowel incremental point (mm) with time (seconds) (Figure 4-16B) due to the change in the represented colour across the graph from red to green in the oral to anal direction. To improve data analysis, contraction depth was calculated based on the percentage change in bowel diameter from the calculated mean diameter on vertical slice analysis at each 0.022mm incremental point along the bowel length. This data was then plotted on a spatiotemporal map showing percentage change from mean diameter against bowel length with time (Figure 4-16C) providing a clearer visual plot of contractions. Finally, oxygenation of the Ringer's solution resulted in the formation of bubbles, some of which adhered to the edge of the bowel. Dislodgement of these bubbles resulted in paralysis of the bowel requiring a period of recovery therefore it was not possible to dislodge all bubbles. Where a bubble is adherent to the bowel it led to an artefact in measurement of the diameter change (Figure 4-16A – C). However, due to the large number of vertical slice analyses performed these bubble artefacts had minimal impact on the results.

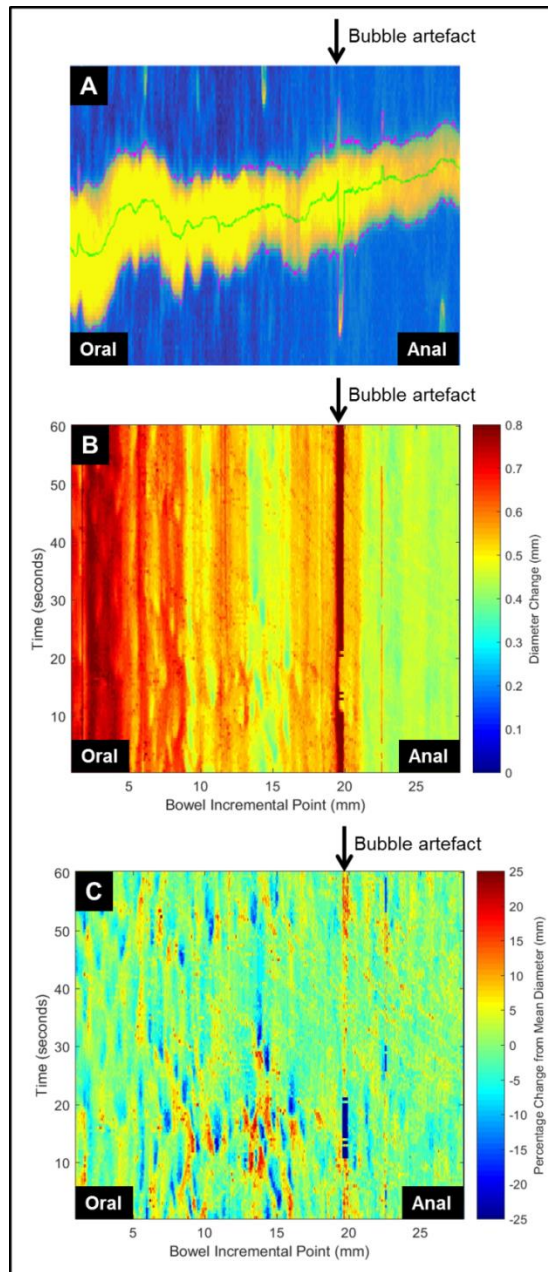


**Figure 4-16:** Analysis optimisation using MATLAB software. **A.** Bowel edge detection performed by light thresholding showing reducing light intensity in the oral to anal direction and the presence of a bubble artefact. Gut appears in yellow, pink line marks ileal edge, green line marks centre point of bowel. **B.** Spatiotemporal map of change in bowel diameter in absolute millimetres showing decreasing bowel diameter from the oral to anal direction (normal bowel anatomy) and bubble artefact (black arrow). **C.** Spatiotemporal map of change in bowel diameter as a percentage change from the mean diameter providing uniform analysis of contraction depth along the length of the bowel. Black arrow indicates bubble artefact.



#### **4.3.4 Conclusion**

The ACLP knockout mouse model is another example of inaccurate phenotyping resulting from a lack of detailed assessment of the AWD and associated membranes. Rather than expressing a gastroschisis defect, the ACLP knockout mouse exhibits an unusual exomphalos defect with failed adhesion of the amniotic membrane to the umbilical vessels placing the externalised bowel free floating within the exocoelomic fluid, which is an ultra-filtrate of the maternal serum. This could explain the lack of bowel wall thickening and normal ICC architecture present within the untreated AWD fetuses. The whole mount ICC data presented here did not agree with the previously published data acquired through analysis of cross-sectioned small bowel (Danzer et al., 2010) and therefore calls into question the validity of results obtained from analysis of small animal cross-sectioned bowel. Although not an ideal model of gastroschisis, the ACLP model enabled the in-utero manipulation of serosal and mucosal inflammatory exposure as two independent variables. These results suggest there is a link between increased inflammation, reduced ICC and bowel dysmotility. As such, these data support the potential for GRID to be caused by an ICC deficiency but interpretation of these results and direct application to human gastroschisis must be undertaken with care.

## **Chapter 5: Analysis of Gastroschisis ICC and Enteric Neurons in Infant Human Pathological Gut Tissue**

### **5.1 Introduction**

At the start of this study only one paper (Midrio et al., 2008) had been published investigating ICC development in gastroschisis bowel. This study involved a single case of gastroschisis. The infant was born at 36 weeks GA and required resection of necrotic bowel and stoma formation shortly after delivery. One month later when partial enteral feeding was tolerated, the stoma was closed. The resected tissue was immunostained for CD117 and ICC differentiation at the level of the myenteric plexus (the first ICC population to develop in the human bowel, which is also well developed at full term (Faussone-Pellegrini et al., 2007)) was described. At the time of the first operation the authors described the ICCs as infrequent and ultrastructurally immature but at one month of age the cells had matured and formed rows or groups, suggesting that ICC differentiation is delayed in gastroschisis and may be the cause of GRID. However, the method used was not quantitative and no controls were included in the study.

Gastroschisis infants are hypothesised to exhibit deficient and architecturally immature bowel wall ICC, which may be the cause of GRID. As such, the aim for this part of the study was to determine with a larger patient series whether development of ICC at the level of the myenteric plexus was impaired in gastroschisis infants compared to control infants.

### **5.2 Results**

#### **5.2.1 Study Population and Demographics**

Following ethical approval a total of 17 control and 20 gastroschisis small bowel specimens were included in the study, which had been resected between 1988 and 2012. Bowel resection had been performed in the control and gastroschisis groups for pathologies as outlined in Table 5-1.

	Control n=17	Gastroschisis n=20
Dysmotile bowel	-	9
Ischaemia/necrosis	-	6
Anastomotic stricture	-	1
Stenosis	1	3
Perforation	3	1
Intussusception	7	-
Meckel's diverticulum	2	-
Strangulated hernia	2	-
Volvulus	2	-

**Table 5-1:** Pathology resulting in small bowel resection in the control and gastroschisis groups.

There was no significant difference in the age at time of bowel resection (control median 58, range [1-378] days and gastroschisis 72 [1-717] days,  $p=0.39$ ) or the corrected gestational age (CGA) at time of bowel resection (control 40 [26-94] weeks and gastroschisis 48 [34-140] weeks,  $p=0.34$ ) between the control and gastroschisis groups. Linked clinical data was not possible to obtain for 4 gastroschisis small bowel specimens as the samples were transferred from another hospital for a second opinion regarding the cause of persistent dysmotility. Hence, CGA for these patients was estimated using a delivery at 38 weeks GA as this is the time point at which planned delivery for gastroschisis is commonly undertaken. Linked time to full enteral feeds (ENT) data was available for 11 gastroschisis small bowel specimens (ENT 62 [18-204] days) the reason for missing data included; PN dependency ( $n=5$ ) and specimens that were transferred from another hospital ( $n=4$ ).

## 5.2.2 ICC and Enteric Neurons

### 5.2.2.1 Optimisation of Immunofluorescence ICC Staining Protocols

The previous human gastroschisis study utilised immunohistochemistry techniques for staining of ICC. However, initial protocols with both immunohistochemistry (Table 5-1A) and immunofluorescence (Table 5-1B) revealed ICC cell bodies to be more easily identified with immunofluorescence. Additional advantages of immunofluorescence included; the ability to triple label sections for ICC, enteric neurons and nuclei, which reduced the number of sections required and improved identification of both ICC and enteric neuron cell bodies. Therefore, it was decided to continue the study using immunofluorescence.

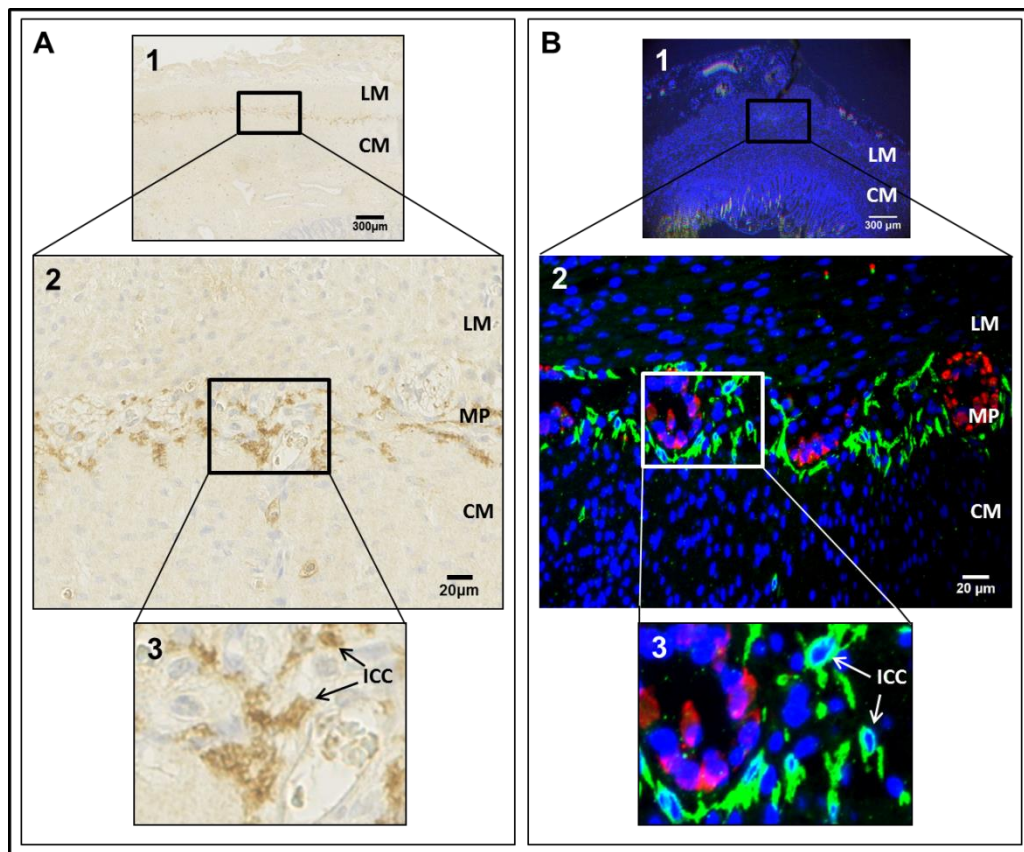


**Figure 5-1:** Images taken with; (1) 5x and (2) 40x objective. Image (3) is an enlarged section of 40x objective image. **A.** Immunohistochemistry. ICC stained with CD117 and DAB detection kit (dark brown staining), nuclei stained with Eosin counterstain (purple). **B.** Immunofluorescence. Composite images showing triple staining for ICC with anti-CD117 (green), enteric neurons with anti-HuC/D (red) and nuclei with DAPI (blue). Key: LM – longitudinal muscle, CM – circular muscle, MP – myenteric plexus, ICC – interstitial cells of Cajal.

### 5.2.2.2 ICC and Enteric Neuron Architecture

ICC at the level of the myenteric plexus were well developed in both control (Figure 5-2A and B) and gastroschisis (Figure 5-2C and D) small bowel. ICC intercellular branching connections were evident creating cell networks that were closely associated with the myenteric plexus. ICC networks were found to surround and be continuous either side of the myenteric ganglion cells. The myenteric neuronal plexus was also well developed in both groups. The enteric neurons formed regular clumps of cells consistent with myenteric ganglia.

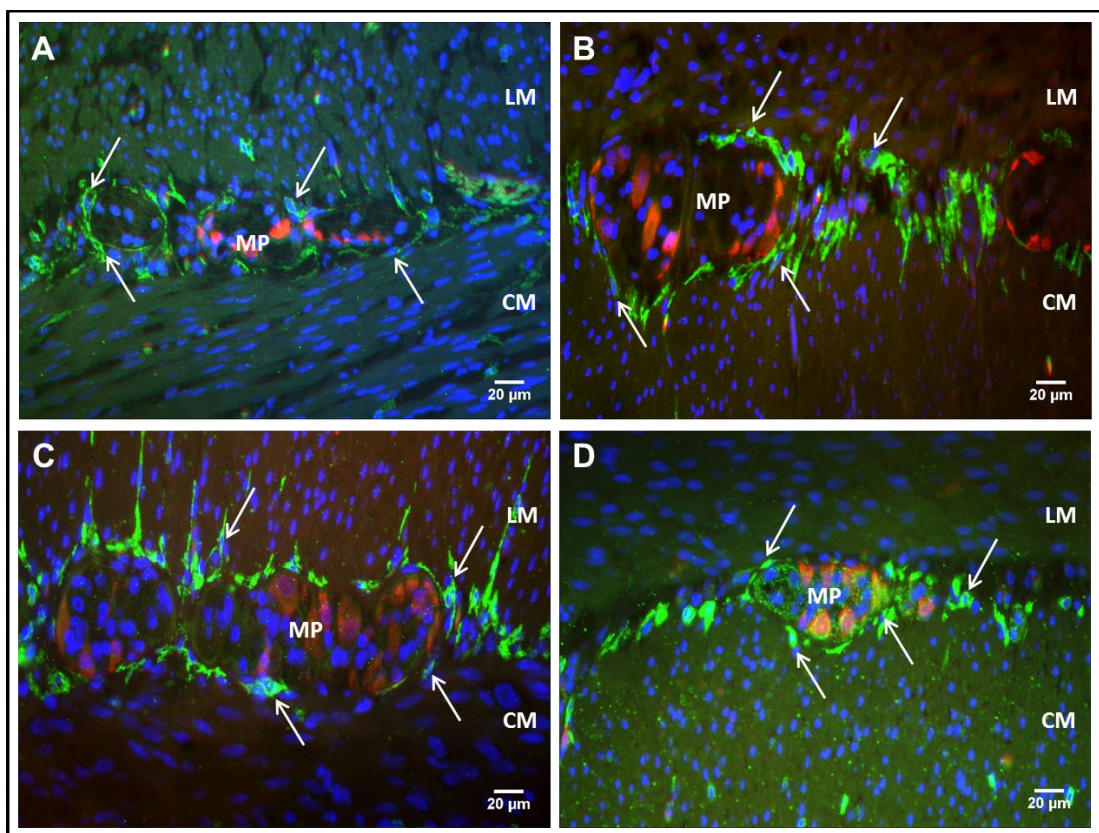


**Figure 5-2:** Composite images showing triple staining of ICC (green), enteric neurons (red) and nuclei (blue), images taken with 40x objective. **A and B.** Control small bowel images. **C and D.** Gastroschisis small bowel images. Key: LM – longitudinal muscle, CM – circular muscle, MP – myenteric plexus, arrows indicating example ICC adjacent to ganglia.

### 5.2.2.3 ICC and Enteric Neuron Numbers

On group comparison with t-test analysis there were no differences in either the number of ICC per high powered field (control  $16.2 \pm 1.9$  [mean  $\pm$  SEM] and gastroschisis  $15.2 \pm 1.7$ ,  $p=0.71$ ) or enteric neurons per high powered field (control  $13.2 \pm 2.2$  and gastroschisis  $10.6 \pm 1.1$ ,  $p=0.23$ ) between control and gastroschisis small bowel (Figure 5-3).

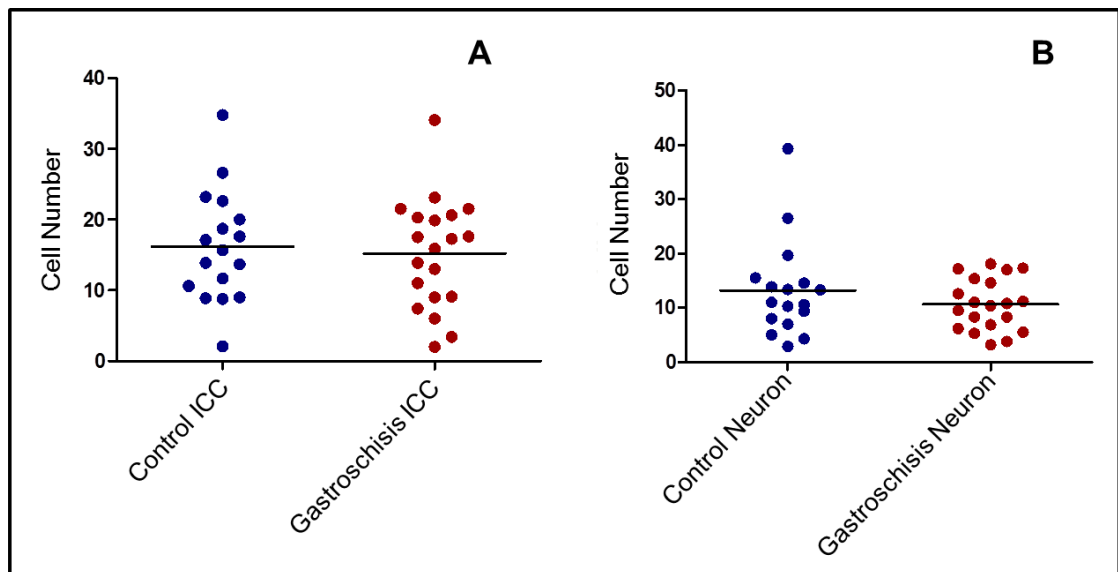


**Figure 5-3:** Correlation between ICC numbers (A) and enteric neuron numbers (B) between control and gastroschisis small bowel.

### 5.2.2.4 ICC and Enteric Neuron Numbers and Age at Bowel Resection

Given that ICC networks continue to develop after birth (Faussonne-Pellegrini et al., 2007), a linear regression analysis was performed of all bowel resection specimens to determine whether there was a relationship between ICC numbers and age at time of bowel resection. This showed no significant relationship ( $R^2=0.02$ ,  $p=0.44$ , **Error! Reference source not found.A**). However, this analysis may have been skewed by the outlier that underwent bowel resection at 717 days. Removing this outlier from the analysis resulted in a significant relationship ( $R^2=0.21$ ,  $p=0.005$ , **Error! Reference source not found.B**) showing an increase in ICC numbers with age. A similar linear regression analysis was performed for neuron numbers, which showed a significant trend of decreasing neuron numbers with age when the outlier was included

( $R^2=0.11$ ,  $p=0.049$ , **Error! Reference source not found.C**) but no significant trend when the outlier was excluded ( $R^2=0.07$ ,  $p=0.11$ , **Error! Reference source not found.D**). Further analysis was performed using multiple regression analysis taking into account both the effect of age at time of bowel resection and diagnosis of gastroschisis. Results showed neither factor to be significant when considering ICC or neuronal cell number (Table 5-2).

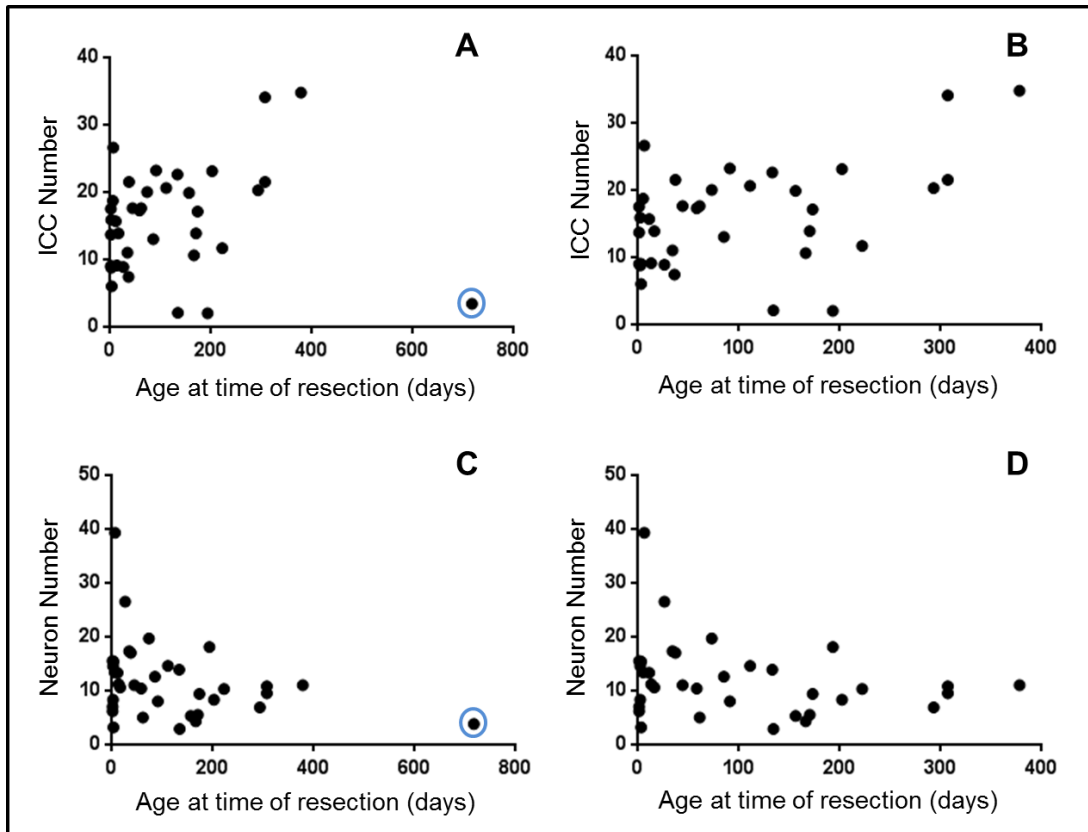


**Figure 5-4:** Linear regression analysis comparing ICC (A and B) and neuron (C and D) numbers with age at time of bowel resection, including all bowel resection specimens. A and C. Including the outlier (indicated by the blue circles). B and D. Excluding the outlier.



ICC Number	Regression Coefficient (95% CI)	p-value
Age at time of bowel resection	0.008 (-0.01, +0.03)	0.36
Gastroschisis	-1.4 (-6.8, +3.9)	0.59
Neuron Number	Regression Coefficient (95% CI)	p-value
Age at time of bowel resection	-0.014 (-0.03, +0.001)	0.07
Gastroschisis	-1.8 (-6.4, +2.776)	0.43

**Table 5-2:** Multiple regression analysis of ICC and neuron numbers taking into account age at time of bowel resection and diagnosis of gastroschisis, including all bowel resection specimens.

#### ***5.2.2.5 ICC and Enteric Neuron Numbers and Time to Full Enteral Feeds***

To determine whether ICC or neuron numbers were associated with ENT in the gastroschisis population, a Spearman's correlation was performed, which showed no significant correlation with ICC ( $r_s=0.3$ ,  $p=0.33$ ,) or neuron ( $r_s=0.2$ ,  $p=0.66$ ) numbers (Figure 5-5).



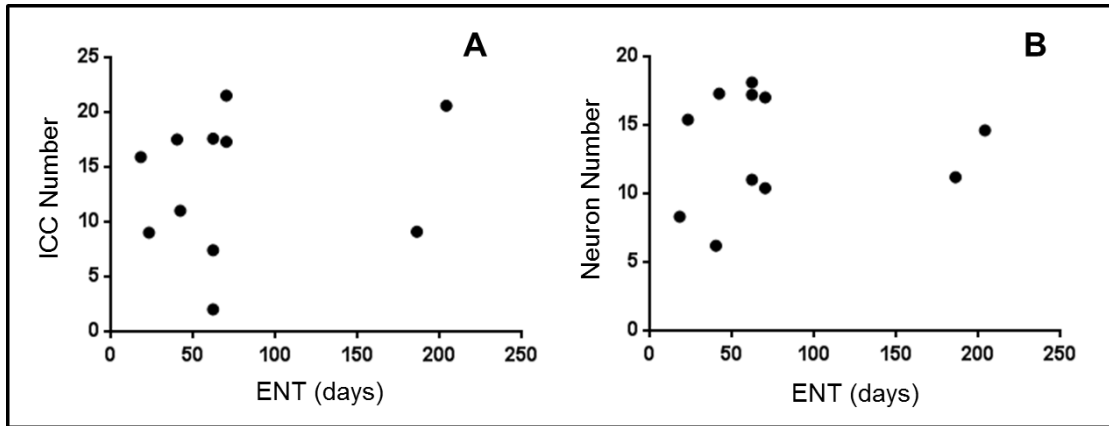


**Figure 5-5:** Relationship between gastroschisis ICC (A) and neuron (B) numbers with time to full enteral feeds (ENT).

#### 5.2.2.6 ICC in Meconium Ileus

As a positive control, two bowel resection specimens from patients with meconium ileus without cystic fibrosis were immunostained and imaged. Both cases showed immature, scanty ICC (ICC number across both specimens  $1.4 \pm 0.4$ ) that lacked intercellular branching connections. The enteric neurons were architecturally normal forming regular myenteric ganglia but also appeared to be low in number ( $5.4 \pm 1.1$ ) (Figure 5-6).

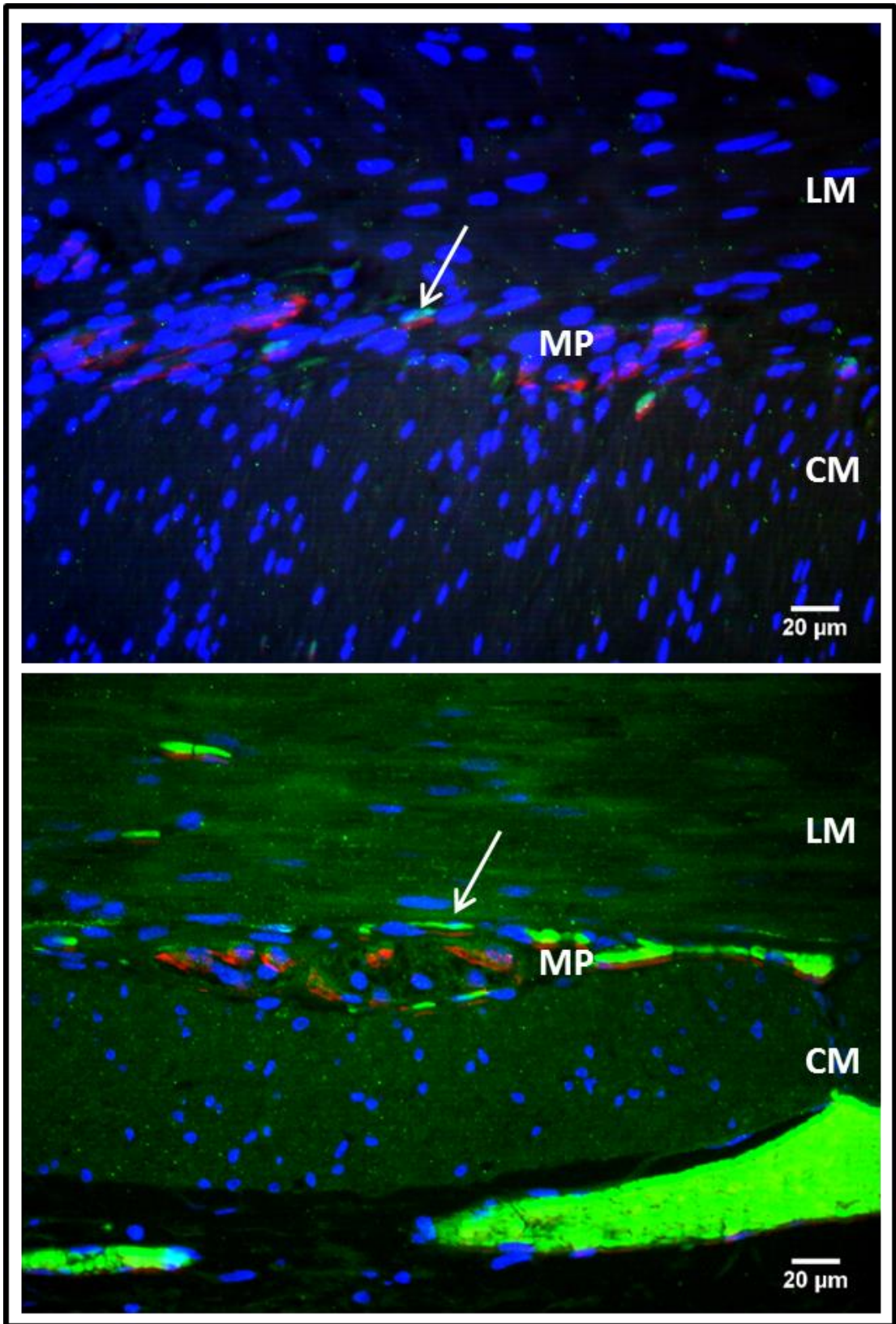


**Figure 5-6:** Composite images from 2 different meconium ileus small bowel specimens, showing triple staining of ICC (green), enteric neurons (red) and nuclei (blue), images taken with 40x objective. Key: LM – longitudinal muscle, CM – circular muscle, MP – myenteric plexus, arrows indicating example ICC adjacent to ganglia.

## **5.3 Discussion**

### **5.3.1 Tissue Selection for Inclusion in the Study**

Small bowel is only resected in gastroschisis or otherwise normal infants when there is concomitant intestinal pathology. Therefore, it is impossible to compare bowel from uncomplicated gastroschisis infants with completely healthy infants. To reduce the confounding effect of concomitant pathologies, bowel conditions described in the literature to have reduced ICC such as atresia (Tander et al., 2010, Midrio et al., 2010) and meconium ileus (Toyosaka et al., 1994, Yoo et al., 2002) and those associated with significant bowel wall inflammation that may adversely impact ICC numbers including necrotising enterocolitis (NEC), stoma closure and post-mortem specimens were excluded. Additionally, only grossly normal resection margins were included thus selecting as near macroscopically normal small bowel as possible. Where available pathologies that involved mechanical compromise of healthy bowel were included to ensure selection of as near normal bowel resection margins as possible. However, the worst cases of gastroschisis with prolonged intestinal dysmotility were included in this cohort. If ICC deficiency is the cause of GRID, a significant reduction in ICC numbers between gastroschisis and control small bowel resections would be expected. Finally, the gastroschisis and control groups were aged matched to reduce the impact of potential continued ICC development in the infant period.

### **5.3.2 ICC and Enteric Neuron Numbers and Architecture**

This study found no differences in the number or architecture of ICC or enteric neurons between the gastroschisis and control groups. Additionally, regression analysis revealed no effect of gastroschisis on ICC or enteric neurons. In comparison, as a positive control two meconium ileus small bowel specimens were immunostained and analysed revealing immature, scanty ICC as expected (Toyosaka et al., 1994, Yoo et al., 2002). This indicates validity of the staining and quantification method for analysis of ICC and enteric neurons and supports the lack of effect of gastroschisis on ICC or enteric neuron cell numbers.

Age at resection also did not appear to significantly affect the number of ICC or enteric neurons at the level of the myenteric plexus. This is in keeping with a study that documented the development of different ICC populations within the bowel wall during fetal life, which suggested the ICC of the myenteric plexus appeared early in gestation (17 weeks GA) and were well differentiated by full term (Faussone-Pellegrini et al., 2007). Finally, no correlation was found between ICC and enteric neuron numbers and the time to achieve full enteral feeds.

### **5.3.3 Quantification of ICC and Enteric Neurons**

Reliable ICC and enteric neuron immunofluorescence staining was possible with anti-CD117 and HuC/D (respectively) antibodies following antigen retrieval of paraffin embedded human gut sections. Due to the relatively large size of the small bowel specimens (unlike rodent small bowel), ICC and enteric neurons were easily identified and architecture discerned following imaging of cross-sectioned tissue with 40x objective. Therefore it was possible to perform accurate cell counts providing a robust and reliable method of cell quantification. Background staining was present, which did not affect manual cell counting. However, if an automated method was used such as the use of image software processing to calculate the area of positive staining (Wang et al., 2009, Bernardini et al., 2012), background staining may have led to inaccurate results. The two meconium ileus small bowel specimens, which were processed as positive controls confirmed that the quantification method used in this study can discriminate between varying degrees of ICC numbers and architecture.

### **5.3.4 Comparison with Other Studies**

The original human gastroschisis ICC data was derived from a single case report (Midrio et al., 2008) as previously described. Recently, another larger study has been published investigating the differences in ICC numbers between gastroschisis and control small bowel specimens (Zani-Ruttenstock et al., 2015). This larger study has several fundamental differences in the methods used for specimen selection, immunostaining, cell quantification and data analysis compared to the data presented here. Zani-Ruttenstock et al. only included patients who underwent stoma formation

(time point 1) and later stoma closure (time point 2). The gastroschisis group (n=24 in total) consisted of patients who took >42 days to achieve ENT, however, the reason for stoma formation was not fully documented for patients within this group. The control group (n=22 in total) included patients with NEC, atresia, atresia with volvulus and malrotation/volvulus. Resection margins included evidence of inflammation as outline in Table 5-3. Quantification was performed on sections stained by immunohistochemistry (DAB detection kit) from 25 randomly orientated fields of view taken with 20x objective.

Categorisation of Inflammation	Number of Gastroschisis Samples	Number of Control Samples
Severe	10	8
Transmural	12	10
Necrosis	6	9
Ulceration	13	16
Peritonitis	10	9

**Table 5-3:** Degree, distribution and type of inflammation present in resected bowel sections included in Zani-Ruttenstock et al. study.

The results showed at time point 1 there was no significant difference between the control (mean ICC number 6) and gastroschisis (mean ICC number 2.5, p=0.06) groups but at time point 2 there were significantly more cells in the control (mean ICC number 11) compared to gastroschisis (mean ICC number 3.5, p=0.01) group. Overall ICC numbers were higher in the control (mean ICC number 11) compared to gastroschisis (mean ICC number 3, p<0.003) group. Morphological analysis showed no difference in cell architecture between the groups with branching, interconnecting cells seen in both.

Although, the results of that study appear to be contradictory to this one it is important to note that at time point 1 Zani-Ruttenstock, et al. also showed no

significant difference in ICC numbers and overall ICC maturity was the same in both groups. It is also interesting to note that the mean number of ICC quantified within the Zani-Ruttenstock study were significantly lower than that of the study presented here even though quantification was performed at a lower magnification. It is possible that this lower cell number could have occurred secondary to the use of inflamed, grossly abnormal resection tissue (including stoma reversal tissue, which is known to exhibit chronic inflammation) or from inclusion of conditions such as atresia (Tander et al., 2010, Midrio et al., 2010) both of which could have negatively impacted on ICC numbers. Finally, the accuracy of their data is unknown due to quantification being performed on randomly orientated fields of view. As such, this study may have resulted in bias and the incorrect rejection of a true null hypothesis (type 1 error).

### **5.3.5 Limitations of the Current Study**

This was a retrospective study and therefore the original handling and paraffin embedding of the small bowel tissue was not performed uniformly although it would have followed normal histopathology protocols. It was also only possible to analyse gut tissues from patients requiring bowel resection therefore patients with simple gastroschisis or healthy control infants could not be included in the study.

Additionally, the most common reason for bowel resection in gastroschisis infants is intestinal atresia and therefore the number of small bowel specimens available for analysis was limited. Although cell numbers and architecture can be analysed it is not possible to assess function of ICC or enteric neurons from paraffin embedded tissue. Finally, clinical data was not available for all small bowel specimens due to tissue being transferred from outside hospitals for a second opinion.

## **5.4 Conclusion**

The data showed no differences in the number or architecture of ICC or enteric neurons at the level of the myenteric plexus in gastroschisis small bowel compared to control tissues. Additionally, no association was found between numbers of ICC or enteric neurons with age at bowel resection or duration of GRID (measured as ENT). Therefore, this study does not support the hypothesis that GRID is secondary to

reduced or poorly differentiated ICC and contradicts the published literature to date. This finding was unexpected particularly as only bowel specimens from infants with the worst postnatal outcomes were included and highlights the need for further investigation into the bowel wall development of gastroschisis fetuses before a therapy to improve gastroschisis gut function can be developed. A further detailed morphological analysis of the small bowel specimens was performed to determine whether another factor could be identified for the cause of GRID (Chapter 6).

## **Chapter 6: Analysis of Gastroschisis Bowel Wall Morphology in Infant Human Pathological Gut Tissue**

### **6.1 Introduction**

At birth the bowel wall of infants with gastroschisis has frequently been described as appearing thickened and inflamed (Tibboel et al., 1986) and investigations using surgical animal models (Api et al., 2001, Correia-Pinto et al., 2002, Langer et al., 1989, Srinathan et al., 1995) have shown increased serosal and muscle layer thickening of gastroschisis bowel compared to normal controls. The serosal and muscle layer thickening in animal studies has been hypothesised to be induced by inflammation secondary to amniotic fluid exposure (Api et al., 2001, Correia-Pinto et al., 2002, Olguner et al., 2006, Guo et al., 1995, Bittencourt et al., 2006, Yu et al., 2004, Langer et al., 1989) or constriction at a tight abdominal wall defect (Shah et al., 2012, Langer et al., 1989). In human gut, increased levels of the inflammatory cytokine transforming growth factor-beta 3 (TGF- $\beta$ 3) have been found in gastroschisis infants compared to control infants (Moore-Olufemi et al., 2015) and TGF- $\beta$ 3 has been hypothesised to be a mediator of bowel wall thickening in gastroschisis. However, to date there are no published morphological studies of histological human gastroschisis gut therefore the nature of the observed bowel wall thickening at birth in gastroschisis infants remains unknown.

Gastroschisis infants are hypothesised to exhibit thickened bowel wall, which may be the cause of GRID. The aims of this part of the study were to; (i) determine whether bowel wall thickening was present in human gastroschisis infants compared to controls and (ii) determine the architectural basis of any differences.

### **6.2 Results**

#### **6.2.1 Study Population and Demographics**

This study included the same small bowel specimens that were used for the ICC and enteric neuron analysis in Chapter 5 with the addition of specimens resected from



infants with atresia and meconium ileus. However, due to the young age at bowel resection of the control atresia infants, one gastroschisis small bowel specimen from the original cohort, who underwent bowel resection at 717 days of life for persistently dysmotile bowel, was excluded from this study in order to maintain age matching between the groups. Additionally, one control small bowel specimen from the original cohort, who underwent bowel resection for a strangulated hernia, was excluded from this study due to significant abnormal thickening of the bowel wall (entire bowel wall measured 5437 $\mu$ m). In total, 26 control and 21 gastroschisis small bowel specimens were included, which were resected for pathologies as outlined in Table 6-1.

	Control n=26	Gastroschisis n=21
Dysmotile bowel	-	8
Ischaemia/necrosis	-	6
Anastomotic stricture	-	1
Stenosis	1	3
Perforation	3	1
*Atresia	8	1
*Meconium Ileus	2	-
Intussusception	7	-
Meckel's diverticulum	2	-
Strangulated hernia	1	-
Volvulus	2	-

**Table 6-1:** Pathology resulting in small bowel resection in the control and gastroschisis groups. \*Indicates the pathologies that are different to those infants included in the analysis of ICC and enteric neurons in human gut tissue.

There was no significant difference in age at time of bowel resection (control median 6, range [1-378] days and gastroschisis 44 [1-322] days,  $p=0.06$ ) or the corrected gestational age (CGA) at time of bowel resection (control 40 [26-94] weeks and gastroschisis 43.2 [34-92] weeks,  $p=0.1$ ) between the control and gastroschisis groups. Linked ENT data was available for 11 of the 21 gastroschisis small bowel specimens (ENT 62 [18-204] days). The reasons for missing data included; PN dependency ( $n=5$ ), death before attaining full enteral feeds ( $n=1$ ) and specimens that were transferred from another hospital ( $n=4$ ).

### 6.2.2 Bowel Wall Thickness

The bowel wall of gastroschisis infants was found to be significantly thicker (median 1284, range [755-2258]  $\mu\text{m}$ ) compared to controls (703 [340-1601]  $\mu\text{m}$ ,  $p=0.0001$ , Mann-Whitney analysis, Table 6-2 and Figure 6-1). This increased small bowel wall thickness in gastroschisis infants was comprised of proportional thickening of the serosa (266 [80-1031]  $\mu\text{m}$  versus 76 [35-231]  $\mu\text{m}$ ,  $p<0.0001$ ), longitudinal muscle (317 [131-675]  $\mu\text{m}$  versus 138 [63-395]  $\mu\text{m}$ ,  $p<0.0001$ ), circular muscle (308 [137-834]  $\mu\text{m}$  versus 245 [104-684]  $\mu\text{m}$ ,  $p=0.04$ ) and entire muscle layer (644 [755-2258]  $\mu\text{m}$  versus 429 [199-1044]  $\mu\text{m}$ ,  $p=0.0003$ ). However, there was no difference in the villus height or crypt depth between the groups, but the villus to crypt ratio was greater in controls (2.7 [1.4-5.0]) compared to the gastroschisis group (2.1 [0.4-3.3],  $p=0.01$ ). In children, a ratio of  $>2:1$  is considered normal (Dickson et al., 2006) suggesting normal villus and crypt development was present within both groups and the decreased villus crypt ratio in gastroschisis may reflect the lack of stimulation from enteral feeds. The longitudinal muscle comprised significantly more muscle cells (quantified as the number of muscle fibres that bisected the measurement line) in the gastroschisis group (33 [12-66]) than controls (19 [9-50],  $p<0.0001$ , Table 6-3, Figure 6-2A). However, the muscle cell thickness (muscle layer thickness/number of muscle fibres) was similar between the groups. Although the number of circular muscle cells was greater in the gastroschisis group, this did not reach significance and the circular muscle cell thickness was not different between the two groups (Table 6-3, Figure 6-2).

Bowel Wall Layer Measured	Control Median [range] $\mu\text{m}$	Gastroschisis Median [range] $\mu\text{m}$	p-value
Serosa	76 [35-231]	266 [80-1031]	* $<0.0001$
Longitudinal muscle	138 [63-395]	317 [131-675]	* $<0.0001$
Circular muscle	245 [104-684]	308 [137-834]	*0.04
Submucosa	193 [49-971]	223 [67-843]	0.35
Villus height	445 [233-771]	346 [67-783]	0.054
Crypt depth	161 [112-222]	172 [127-320]	0.09
Villus to Crypt ratio	2.7 [1.4-5.0]	2.1 [0.4-3.3]	*0.01
Entire wall layer thickness	703 [340-1601]	1284 [755-2258]	* 0.0001
Entire muscle layer thickness	429 [199-1044]	644 [377-1344]	*0.0003

**Table 6-2:** Comparison of bowel wall measurements between control and gastroschisis small bowel. Entire wall layer thickness measurement includes all bowel wall layers from the serosa to submucosa. Entire muscle layer thickness measurement includes the circular and longitudinal muscle layers. \*Indicates p-values that reached significance.

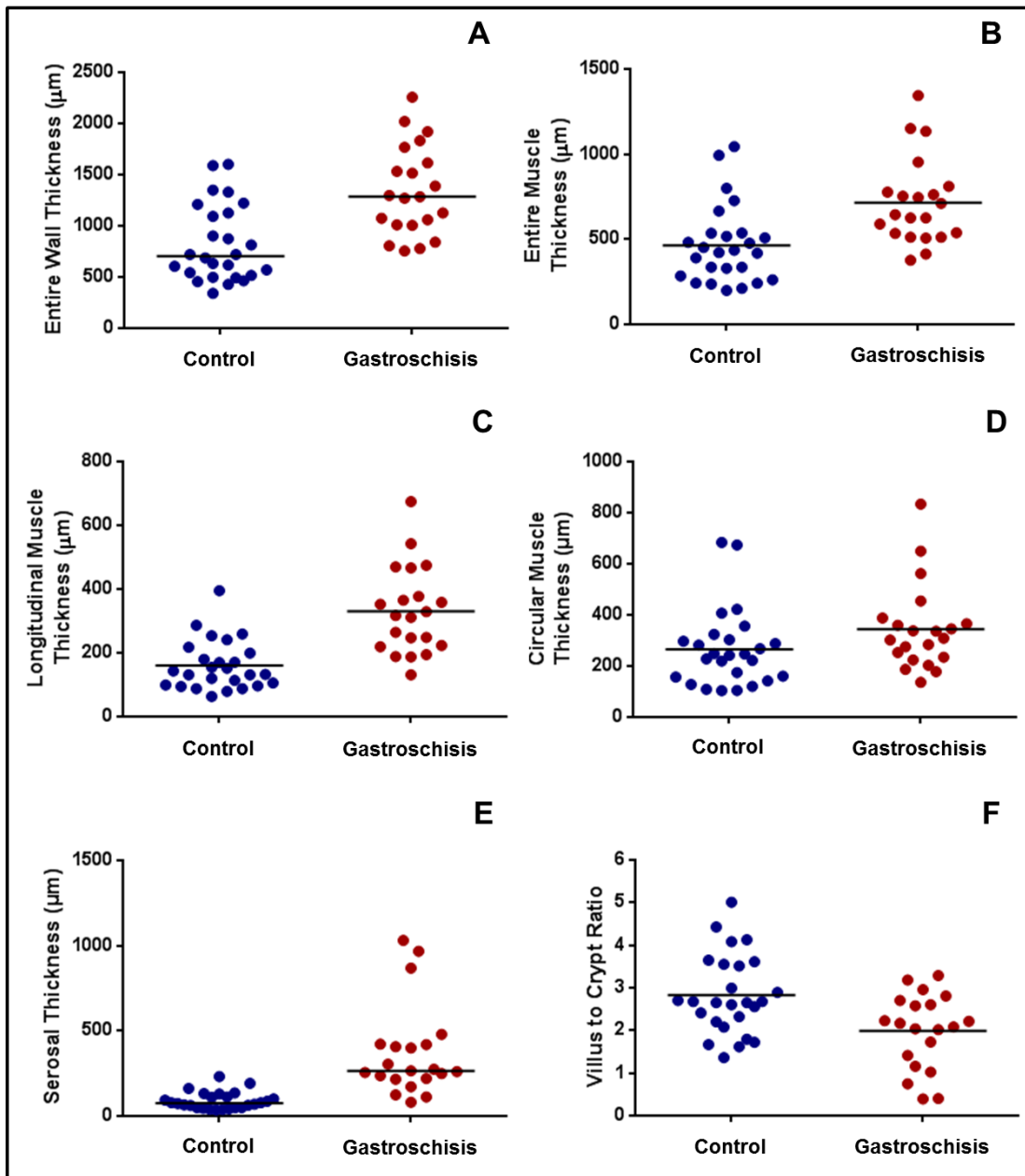


**Figure 6-1:** Comparison of **A.** entire wall thickness, **B.** entire muscle thickness, **C.** longitudinal muscle thickness **D.** circular muscle thickness, **E.** serosal thickness and **F.** villus to crypt ratio between the control and gastroschisis groups. All comparisons reached statistical significance.

Muscle layer	Control Median [range]	Gastroschisis Median [range]	p-value
Longitudinal number of cells	19 [9-50]	33 [12-66]	*<0.0001
Longitudinal thickness of cells	8.0 [5.1-11.0] $\mu\text{m}$	8.7 [6.3-7.6] $\mu\text{m}$	0.12
Circular number of cells	29 [14-69]	40 [16-68]	0.08
Circular thickness of cells	7.8 [4.8-11.3] $\mu\text{m}$	8.2 [5.7-12.4] $\mu\text{m}$	0.20

**Table 6-3:** Number and thickness of muscle cells within the longitudinal and circular muscle layers of control and gastroschisis small bowel specimens. \*Indicates p-values that reached significance.

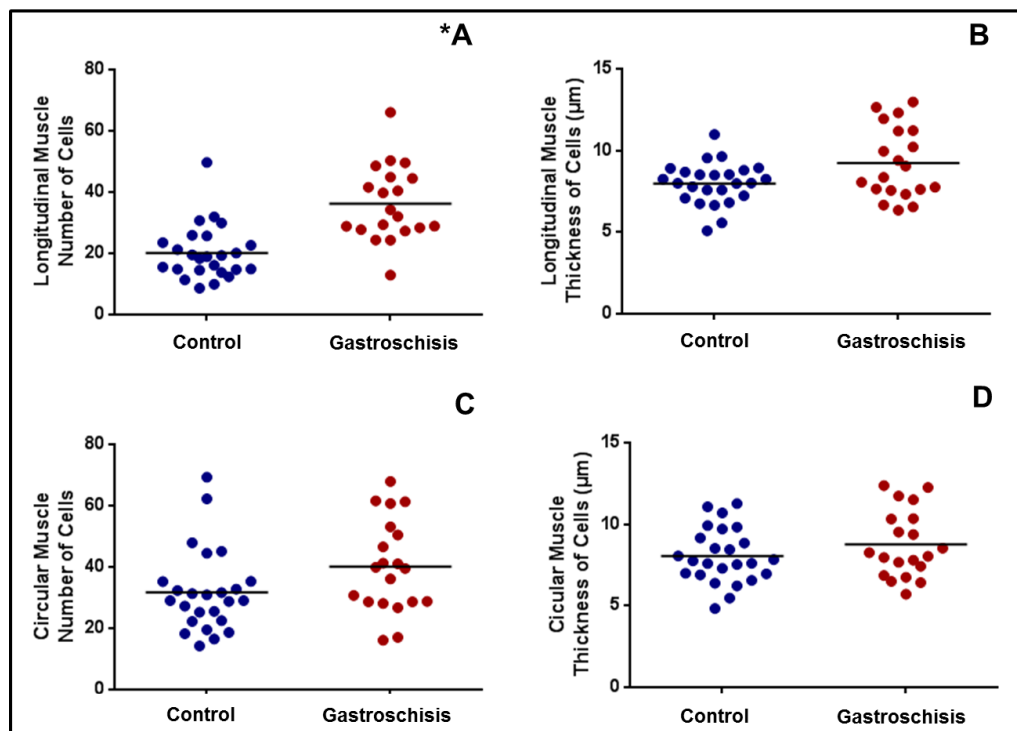


**Figure 6-2:** Comparison of **A.** longitudinal muscle number of cells, **B.** longitudinal muscle thickness of cells, **C.** circular muscle number of cells and **D.** circular muscle thickness of cells. \*Comparison that reached statistical significance.

### ***6.2.2.1 Bowel Wall H&E Qualitative Description***

Significant serosal and muscle layer thickening was observed in three of the gastroschisis cases. The H&E slides for these three outlier gastroschisis cases were blindly reviewed alongside two randomly selected gastroschisis cases and two randomly selected control cases by Professor Neil Sebire, Professor of Paediatric and Developmental Pathology, Great Ormond Street Hospital. The three outlier gastroschisis cases showed fibrosis and loose connective tissue with mild chronic inflammatory infiltrate, foreign body giant cells and foreign body granulomata. There was no evidence of acute inflammation and findings were in keeping with organising granulation tissue. In these cases there was no evidence of inflammatory infiltrate within the muscle layers. The two randomly selected gastroschisis cases showed dense serosal fibrosis, inflammation and granulation tissue with no evidence of inflammatory infiltrate within the muscle layers. The two control cases were almost normal in appearance with very mild chronic inflammatory infiltrate of the serosa and normal muscle layers. There was no evidence of cutting artefacts in any of the slides. Figure 6-3 shows representative H&E images of control and gastroschisis bowel.

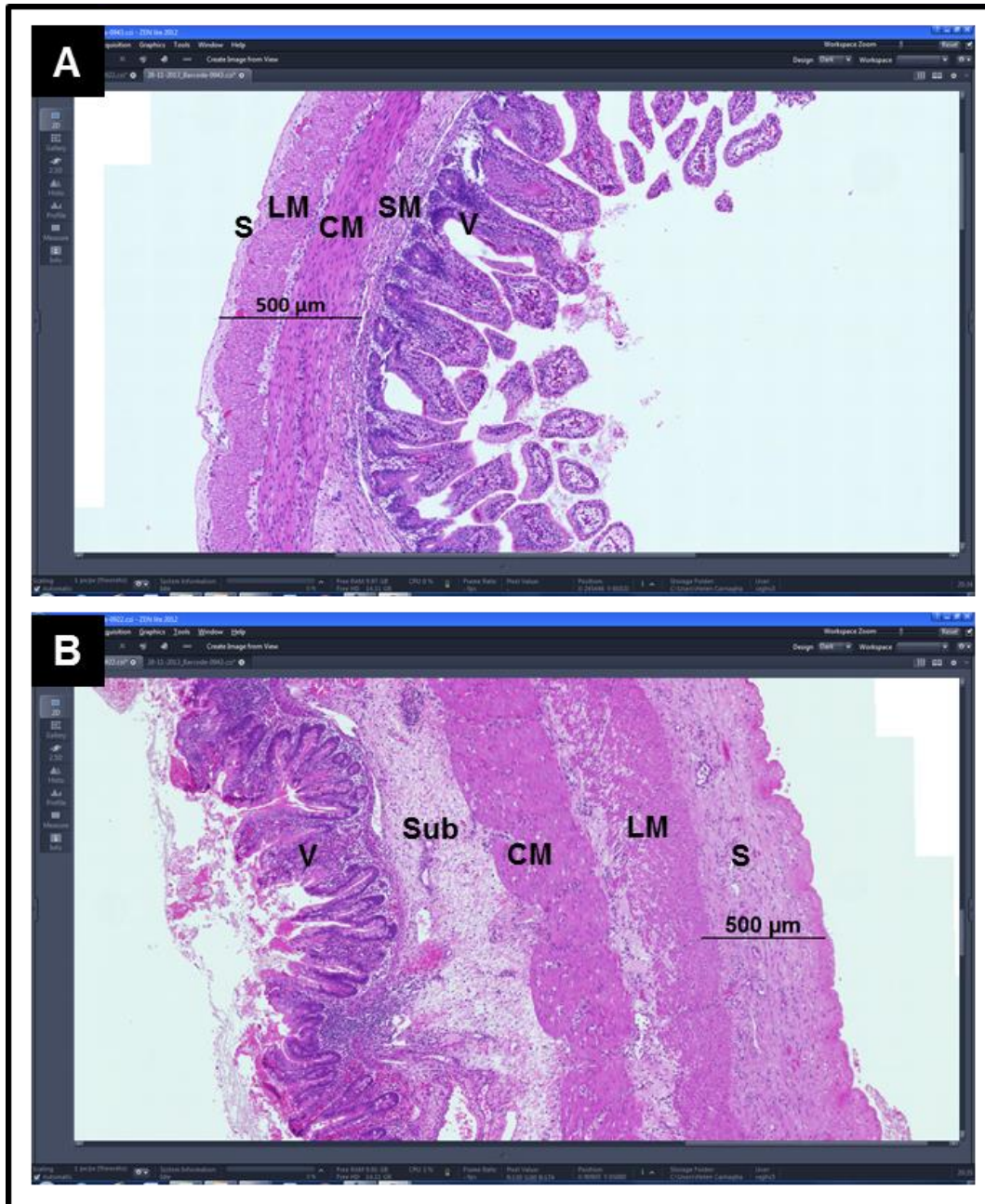


**Figure 6-3:** Representative H&E images of **A.** control and **B.** gastroschisis bowel. Bowel sections imaged using Zeiss AxioScan Z1 slide scanner using 40x objective and analysed with Zeiss ZEN lite imaging software. Key: S – serosa, LM – longitudinal muscle, CM – circular muscle, Sub – submucosa, V – villi. Images showing scale bar indicating 500μm. Control bowel (**A**) shows very mild serosal inflammatory infiltrate. Gastroschisis bowel (**B**) shows serosal fibrosis, loose connective tissue and chronic inflammatory infiltrate.



### 6.2.2.2 Bowel Wall Thickness and Age at Bowel Resection

Linear regression analysis was performed to determine whether there was a relationship between bowel wall thickness and age at time of bowel resection. Analysis of control small bowel specimens revealed no significant relationship between entire bowel wall thickness ( $p=0.06$ ,  $R^2=0.27$ , Figure 6-4A) or entire muscle layer ( $p=0.7$ ,  $R^2=0.007$ , Figure 6-4C) thickness with age at time of bowel resection. However, analysis of gastroschisis small bowel specimens showed a significant relationship between increasing entire bowel wall ( $p=0.003$ ,  $R^2=0.4$ , Figure 6-4B) and entire muscle layer ( $p=0.006$ ,  $R^2=0.35$ , Figure 6-4D) thickness with older age at time of bowel resection.

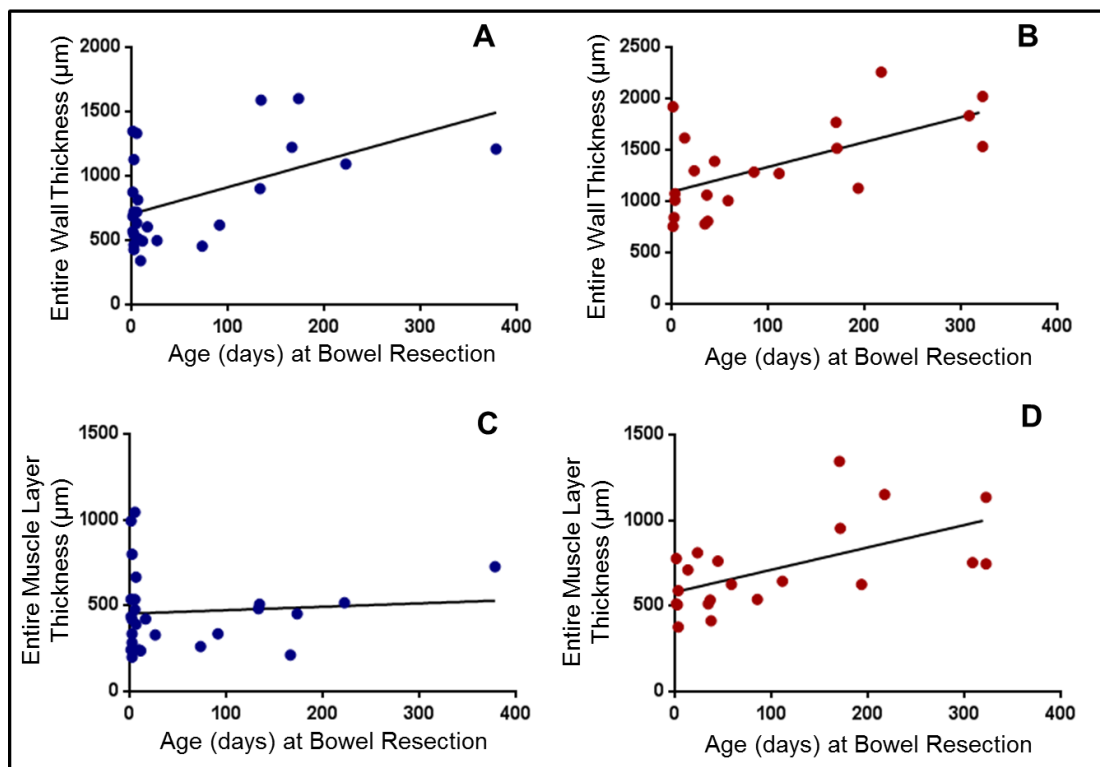


**Figure 6-4:** Linear regression analysis comparing entire bowel wall and age at time of bowel resection. **A.** Control group ( $p=0.06$ ,  $R^2=0.27$ ). **B.** Gastroschisis group  $p=0.003$ ,  $R^2=0.4$ . Linear regression analysis comparing entire muscle thickness and age at time of bowel resection. **C.** Control group  $p=0.7$ ,  $R^2=0.007$ . **D.** Gastroschisis group ( $p=0.006$ ,  $R^2=0.35$ ).

### 6.2.2.3 Bowel Wall Thickness and Time to Full Enteral Feeds

Additionally, a linear regression analysis was performed to determine whether the degree of entire bowel wall thickening impacted ENT in the gastroschisis population, which showed that increasing bowel wall thickness was significantly correlated with increased time to ENT ( $p=0.01$ ,  $R^2=0.5$ , Figure 6-5A). However, increasing entire muscle layer thickness ( $p=0.08$ ,  $R^2=0.3$ , Figure 6-5 B) and increasing serosal thickness ( $p=0.6$ ,  $R^2=0.34$ , Figure 6-5C) were not significantly correlated with increased time to ENT. However, these analyses are limited by the number of data points and may be influenced by the outliers with a very long ENT.

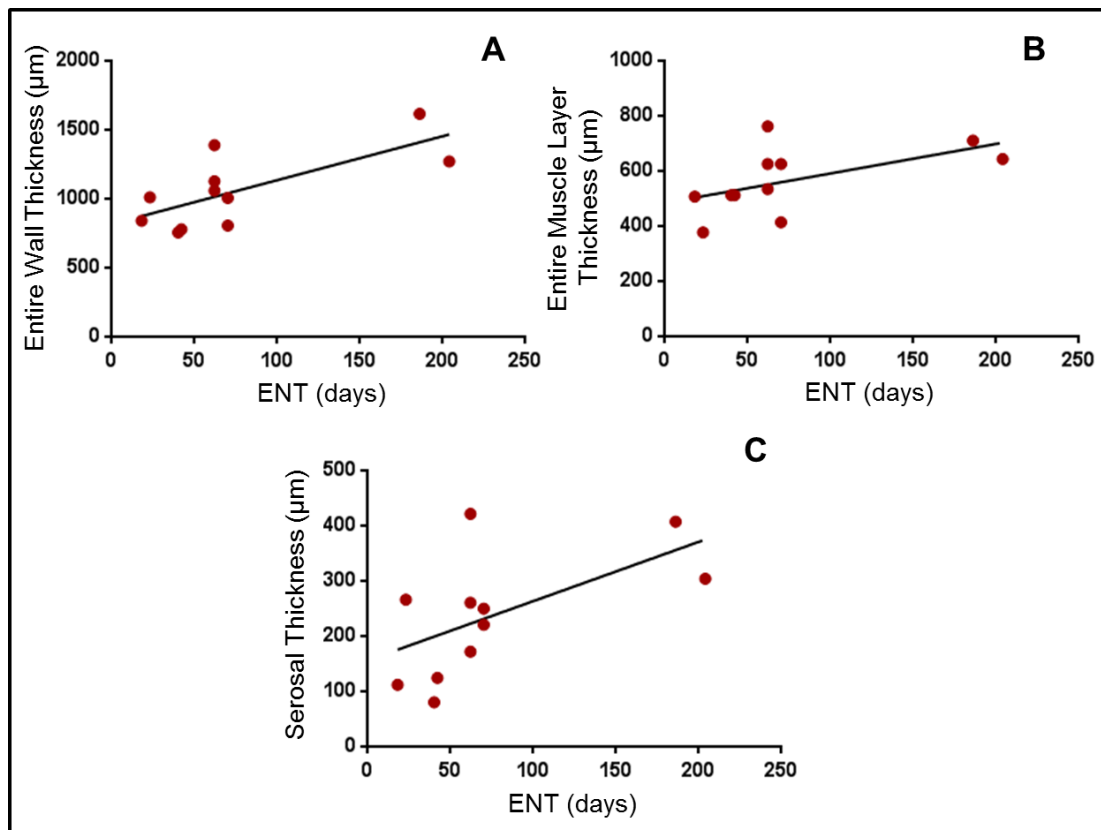


**Figure 6-5:** Linear regression comparing gastroschisis (A) entire bowel wall thickness ( $p=0.01$ ,  $R^2=0.5$ ), (B) entire muscle layer thickness ( $p=0.08$ ,  $R^2=0.3$ ) and (C) serosal thickness ( $p=0.6$ ,  $R^2=0.34$ ) with time to full enteral feeds (ENT). Bowel Wall Architecture.

#### **6.2.2.4 *$\alpha$ -Smooth Muscle Actin***

To determine whether a myopathy was present in the thickened bowel wall of gastroschisis infants, specimens were stained for  $\alpha$ -smooth muscle actin ( $\alpha$ -SMA). The total area of longitudinal or circular muscle within the high power (40x objective) field of view and the percentage of positive  $\alpha$ -SMA staining within these muscle layers were quantified using ImageJ software. For the thicker small bowel specimens the muscle was too large for the entire muscle thickness to be fully imaged in a single high power field of view so the image is a representative view of the muscle architecture and area (Figure 6-7B). However, as expected the total area of longitudinal and circular muscle was significantly greater in the gastroschisis group compared to the control group (Table 6-4, Figure 6-6). The percentage of positive  $\alpha$ -SMA staining in the longitudinal muscle layer was significantly lower in the gastroschisis group compared to the control group with areas of absent staining appearing as loculations within the smooth muscle (Table 6-4, Figure 6-6, Figure 6-7A and B). However, there was no difference in the percentage of positive  $\alpha$ -SMA staining in the circular muscle layer between the groups (Table 6-4, Figure 6-6, Figure 6-7C and D).

	Control Mean±SEM	Gastroschisis Mean±SEM	p-value
Longitudinal muscle area (mm <sup>2</sup> )	0.052±0.004	0.079±0.004	*0.0001
Circular muscle area (mm <sup>2</sup> )	0.075±0.004	0.086±0.002	*0.03
α-SMA longitudinal muscle % positive staining	81±2.02	69.4±3.1	*0.0027
α-SMA circular muscle % positive staining	69.5±2.8	72.8±2.5	0.40

**Table 6-4:** Muscle area and percentage (%) of positive α-smooth muscle actin (α-SMA) staining within the longitudinal and circular muscle layers of control and gastroschisis small bowel specimens. \*Indicates p-values that reached significance.

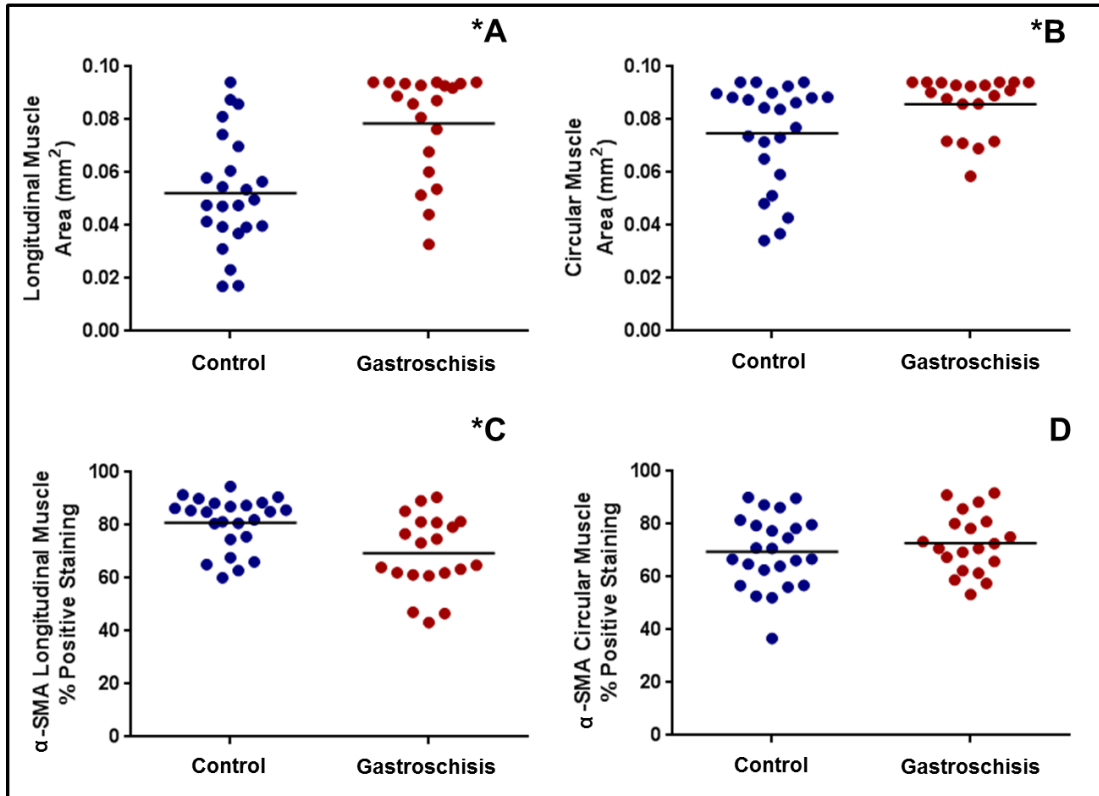


**Figure 6-6:** Comparison of **A.** longitudinal muscle area, **B.** circular muscle area, **C.** α-SMA longitudinal muscle % positive staining and **D.** α-SMA circular muscle % positive staining. \*Comparison that reached statistical significance.

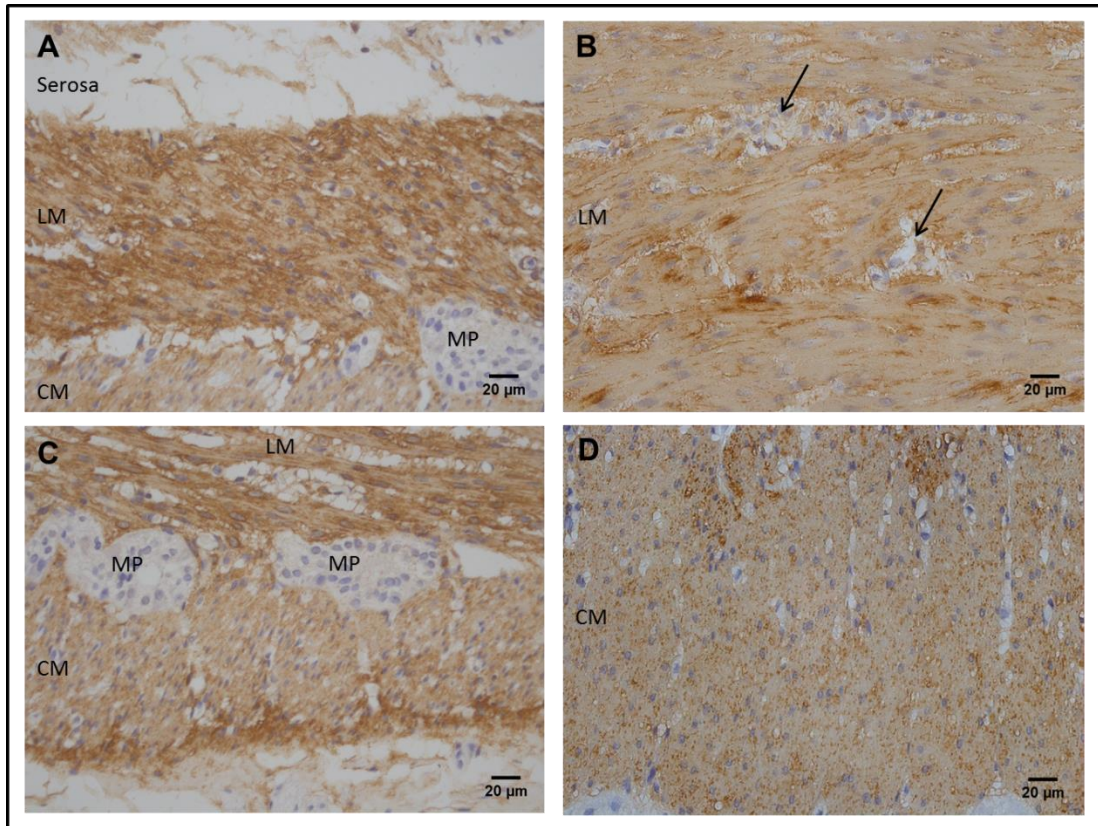


**Figure 6-7:** Images showing  $\alpha$ -smooth muscle actin ( $\alpha$ -SMA) staining, taken with 40x objective. **A and C:** control small bowel centred on **A.** longitudinal muscle, **C.** circular muscle. **B and D:** Gastroschisis small bowel centred on **B.** longitudinal muscle, **D.** circular muscle. Key: LM – longitudinal muscle, CM – circular muscle, MP – myenteric plexus.

#### 6.2.2.5 Collagen

To determine whether there was an increase in collagen deposition in the thickened gastroschisis bowel wall, specimens were stained with picrosirius red (PS). The total area of the serosa and submucosa within the high power field of view and the percentage of positive PS staining in all bowel wall layers was quantified using ImageJ software. Again, for the thicker small bowel specimens the serosa and submucosa was too large for the entire thickness to be fully imaged in a single high power field of view therefore the image is a representative view of the architecture and area of these layers (Figure 6-8B, D, F, G and H). However, in keeping with the bowel wall thickness measurements, the serosal layer area was significantly larger in the gastroschisis group compared to the control group (Table 6-5) and there was no difference in the submucosal area between the groups. There was no significant difference in the percentage of positive PS staining in the longitudinal muscle, circular muscle or submucosa between the two groups (Figure 6-8C-H). However,

the percentage of positive PS serosal staining was significantly lower in gastroschisis small bowel compared to controls with areas of separation seen between the collagen fibres (Figure 6-8A and B). These findings are likely due to the presence of loose connective tissue and ongoing low grade serosal fibroinflammatory reaction within the gastroschisis bowel as described in 6.2.2.1 Bowel Wall H&E Qualitative Description.

	Control Mean±SEM	Gastroschisis Mean±SEM	p-value
Serosal area (mm <sup>2</sup> )	0.038±0.005	0.079±0.004	*<0.0001
Submucosal area (mm <sup>2</sup> )	0.030±0.002	0.035±0.003	0.14
PS serosal % positive staining	44.1±3.3	34.4±3.3	*0.046
PS longitudinal muscle % positive staining	26.3±3.2	29.6±2.5	0.45
PS circular muscle % positive staining	20.0±2.6	25.7±2.5	0.13
PS submucosal % positive staining	47.6±2.8	46.3±3.1	0.76

**Table 6-5:** Serosal and submucosal layer area and percentage (%) of positive picosirius red (PS) staining in all bowel wall layers of control and gastroschisis small bowel specimens. \*Indicates p-values that reached significance.



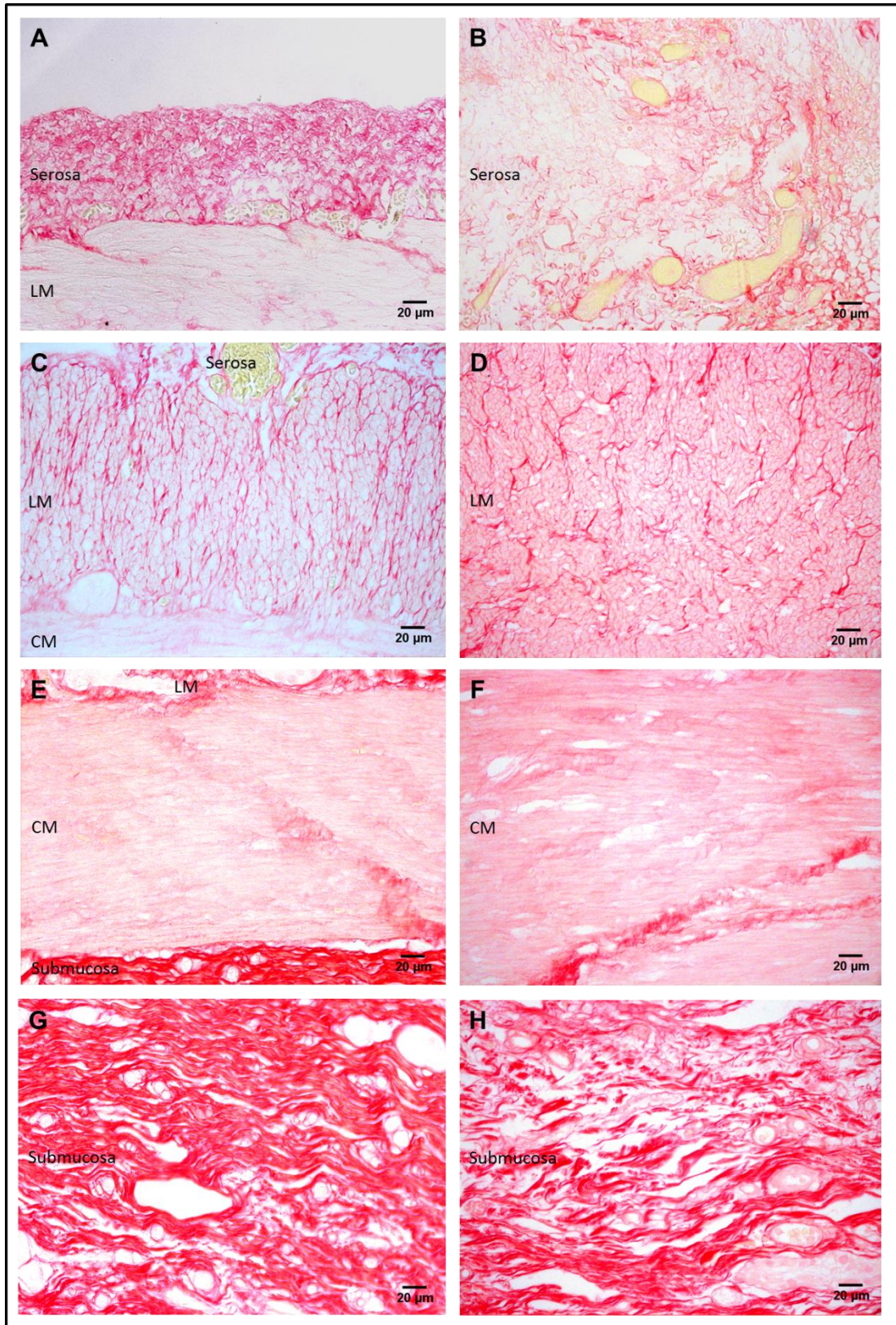


**Figure 6-8:** Images showing picrosirius red (PS) staining, taken with 40x objective. **A, C, E and G:** control small bowel centred on **A.** serosa, **C.** longitudinal muscle, **E.** circular muscle and **G.** submucosa. **B, D, F and H:** Gastroschisis small bowel centred on **B.** serosa, **D.** longitudinal muscle, **F.** circular muscle and **H.** submucosa. Key: LM – longitudinal muscle, CM – circular muscle.



#### **6.2.2.6 *Ki67 Staining***

To determine whether muscle layer thickening in gastroschisis is linked to hypertrophied cells or increased cell proliferation, specimens were stained for ki67, which stains dividing nuclei. The total number of nuclei per muscle area (longitudinal and circular) and the percentage of proliferating nuclei in these muscle layers were calculated. There was no significant difference in the number of nuclei/mm<sup>2</sup> within the longitudinal or circular muscle layers between the groups (Table 6-6) suggesting the gastroschisis muscle cells are not hypertrophic. Equally, there was no difference in the percentage of proliferating nuclei in the longitudinal or circular muscle layers between the two groups. As cell proliferation in gastroschisis small bowel may reduce after birth following cessation of exposure to amniotic fluid, the analysis of percentage of proliferating cells was repeated including only those specimens resected at <40 days. There was no significant difference in the age at time of bowel resection (control median 4, range [1-26] days, n=18 and gastroschisis 3 [1-37] days, n=9, p=0.08) between the groups. However, again there was no significant difference in percentage of proliferating nuclei within the longitudinal or circular muscle layers between the groups.

	Control Mean±SEM	Gastroschisis Mean±SEM	p-value
Longitudinal muscle nuclei/mm <sup>2</sup>	5770±494	5313±735	0.60
Circular muscle nuclei/mm <sup>2</sup>	5474±600	5945±624	0.59
Longitudinal muscle % proliferating nuclei	2.0±0.5	2.7±0.7	0.40
Circular muscle % proliferating nuclei	2.1±0.5	1.8±0.5	0.68
Longitudinal muscle % proliferating nuclei (<40 days)	2.6±0.6	4.2±1.2	0.21
Circular muscle % proliferating nuclei (<40 days)	2.7±0.6	3.3±0.7	0.56

**Table 6-6:** Total number of nuclei per area and the percentage (%) of proliferating nuclei within the longitudinal and circular muscle layers of control and gastroschisis small bowel specimens.

#### **6.2.2.7 Transforming Growth Factor-Beta 3 Staining**

A previous study (Moore-Olufemi et al., 2015) linked gastroschisis with increased levels of transforming growth factor-beta 3 (TGF-β3), which was hypothesised to be the mediator of bowel wall thickening in gastroschisis. Therefore, TGF-β3 staining was performed to determine whether there were increased levels within this gastroschisis cohort. There was no significant difference in the percentage of positive TGF-β3 staining for any bowel wall layer between gastroschisis and control groups

(Table 6-7). However, there was high level background staining, which prevented analysis using automated colour thresholding. Although manual thresholding was performed the results may still have been affected by the considerable background staining present across all bowel specimens (Figure 6-9).

	Control Mean±SEM	Gastroschisis Mean±SEM	p-value
Longitudinal muscle % positive staining	26.7±3.2	26.4±4.4	0.96
Circular muscle % positive staining	31.0±3.6	23.8±3.5	0.17
Submucosa % positive staining	10.0±0.9	8.6±1.0	0.29
Villi epithelium % positive staining	38.1±3.9	38.7±4.2	0.91

**Table 6-7:** Percentage (%) of positive transforming growth factor-beta 3 (TGF-β3) staining within all bowel wall layers of control and gastroschisis small bowel specimens.

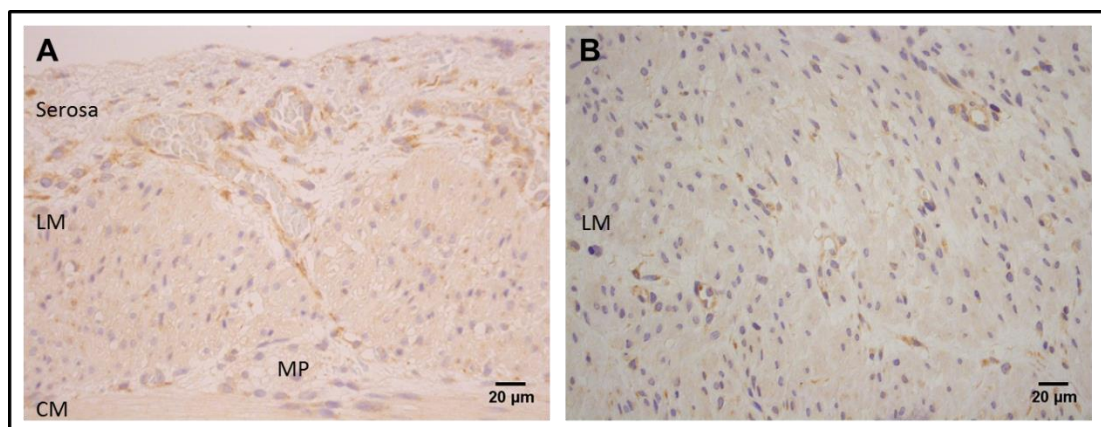


**Figure 6-9:** Images showing transforming growth factor-beta 3 (TGF-β3) staining, centred on longitudinal muscle, taken with 40x objective. **A.** Control small bowel. **B.** Gastroschisis small bowel. Both images showing significant background staining.

## **6.3 Discussion**

### **6.3.1 Bowel Wall Thickness and Mucosal Morphology**

The bowel wall of gastroschisis infants is significantly thicker compared with controls, comprising thickened serosa, longitudinal muscle and circular muscle. However, there was no difference in submucosal thickness. These findings were consistent both on direct linear measurement of H&E sections and calculation of the area per high powered field of view following  $\alpha$ -SMA and PS staining. Additionally, the mucosa of both gastroschisis and control small bowel exhibited normal development without evidence of villus blunting or crypt hyperplasia. Although the villus to crypt ratio of gastroschisis small bowel was lower than the control group, the ratio was  $>2:1$ , which is within the normal limits for children (Dickson et al., 2006). These results suggest that the inner layers of gastroschisis small bowel develop normally but there is altered development of the outer layers, which is consistent with a signal originating at the serosal surface.

Included in this cohort were bowel wall specimens resected from birth up to approximately 1 year of age. In the control group there was no significant change in wall thickness during this time period suggesting the process of normal infant bowel growth results in a fairly constant bowel wall thickness during the first year of life. However, the gastroschisis bowel showed a significant increase in bowel wall thickness with increasing age implying that within this complex/dysmotile gastroschisis cohort abnormal bowel growth continued to be present during the postnatal period. Additionally, increased thickness of the entire bowel wall was significantly associated with prolonged ENT feeds in this complex gastroschisis cohort suggesting that these morphological changes may cause GRID or be a result of GRID.

### **6.3.2 Bowel Wall Architecture and Composition**

The circular muscle, although thicker in the gastroschisis small bowel, showed no other significant structural differences between the groups. However, the gastroschisis longitudinal muscle and serosa showed significant morphological

differences compared to the control small bowel. This may suggest that the trigger for gastroschisis bowel morphological changes is extrinsic to the bowel and may originate from the amniotic fluid. This could result in the outer longitudinal muscle providing an element of protection and partial ‘sparing’ of circular muscle development.

The gastroschisis longitudinal muscle exhibited an increased number of muscle fibres without an increased number of nuclei/mm<sup>2</sup> suggesting the presence of muscle hyperplasia without cell hypertrophy. Although there was no difference in the percentage of proliferating nuclei between the groups to support the presence of hyperplasia, this could be due to the high powered field of view not including the entire muscle thickness for all samples or that following gastroschisis delivery the triggers for cell proliferation are removed reducing the rate of cell proliferation to normal levels. However, it is also worth noting that although the percentage of proliferating cells is the same between the groups this would equate in absolute terms to a larger total number of proliferating cells in the thicker gastroschisis muscle layer. Additionally, the gastroschisis longitudinal muscle exhibited a lower percentage of positive  $\alpha$ -SMA staining with areas of loculation in the muscle layers without increased PS staining or evidence of cutting artefact suggesting the development of these hyperplastic muscle fibres is abnormal. Coordinated and effective bowel peristalsis requires normal neuromuscular function involving the interaction between enteric neurons, ICC and smooth muscle cells. The results from the previous chapter have shown that the numbers of both enteric neurons and ICC are normal in human gastroschisis small bowel. This suggests the cause of GRID may be a myopathic disturbance of the muscularis smooth muscle rather than a neuropathy.

As expected and in keeping with observations of serosal peel/thickening at birth, the serosa within the gastroschisis cohort was significantly thicker mainly due to an ongoing low grade chronic fibroinflammatory reaction that was associated with loose connective tissue and lower percentage of positive PS staining.

### **6.3.3 Hypothesised Cause of Bowel Wall Thickening**

Throughout life, smooth muscle has the ability to adapt morphologically in response to internal and external stimuli for which inflammation is an identified trigger and has been shown to cause remodelling of respiratory (Bousquet et al., 2000), vascular (Kranzhofer et al., 1999) and intestinal (Shea-Donohue et al., 2012, Nair et al., 2014) smooth muscle cells. Inflammation at the intestinal mucosal surface secondary to gastrointestinal infection results in smooth muscle hyperplasia and hypertrophy causing smooth muscle thickening (Bettini et al., 2003, Blennerhassett et al., 1992) providing evidence that extrinsic environmental influences can alter intestinal smooth muscle morphology.

Animal studies investigating gastroschisis bowel wall thickening have shown that increased serosal and smooth muscle thickening occurs secondary to amniotic fluid exposure (Langer et al., 1989, Guo et al., 1995, Yu et al., 2004, Bittencourt et al., 2006, Shah et al., 2012, Albert et al., 2001) suggesting that amniotic fluid contains extrinsic triggers for intestinal remodelling. Manipulation of the amniotic fluid inflammatory environment has previously shown increased amniotic fluid IL-8 concentrations to be associated with increased bowel wall thickening (Api et al., 2001, Correia-Pinto et al., 2002), and with decreased IL-8 concentrations associated with decreased bowel wall thickening (Hakguder et al., 2011, Olguner et al., 2006). Additionally, surgical gastroschisis animal models treated with either intra-amniotic (Guo et al., 1995, Yu et al., 2004) or maternal intraperitoneal (Bittencourt et al., 2006) injections of dexamethasone have also shown reduced bowel wall thickness.

Other researchers have investigated the potential of bowel constriction at a tight abdominal wall defect as the cause for bowel wall morphological changes. Bowel constriction creates lymphatic and vascular stasis resulting in intrinsic bowel wall inflammation (Langer et al., 1989). One study using a surgical lamb gastroschisis model placed a surgical tie around the bowel to create a point of constriction mimicking a tight abdominal wall defect. This resulted in smooth-muscle thickening and mucosal blunting without serosal thickening (Langer et al., 1989). However, a study using a rabbit model showed the degree of gastroschisis bowel wall thickening was independent of the abdominal wall defect size and that bowel wall thickening

was unchanged by increased bowel compression. This study therefore concluded that abnormal serosal exposure to amniotic fluid was the trigger of the gastroschisis bowel wall morphological changes (Albert et al., 2001).

The results presented in this chapter reveal the morphological changes within human gastroschisis small bowel are located within the outer bowel wall layers (serosa and smooth muscle) with mucosal and submucosal sparing. Given an intrinsic inflammatory trigger secondary to bowel compression at a tight abdominal wall defect would more likely cause transmural remodelling it is possibly more likely that the trigger for bowel wall thickening has an extrinsic origin associated with direct contact of the serosa with the amniotic fluid. It has been previously documented that overt signs of bowel wall thickening and serosal peel do not develop until the third trimester (Tibboel et al., 1986) when significant changes in the amniotic fluid composition take place. Abnormal exposure of the serosal surface to increasing levels of meconium, enteric enzymes, urine and airway secretions within the amniotic fluid (Underwood et al., 2005) could be the trigger for the pro-inflammatory amniotic fluid environment, which has previously been reported within the third trimester of gastroschisis pregnancies (Morrison et al., 1998, Guibourdenche et al., 2006). Given inflammation located at the mucosal surface secondary to infection can stimulate smooth muscle remodelling it is therefore possible that inflammation located at the serosal surface could also induce smooth muscle remodelling and be the cause of the morphological changes present in the gastroschisis small bowel.

Another source of external stimulus could come from abnormal mechanical forces being applied to the externalised bowel particularly during birth and postnatal manipulation of the externalised bowel prior to abdominal wall closure. Transient post-operative ileus (intestinal dysmotility) is a common source of morbidity following abdominal and pelvic surgery whereby manipulation of the bowel induces inflammation and two phases of intestinal inhibition (Boeckxstaens and de Jonge, 2009). The first phase occurs during surgery and is mediated by neurotransmitters and the second develops 3 to 4 hours after surgery secondary to a leukocytic infiltrate within the muscularis externa (Kalff et al., 1998, Kalff et al., 1999a, Kalff et al.,

1999b). Therefore, postnatal manipulation of the externalised bowel of gastroschisis neonates may further compound smooth muscle remodelling and dysfunction.

The composition of amniotic fluid is complex and its constituents originate both from the fetus and the amniotic membranes. In addition to containing products from urine, respiratory secretions and meconium, the amniotic fluid also contains growth factors produced by the amniotic membranes, which have a trophic effect on the bowel and include; epidermal growth factor, transforming growth factor alpha and beta, erythropoietin, insulin-like growth factor-1 and granulocyte colony-stimulating factor (Underwood et al., 2005). A previous study showed that ligation of the fetal rabbit oesophagus preventing swallowing of amniotic fluid resulted in poorly developed gut whilst normal gut development was achieved by infusions of amniotic fluid distal to the oesophageal ligation (Mulvihill et al., 1986). Fetal swallowing results in mucosal exposure to the amniotic fluid growth factors and regulates normal fetal bowel development. However, in gastroschisis the serosal surface is abnormally exposed to these growth factors, which could cause abnormal hyperplasia and development of dysfunctional smooth muscle cells. TGF- $\beta$ 3 has previously been shown to be increased in human gastroschisis small bowel specimens compared to controls (Moore-Olufemi et al., 2015) and has been hypothesised to be the mediator of bowel wall thickening and disordered contractility in gastroschisis. However, this finding of increased levels of TGF- $\beta$ 3 could not be replicated in the study presented in this chapter but this may have been due to the high levels of associated background staining and therefore cannot be used to confirm or deny the findings of Moore-Olufemi et al.

Finally, close regulation of organ size during fetal development is essential requiring contact inhibition of proliferation, which is regulated by the Hippo pathway. Dysregulation of this pathway leads to tissue overgrowth (Zhao et al., 2011). The precise events that integrate mechanical and biochemical signals are not fully understood. However, it is thought that yes-associated protein (YAP) and transcriptional coactivator with PDZ-binding motif (TAZ) are the nuclear relays of mechanical cues such as confined adhesiveness and extracellular matrix stiffness (Dupont et al., 2011, Low et al., 2014). In normal fetal organogenesis the bowel develops within the confines of the abdominal cavity, which exerts mechanical



pressure on the bowel wall. However, the bowel of gastroschisis fetuses herniates through the abdominal wall defect without being contained within a peritoneal membrane and lies free floating within the amniotic cavity. As such, the mechanical pressure exerted and contact stimuli on the bowel is greatly reduced compared to that of a structurally normal fetus or even a fetus with an exomphalos. Therefore, it is feasible that the loss of regulatory mechanical cues could result in dysregulation of the Hippo pathway and over proliferation of bowel smooth muscle. Liver regeneration is a good example of this possible mechanism. The liver is able to regenerate following hepatic resection until the original liver-to-body weight ratio is restored (Michalopoulos, 2007). One study in rats revealed that partial hepatic resection resulted in increased nuclear YAP until the original liver-to-body weight ratio was achieved following which nuclear YAP levels returned to baseline levels (Grijalva et al., 2014). As such, within fetal gastroschisis bowel it is possible that nuclear YAP is over expressed due to loss of normal bowel to abdominal cavity sizing cues. However, going against this theory, the findings from the ACLP mouse model presented in chapter 4 did not show any evidence of bowel wall thickening within the AWD group compared to controls. Given the bowel of AWD fetuses was contained within the relatively large exocoelomic cavity compared to the smaller abdominal cavity if the YAP-TAZ theory was correct the AWD bowel would be hypothesised to be thicker. As such, this suggests the YAP-TAZ pathway may not be a factor in human gastroschisis bowel wall changes. Additionally, this theory would be very difficult to test in human gastroschisis as the molecular events of the YAP-TAZ pathway may have ceased long before delivery of gastroschisis fetuses and therefore may not be easily accessible for investigation.

The results from this study show that the control small bowel wall thickness did not significantly change over the first year of life. This finding is supported by a study that investigated bowel wall architecture including fetuses of 10 weeks GA through to adults of 70 years old (Bruhin-Feichter et al., 2012). As expected over the entire age range the bowel wall increased in thickness but the detailed breakdown of results showed similar bowel wall thickness throughout the first year of life. However, within the gastroschisis group increasing bowel wall thickness was significantly associated with increasing age at time of bowel resection and prolonged ENT. This may be due to the presence of ongoing chronic serosal inflammation that was

identified within the gastroschisis cases post-partum. This ongoing serosal fibroinflammatory reaction may be exerting a persistent smooth muscle remodelling effect on the bowel muscle layers prolonging the duration of GRID in these infants.

#### **6.3.4 Smooth Muscle $\alpha$ -SMA Deficiency and Chronic Idiopathic Intestinal Pseudo-Obstruction**

Smooth muscle contains thick myosin and thin actin filaments both of which are essential for normal muscular contractions. The actin filaments regulate changes in cell size, cell contraction, mechanical support and cellular adhesion. As such,  $\alpha$ -SMA is a major constituent of the intestinal muscularis smooth muscle apparatus and is essential for normal intestinal motility (Hartshome, 1987). Chronic idiopathic intestinal pseudo-obstruction (CIPO) is a condition that presents with chronic obstructive symptoms including intractable constipation, nausea, vomiting, abdominal pain and distension often with episodic exacerbations. The cause of CIPO is not fully understood. However, absence of intestinal  $\alpha$ -SMA staining has been found in some patients most frequently reported to be isolated to the circular muscle (Knowles et al., 2004, Donnell et al., 2008, Moore et al., 2002, Smith et al., 1992) but occasionally within both the circular and longitudinal muscle layers (Koh et al., 2008). The findings in CIPO suggest absence of  $\alpha$ -SMA staining within only one layer of the intestinal muscularis may be sufficient to cause bowel dysmotility and obstruction. However, in contrast to CIPO, the small bowel function of gastroschisis infants over time generally improves enabling normal bowel transit and full enteral tolerance suggesting the  $\alpha$ -SMA changes seen in gastroschisis small bowel are not persistent and recovers to normal levels with time.

#### **6.3.5 Limitations of the Study**

As discussed within the previous chapter this was a retrospective study with the limitations associated with the use of archival specimens and the ability to only include the most severely affected gastroschisis infants. The use of automated software analysis was effective for  $\alpha$ -SMA and PS staining but due to significant background staining associated with the TGF- $\beta$ 3 automated colour thresholding could not be used and even following manual colour thresholding results may have

been affected by the background staining. Additionally there was no significant increase in the proportion of proliferating nuclei measured by ki67, which suggests that the molecular triggers that lead to increase in number of smooth muscle cells were no longer persistent at the time of bowel resection. Finally, on review of H&E sections by a Consultant Pathologist there was evidence of a serosal inflammatory infiltrate in gastroschisis bowel, which did not extend to the smooth muscle. Although TGF- $\beta$ 3 staining was performed, inflammation was not quantitatively evaluated by another method and further work with specific inflammatory immunohistochemical stains should be performed to verify the presence or absence of inflammation within the bowel wall layers.

## **6.4 Conclusion**

This study shows increased bowel wall thickening in gastroschisis infants compared to controls. Comprising of serosal and smooth muscle thickening with normal inner submucosal and mucosal layers. The most significant morphological changes were present in the outer bowel wall layers with smooth muscle hyperplasia and deficiency of  $\alpha$ -SMA within the longitudinal muscle layer. These findings suggest bowel wall thickness could be a biomarker for infant outcome and that GRID maybe secondary to a myopathic disturbance of the muscularis smooth muscle rather than a neuropathy secondary to ICC deficiency. The trigger for these morphological changes could be linked to bowel inflammation or abnormal exposure of the bowel serosal surface to growth factors contained within the amniotic fluid.

# **Chapter 7: Gestational Age at Delivery and Maternal Corticosteroid Administration: Association with Outcomes in Gastroschisis**

## **7.1 Introduction**

### **7.1.1 Timing of Delivery**

The optimisation of gastroschisis antenatal management, including timing of delivery, may improve neonatal outcomes. Currently many centres worldwide electively deliver gastroschisis pregnancies at 37 to 38 weeks GA following the report of in-utero fetal deaths in late term pregnancies (Burge and Ade-Ajayi, 1997). Additionally, more recent publications have also suggested that early term birth at around 37 weeks GA is associated with decreased neonatal morbidity and mortality compared with late term birth (Baud et al., 2013, Meyer et al., 2014, Harper et al., 2014). Furthermore, it has been hypothesized that amniotic fluid negatively impacts on bowel development and longer exposure of bowel to amniotic fluid worsens postnatal GRID (Morrison et al., 1998, Api et al., 2001). Some surgeons therefore propose that elective delivery of otherwise healthy gastroschisis pregnancies in the late pre-term period between 34 and 36<sup>+6</sup> weeks GA would reduce bowel exposure to amniotic fluid and result in improved postnatal gut function.

The literature presents conflicting evidence both for (Gelas et al., 2008, Serra et al., 2008, Moore et al., 1999, Moir et al., 2004) and against (Maramreddy et al., 2009, Youssef et al., 2015, Cain et al., 2014, Logghe et al., 2005, Charlesworth et al., 2007) elective delivery in the late pre-term period as a means to protect bowel from ongoing damage. The majority of these studies include small numbers of patients and a randomised control study with enough power to determine the optimal timing for delivery is elusive due to the relatively small numbers of gastroschisis neonates seen per centre per year.

### 7.1.2 Maternal Antenatal Corticosteroids

Experiments using surgical gastroschisis animal models (rabbit, rat and chick) treated either with intra-amniotic (Guo et al., 1995, Yu et al., 2004) or maternal intraperitoneal (Bittencourt et al., 2006) injections of dexamethasone have shown reduced bowel wall thickness, increased bowel glucose uptake and increased levels of bowel protein, DNA and enzymes, suggesting a beneficial effect of dexamethasone on intestinal function (Table 7-1). In humans, a small prospective study (only published in abstract form) investigating the impact of maternal antenatal corticosteroid administration in gastroschisis pregnancies suggested that gastroschisis infants who received maternal antenatal corticosteroids had a reduced duration of PN, ENT and LOS (Polnik et al., 2012). Additionally, a study of duodenal contractility in normal premature neonates showed that antenatal corticosteroids was associated with improved duodenal contractility particularly in those neonates born between 29 to 32 weeks gestation suggesting corticosteroids may have a maturational effect on the bowel (Morriss et al., 1986) similar to that on the lungs.

Effect of Antenatal Corticosteroids	Chick	Rat	Rabbit
Protein	↑ Protein and DNA content	↑ Protein and DNA content	↑ Protein content
Wall thickening	↓ Wall thickening	↓ Wall thickening	No reported
Other parameters	↓ Inflammation	↑ proliferation and ↓ apoptosis	↑ glucose uptake, lactase and maltase content

**Table 7-1:** Impact of antenatal corticosteroids on bowel and intestinal function in animal surgical models of gastroschisis.

Within placental syncytiotrophoblasts, the corticosteroid enzyme 11- $\beta$ -hydroxysteroid dehydrogenase isozyme 2 (11 $\beta$ -HSD2) protects the fetus from the potentially harmful effects of endogenous maternal glucocorticoids (Benediktsson et al., 1997). However, synthetic steroid derivatives such as dexamethasone and

betamethasone are minimally metabolised by 11 $\beta$ -HSD2 and therefore cross into the fetal circulation (Murphy et al., 2007b). Experiments in fetal animals showed that corticosteroid stimulation accelerates type 1 and 2 pneumocyte development leading to increases in surfactant production and improved lung biomechanics (Liggins, 1969, DeLemos et al., 1970, Kotas and Avery, 1971). In a landmark randomised controlled trial (RCT), a single course of maternal antenatal corticosteroids in women at risk from preterm delivery was shown to reduce neonatal morbidity and mortality from respiratory distress syndrome (Liggins and Howie, 1972). Since then antenatal corticosteroids are part of routine clinical care for threatened preterm labour and have revolutionised the neonatal management of premature neonates, reducing respiratory distress syndrome, neonatal death, intraventricular haemorrhage, necrotising enterocolitis and sepsis within the first 48 hours of birth without increased risks to otherwise healthy mothers (Roberts and Dalziel, 2006). As such, maternal antenatal corticosteroid administration for the improvement of GRID is a very attractive option and would be a relatively easy intervention to implement.

### **7.1.3 Hypothesis, Aims and Study Design**

It is hypothesised that early delivery and maternal antenatal corticosteroids improve infant outcomes. The primary outcome measure is time to full enteral feeds (ENT) and to be considered a surrogate for bowel function. The secondary outcome measure is length of hospital stay (LOS). As such, the aims for this retrospective study were: (i) to assess the association of timing of birth in gastroschisis fetuses with ENT and LOS; (ii) to determine whether maternal antenatal corticosteroids were associated with improvement of postnatal intestinal function (measured as ENT) in gastroschisis infants.

This was an international multicentre retrospective cohort study, data were obtained from three centres: (i) Fetal Medicine Unit, University College London Hospital (UCLH) and the Paediatric Surgery Department at Great Ormond Street Hospital for Children (GOSH), London, UK; (ii) Fetal Medicine Unit and Paediatric Surgery Department at King's College Hospital (KCH), London, UK; (iii) Fetal Medicine Unit at Mount Sinai Hospital (MSH) and the Division of General and Thoracic Surgery at The Hospital for Sick Children, University of Toronto, Canada. Data were

analysed by Mann-Whitney test, Fisher's exact test, linear regression and Cox regression.

## **7.2 Results**

### **7.2.1 Timing of Delivery and Impact on Time to Full Enteral Feeds and Length of Hospital Stay**

#### ***7.2.1.1 Study Population and Demographics***

A total of 510 gastroschisis infants were included in the analysis (n=153 from UCLH/Great Ormond Street, 125 from King's College London, and 232 from Toronto, Figure 7-1). In the combined cohort there were 76 infants with complex gastroschisis comprising; 42 atresias, 28 necrosis, 8 stenosis and 14 perforations (there was more than one pathology in 9 complex patients). Twenty-three infants died, causes of death were: sepsis in 1 atresia patient; 1 volvulus at birth; 1 volvulus following primary closure at day 10 of life; 1 respiratory failure, 2 unexpected infant deaths following discharge; 1 patient due to necrotic bowel and multi-organ failure, 1 due to necrotising enterocolitis, 2 due to parenteral nutrition associated liver failure and 1 due to overwhelming sepsis. In the other infants cause of death was unclear. 284 infants were delivered at <37 weeks GA. The reasons for semi-elective early induction of labour/emergency delivery and documented triggers for spontaneous delivery are delineated in Table 7-2. Onset of labour in infants delivered at  $\geq 37$  weeks GA was; spontaneous (n=51), elective induction of labour/caesarean section (n=155), emergency caesarean section (n=6) and unknown (n=14).

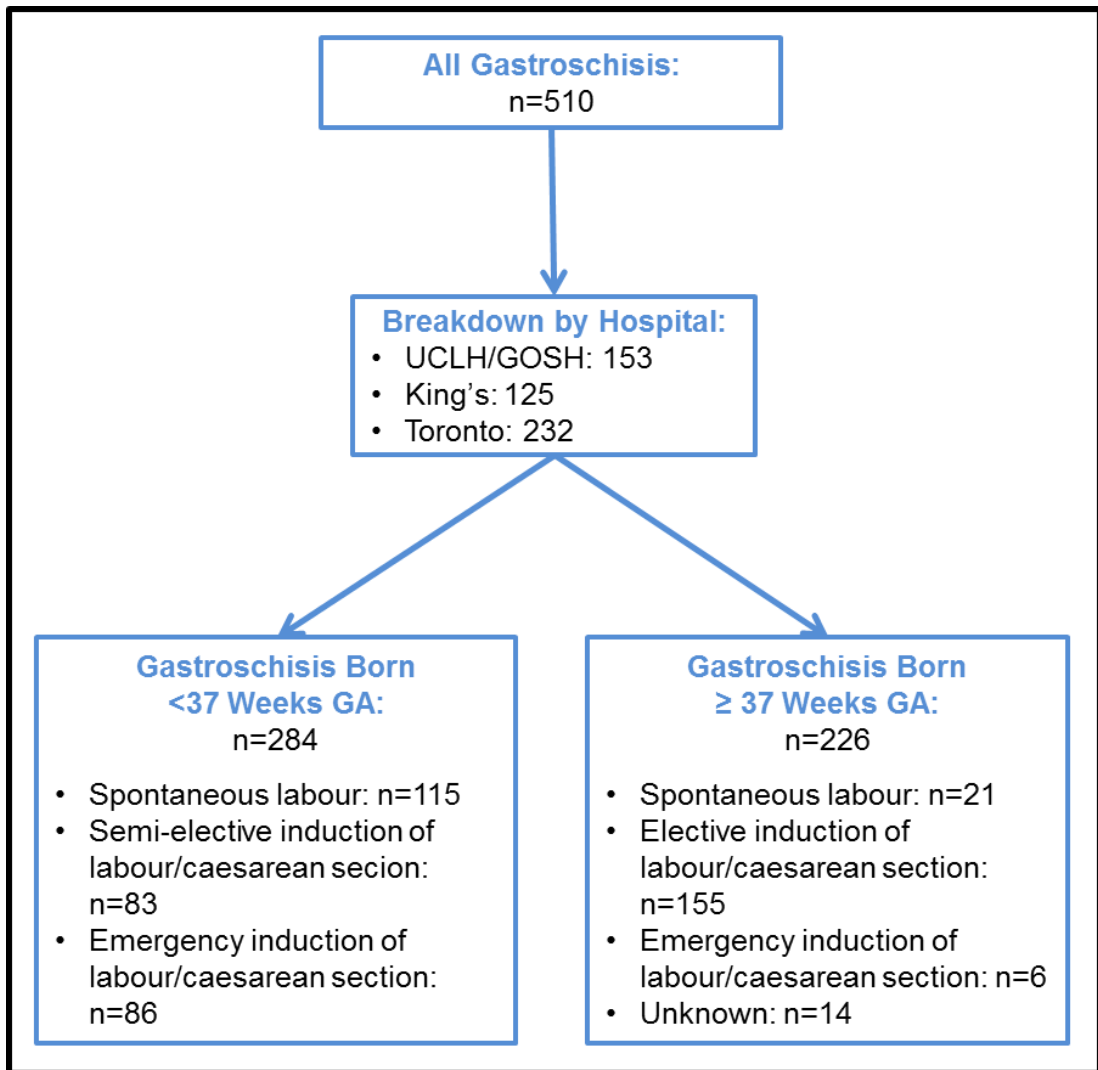


**Figure 7-1:** Study population and demographics



Reason for Early Delivery/Documented Trigger for Spontaneous Delivery	<37 weeks GA Spontaneous Labour (n=115)	<37 weeks GA Early Induction of Labour (n=83)	<37 weeks GA Emergency Delivery (n=86)
No antenatal concerns	93	17	0
<b>Maternal Factors</b>			
Prolonged rupture of membranes	4	7	1
Maternal alcohol/smoking/drug use	8	0	0
Maternal health reasons	0	2	1
Maternal infection	1	0	0
<b>Fetal Factors</b>			
Bowel dilatation	5	27	25
Intrauterine growth restriction	1	9	5
Reduced fetal movements	2	3	10
Non-reassuring fetal heart rate	0	5	16
Fetal distress / Non-reassuring biophysiological profile	1	3	8
Oligohydramnios	0	0	2
Unknown	0	10	18

**Table 7-2:** Reasons for early delivery and documented triggers of spontaneous delivery in infants born at <37 weeks GA.

### 7.2.1.2 Linear Regression Analysis

Linear regression analysis of log transformed data (due to non-normally distributed data, Table 7-3) revealed that ENT ( $p < 0.0001$ , Figure 7-2A) and LOS ( $p < 0.0001$ , Figure 7-2B) were significantly longer at lower birth GA. This resulted in an increase of 9 days for ENT and 13 days for LOS if delivery occurred at 34 weeks instead of 37 weeks. The analysis was repeated including only infants delivered at  $\geq 34$  weeks ( $n=468$ ) in order to remove the effect of extreme prematurity and the relationship remained significant for both ENT ( $p < 0.0005$ ) and LOS ( $p < 0.0005$ ). Lower birth weight showed an association with longer LOS ( $p=0.002$ ) and with longer ENT ( $p=0.007$ ) on linear regression analysis.

Linear Regression Category	Impact on ENT	p-value	Impact on LOS	p-value
Gestational age at birth (including all infants)	↑ with ↓GA	<0.0001	↑ with ↓GA	<0.0001
Gestational age at birth (including infants born at $\geq 34$ weeks GA)	↑ with ↓GA	<0.0005	↑ with ↓GA	<0.0005
Birth weight (including all infants)	↑ with ↓birth weight	0.002	↑ with ↓birth weight	0.007

**Table 7-3:** Effect of gestational age at birth and birth weight on ENT and LOS (linear regression of log transformed ENT or LOS data).

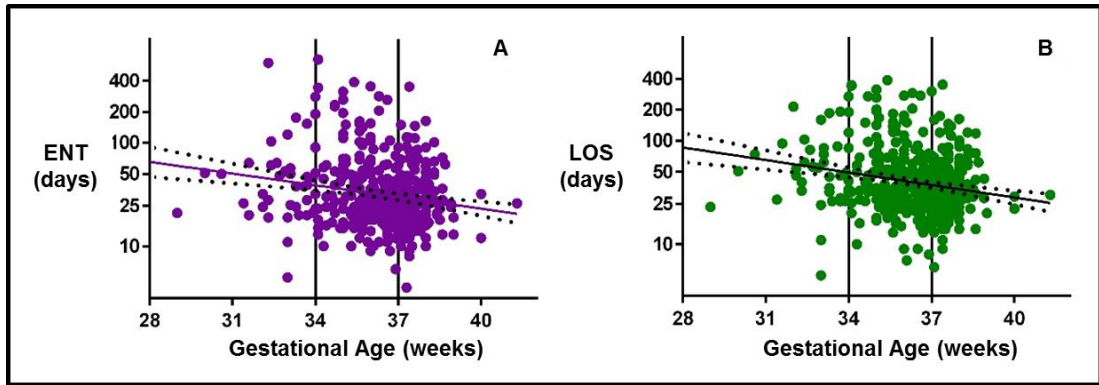


**Figure 7-2:** Effect of gestational age at birth on; **A.** ENT and **B.** LOS. Linear regression of log transformed ENT or LOS data with 95% confidence interval (dotted lines) of best fit line. Vertical lines highlight 34 and 37 weeks GA.

### 7.2.1.3 Group Univariate Analysis

To remove the effect of extreme prematurity group analysis was performed comparing infants born at 34 to 36<sup>+6</sup> weeks GA with those born at  $\geq 37$  weeks GA. Mann-Whitney comparison of ENT and LOS (results outlined in Table 7-4, excluding those patients not achieving full feeds or discharge from hospital, as appropriate) revealed no difference in ENT between groups. However, LOS was significantly longer in infants born at 34 to 36<sup>+6</sup> weeks GA compared with those born at  $\geq 37$  weeks GA. Analysis of corrected GA at ENT and LOS was performed in order to remove the effect of earlier birth. Infants born at 34 to 36<sup>+6</sup> weeks GA had a slightly lower corrected GA at ENT compared to those born at  $\geq 37$  weeks GA. However, corrected GA at hospital discharged was not significantly different between the two groups. There was a significantly higher risk (Fisher's exact test) of an episode of sepsis in those infants born at 34 to 36<sup>+6</sup> weeks GA compared to infants born at  $\geq 37$  weeks GA.

Neonatal Outcomes on Univariant Analysis	34 to 36 <sup>+6</sup> weeks GA (n=242)	≥37 weeks GA (n=226)	p-value
Time to full enteral feeds (days)	27 [6-283]	26 [4-163]	0.16
Length of hospital stay (days)	38 [7-346]	32 [11-349]	0.001
Corrected GA at time to full enteral feed (weeks)	40 [36-77]	42[38-61]	<0.0005
Corrected GA at time of hospital discharge (weeks)	42 [37-84]	42 [39-87]	0.017
*Patients with sepsis episode	83/242 (34%)	50/226 (22%)	0.004

**Table 7-4:** Univariate analysis of postnatal outcomes using Mann-Whitney (median [range]) and \*Fisher’s exact test.

#### 7.2.1.4 Cox Regression Analysis

Cox regression analysis was performed for infants delivered at ≥34 weeks in order to determine the effect of GA on ENT and LOS (Table 7-5). The model was adjusted for complexity and GA. Censoring was performed for death, not achieving full feeds and not being discharged from hospital as appropriate. Complex gastroschisis compared with simple gastroschisis significantly prolonged ENT (hazard ratio for reaching full feeds 0.28 [95% CI: 0.21-0.38], p<0.0005) and LOS (hazard ratio for hospital discharge 0.1 [95% CI: 0.23-0.42], p<0.0005). Lower birth GA was also associated with a longer ENT (hazard ratio for reaching full feeds 0.87 per week earlier birth [95% CI: 0.82-0.93], p<0.0005) and LOS (hazard ratio for hospital discharge 0.84 per week earlier birth [95% CI: 0.79-0.90], p<0.0005). In order to graphically illustrate these findings the patients were divided into categories of birth GA (≥34 to <35 weeks, ≥35 to <36 weeks, ≥36 weeks to <37 weeks, ≥37 to <38

weeks and  $\geq 38$  weeks) and a cox regression curve is shown for each category for ENT (Figure 7-3A) and LOS (Figure 7-3B).

Cox Regression Category	Impact on ENT	HR [95% CI] p-value	Impact on LOS	HR [95% CI] p-value
Complexity of gastroschisis	↑ with complex gastroschisis	0.28 [0.21-0.38] <0.0005	↑ with complex gastroschisis	0.1 [0.23-0.42] <0.0005
Gestational age (GA) at birth	↑ with ↓GA	0.87 [0.82-0.93] <0.0005	↑ with ↓GA	0.84 [0.79-0.90] <0.0005

**Table 7-5:** The effect of gestational age at birth and complexity of gastroschisis on ENT and LOS. Cox regression adjusted for complexity and gestational age and censored for death, not achieving full feeds and not being discharged from hospital. Data for gestational age at birth is per week earlier birth. HR = hazard ratio, CI = confidence interval.

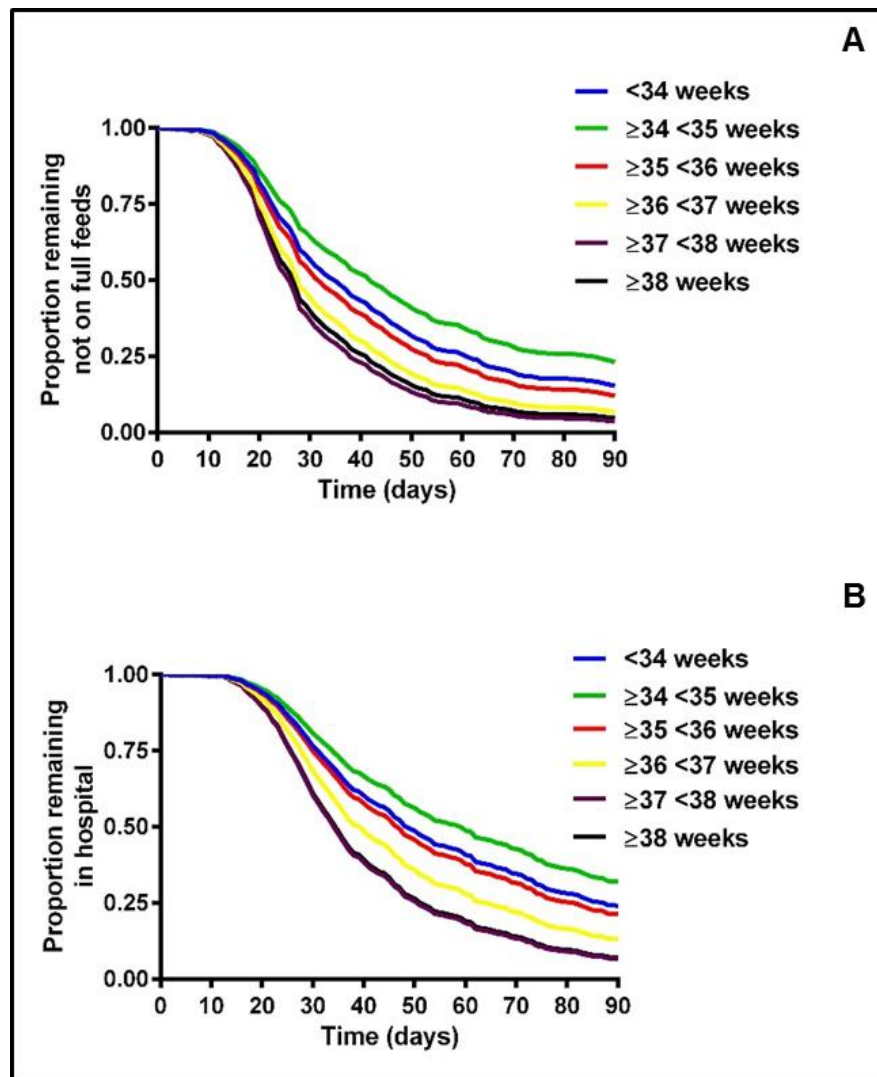


**Figure 7-3:** Cox regression of effect of gestational age category on: **A.** ENT and **B.** LOS.

As infants delivered at <37 weeks GA were delivered for obstetric concerns rather than elective early induction of labour, a post-hoc analysis was performed to determine whether the mode of labour onset for those infants born at 34 to 36<sup>+6</sup> weeks affected ENT or LOS. Spontaneous labour (14/92 complex patients, mean birth GA 35.8±0.1 weeks) was compared with (i) semi-elective early induction of labour/caesarean section (7/59 complex patients, mean GA at birth 36.2±0.1 weeks) and (ii) emergency (15/68 complex patients, mean GA at birth 35.5±0.1 weeks). The association of lower birth GA and longer ENT (hazard ratio for reaching full feeds 0.69 per week earlier birth [95% CI: 0.55-0.86], p=0.001) and LOS (hazard ratio for hospital discharge 0.70 per week earlier birth [95% CI: 0.55-0.89], p=0.003) remained significant for those infants born between 34 to 36<sup>+6</sup> weeks. However, the mode of labour onset had no significant effect on ENT (hazard ratio 1.0 [0.7-1.5])

p=0.86 for non-urgent compared with spontaneous, hazard ratio 0.9 [0.7-1.6] p=0.78 for emergency), or on LOS (hazard ratio 0.9 [0.6-1.3] p=0.61 for non-urgent compared with spontaneous, hazard ratio 1.0 [0.7-1.6] p=0.91 for emergency).

Analysis was also performed for mode of Labour onset in infants born at  $\geq 37$  weeks GA comparing spontaneous labour (4/48 complex patients, mean GA at birth  $37.6 \pm 0.09$  weeks) with planned induction of labour/caesarean section (15/148 complex patients, mean GA at birth  $37.6 \pm 0.04$  weeks), and emergency delivery (2/6 complex patients, mean GA at birth  $37.8 \pm 0.19$  weeks). There was no effect of lower GA on ENT (hazard ratio per week 1.0 [95% CI:0.8-1.3], p=0.96) or LOS (hazard ratio per week 1.0 [95% CI:0.7-1.4], p=0.78) in the  $\geq 37$  weeks GA group.

Additionally, mode of delivery had no impact on ENT (hazard ratio 0.64 [0.25-1.7] p=0.36 for non-urgent induction/Caesarean section compared with spontaneous, hazard ratio 0.52 [0.21-1.29] p=0.16 for emergency), or on LOS (hazard ratio 0.6 [0.24-1.58] p=0.31 for non-urgent induction/Caesarean section compared with spontaneous, hazard ratio 0.5 [0.22-1.4] p=0.2 for emergency).

#### ***7.2.1.5 Timing of Delivery and Impact on Macroscopic Bowel Wall Inflammation***

Bowel exposure to amniotic fluid has been hypothesised to cause bowel inflammation (Morrison et al., 1998) and therefore later birth GA may be associated with increased macroscopic bowel inflammation due to prolonged exposure to amniotic fluid. The visual appearance of bowel at birth was documented in 425 (83%) infants of whom 137 (32%) were reported to demonstrate bowel inflammation/serosal peel. There was no significant difference in birth GA between infants with inflammation/peel (GA median 36.6, range [30.0-41.3] weeks) and those without inflammation/peel (GA 36.9 [25.0-39.0] weeks, P=0.24). There was a small, but significantly longer time to full feeds 31 [6-1103] days vs. 27 [4-386] days, P=0.008) in those infants with inflammation/peel, but no significant difference in LOS (42.5 [8-349] days vs. 35 [5-386] days, P=0.06, Table 7-6).

Neonatal Outcome	With Bowel Inflammation / Serosal Peel	Without Bowel Inflammation / Serosal Peel	p-value
Gestational Age at birth (weeks)	36.6 [25.0-39.0]	36.9 [25.0-39.0]	0.24
Time to full enteral feeds (days)	31 [6-1103]	27 [4-386]	0.008
Length of Hospital Stay (days)	42.5 [8-349]	35 [5-386]	0.06

**Table 7-6:** Comparison of postnatal outcomes between those infants with and without bowel inflammation/serosal peel using Mann-Whitney (median [range]).

## 7.2.2 Maternal Antenatal Corticosteroid Administration and Impact on Infant Outcomes

### 7.2.2.1 Demographics

From the complete 3 centre dataset of 510 infants with linked fetal and neonatal data, 10 infants were excluded as it was not possible to ascertain whether maternal antenatal corticosteroids had been administered or not. Of the 500 infants included in the corticosteroid analysis, 431 (GA at birth median 37, range [31-41] weeks) did not receive maternal antenatal corticosteroids whereas 69 (GA at birth 34 [25-38] weeks) did receive maternal antenatal corticosteroids. Of those infants who received maternal antenatal corticosteroids, 56 received a full single course and 13 received a partial single course. The numbers of infants who received and did not receive antenatal corticosteroids were evenly distributed across the study centres (Table 7-7). The timing of antenatal corticosteroid administration varied across the group, 2 infants received corticosteroids <24 hours before birth, 42 infants between >24 hours and ≤7 days before birth, 23 infants at >7 days before birth and for 2 infants the timing of administration was not known. Antenatal corticosteroids were administered for the following reasons: premature labour (n=15); threatened premature labour (n=18); elective caesarean section delivery at 36 weeks GA (n=3); planned delivery



at <37 weeks GA for bowel dilatation (n=20); premature delivery for obstetric reasons (n=10) or unknown (n=3). As expected, infants who received antenatal corticosteroids were born at a significantly earlier GA and lower birth weight than those infants who did not receive antenatal corticosteroids (Table 7-7).

	Maternal Antenatal Corticosteroids		
	No Steroids	Steroids	
<b>Study Population:</b>			
Total patients included (n=500)	431 (86%)	69 (14%)	
Centre 1 (n=150)	128 (85%)	22 (15%)	
Centre 2 (n=122)	103 (84%)	19 (16%)	
Centre 3 (n=228)	200 (88%)	28 (12%)	
<b>Birth Demographics:</b>			<b>p-value</b>
Birth gestational age (weeks)	37.0 [30.6-41.3]	34.0 [25.1-38.3]	<0.0001
Birth weight (g)	2500 [220-3884]	1960 [540-3380]	<0.0001
Male	217	36	0.99
Female	214	33	

**Table 7-7:** Gastroschisis antenatal maternal corticosteroid study population and demographics.

### **7.2.3 Postnatal Outcomes**

#### ***7.2.3.1 Univariate analysis***

A significantly higher proportion of complex gastroschisis infants (22%) received maternal antenatal corticosteroids compared with simple gastroschisis infants (12%,  $p=0.03$ ). Table 7-8 indicates the number of complex and simple gastroschisis infants who received maternal antenatal corticosteroids, the reason for classification as complex and neonatal outcomes. Univariate analysis showed infants who received maternal antenatal corticosteroids had a significantly longer time to ENT and LOS than those who did not receive maternal antenatal corticosteroids. This is likely due to the higher proportion of complex patients and lower gestational age and birthweight in the group who received corticosteroids.

	No Steroids	Steroids	p-value
<b>*Simple and complex gastroschisis patients:</b>			
Simple (n=424, 85%)	372 (88%)	52 (12%)	0.03
Complex (n=76, 15%)	59 (78%)	17 (22%)	
Atresia (n=42)	30	12	
Necrosis (n=28)	22	6	
Perforation (n=14)	13	1	
Stenosis (n=8)	7	1	
<b>Neonatal outcomes in univariate analyses:</b>			
**Time to first enteral feed (days)	12 [2-101]	13.5 [2-186]	0.58
**Time to full enteral feeds (days)	26 [4-283]	30 [2-590]	0.01
**Length of hospital stay (days)	35 [7-349]	46 [20-346]	0.003
Deaths (n=23, 5%)	18 (4%)	5 (7%)	0.23

**Table 7-8:** Gastroschisis complexity, corticosteroid administration and postnatal outcomes. \*>1 pathology in 9 complex patients. Univariate analysis was \*\*Mann-Whitney (median [range]) and Fisher's exact tests.

### 7.2.3.1.1 *Multivariate Analysis*

Cox regression analysis was performed in order to account for likely confounders within the univariate analysis (Table 7-9). The Cox model was adjusted for complex gastroschisis, birth GA, source hospital and antenatal corticosteroid administration. Censoring was performed for death, not achieving full feeds and not being discharged from hospital. Analysis revealed that maternal antenatal corticosteroid administration was not associated with faster time to ENT (hazard ratio reaching full feeds 1.0 [95% CI: 0.8-1.4],  $p=0.8$ ) or LOS (hazard ratio for hospital discharge 1.1 [95% CI: 0.7-1.5],  $p=0.8$ ) (Figure 7-4A and B). Complex gastroschisis significantly increased ENT (hazard ratio 0.3 [95% CI: 0.2-0.4],  $p<0.001$ ) and LOS (hazard ratio 0.3 [95% CI: 0.2-0.4],  $p<0.001$ ) (Figure 7-4C and D) compared to simple gastroschisis infants. Conversely, later birth GA significantly decreased ENT (hazard ratio for reaching full feeds 1.1 per week of later birth [95% CI: 1.1-1.2],  $p<0.001$ ) and LOS (hazard ratio for hospital discharge 1.2 per week of later birth [95% CI: 1.1-1.3],  $p<0.001$ ). Source hospital had no effect on ENT (comparing against centre 3: centre 1 hazard ratio 1.2 [95% CI: 0.9-1.5],  $p=0.2$  and centre 2 hazard ratio 1.2 [95% CI: 1.0-1.5],  $p=0.1$ ) but had a significant effect on LOS (comparing against centre 3: centre 1 hazard ratio 1.3 [95% CI: 1.0-1.6],  $p=0.07$  and centre 2 hazard ratio 1.5 [95% CI: 1.2-1.9],  $p=0.001$ ) possibly due to a differing feeding and/or discharge policy in Centre 3.

Cox Regression Category	Impact on ENT	HR [95% CI] p-value	Impact on LOS	HR [95% CI] p-value
Maternal antenatal corticosteroids	No effect	1.0 [0.8-1.4] 0.8	No effect	1.1 [0.7-1.5] 0.8
Complexity of gastroschisis	↑ with Complex gastroschisis	0.3 [0.2-0.4] <0.001	↑ with Complex gastroschisis	0.3 [0.2-0.4] <0.001
Gestational age (GA) at birth	↓ with ↑ GA	1.1 [1.1-1.2] <0.001	↓ with ↑ GA	1.2 [1.1-1.3] <0.001

**Table 7-9:** The effect of antenatal maternal corticosteroids, complexity of gastroschisis and gestational age at birth on ENT and LOS. Cox regression adjusted for complex gastroschisis, birth GA, source hospital and antenatal corticosteroid administration and censored for death, not achieving full feeds and not being discharged from hospital as appropriate. Data for gestational age at birth is per week later birth. HR = hazard ratio, CI = confidence interval.

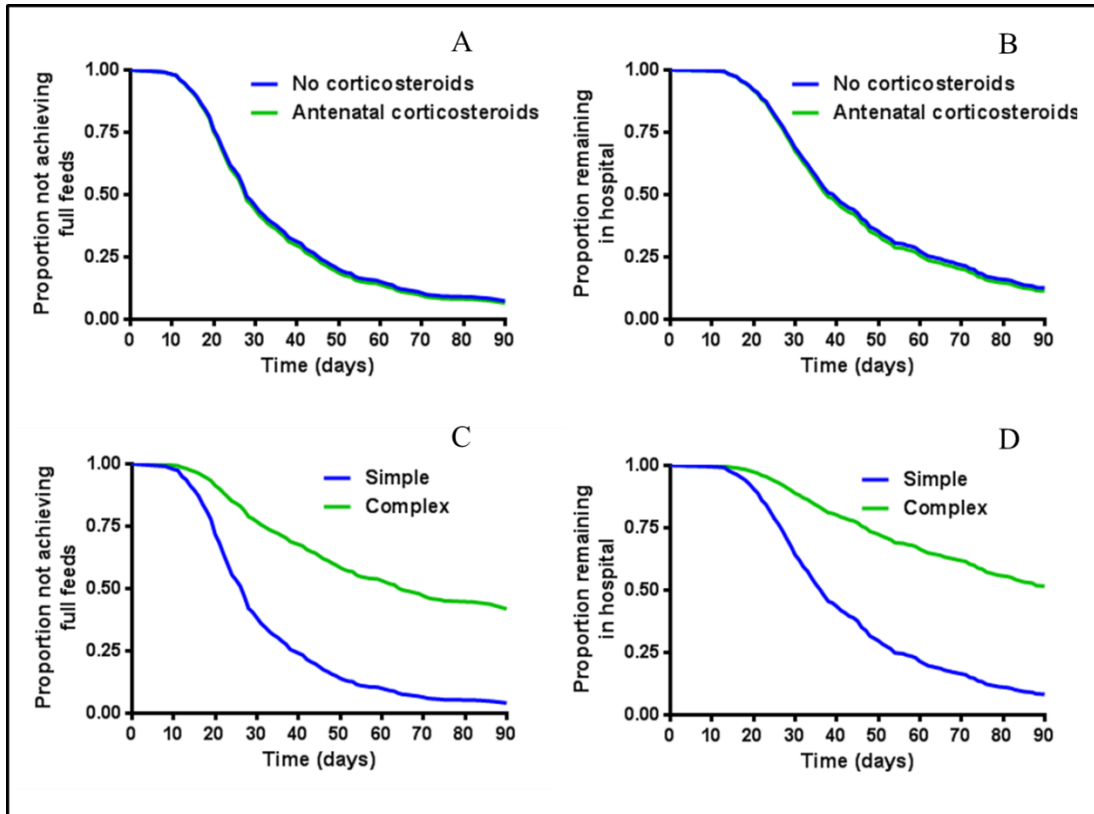


**Figure 7-4:** Cox regression analysis of effect of maternal antenatal corticosteroids on **A.** ENT and **B.** LOS and effect of gastroschisis complexity on **C.** ENT and **D.** LOS.

### 7.2.3.2 Post-hoc Exploratory Analyses

To determine whether maternal antenatal corticosteroids administration was associated with any effect on postnatal gastroschisis outcomes in any patient subset, further exploratory analyses were performed.

As the therapeutic effect of maternal antenatal corticosteroids may have been impacted by an incomplete course, the analysis was repeated only including infants who received a complete course (n=56), which again showed no difference in ENT (hazard ratio 0.9 [95% CI: 0.4-1.2], p=0.4) or LOS (hazard ratio 0.9 [95% CI: 0.6-1.2], p=0.4).

Extreme prematurity or later birth GA (as very few patients with late birth GA received maternal antenatal corticosteroids) may influence results therefore to remove this potential confounder only patients born between 31<sup>+0</sup> to 36<sup>+6</sup> weeks gestation were included in the analysis (n=207 did not receive corticosteroids, n=65

received corticosteroids), which showed no effect on ENT (hazard ratio 0.9 [95% CI: 0.6-1.2],  $p=0.4$ ) or LOS (hazard ratio 1.2 [95% CI: 0.8-1.7],  $p=0.4$ ). This was also repeated including only those infants born at 34 weeks GA or above ( $n=44$  received steroids,  $n=420$  did not). There was no association between administration of antenatal corticosteroids and ENT (hazard ratio 1.2 [95% CI: 0.7-1.5],  $p=0.9$ ) or LOS (hazard ratio 1.0 [95% CI: 0.7-1.5],  $p=1.0$ ). Those born at  $<34$  weeks were also analysed separately ( $n=25$  with steroids,  $n=11$  no steroids), again with no association either for ENT (hazard ratio 1.0 [95% CI: 0.4-2.2],  $p=0.9$ ) or LOS (hazard ratio 0.7 [95% CI: 0.3-1.6],  $p=0.4$ )

Maternal antenatal corticosteroid administration may affect the time to start feeding, however, analysis of whether antenatal corticosteroids reduced time to first enteral feed, again showed no difference (hazard ratio 1.0 [95% CI: 0.7-1.5],  $p=0.8$ ).

As the intestinal function of infants with complex gastroschisis may be adversely affected by concomitant intestinal pathologies (atresia, stenosis, necrosis and perforation) an analysis including only simple gastroschisis patients ( $n=372$  did not receive corticosteroids  $n=52$  received corticosteroids) was performed. Similarly this analysis showed no difference in ENT (hazard ratio 1.0 [95% CI: 0.7-1.4],  $p=0.8$ ) or LOS (hazard ratio 1.0 [95% CI: 0.7-1.5],  $p=1.0$ ).

To determine whether the timing of antenatal corticosteroid administration prior to birth was an important factor, only infants who received corticosteroids between  $>24$  hours and  $\leq 7$  days ( $n=42$ ) before birth were included also showing no effect on time to ENT (hazard ratio 1.0 [95% CI: 0.7-1.5],  $p=0.9$ ) or LOS (hazard ratio 1.0 [95% CI: 0.7-1.6],  $p=0.8$ ). Additionally, only infants who received corticosteroids at  $>7$  days ( $n=23$ ) before birth were analysed, which also showed no effect on ENT (hazard ratio 1.1 [95% CI: 0.7-1.7],  $p=0.7$ ) or LOS (hazard ratio 1.0 [95% CI: 0.5-1.7],  $p=0.9$ ).

Finally, to investigate whether changes in neonatal practices over the 22 year study period influenced gastroschisis outcomes, the year of birth was added into the Cox regression model. This again showed no difference in ENT (hazard ratio 1.0 per year

later birth [95% CI: 1.0-1.0],  $p=0.5$ ) or LOS (hazard ratio 1.0 per year later birth [95% CI: 1.0-1.0],  $p=0.6$ ).

## **7.3 Discussion**

### **7.3.1 Timing of Delivery and Impact on Postnatal Outcomes**

The data from this international multicentre retrospective cohort study refuted the original study hypothesis and shows a significant association between earlier birth GA and prolonged ENT and LOS. These findings were independent of gastroschisis complexity. As these data only include infants with gastroschisis it is not possible to determine whether these associations are due to a general effect of prematurity or specific to gastroschisis. Univariate analysis of corrected GA at time of ENT suggests that delivery at 34 to 36<sup>+6</sup> weeks GA confers a small improvement in neonatal gut function. However, this is not translated into a faster time to achieve ENT. Furthermore, delivery at 34 to 36<sup>+6</sup> weeks GA did not reduce the corrected GA at hospital discharge and regression analysis showed these infants spend longer in hospital. The prolonged time taken to ENT and LOS places infants delivered at <37 weeks GA at increased risk of sepsis as indicated by the nearly doubled (32 vs. 17%) risk of blood-culture positive sepsis in the 34 to 36<sup>+6</sup> week GA group. Additionally, visual evidence of bowel inflammation/serosal peel was not associated with later GA at birth or duration of LOS but there was a small, but significantly longer time to ENT

### **7.3.2 Relationship between Maternal Antenatal Corticosteroid Administration and Gastroschisis Outcomes**

Again the of linked fetal and neonatal data from this international multicentre retrospective cohort study contested the original study hypothesis and showed that maternal antenatal corticosteroid administration was not associated with any effect, positive or negative, on ENT or LOS. Post-hoc exploratory analysis was performed in order to determine if there were any patient subsets in which corticosteroids were beneficial. These analyses included effect on time to first enteral feed, timing of maternal corticosteroid administration prior to birth, and exclusion of factors that



might skew the data such as extreme prematurity, complex gastroschisis and those who did not receive a full course of corticosteroids. However, none of these analyses were associated with any differences in gastroschisis infant outcomes. These data suggest, contrary to the published literature from animal studies and a single abstract in humans, that a single course of maternal antenatal corticosteroids with the aim of decreasing intestinal inflammation and improving intestinal maturation does not prevent or reverse the bowel changes that cause GRID.

### **7.3.3 Impact of Other Factors on Gastroschisis Outcomes**

In keeping with previous published studies complex gastroschisis (Bradnock et al., 2011, Bergholz et al., 2014) was shown to be associated with a significant increase in ENT and LOS. This is unsurprising given that atresia, perforation, stenosis and necrosis all requires surgical intervention and have a significant concomitant impact on bowel function. Source hospital had no impact on ENT but LOS was prolonged in one centre likely due to differing management and discharge practices. Interestingly, these data showed that changes in neonatal practices over the 22 year study period had no impact on postnatal gastroschisis outcomes.

### **7.3.4 Timing of Delivery Review of the Literature**

Optimal timing for elective delivery of gastroschisis fetuses remains controversial. As previously stated there is conflicting evidence both for (Gelas et al., 2008, Serra et al., 2008, Moore et al., 1999, Moir et al., 2004) and against (Maramreddy et al., 2009, Youssef et al., 2015, Cain et al., 2014, Logghe et al., 2005, Charlesworth et al., 2007) elective delivery at <37 weeks GA (Table 7-10). The majority of studies are small and retrospective in nature. However, there are two prospective studies (Serra et al., 2008, Moir et al., 2004) and one randomized control trial (Logghe et al., 2005) in the literature. The prospective studies compared outcomes from patients delivered prospectively at 34-35 weeks GA with retrospective controls. The numbers were small including; 13 prospective and 10 retrospective infants in the Serra, et al study and 13 prospective and 14 retrospective infants in the Moir, et al study, but both studies showed a significant reduction in ENT and LOS. However, due to the small cohort size, partial retrospective nature of the studies and lack of randomisation it is

not possible to assess true validity of these results. The only randomised control trial (Logghe et al., 2005) included one treatment centre and recruited 42 gastroschisis pregnancies that were randomly allocated to either elective delivery at <36 weeks GA or continuation of pregnancy to full term with spontaneous delivery. The study showed no benefit from early delivery. However, due to early spontaneous labour in the control group there was little difference in birth GA between the early delivery group (35.8 weeks) and controls (36.7 weeks) hence significantly larger numbers are required to determine the true impact of birth GA on postnatal outcomes.

Study	Number of Centres	Study Inclusion Period, Number of Patients	Study Type	Study Groups	Outcome Measures	Impact on Primary Outcome	Impact on Secondary Outcome	Comments
*Gelas et al., 2008	1	1990-2004 n=69	Retrospective cohort	<b>Group 1 (n=33):</b> 1990-1997 delivery at any time <b>Group 2 (n=36):</b> 1997-2004, elective delivery at 35 weeks by c-section + antenatal steroids	<b>Primary outcome:</b> -Initiation of enteral feeds <b>Secondary outcome:</b> -Duration of parenteral nutrition -Length of hospital stay	<b>Group 2 showed:</b> Faster initiation of first feeds (p<0.0001)	<b>No difference between groups for:</b> -Duration of parenteral nutrition -Length of hospital stay	-Authors support elective delivery at 35 weeks -Changes in group 2 not limited to timing of delivery also included mode of delivery and antenatal steroids
*Seira et al., 2007	1	1994-2004 n=23	Prospective cohort versus retrospective cohort	<b>Prospective group (n=13):</b> Prospective, 1999-2004, elective delivery at 34 weeks + corticosteroids <b>Retrospective group (n=10):</b> Retrospective, 1994-1999 delivery at anytime	<b>Primary outcome:</b> -Initiation of enteral feeds -Length of hospital stay	<b>Prospective group showed:</b> -Faster initiation of first feeds (p=0.0012) -Shorter length of hospital stay (p=0.016)		-Authors support elective preterm delivery -Changes in prospective group management not limited to timing of delivery but also included antenatal steroids
*Moore et al., 1999	1	1951-1999 n=77	Retrospective cohort	<b>Group 1 (n=44):</b> Born after spontaneous labour either vaginal or c-section <b>Group 2 (n=33):</b> Elective early c-section (GA not specified)	<b>Primary outcome:</b> -Presence of serosal 'peel' at birth <b>Secondary outcome:</b> -Presence of complex gastroschisis	<b>Group 1:</b> -All 44 patients had presence of 'peel' <b>Group 2:</b> -None of the 33 infants had 'peel'	<b>Group 1:</b> -19.1% had complex gastroschisis <b>Group 2:</b> -3% had complex gastroschisis	-Authors conclude preterm delivery without labour onset prevented 'peel' and complex gastroschisis. -No correlation with any other infant outcome measure discussed

Study	Number of Centres	Study Inclusion Period, Number of Patients	Study Type	Study Groups	Outcome Measures	Impact on Primary Outcome	Impact on Secondary Outcome	Comments
*Moir et al., 2004	1	Study period not specified n=27	Prospective cohort versus retrospective cohort	<b>Prospective group (n=13):</b> - Weekly antenatal monitoring, delivery if concerns at >30 weeks by c-section + corticosteroids <b>Retrospective group (n=14):</b> Minimal monitoring, spontaneous labour	<b>Primary outcome:</b> - Time to full enteral feeds <b>Secondary outcome:</b> - Length of hospital stay	<b>Prospective group showed:</b> - Shorter time to full feeds (p=0.039) NB: Group 1 mean GA at birth 34.2±2.4 weeks Group 2 mean GA at birth 37.7±1.8 weeks	<b>Prospective group showed:</b> - Shorter length of hospital stay (p=0.028)	- Authors conclude elective preterm delivery improves infant outcomes - Changes in prospective group management not limited to timing of delivery but also included mode of delivery and antenatal steroids
*Maramreddy et al., 2009	1	1989-2007 n=49	Retrospective cohort	<b>Preterm infants (n=24):</b> Mean GA at birth 33±2 (26-36) weeks <b>Term infants (=12):</b> Mean GA at birth 38±1 (37-40) weeks	<b>Primary outcome:</b> - Time to full enteral feeds <b>Secondary outcome:</b> - Length of hospital stay	<b>Preterm group showed:</b> - Longer time to full feeds (p=0.002)	<b>Preterm group showed:</b> - Longer length of hospital stay (p=0.001)	Authors do not support elective preterm delivery - Preterm group included extreme prematurity so reanalysed excluding <34 weeks (n=15) results remained the same Authors do not support elective preterm delivery - No other infant outcome measure assessed
Youssef et al., 2015	Canadian national database	2005-2013 n=692	Retrospective cohort	<b>Regression modelling:</b> excluding infants born at <29 weeks GA and >40 weeks GA	<b>Primary outcome:</b> - Severe bowel matting	Linear regression showed correlation between ↑GA and ↓ bowel matting		

Study	Number of Centres	Study Inclusion Period, Number of Patients	Study Type	Study Groups	Outcome Measures	Impact on Primary Outcome	Impact on Secondary Outcome	Comments
Cain et al., 2014	Florida database	1998-2009 (n=324)	Retrospective cohort	<b>Infants born at weeks GA:</b> <34 weeks (n=26) 34-36 weeks (n=131) 37-38 weeks (n=135) >38 weeks (n=32)	<b>Primary outcome:</b> -Adverse pregnancy outcome (jaundice and respiratory distress) <b>Secondary outcome:</b> -Length of hospital stay -Medical costs	<b>37-38 week GA showed:</b> Decreased adverse pregnancy outcomes compared to earlier delivery (p<0.001)	<b>↑ GA associated with ↓ in both:</b> -Length of hospital stay -Medical costs	Authors do not support elective preterm delivery
Logghe et al., 2005	1	1995-1999 n=42	Randomised controlled trial	<b>Elective delivery at 36 weeks (n=21)</b> Mean GA at birth 35.8 weeks <b>Await spontaneous labour (n=21)</b> Mean GA at birth 36.7 weeks	<b>Primary outcome:</b> -Time to full enteral feeds -Length of hospital stay <b>Secondary outcome:</b> -Primary defect closure	No significant difference between the groups for either primary outcome measure	No difference in rates of primary closure between the groups	-Authors concluded no significant benefit from elective preterm delivery -Little difference in terms of mean GA at birth between the groups
Charlesworth et al., 2007	1	1993-2005 n=110	Retrospective cohort	Divided into delivery groups <b>Group A (n=18):</b> <35 weeks <b>Group B (n=33):</b> 35-37 weeks <b>Group C (n=59):</b> >37 weeks	<b>Primary outcome:</b> -Time to full enteral feeds <b>Secondary outcome:</b> - Length of hospital stay	<b>Group A showed:</b> -Longest time to achieve full enteral feeds (p=0.05)	<b>Group A showed:</b> -Longest length of hospital stay (p<0.01)	Authors conclude: -No evidence early birth improves outcomes -Low birth weight associated with worst outcomes and a better predictor of prognosis

**Table 7-10:** Summary of literature investigating effect of timing of delivery on gastroschisis infant outcomes. \*Indicates studies supporting elective preterm delivery. GA=gestational age.

### **7.3.5 Hypothesised Reason for Prolonged Postnatal Outcomes at Lower Birth Gestational Age**

These data suggest that earlier delivery marginally improves corrected GA at time of ENT but has no impact on absolute duration of ENT and prolongs absolute LOS. Additionally, visual evidence of bowel inflammation/peel at birth was not related to later GA at birth. Therefore, GRID in gastroschisis is likely to be more multifactorial than simple duration of bowel exposure to amniotic fluid. As such, these data suggest that a longer time in utero is more protective from prolonged use of PN or hospital stay and risk of developing sepsis. Furthermore, the positive effects of fetal bowel maturation in the later stages of pregnancy appear to have a greater influence on postnatal outcomes than the detrimental effects of prolonged amniotic fluid exposure.

### **7.3.6 Hypothesised Reason for Lack of Effect from Maternal Antenatal Corticosteroid Administration**

The composition of amniotic fluid changes significantly after 25 weeks gestation with increases in creatinine, urea, enteric enzymes and bile acids, and reduction in sodium, chloride and osmolality (Underwood et al., 2005). These changes in amniotic fluid composition coincide with increases in bowel wall inflammation in fetuses with gastroschisis in the third trimester (Tibboel et al., 1986). As such, the lack of effect on ENT and LOS within this cohort may be due to the administration of maternal antenatal corticosteroids occurring too late in gestation. Potentially, earlier administration of corticosteroids at the start of the third trimester may act to prevent the onset of bowel inflammation and in turn the gastrointestinal damage leading to intestinal dysfunction.

In addition, corticosteroids are quickly removed from the systemic circulation and therefore the therapeutic effectiveness of antenatal corticosteroids may have been impeded by the short lived effect. Although corticosteroids given to the mother are readily available to the fetus (Della Torre et al., 2010), animal experiments have shown that the peak maternal concentration following administration occurs after 15 minutes and declines rapidly over 3 hours whilst the peak fetal concentration occurs

after 1 hour and becomes undetectable at 8 hours (Schwab et al., 2006). Interestingly, delivery of corticosteroids via the maternal route provides a longer half-life in the fetus than direct fetal administration (Moss et al., 2003).

Considering both the uncertainty of the optimal timing for administration and the short half-life of corticosteroids, it may be that multiple courses throughout the third trimester are required in order to exert a prolonged therapeutic anti-inflammatory or maturational effect. Multiple courses of antenatal corticosteroids are controversial and have been considered for otherwise normal pregnancies at risk of preterm birth that remain pregnant for a further 7 to 14 days after initial antenatal corticosteroid administration. Current research is lacking conclusive evidence for the benefit and safety of multiple antenatal corticosteroid courses (Murphy et al., 2008, Asztalos, 2012, Asztalos et al., 2013), which may be associated with adverse events such as low birth weight, neurological developmental impairment (Kanagawa et al., 2006, Church et al., 2012) and increased risk of developing type 2 diabetes mellitus and cardiovascular disease later in life (Asztalos, 2012, Norberg et al., 2013). Due to this uncertainty and lack of proven benefit it would be difficult to develop a trial involving administration of multiple courses of maternal antenatal corticosteroids in gastroschisis pregnancies unless more data was available from relevant animal models.

Finally, the cause of GRID may be more complicated than simply inflammation. Intestinal dysfunction may result from bowel morphological changes that occurred from abnormal serosal exposure to amniotic fluid growth factors or lack of mechanical constraint from the abdominal cavity. Alternatively, inflammation may have been caused by mechanical compression at the exit point from the small abdominal wall defect resulting in ischaemic intestinal changes. As such, further research is required to determine if antenatal corticosteroid administration could be beneficial in improving GRID and in turn infant outcomes.

### **7.3.7 Limitations of the Study**

These data were collected retrospectively without control over the method/timing of delivery or the administration (dosage and timing) of antenatal corticosteroids and

the general antenatal and postnatal management were not standardised. Hence, the cohort included infants delivered on a semi-urgent or emergency basis due to maternal or fetal concerns at <37 weeks GA, infants delivered by spontaneous labour at <37 weeks GA and infants delivered as per standard elective induction of labour at  $\geq 37$  weeks GA. Therefore comparisons between infants could be affected by the overall health of the neonates who were delivered early for maternal or fetal concerns and who could conceivably have poorer outcomes as a result. In addition, administration of maternal antenatal corticosteroids occurred in patients with threatened preterm delivery or those who had maternal or fetal concerns resulting in early delivery in order to improve lung maturation and not for the purpose of bowel maturation or anti-inflammatory action. As such, the antenatal corticosteroid group were born at an earlier GA, which may have resulted in potentially worse infant outcomes. To account for these factors the birth GA was adjusted for in the analysis. Additionally, a posthoc analysis removing extreme outliers was performed through inclusion of patients born between  $31^{+0}$  and  $36^{+6}$  weeks gestation. Also, the definition of ENT was not protocolised and LOS may be affected by socio-economic factors surrounding young maternal age. Finally, there may be other sources of bias and confounders that were not considered or could not be accounted for in this study.

### **7.3.8 Strength of the Study**

These data consistently show lower birth GA to be associated with prolonged ENT and LOS and no associated effect of antenatally corticosteroids on postnatal outcomes even following detailed post-hoc analysis. These data were collected from two UK and one Canadian tertiary referral centres therefore the data includes variation in antenatal and neonatal management improving the generalisability of the study to other centres. Finally, this retrospective cohort study contains over 500 patients forming one of the largest published data sets to date.

## **7.4 Conclusion**

Similarly to other tested but failed therapeutic strategies for improving postnatal intestinal function in gastroschisis including antenatal amniotic fluid exchange (Midrio et al., 2007, Burc et al., 2004, Demir et al., 2013) and postnatal prokinetics



(Curry et al., 2004), these data showed; (i) early delivery does not appear to reduce bowel damage or improve bowel function and is associated with prolonged ENT and LOS and (ii) no association between maternal antenatal corticosteroids and improved ENT or LOS in gastroschisis infants. As such, these data do not support elective delivery at <37 weeks GA or the routine administration of maternal antenatal corticosteroids as strategies to improve postnatal outcomes and enteral feeding. This study was not designed to identify antenatal findings that would predict worse postnatal outcomes therefore timing of delivery for gastroschisis fetuses with evidence of maternal or fetal compromise should continue to be directed by clinical indication rather than a specific target gestational age. Further investigation is required into the cause of gastroschisis bowel morphological changes as described in Chapter 6 in order to develop a therapy that could prevent such changes from occurring.

## **Chapter 8: Does Antenatally Detected Bowel Dilatation Predict Gastroschisis Infant Outcomes?**

### **8.1 Introduction**

The ability to predict gastroschisis postnatal outcomes based on antenatal ultrasound markers would greatly aid prenatal counselling and inform clinical management both antenatally and postnatally. It would be of particular benefit if fetuses with impending bowel necrosis secondary to closing gastroschisis or a tight abdominal wall defect could be detected before extensive ischaemic damage develops enabling bowel salvage by urgent antenatal intervention (early delivery or fetoscopic widening of the tight defect ring). Intra-abdominal bowel dilatation (IABD) has been found in several studies to be associated with complex gastroschisis (Huh et al., 2010, Houben et al., 2009, Ghionzoli et al., 2012, Nick et al., 2006, D'Antonio et al., 2015, Goetzinger et al., 2014, Contro et al., 2010) and bowel dilatation has been hypothesised to represent poorly functioning bowel in cases of simple gastroschisis resulting in prolonged ENT and LOS (Langer et al., 1993). However, some studies have also found IABD not to be associated with complex gastroschisis (Mears et al., 2010, Badillo et al., 2008). Conversely, Extra-abdominal bowel dilatation (EABD) has been considered by some to be a normal occurrence in gastroschisis (Huh et al., 2010, Contro et al., 2010) and not to be predictive of either complex gastroschisis or outcomes in simple gastroschisis (Badillo et al., 2008, Mears et al., 2010). As such, some clinicians instigate early delivery based on the antenatal findings of IABD with the aim to prevent development of bowel necrosis from closing gastroschisis. However, the data relating to IABD and EABD is limited due to the small number of patients included in most studies and little is known regarding the predictive value of combined IABD and EABD with complex gastroschisis and infant outcomes.

Antenatal intra-abdominal bowel dilatation is hypothesised to be predictive of complex gastroschisis and poor infant outcomes. The aim of this study is to determine the association of IABD and EABD with (i) complex gastroschisis and (ii) infants outcomes using ENT and LOS as surrogate markers of outcome.

## 8.2 Results

Of the 246 gastroschisis infants included from the London centres, 110 had IABD detected antenatally (including gastric dilatation), which resolved in 18 fetuses (16 simple gastroschisis, 2 complex gastroschisis) during the antenatal period after a median 1, range [1-3] ultrasound scans. The remaining 92 fetuses had persistent IABD that remained detectable at the last antenatal scan before birth, of whom 68 (74%) were simple gastroschisis and 24 (26%) complex gastroschisis giving a positive predictive value (PPV) for detecting complex gastroschisis of 26% (Table 8-1). IABD was detected prior to 30 weeks GA in 34 fetuses of whom 21 were simple gastroschisis and 13 complex gastroschisis giving a PPV for detecting complex gastroschisis of 38% (Table 8-1). Of the 136 fetuses who never had antenatal IABD detected, 130 were simple gastroschisis and 6 were complex gastroschisis (1 perforation, 3 atresia, 2 necrosis) giving a negative predictive value (NPV) for detecting complex gastroschisis of 96% (Table 8-1).

EABD was detected in 65 fetuses, which resolved in 7 fetuses after 1 [1-3] scans and was persistent to the last antenatal scan before delivery in 58, fetuses of whom 46 were simple gastroschisis and 12 complex (9 atresia, 2 necrosis and 1 stenosis, PPV 21%, Table 8-1). The detection of EABD prior to 30 weeks GA gave a higher PPV of 64%. EABD was never detected in 19 (59%) complex gastroschisis giving an NPV for detecting complex gastroschisis of 90% (Table 8-1).

Combined IABD and EABD (combined dilatation) was present in 22 fetuses of whom 14 were simple gastroschisis and 8 complex (7 atresia, 1 necrosis). When combined dilatation was present prior to 30 weeks GA the PPV for detecting complex gastroschisis was relatively high at 75% (Table 8-1). Additionally, IABD with collapsed extra-abdominal bowel loops was detected in 3 patients all of whom were complex gastroschisis (1 atresia, and 2 necrosis) and in all of whom these findings were detectable prior to 30 weeks GA.

All Intra-Abdominal Bowel Dilatation (IABD)					
Group (n=total in group)	IABD at Last Scan Number (% of group)	IABD at $\geq 30$ to $\leq 34$ Weeks GA Number (% of group)	IABD at $< 30$ Weeks GA Number (% of group)	Resolved IABD Number (% of group)	Never had IABD Number (% of group)
Simple n=214	68 (32%)	47 (22%)	21 (10%)	16 (7%)	130 (61%)
Complex n=32	24 (75%)	21 (66%)	13 (41%)	2 (6%)	6 (19%)
PPV or NPV	26% PPV	31% PPV	38% PPV	89% NPV	96% NPV
All Extra-Abdominal Bowel Dilatation (EABD)					
Group (n=total in group)	EABD at Last Scan Number (% of group)	EABD at $\geq 30$ to $\leq 34$ Weeks GA Number (% of group)	EABD at $< 30$ Weeks GA Number (% of group)	Resolved EABD Number (% of group)	Never had EABD Number (% of group)
Simple n=214	46 (21%)	28 (13%)	4 (2%)	6 (3%)	162 (76%)
Complex n=32	12 (38%)	11 (0.34%)	7 (22%)	1 (3%)	19 (59%)
PPV or NPV	21% PPV	28% PPV	64% PPV	86% NPV	90% NPV
Combined Intra and Extra-Abdominal Bowel Dilatation (Combined)					
Group (n=total in group)	Combined at Last Scan Number (% of group)	Combined at $\geq 30$ to $\leq 34$ Weeks GA Number (% of group)	Combined at $< 30$ Weeks GA Number (% of group)	Resolved Combined Number (% of group)	Never had Combined Number (% of group)
Simple n=214	14 (26%)	13 (6%)	1 (0.5%)	1 (0.5%)	200 (93%)
Complex n=32	8 (25%)	8 (25%)	3 (9%)	1 (3%)	24 (75%)
PPV or NPV	36% PPV	38% PPV	75% PPV	50% NPV	89% NPV

**Table 8-1:** Presence of intra-abdominal bowel dilatation (IABD), extra-abdominal bowel dilatation (EABD) and both IABD/EABD (combined) throughout pregnancy by gastroschisis complexity group. Positive predictive value and negative predictive value are for complex gastroschisis.

The diameter of the IABD was measured and documented for 55 fetuses (42 simple gastroschisis, 13 complex gastroschisis) revealing no significant difference in diameter of IABD between simple (19 [7.2-36.0] mm) and complex gastroschisis (20 [13-36] mm,  $p=0.064$ , Figure 8-1). Additionally, when considering fetuses with measured large IABD (diameter  $\geq 18$ mm), this was present in 64% of simple and 69% of complex gastroschisis giving a PPV for detected complex patients of only 25% (Table 8-2). When considering all infants with measured IABD there was no correlation between the degree of dilatation and ENT ( $p=0.33$ ) but larger bowel dilatation was weakly associated with prolonged LOS ( $p=0.049$ ). However, this association was not present when LOS for simple ( $p=0.26$ ) and complex ( $p=0.42$ ) gastroschisis were analyzed separately. Within the simple gastroschisis group, there was no significant difference between those patients with IABD and without IABD in ENT (24.5 [11-112] days vs. 26.0 [4-365] days,  $p=0.65$ ) or LOS (32.0 [15-94] days vs. 29.0 [7-167] days  $p=0.13$ ).

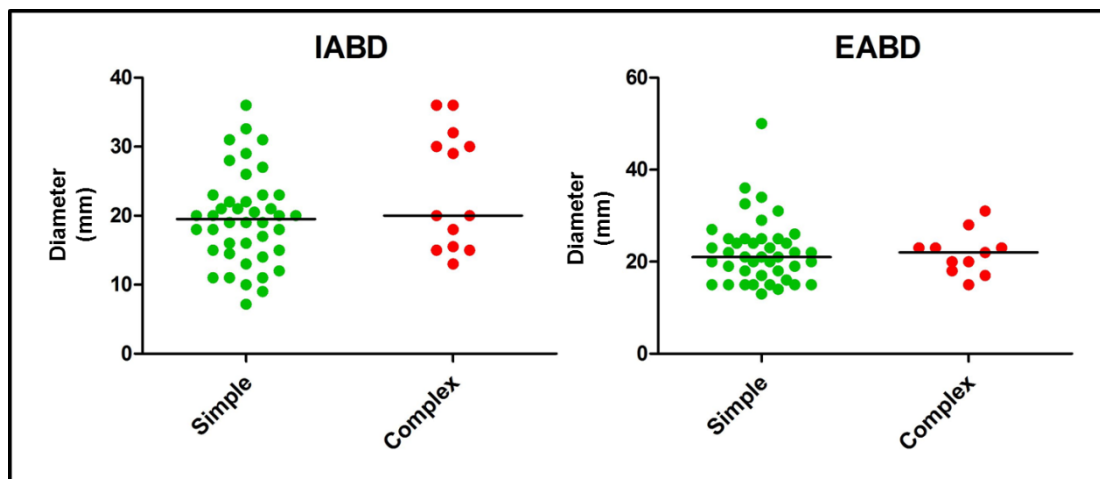


**Figure 8-1:** Relationship of measured intra-abdominal bowel dilatation (IABD) and extra-abdominal bowel dilatation (EABD) with simple and complex gastroschisis. Horizontal line at median.

The diameter of the EABD was measured and documented for 51 fetuses (40 simple gastroschisis, 11 complex gastroschisis) revealing no significant difference in diameter of EABD between simple (21 [13-50] mm) and complex gastroschisis (22 [15-31] mm,  $p=0.91$ , Figure 8-1). When considering fetuses with measured large EABD (diameter of  $\geq 18$ mm) this was present in 82% of complex and 72% of simple gastroschisis giving a PPV for detected complex patients of only 24% (Table 8-2).

Additionally, there was no correlation between size of EABD and ENT ( $p=0.50$ ) or LOS ( $p=0.47$ ). However, patients with combined IABD/EABD had longer ENT (30 [15-365] days vs. 26.5 [4-365] days,  $p=0.14$ ) and LOS (37 [16-273] vs. 32 [7-300] days,  $p=0.17$ ) but neither reached significance.

<b>Degree of Intra-Abdominal Bowel Dilatation (IABD)</b>			
<b>IABD Diameter (mm)</b>	<b>Simple Gastroschisis n=42 Number (% in group)</b>	<b>Complex Gastroschisis n=13 Number (% in group)</b>	<b>Positive Predictive Value</b>
<10	2 (5%)	0	0%
10 to <18	13 (31%)	4 (31%)	24%
$\geq 18$	27 (64%)	9 (69%)	25%
<b>Degree of Extra-Abdominal Bowel Dilatation (EABD)</b>			
<b>EABD Diameter (mm)</b>	<b>Simple Gastroschisis n=40 Number (% in group)</b>	<b>Complex Gastroschisis n=11 Number (% in group)</b>	<b>Positive Predictive Value</b>
<10	0	0	0%
10 to <18	11 (28%)	2 (18%)	15%
$\geq 18$	29 (72%)	9 (82%)	24%

**Table 8-2:** Size of measured intra-abdominal bowel dilatation (IABD) and extra-abdominal bowel dilatation (EABD) for both simple and complex gastroschisis

At birth, 23 neonates with simple gastroschisis were considered at risk of impending closing gastroschisis either due to the presence of ischaemic bowel or the need for widening of a tight defect prior to definitive surgical management. Of these 23 neonates, 5 (22%) had persistent IABD (combined with EABD from >30 weeks GA

in 2 cases), 5 (22%) had resolved IABD, 4 had persistent EABD but 8 (36%) never had IABD or EABD detected.

Finally, clinical concerns were raised antenatally of impending closing gastroschisis resulting in early delivery based on IABD in 20 patients. These concerns were due to: persistent/static dimension of IABD (5 simple, 3 atresia, 1 necrosis), sudden onset of large IABD in the 3<sup>rd</sup> trimester (6 simple, 1 atresia), increasing IABD throughout pregnancy (3 atresia). There was no difference in the number of infants with necrosis in the early delivery and non-early delivery groups (Table 8-3). Of those infants with simple gastroschisis who were delivered early, only one was reported to have dusky bowel and therefore born with possible signs of impending closing gastroschisis. Overall, 59 patients had persistent/static IABD (45 simple, 11 atresia, 3 necrosis), 27 sudden (21 simple, 5 atresia, 1 necrosis) and 6 increasing (2 simple, 4 atresia).

	Planned Early Delivery for IABD (n=20)	IABD at Any Time but no Early Delivery (n=90)	p-value
IABD Diameter (mm)	20 [12-36]	19.0 [7.2-36]	0.17
Patients with Bowel Necrosis Number (% in group)	1 (5%)	3 (3%)	0.56
Patients with Atresia Number (% in group)	8 (40%)	13 (14%)	0.023

**Table 8-3:** Comparison of complex patients and the diameter of bowel dilatation between the planned early delivery for intra-abdominal bowel dilatation (IABD) versus no early delivery for IABD.

## **8.3 Discussion**

### **8.3.1 Predictive Value of Antenatal Bowel Dilatation**

Evaluating the presence of IABD and EABD in isolation gave mixed results. IABD was present in a relatively large number of simple and complex gastroschisis fetuses resulting in a low PPV for predicting complex gastroschisis. Although the absence of IABD yielded a high NPV of 96% it is also important to note that 6 (19%) complex gastroschisis fetuses did not exhibit IABD at any time antenatally. EABD at <30 weeks GA yielded the highest PPV (64%) but the absence of EABD gave a lower NPV (90%). There were no apparent pattern of evolving IABD or EABD over the course of gestation that was indicative of complex gastroschisis and several infants at birth with signs of impending closing gastroschisis had not exhibited any bowel dilatation antenatally. However, combined dilatation present at <30 weeks GA yielded a relatively high PPV of 75% for detecting complex gastroschisis. Additionally, IABD combined with collapsed extra-abdominal bowel was only present in complex gastroschisis fetuses and was detected from <30 weeks GA in all cases.

The diameter of IABD and EABD was similar in both simple and complex gastroschisis even when considering only large bowel dilatation of >18mm. As such, the degree of measured bowel dilatation was poorly predictive of gastroschisis complexity. Finally, increasing bowel diameter size was not associated with poorer infant outcomes (measured as ENT and LOS) for simple or complex gastroschisis infants in this cohort

### **8.3.2 Implications of Findings**

Overall, the absence of IABD or EABD (when considered in isolation) is suggestive of simple gastroschisis. As such, expectant parents could be cautiously counselled accordingly with the caveat that absence of dilatation does not completely rule out the possibility of complex gastroschisis. Although the presence of bowel dilatation increases the chance of complex gastroschisis, it is also frequently associated with simple gastroschisis and the presence of bowel dilatation in simple gastroschisis did



not negatively impact postnatal outcomes. Therefore, IABD or EABD considered in isolation are not reliable markers for predicting postnatal outcome. On the other hand, the presence of combined dilatation or IABD and collapsed extra-abdominal bowel particularly when present at <30 weeks GA was highly predictive of complex gastroschisis in this cohort. These antenatal findings may suggest that bowel damage has already occurred rather than these signs being a prelude to the development of bowel complications. As such, it may be too late to achieve bowel salvage by the time these findings are detected. Even so, it may still be prudent to consider early delivery or fetoscopic intervention with the aim to lessen the degree of bowel damage or achieve bowel salvage where possible.

### **8.3.3 Literature Review**

It has previously been hypothesised that the presence of IABD in particular is prognostically useful in detecting fetuses with poorer postnatal outcomes or impending bowel damage (e.g. necrosis or atresia, literature summarised in Table 8-4) enabling selection of patients who would benefit from fetal intervention such as early delivery before further deterioration (Houben et al., 2009). A meta-analysis (D'Antonio et al., 2015) assessing prenatal risk factors showed that IABD was associated with an increased risk of bowel atresia but the study was unable to identify a marker that could accurately predict complex gastroschisis. Additionally, it showed that fetuses with EABD were not at increased risk of bowel atresia. Interestingly, the results presented in this chapter revealed the highest PPV for detecting complex gastroschisis based solely on IABD or EABD was fetuses with the presence of EABD at <30 weeks GA. A previous study from UCLH and GOSH found that the absence of bowel dilatation excluded atresia (Ghionzoli et al., 2012). However, the results presented in this chapter did not fully agree with this finding and showed that the absence of IABD could not fully exclude atresia. Another study concluded that second trimester IABD predicts bowel atresia (Nick et al., 2006) and may indicate the need for prenatal intervention or early delivery to prevent ongoing damage. Again the data presented in this chapter disagrees with this finding given the PPV of IABD at <30 weeks GA was only 38%, as such, instigating prenatal intervention or early delivery on the basis of IABD would lead to a large number of simple gastroschisis infants being born early for no clinical benefit and could in fact

result in poorer infant outcomes in terms of ENT and LOS as discussed in **Error! eference source not found.**pter 7. Additionally, there are conflicting data in terms of the association of bowel dilatation and prolonged ENT and LOS. Some studies found IABD (Goetzinger et al., 2014, Huh et al., 2010) to be associated with worse infant outcomes whilst others found unspecified bowel dilatation (Tower et al., 2009), IABD (Badillo et al., 2008, Mears et al., 2010) and EABD (Japaraj et al., 2003, Goetzinger et al., 2014, Badillo et al., 2008, Mears et al., 2010) not to be associated with poorer outcomes. The data presented in this chapter provides extra support to the studies that found no association between bowel dilatation or bowel diameter and infant outcomes. Finally, a previous case report has reported IABD combined with vanishing externalised bowel detected antenatally (i.e. antenatal ultrasound diagnosis of gastroschisis with evidence of externalised bowel followed by disappearance of the externalised bowel on subsequent ultrasound scans) to be associated with closed gastroschisis at birth including the following features; bowel atresia, short bowel syndrome, closed abdominal wall and an intestinal tissue remnant to the right of the umbilicus (Winter et al., 2005). Vanishing gastroschisis is a rare occurrence and was not present in the cohort presented here but is in keeping with the finding that IABD and collapsed extra-abdominal bowel was associated with complex gastroschisis particularly bowel necrosis.

Study	Number of Centres	Study Inclusion Period, Number of Patients	Study Type	Type of Bowel Dilatation Reviewed	Outcomes Associated with IABD	Outcomes Associated with EABD	Author Comments
D'Antonio et al., 2015	Multiple	26 studies n=2023	Meta-Analysis	-Intra-abdominal -Extra-abdominal	-High risk of atresia (OR: 5.48, 95% CI: 3.1-9.8) IABD with bowel diameter >14mm: -Higher risk of atresia (RR: 3.1, 95% CI: 1.2-8.2) -Increased LOS	-EABD not associated with increased risk of atresia -EABD not significantly associated with adverse outcomes	IABD increases risk of atresia.  IABD >14mm associated with atresia and poorer infant outcomes. May be useful for prenatal counselling
Goetzing et al., 2014	1	2001-2010 n=109	Retrospective cohort	-Intra-abdominal -Extra-abdominal			
Ghionzoli et al., 2012	1	1992-2010 n=130	Retrospective cohort	-Intra-abdominal and extra-abdominal (dilatation considered as bowel diameter >18mm) grouped together and termed 'fetal bowel dilatation'	-Unspecified fetal bowel dilatation associated with a 99% negative predictive value for atresia and 17% positive predictive value for atresia		Absence of any fetal bowel dilatation excludes atresia
Huh et al., 2010	1	2002-2008 n=43	Retrospective cohort	-Intra-abdominal -Extra-abdominal	-Single dilated loop (n=10) no complex gastrochisis reported -Multiple dilated loops (n=6) all had complex gastrochisis. -Multiple dilated loops compared to single dilated loop had increased ENT and LOS	-Incidence of EABD was the same between IABD and non-IABD groups and not associated with outcomes	IABD is associated with increased postnatal complications but limited to those with multiple loops of dilated IABD
Contro et al., 2010	1	1998-2008 n=62	Retrospective cohort	-Intra-abdominal -Extra-abdominal	-Increased risk of complex gastrochisis (RR: 4.05, 95% CI: 1.12-14.7)	- Not associated with increased risk of complex gastrochisis	-IABD predictive of complex gastrochisis -EABD common and not predictive of complex gastrochisis

Study	Number of Centres	Study Inclusion Period, Number of Patients	Study Type	Type of Bowel Dilatation Reviewed	Outcomes Associated with IABD	Outcomes Associated with EABD	Author Comments
Mears et al., 2010	1	2004-2008 n=60	Retrospective cohort	-Intra-abdominal -Extra-abdominal	-No increased risk of complex gastroschisis -No association with prolonged ENT or LOS	-No increased risk of complex gastroschisis -No association with prolonged ENT or LOS	Bowel dilatation is not a prognostic indicator of infant outcomes
Houben et al., 2009	1	1994-2007 n=146	Retrospective cohort	-Intra-abdominal	Of the 146 infants 9 found to have evidence of closing gastroschisis at birth of whom 6 had IABD on antenatal scans		Key fetal sign of closing gastroschisis is persistent or progressive IABD and advise early delivery to achieve bowel salvage
Tower et al., 2009	Multiple	10 studies n=273	Systematic review of cohort studies	-Unspecified bowel dilatation	Bowel dilatation was not associated with increased death, bowel resection or LOS. There was insufficient data to compare bowel dilatation with ENT		Antenatal bowel dilatation does not appear to worsen perinatal morbidity and mortality
Badillo et al., 2008	1	2000-2007 n=64	Retrospective cohort	-Intra-abdominal -Extra-abdominal	-No increased risk of complex gastroschisis -No association with prolonged ENT or LOS	-No increased risk of complex gastroschisis -No association with prolonged ENT or LOS	Bowel dilatation does not correlate with adverse infant outcome
Japaraj et al., 2003	1	1993-2001 n=45	Retrospective cohort	-Extra-abdominal		-No increased risk of complex gastroschisis -No association with prolonged ENT or LOS	EABD not associated with adverse neonatal outcome
Nick et al., 2006	1	1998-2004 n=58	Retrospective cohort	-Intra-abdominal	-IABD present in 10 fetuses and all had atresia		IABD in second trimester predicts atresia
Langer et al., 1993	2	n=24	Prospective	-Unspecified bowel dilatation (dilatation considered as bowel diameter > 18mm)	Unspecified bowel dilatation associated with significantly longer ENT and greater need for bowel resection		Bowel dilatation may be a marker of bowel damage

**Table 8-4:** Summary of studies investigating the association of antenatally detected intra-abdominal bowel dilation (IABD) and extra-abdominal bowel dilatation (EABD) with complex gastroschisis and surrogate infant outcomes (ENT and LOS).

### **8.3.4 Limitations of the Study**

This was a retrospective study with non-protocolised methods for the measurement of bowel diameter. Many of the ultrasound images were not stored and therefore it was not possible to design a retrospective study whereby stored images were assessed for the presence of bowel dilatation by a single blinded investigator. Bowel dilatation was therefore classified based on documentation within the fetal notes and hence subject to inter-observer variability. Due to the way IABD was documented, it was not possible to distinguish between intestinal or gastric dilatation. It was not possible to apply a threshold diameter to define the severity of bowel dilatation as only 55 of the 110 patients with IABD and 51 of 65 patients with EABD had bowel diameter measurements documented in their notes. This was a retrospective study and relies on accurate documentation of clinical findings within the fetal notes as such the presence of bowel dilatation may not have been documented accurately for all fetuses. Additional, data collection such as volume of amniotic fluid would have provided an additional factor that may have aided the reliability of predicting postnatal outcomes based on the presence antenatal bowel dilatation.

### **8.3.5 Strength of the Study**

This study included two large London centres both of whom routinely assess bowel diameter during antenatal monitoring of fetuses with gastroschisis. As such, the number of patients included in this study is relatively high improving the validity of the results. It was possible to track the presence of documented bowel dilatation throughout the course of gestation enabling the identification of bowel diameter patterns overtime if any were present. Finally, to date previous studies have focused on the presence of IABD or EABD in isolation whilst this study has identified that the presence of combined dilatation or IABD with extra-abdominal bowel collapse more reliably detects fetuses with bowel necrosis or atresia. However, there were only a small number of patients with combined findings and therefore continued investigation is required before the reliability of these markers can be fully known.

### **8.3.6 Conclusion**

Prediction of gastroschisis infant outcomes is unreliable when considering IABD or EABD as independent antenatal markers. As such, fetal intervention based solely on IABD or EABD is not warranted due the lack of difference in size of bowel dilatation diameter between simple and complex gastroschisis, lack of association between bowel dilatation and infant outcomes (ENT and LOS) and the failure to reliably detect fetuses with impending closing gastroschisis, necrosis or atresia. In this cohort, more accurate predictors of poor outcomes were the presence of combined dilatation or IABD and collapsed extra-abdominal bowel before 30 weeks GA. Although antenatal markers may potentially enable identification of gastroschisis fetuses with poorer infant outcomes, these ultrasound signs possibly occur after the bowel damage has already developed. However, it might still be prudent to consider fetal intervention for such fetuses with the aim to salvage bowel or reduce the extent of bowel damage. Further research is required to identify more reliable antenatal markers that predict infant outcomes, detect fetuses that would benefit from antenatal intervention or detect bowel damage before it happens.

## **Chapter 9: Summary, Discussion and Concluding Remarks**

### **9.1 Discussion**

#### **9.1.1 Gastroschisis Bowel Wall Morphology**

The current literature suggests that the most likely cause of GRID is deficiency and immaturity of bowel wall ICC secondary to bowel wall inflammation based on previous animal (Krebs et al., 2014, Vargun et al., 2007, Danzer et al., 2010, Auber et al., 2013, Midrio et al., 2004) and human studies (Midrio et al., 2008, Zani-Ruttenstock et al., 2015, Morrison et al., 1998). This hypothesis formed the primary line of investigation for the work leading up to this thesis.

Analysis of gastroschisis bowel wall ICC using human pathological gut tissue showed no differences in the number or cell architecture of ICC at the level of the myenteric plexus between gastroschisis and control bowel. Furthermore, this study found no association between the number of ICC and duration of GRID measured as ENT. Additionally, there was no difference in the number or architecture of enteric neurons between gastroschisis and control bowel. Thus, the data in this thesis contradict the current literature and suggests that deficiency and immaturity of ICC may not be the primary cause of GRID. It is important to note that this study only included bowel specimens from gastroschisis infants with the worst postnatal outcomes and therefore if deficient, immature ICC were the cause of GRID it should have been evident from this study.

The ACLP knockout mouse model study using whole mount gut tissue revealed untreated AWD fetuses to have an 11% reduction in ICC numbers compared to untreated controls. However, this was in stark contrast to the original published study using cross-sectioned gut tissue, which reported AWD fetuses to exhibit a 70% reduction in bowel ICC compared to controls (Danzer et al., 2010). Furthermore Danzer et al. reported the AWD bowel ICC to be architecturally immature and enteric neurons to be absent. However, the results presented in this thesis revealed

the untreated AWD bowel ICC to be architecturally normal with no difference in enteric neuron number or architecture between untreated AWD and untreated control bowel. It is not possible to know if the reduced number of ICC in the AWD fetuses was due to ACLP deficiency or exposure to the exocoelomic fluid.

The ICC data presented in this thesis highlights methodological issues of previously published studies including; inaccurate phenotyping of abdominal wall defects in genetic mouse models, the unreliability of quantification and architectural assessment of ICC from cross-sectioned small animal gut tissue and the imprecise nature of semi-quantitative methods for the comparison of gastroschisis and control bowel in both human and animal studies.

The results presented in this thesis suggest that deficiency and immaturity of bowel wall ICC is not the primary cause of GRID. However, the detailed morphological analysis of human pathological gut tissue revealed another possibility for the cause of GRID, i.e. that of increased bowel wall thickness, which is in keeping with the findings of a number of previous animal studies (Api et al., 2001, Correia-Pinto et al., 2002, Langer et al., 1989, Srinathan et al., 1995). The increased bowel wall thickening was found to be due to thickening of the outer bowel wall layers (serosa and muscularis externa) but sparing of the inner bowel wall layers (submucosa and mucosa). Of particular note the muscularis externa was found to be hyperplastic with deficiency of  $\alpha$ -SMA within the outer longitudinal smooth muscle layer. Further, analysis of clinical data revealed increasing bowel wall thickness to be associated with prolonged GRID (measured as ENT). Together, these findings suggest that GRID may be caused by smooth muscle remodelling resulting in cell hyperplasia and possible bowel wall myopathy. However, bowel wall thickening was not present in AWD fetuses of the ACLP knockout mouse model, which is in keeping with the results reported by Danzer et al. This may be due to the externalised bowel being exposed to the exocoelomic fluid (an ultra-filtrate of the maternal serum) instead of the irritant amniotic fluid. Table 9-1 summarises the previously held dogmas within the gastroschisis literature of bowel wall changes that may be the cause of GRID compared to the findings presented in this thesis.



	Dogma within the Gastroschisis Literature	Gastroschisis Findings Presented in this Thesis
<b>Animal</b>	<b>Bowel wall ICC:</b> -Immature architecture -Reduced numbers - 70% reduction of AWD ICC in ACLP model	<b>Bowel wall ICC:</b> -Normal architecture - Slight reduction - 11% reduction of AWD ICC in ACLP model)
	<b>Bowel wall enteric neurons:</b> -Absent in AWD fetuses of ACLP model	<b>Bowel wall enteric neurons:</b> -Normal architecture and numbers in AWD fetuses of ACLP model
	<b>Bowel wall morphology:</b> -Thickened bowel wall (not reported in ACLP model)	<b>Bowel wall morphology:</b> -No bowel wall thickening in ACLP model
<b>Human</b>	<b>Bowel wall ICC:</b> -Immature architecture -Reduced numbers	<b>Bowel wall ICC:</b> -Normal architecture -Normal numbers
	<b>Bowel wall morphology:</b> -Bowel appears grossly thickened at birth (no histological data)	<b>Bowel wall morphology:</b> -Histological analysis shows bowel wall thickening involving serosa and muscularis externa -Muscularis externa hyperplastic - $\alpha$ -smooth muscle actin deficiency -Increased bowel wall thickening associated with prolonged ENT

**Table 9-1:** Summary of the previously held dogmas within the gastroschisis literature of bowel wall changes that may be the cause of GRID compared to the findings presented in this thesis

### 9.1.2 Impact of Inflammatory Modulation on Gastroschisis Bowel Wall Morphology

Previous studies have shown that inflammation causes disruption to bowel wall ICC networks (Der et al., 2000, Wang et al., 2005) and thickening of the muscularis externa (Bettini et al., 2003, Blennerhassett et al., 1992). In-utero injection of IL-8, a pro-inflammatory cytokine, in the ACLP knockout mouse model resulted in

increased IL-8 exposure to the bowel serosal surface of AWD fetuses and the bowel mucosal surface of control fetuses. Results showed that bowel wall thickness was unaffected by IL-8 exposure in both groups, which could be due to the duration of IL-8 exposure being shorter than the time required for smooth muscle remodelling to occur. However, IL-8 exposure resulted in decreased ICC numbers without disrupting cell architecture which was most pronounced in the control group. This suggests that mucosal exposure to IL-8 has a greater negative impact on the myenteric ICC network than serosal exposure and morphological bowel wall changes in gastroschisis may occur from an additive effect of serosal and mucosal exposure to the pro-inflammatory amniotic fluid environment (Morrison et al., 1998). There was also a trend of reduced bowel contractility with increasing fetal manipulation. These results showed that IL-8 exposed bowel was more dysfunctional than the untreated counter-parts suggesting that bowel inflammation impairs intestinal motility.

### **9.1.3 Impact of Clinical Antenatal Interventions on Infant Outcomes**

It has been hypothesised that prolonged serosal exposure to amniotic fluid negatively impacts bowel development (Morrison et al., 1998, Api et al., 2001) and that early delivery of gastroschisis pregnancies would improve bowel function and reduce the duration of GRID (Gelas et al., 2008, Serra et al., 2008, Moore et al., 1999, Moir et al., 2004). However, the International multi-centre retrospective cohort study presented in this thesis showed that although earlier delivery marginally reduced the corrected GA at time of ENT this did not translate into a faster time to achieve ENT and resulted in a prolonged hospital stay and increased risk of sepsis. Therefore, elective delivery at <37 weeks GA is not supported by these data as a strategy to improve infant outcomes. This conclusion is in keeping with several other published studies (Maramreddy et al., 2009, Youssef et al., 2015, Cain et al., 2014, Logghe et al., 2005, Charlesworth et al., 2007) (Table 9-2).

Previous studies investigating antenatal administration of corticosteroids in surgical animal models of gastroschisis have shown a beneficial effect on bowel wall morphology and protein content (Guo et al., 1995, Yu et al., 2004, Bittencourt et al., 2006). Antenatal corticosteroids could therefore have the potential to beneficially remodel the abnormal bowel wall of gastroschisis fetuses. However, the results of the

large International multi-centre retrospective study found no association between the administration of maternal antenatal corticosteroids and improved infant outcomes following multiple analysis strategies. Although results showed no positive benefit of maternal antenatal corticosteroids on infant outcomes, this may reflect the late administration of the corticosteroid or the need for repeated doses during pregnancy for a beneficial effect on bowel function to be apparent (Table 9-2).

The ability to antenatally predict postnatal outcomes would aid the antenatal management of gastroschisis pregnancies. Antenatally detected bowel dilatation has previously been shown to be associated with complex gastroschisis (Huh et al., 2010, Houben et al., 2009, Ghionzoli et al., 2012, Nick et al., 2006, D'Antonio et al., 2015, Goetzinger et al., 2014, Contro et al., 2010) and hypothesised in simple gastroschisis fetuses to be associated with poorer intestinal function (Langer et al., 1993). The multi-centre retrospective study showed that although the absence of IABD or EABD is suggestive of simple gastroschisis the presence of either IABD or EABD is poorly predictive of complex gastroschisis and is not associated with prolonged ENT or LOS. However, the presence of combined IABD and EABD or IABD and collapsed extra-abdominal bowel before 30 weeks, although a rare finding, was highly predictive of complex gastroschisis. Therefore, overall antenatally detected bowel dilatation is a poor predictor of infant outcomes and could not be reliably used to identify fetuses that would benefit from antenatal intervention (Table 9-2).

	Dogma within the Gastroschisis Literature	Gastroschisis Findings Presented in this Thesis
<b>Timing of delivery</b>	-Elective early delivery in the early preterm period improves infant outcomes	-Earlier delivery associated with worse infant outcomes (ENT, LOS and sepsis)
<b>Antenatal maternal corticosteroids administration</b>	-In animals corticosteroids associated with improved bowel wall morphology and function -A small human study suggested corticosteroids may improve infant outcomes	-No improvement in infant outcomes demonstrated from retrospective cohort study
<b>Antenatally detected bowel dilatation</b>	<b>IABD predictive of:</b> -Complex gastroschisis -Poorer infant outcomes <b>EABD not predictive of:</b> -Complex gastroschisis -Poorer infant outcomes (ENT and LOS)	<b>Absence of either IABD or EABD:</b> -Suggestive of simple gastroschisis <b>Presence of either IABD or EABD:</b> -Poor predictor of complex gastroschisis -Not associated with prolonged ENT and LOS <b>Combined IABD/EABD or IABD/collapsed extra-abdominal bowel:</b> -Highly predictive of complex gastroschisis

**Table 9-2:** Summary of the previously held dogmas within the gastroschisis literature of timing of delivery, antenatal corticosteroid administration and predictive value of antenatally detected bowel dilatation compared to the findings presented in this thesis.

#### 9.1.4 Other Findings

Animal models should closely reflect, structurally and functionally, the human disease (Klocke et al., 2007) in order to avoid the generation of misleading data and inaccurate conclusions (Chu et al., 2002, Klocke et al., 2007). Prior to starting this research two genetic mouse models of gastroschisis were described in the literature;

the Scribble knockout mouse model (Murdoch, 2003, Hartleben et al., 2012, Pearson et al., 2011) and the ACLP knockout mouse model (Layne et al., 2001, Danzer et al., 2010). However, neither of these models had a detailed phenotypic description of the abdominal wall defect. A third model, the *Alx-4* mutant mouse model, had previously been reported as having gastroschisis (Qu et al., 1997) but was later re-characterised as exomphalos (Matsumaru et al., 2011). Therefore, based on these published studies, detailed investigations of the abdominal wall defect and amniotic membrane anatomy was performed in both the Scribble and ACLP knockout mouse models. Detailed phenotyping of the Scribble knockout mouse model revealed AWD fetuses to have fine a membrane (intact or ruptured) covering the externalised viscera in keeping with an exomphalos. On the other hand, AWD fetuses of the ACLP knockout mouse model were found to have, as well as failed abdominal wall closure, failed umbilical cord formation whereby the amniotic membrane failed to adhere to the umbilical vessels and attached directly to the abdominal wall defect edge resulting in the externalised viscera lying within the exocoelomic fluid. The anatomy of this defect has never before been described in humans. However, if normal cord formation had occurred then the externalised viscera would have a membrane covering and the phenotype would be that of exomphalos. Given these results there are now no known genetic murine models of gastroschisis (Table 9-3).

	Dogma within the Gastroschisis Literature	Gastroschisis Findings Presented in this Thesis
<b>Scribble knockout mouse model</b>	Gastroschisis phenotype	Exomphalos phenotype
<b>ACLP</b>	Gastroschisis phenotype	-Abdominal wall defect + failed umbilical cord formation -Externalised gut free floating in exocoelomic fluid -Not gastroschisis

**Table 9-3:** Summary of the previously held dogmas within the gastroschisis literature of genetic gastroschisis mouse models compared to the findings presented in this thesis

## 9.2 Future Research

The research presented in this thesis suggests that ICC defects may have less of a role in the cause of GRID than originally expected. However, bowel wall thickening and myopathy of the muscularis externa may be significant factors causing intestinal dysfunction. Further research is required to unravel the mechanisms underlying bowel wall thickening and smooth muscle remodeling, which might only be possible in an animal model due to the obvious difficulties in obtaining human gastroschisis gut tissue of an appropriate gestational age.

The phenotypic analyses of the Scribble and ACLP knockout mouse models suggest that genetic murine models are of limited value in gastroschisis research. As such, if further animal research is to be carried out then an appropriate surgical model could be used. Given the high risk of fetal loss in the surgical rat model (Auber et al., 2013, Hakguder et al., 2011) and risk of operative induced inflammation, it would be of benefit to use a large animal model with a lower risk of fetal loss (Oyachi et al., 2004, Krebs et al., 2014) and a longer gestational period reducing the impact of surgical induced inflammation on bowel development. Bowel wall thickening including the serosa and muscularis externa has previously been demonstrated both in the rabbit (Santos et al., 2003) and sheep (Krebs et al., 2014, Srinathan et al., 1995) surgical models of gastroschisis making these models ideal for further gastroschisis research. However, the research design would need to take into consideration the expense of using large animals and the longer pregnancy duration.

Key features of the gastroschisis bowel wall thickening found on analysis of the human pathological gut tissue included sparing of the inner bowel wall layers, hyperplasia of the muscularis externa and deficiency of  $\alpha$ -SMA within the outer longitudinal smooth muscle layer. As previously discussed in chapter 6 of this thesis the trigger for deranged bowel wall morphology is likely external to the bowel wall and may include inflammation, reduced Hippo pathway signalling or growth factors. Further research investigating these possible triggers may help identify an antenatal therapy for the improvement of GRID.

### 9.2.1 Modulation of Inflammation

The impact of inflammation on exposed bowel can be investigated through in-utero modulations of the amniotic fluid environment. In this thesis in-utero injection of the pro-inflammatory cytokine IL-8 was used to promote inflammation but further inflammatory modulations were not possible due to significant unforeseen experimental delays. However, investigations into the impact of inflammatory amelioration could be achieved using corticosteroids and/or amniotic fluid stem cells.

Corticosteroids are well known for their potent anti-inflammatory action, which may have beneficial remodelling effects on the smooth muscle of the muscularis externa. Corticosteroids may also have a beneficial maturational effect on bowel motility (Morriss et al., 1986). Although the multi-centre retrospective study showed no association of administration of maternal antenatal corticosteroids on infant outcomes, the use of antenatal corticosteroids may still be beneficial in gastroschisis if optimisation of corticosteroid delivery and dosage could be achieved.

Investigations in fetal animals could compare the effect of antenatal intramuscular maternal injection (as used in clinical practice) or direct intra-amniotic injection (which would enable direct serosal exposure to corticosteroid) on bowel wall morphology and motility. Additionally, varying dosages and number of injections could be performed to ascertain a dose-response curve based on recovery of bowel wall morphological changes and motility.

Stem cell therapy has been investigated for the management of other inflammatory gastrointestinal conditions including inflammatory bowel disease (IBD) (Bamba et al., 2006, Legaki et al., 2016, Cassinotti et al., 2008, Ricart, 2012), graft versus host disease (Okamoto et al., 2002) and necrotising enterocolitis (NEC) (Zani et al., 2014) in which multifactorial therapeutic benefits have been found including anti-inflammatory, immunomodulatory and tissue regenerative capabilities (Eaton et al., 2013, Zani et al., 2014). Additionally, stem cells administered systemically in the form of a bone marrow transplant in humans (Okamoto et al., 2002) or topically into the intraperitoneal cavity in rats (Ghionzoli et al., 2010) has revealed that stem cells migrate and integrate into the bowel wall particularly homing to areas of intestinal injury (Zani et al., 2014, Srivastava et al., 2007). Therefore, stem cells have the

potential in gastroschisis to target dysfunctional bowel, reduce bowel wall inflammation and induce remodelling of abnormal smooth muscle providing a targeted therapy for GRID. Also, due to the integration of stem cells into the bowel wall the therapeutic effect could be long acting and therefore potentially only require a one off antenatal treatment. Stem cells could have significant benefits over a therapy such as antenatal corticosteroids, given that corticosteroids would have a systemic, not just local bowel effect, and are short acting therefore potentially requiring multiple injections in order to have a sustained and beneficial effect.

The options for gastroschisis antenatal stem cell therapy could include intra-amniotic injection of (i) autologous amniotic fluid stem cells (harvested by amniocentesis at approximately 15 weeks gestation) (De Coppi et al., 2007), (ii) allogenic stem cells (amniotic fluid stem cells or mesenchymal stem cells derived from bone marrow) but only if administered early enough in gestation when the fetus is still immunologically immature (Loukogeorgakis and Flake, 2014), and (iii) conditioned medium (containing the secreted factors from stem cell culture) also known as cell free therapy which would exert a paracrine effect on the bowel (Legaki et al., 2016). Animal investigations could involve intra-amniotic injections of labelled amniotic fluid stem cells, conditioned medium from amniotic fluid stem cells, labelled mesenchymal stem cells and conditioned medium from mesenchymal stem cells. Labelled stem cells would enable the assessment of stem cell integration and location of homing within the bowel. The experimental use of conditioned medium would determine whether the therapeutic effect of stem cell therapy was contingent on cell integration or could be achieved by a paracrine effect alone.

### **9.2.2 Regulation of the Hippo Pathway**

The Hippo pathway closely regulates organ size during fetal development and is contingent on external mechanical pressure regulating molecular feedback through the YAP-TAZ pathway, which influences nuclear cues that prevent tissue overgrowth (Dupont et al., 2011, Low et al., 2014). During normal organogenesis the bowel is contained within the abdominal cavity which exerts an external mechanical pressure stimulating the YAP-TAZ pathway. However, in gastroschisis the bowel is free floating within the relatively large amniotic fluid cavity, which potentially exerts



a lower external mechanical pressure thus reducing YAP-TAZ activation resulting in smooth muscle hyperplasia of the muscularis externa. The effect of external mechanical pressure on bowel wall morphology and bowel wall nuclear YAP levels (Grijalva et al., 2014) could be investigated within a gastroschisis surgical large animal model whereby the externalised bowel could be surgically covered with varying sizes of membrane thus exerting differing degrees of external mechanical pressure. Given varying amounts of bowel may be externalised in each fetus the ability to measure the force exerted on the bowel wall by the membrane would greatly improve the validity and reproducibility of the data analysis. The use of a permeable membrane would enable the investigation of external mechanical pressure on the bowel whilst the serosal surface of the bowel remains in contact with the amniotic fluid thus enabling the investigation of only one variable at time.

### **9.2.3 Growth Factors**

Growth factors are essential for fetal development and are ubiquitous in the amniotic fluid originating from the amniotic membranes (Underwood et al., 2005). The effect of mucosal bowel exposure to growth factors during fetal development has previously been investigated by ligation of the fetal rabbit oesophagus to prevent amniotic fluid swallowing followed by injection of amniotic fluid distal to the ligation (Mulvihill et al., 1986). A similar experimental design within a gastroschisis surgical large animal model could be coverage of the bowel with an impermeable membrane followed by injection of specific growth factors into the space between the bowel and the membrane. The difficulties with this experimental design are; the creation of a water tight seal may not be possible, the membrane coverage will also exclude all other amniotic fluid contents, and the pressure of the membrane on the bowel wall may also increase YAP-TAZ signalling resulting in a multi-factorial change that may be difficult to interrupt. Alternatively, intra-amniotic injection of a growth factor inhibitor or increased concentration of a growth factor could be undertaken but may have other systemic effects on the fetus, which could indirectly affect the development of the bowel. As such, investigating the effect of growth factors on bowel wall development may be challenging.

#### **9.2.4 Prospective Cohort Study**

Although it is not possible to investigate the impact of potential triggers on bowel wall development in humans, other minimally-invasive research may be of benefit in understanding the pathophysiological cause of GRID and help develop reliable predictors of infant outcomes. A large scale, multi-centre, prospective cohort study would be required in order to obtain enough data to accurately correlate potential biomarkers with prognosis and possibly uncover a therapeutic target for GRID. Such a study would ideally involve clinical data collection and collection of samples (such as amniotic fluid, blood and stool) both in the antenatal and postnatal period. The aim of the study would be to standardise obstetric monitoring, optimise antenatal and postnatal management and provide further insight into the pathophysiological cause of GRID.

Antenatally a standardised study protocol would be required to ensure uniformity and reproducibility of antenatal ultrasound measurements such as bowel diameter, bowel wall thickness, stomach diameter, stomach position, amniotic fluid volume and fetal growth and Doppler assessment of umbilical cord and mesenteric perfusion. Clinical data such as maternal complications, administration of maternal antenatal corticosteroids, onset of labour, gestational age at delivery, mode of delivery and location of delivery would be essential. Collection of amniotic fluid, maternal blood and at birth fetal cord blood would provide a unique opportunity to perform biomarker discovery, identify trends between potential biomarkers and correlate markers with infant outcome data.

Postnatally standardised outcome endpoints would be required to robustly define surrogate markers of gut function such as ENT and LOS. All infant outcome variables should be documented such as concomitant bowel pathology at birth, defect closure method, timing of defect closure, initiation of enteral feeds, duration of parenteral nutrition, number of operations, episodes of sepsis, bowel resection, mortality, etc. A photograph at birth would provide documented evidence of bowel appearance at birth and ultrasound could be used postnatally to measure bowel wall thickness. The collection of stool from gastroschisis and carefully selected control infants could provide invaluable insight into the ongoing role of bowel inflammation

and the impact of the bowel microbiome composition on GRID. Faecal calprotectin is being routinely measured to distinguish between inflammatory bowel disease and non-inflammatory bowel diseases in older children and adults (NICE, 2013). Therefore, the analysis of faecal calprotectin from stool collected from gastroschisis and control infants at regular intervals throughout their hospital admission could provide insight into whether ongoing bowel inflammation affects infant outcomes. Additionally, the microbiome plays an essential role in health influencing metabolism, nutrition and immune function and alteration to the microbiome population has been linked to several conditions including inflammatory bowel disease, irritable bowel disease, obesity, diabetes mellitus, neuropsychological conditions and allergies (Jandhyala et al., 2015). The microbiome begins to colonize the gut in-utero and alterations in the microbiota composition have been found in neonates that are delivered by caesarean section, premature or develop NEC (Torrizza and Neu, 2013, Slattery et al., 2016) and in animal studies the composition of the microbiome has been found to influence gut motility (Dey et al., 2015). As such, dysbiosis of the microbiome in gastroschisis infants may influence GRID and be associated with prolonged ENT and LOS.

### **9.3 Concluding Statement**

The incidence of gastroschisis is increasing (Kilby, 2006) and although the advent of PN and improved surgical techniques have reduced the mortality rate from 90% to 3-10% of live born gastroschisis neonates (Bradnock et al., 2011, McClellan et al., 2011, Kassa and Lilja, 2011, Skarsgard et al., 2008) no improvements have been made in reducing the severity and duration of GRID. The most popular theory in the literature for the cause of GRID is deficiency and immaturity of ICC. However, the research presented in this thesis suggests that ICC may be less significant in the development of GRID than originally thought. Analysis of human pathological gut tissue suggests that bowel wall thickening with an element of smooth muscle myopathy may be another possibility for the cause of GRID. There are several hypothesised triggers for bowel wall thickening, all of which require further research in order to fully understand the pathophysiological basis of GRID. With this knowledge, it may be possible to develop targeted antenatal therapies that could improve postnatal outcomes for infants with gastroschisis.

## References

- ABDEL-LATIF, M. E., BOLISSETTY, S., ABEYWARDANA, S. & LUI, K. 2008. Mode of delivery and neonatal survival of infants with gastroschisis in Australia and New Zealand. *J Pediatr Surg*, 43, 1685-90.
- ABUHAMAD, A. Z., MARI, G., CORTINA, R. M., CROITORU, D. P. & EVANS, A. T. 1997. Superior mesenteric artery Doppler velocimetry and ultrasonographic assessment of fetal bowel in gastroschisis: a prospective longitudinal study. *Am J Obstet Gynecol*, 176, 985-90.
- ADZICK, N. S., THOM, E. A., SPONG, C. Y., BROCK, J. W., 3RD, BURROWS, P. K., JOHNSON, M. P., HOWELL, L. J., FARRELL, J. A., DABROWIAK, M. E., SUTTON, L. N., GUPTA, N., TULIPAN, N. B., D'ALTON, M. E. & FARMER, D. L. 2011. A randomized trial of prenatal versus postnatal repair of myelomeningocele. *N Engl J Med*, 364, 993-1004.
- AKOLEKAR, R., BETA, J., PICCIARELLI, G., OGILVIE, C. & D'ANTONIO, F. 2015. Procedure-related risk of miscarriage following amniocentesis and chorionic villus sampling: a systematic review and meta-analysis. *Ultrasound Obstet Gynecol*, 45, 16-26.
- AKTUG, T., UCAN, B., OLGUNER, M., AKGUR, F. M. & OZER, E. 1998a. Amnio-allantoic fluid exchange for prevention of intestinal damage in gastroschisis II: Effects of exchange performed by using two different solutions. *Eur J Pediatr Surg*, 8, 308-11.
- AKTUG, T., UCAN, B., OLGUNER, M., AKGUR, F. M., OZER, E., CALISKAN, S. & ONVURAL, B. 1998b. Amnio-allantoic fluid exchange for the prevention of intestinal damage in gastroschisis. III: Determination of the waste products removed by exchange. *Eur J Pediatr Surg*, 8, 326-8.
- ALBERT, A., SANCHO, M. A., JULIA, V., DIAZ, F., BOMBI, J. A. & MORALES, L. 2001. Intestinal damage in gastroschisis is independent of the size of the abdominal defect. *Pediatr Surg Int*, 17, 116-9.
- ALFIREVIC, Z., MUJEZINOVIC, F. & SUNDBERG, K. 2003. Amniocentesis and chorionic villus sampling for prenatal diagnosis. *The Cochrane database of systematic reviews*, 3, CD003252.
- AMIN, R., DOMACK, A., BARTOLETTI, J., PETERSON, E., RINK, B., BRUGGINK, J., CHRISTENSEN, M., JOHNSON, A., POLZIN, W. & WAGNER, A. J. 2018. National Practice Patterns for Prenatal Monitoring in Gastroschisis: Gastroschisis Outcomes of Delivery (GOOD) Provider Survey. *Fetal Diagn Ther*, 1-6.
- API, A., OLGUNER, M., HAKGÜDER, G., ATEŞ, O., ÖZER, E. & AKGÜR, F. M. 2001. Intestinal damage in gastroschisis correlates with the concentration of intraamniotic meconium. *Journal of Pediatric Surgery*, 36, 1811-1815.
- ARGYLE, J. C. 1989. Pulmonary hypoplasia in infants with giant abdominal wall defects. *Pediatr Pathol*, 9, 43-55.
- ASHRAFI, M., HOSSEINPOUR, M., FARID, M. & SANEI, M. H. 2008. Evaluation of diluted amniotic fluid effects on histological changes of intestine of rabbit fetus with gastroschisis. *Pediatr Surg Int*, 24, 421-4.
- ASZTALOS, E. 2012. Antenatal corticosteroids: a risk factor for the development of chronic disease. *J Nutr Metab*, 2012, 930591.
- ASZTALOS, E. V., MURPHY, K. E., WILLAN, A. R., MATTHEWS, S. G., OHLSSON, A., SAIGAL, S., ARMSON, B. A., KELLY, E. N., DELISLE,

- M. F., GAFNI, A., LEE, S. K., SANANES, R., ROVET, J., GUSELLE, P., AMANKWAH, K., SALEEM, M. & SANCHEZ, J. 2013. Multiple courses of antenatal corticosteroids for preterm birth study: outcomes in children at 5 years of age (MACS-5). *JAMA Pediatr*, 167, 1102-10.
- AUBER, F., DANZER, E., NOCHE-MONNERY, M. E., SARNACKI, S., TRUGNAN, G., BOUDJEMAA, S. & AUDRY, G. 2013. Enteric nervous system impairment in gastroschisis. *Eur J Pediatr Surg*, 23, 29-38.
- BADILLO, A. T., HEDRICK, H. L., WILSON, R. D., DANZER, E., BEBBINGTON, M. W., JOHNSON, M. P., LIECHTY, K. W., FLAKE, A. W. & ADZICK, N. S. 2008. Prenatal ultrasonographic gastrointestinal abnormalities in fetuses with gastroschisis do not correlate with postnatal outcomes. *J Pediatr Surg*, 43, 647-53.
- BAMBA, S., LEE, C. Y., BRITAN, M., PRESTON, S. L., DIREKZE, N. C., POULSOM, R., ALISON, M. R., WRIGHT, N. A. & OTTO, W. R. 2006. Bone marrow transplantation ameliorates pathology in interleukin-10 knockout colitic mice. *J Pathol*, 209, 265-73.
- BARGY, F. & BEAUDOIN, S. 2014. Comprehensive developmental mechanisms in gastroschisis. *Fetal Diagn Ther*, 36, 223-30.
- BARRETT, A. N., ZIMMERMANN, B. G., WANG, D., HOLLOWAY, A. & CHITTY, L. S. 2011. Implementing Prenatal Diagnosis Based on Cell-Free Fetal DNA: Accurate Identification of Factors Affecting Fetal DNA Yield. *PLoS ONE*, 6, e25202.
- BAUD, D., LAUSMAN, A., ALFARAJ, M. A., SEAWARD, G., KINGDOM, J., WINDRIM, R., LANGER, J. C., KELLY, E. N. & RYAN, G. 2013. Expectant management compared with elective delivery at 37 weeks for gastroschisis. *Obstet Gynecol*, 121, 990-8.
- BAUMGARTNER, S., HOFMANN, K., CHIQUET-EHRISMANN, R. & BUCHER, P. 1998. The discoidin domain family revisited: new members from prokaryotes and a homology-based fold prediction. *Protein Sci*, 7, 1626-31.
- BEAUCHEMIN, R. R., JR., GARTNER, L. P. & PROVENZA, D. V. 1984. Alcohol induced cardiac malformations in the rat. *Anat Anz*, 155, 17-28.
- BECKETT, E. A., RO, S., BAYGUINOV, Y., SANDERS, K. M. & WARD, S. M. 2007. Kit signaling is essential for development and maintenance of interstitial cells of Cajal and electrical rhythmicity in the embryonic gastrointestinal tract. *Dev Dyn*, 236, 60-72.
- BEN-CHAIM, J., DOCIMO, S. G., JEFFS, R. D. & GEARHART, J. P. 1996. Bladder exstrophy from childhood into adult life. *J R Soc Med*, 89, 39p-46p.
- BENEDIKTSSON, R., CALDER, A. A., EDWARDS, C. R. & SECKL, J. R. 1997. Placental 11 beta-hydroxysteroid dehydrogenase: a key regulator of fetal glucocorticoid exposure. *Clin Endocrinol (Oxf)*, 46, 161-6.
- BERGHOLZ, R., BOETTCHER, M., REINSHAGEN, K. & WENKE, K. 2014. Complex gastroschisis is a different entity to simple gastroschisis affecting morbidity and mortality-a systematic review and meta-analysis. *J Pediatr Surg*, 49, 1527-32.
- BERGHOLZ, R., KREBS, T., WENKE, K., ANDREAS, T., TIEMANN, B., PAETZEL, J., JACOBSEN, B., FAHJE, R., SCHMITZ, C., MANN, O., ROTH, B., APPL, B. & HECHER, K. 2012. Fetoscopic management of gastroschisis in a lamb model. *Surg Endosc*, 26, 1412-6.
- BERNARDINI, N., SEGNANI, C., IPPOLITO, C., DE GIORGIO, R., COLUCCI, R., FAUSSONE-PELLEGRINI, M. S., CHIARUGI, M., CAMPANI, D.,

- CASTAGNA, M., MATTII, L., BLANDIZZI, C. & DOLFI, A. 2012. Immunohistochemical analysis of myenteric ganglia and interstitial cells of Cajal in ulcerative colitis. *J Cell Mol Med*, 16, 318-27.
- BETTINI, G., MURACCHINI, M., DELLA SALDA, L., PREZIOSI, R., MORINI, M., GUGLIELMINI, C., SANGUINETTI, V. & MARCATO, P. S. 2003. Hypertrophy of intestinal smooth muscle in cats. *Res Vet Sci*, 75, 43-53.
- BIARD, J. M., LU, H. Q., VANAMO, K., MAENHOUT, B., DE LANGHE, E., VERBEKEN, E. & DEPREST, J. 2004. Pulmonary effects of gastroschisis in a fetal rabbit model. *Pediatr Pulmonol*, 37, 99-103.
- BICKEL, M. 1993. The role of interleukin-8 in inflammation and mechanisms of regulation. *J Periodontol*, 64, 456-60.
- BITAR, K. N. 2003. Function of gastrointestinal smooth muscle: from signaling to contractile proteins. *Am J Med*, 115 Suppl 3A, 15s-23s.
- BITTENCOURT, D. G., BARRETO, M. W., FRANCA, W. M., GONCALVES, A., PEREIRA, L. A. & SBRAGIA, L. 2006. Impact of corticosteroid on intestinal injury in a gastroschisis rat model: morphometric analysis. *J Pediatr Surg*, 41, 547-53.
- BLENNERHASSETT, M. G., VIGNJEVIC, P., VERMILLION, D. L. & COLLINS, S. M. 1992. Inflammation causes hyperplasia and hypertrophy in smooth muscle of rat small intestine. *Am J Physiol*, 262, G1041-6.
- BOECKXSTAENS, G. E. & DE JONGE, W. J. 2009. Neuroimmune mechanisms in postoperative ileus. *Gut*, 58, 1300-11.
- BONNANS, C., CHOU, J. & WERB, Z. 2014. Remodelling the extracellular matrix in development and disease. *Nat Rev Mol Cell Biol*, 15, 786-801.
- BORNSTEIN, J. C., COSTA, M. & GRIDER, J. R. 2004. Enteric motor and interneuronal circuits controlling motility. *Neurogastroenterol Motil*, 16 Suppl 1, 34-8.
- BOUSQUET, J., JEFFERY, P. K., BUSSE, W. W., JOHNSON, M. & VIGNOLA, A. M. 2000. Asthma. From bronchoconstriction to airways inflammation and remodeling. *Am J Respir Crit Care Med*, 161, 1720-45.
- BRADNOCK, T. J., MARVEN, S., OWEN, A., JOHNSON, P., KURINCZUK, J. J., SPARK, P., DRAPER, E. S., KNIGHT, M. & BAPS, C. 2011. Gastroschisis: one year outcomes from national cohort study. *BMJ*, 343, d6749.
- BRENT, R. L. 2004. Environmental causes of human congenital malformations: the pediatrician's role in dealing with these complex clinical problems caused by a multiplicity of environmental and genetic factors. *Pediatrics*, 113, 957-68.
- BREWER, S. & WILLIAMS, T. 2004a. Finally, a sense of closure? Animal models of human ventral body wall defects. *Bioessays*, 26, 1307-21.
- BREWER, S. & WILLIAMS, T. 2004b. Loss of AP-2alpha impacts multiple aspects of ventral body wall development and closure. *Dev Biol*, 267, 399-417.
- BROWNING, K. N. & TRAVAGLI, R. A. 2014. Central nervous system control of gastrointestinal motility and secretion and modulation of gastrointestinal functions. *Compr Physiol*, 4, 1339-68.
- BRUHIN-FEICHTER, S., MEIER-RUGE, W., MARTUCCIELLO, G. & BRUDER, E. 2012. Connective tissue in gut development: a key player in motility and in intestinal desmosis. *Eur J Pediatr Surg*, 22, 445-59.
- BUGGE, M. 2012. Body stalk anomaly in Denmark during 20 years (1970-1989). *Am J Med Genet A*, 158a, 1702-8.
- BURC, L., VOLUMENIE, J.-L., DE LAGAUSIE, P., GUIBOURDENCHE, J., OURY, J.-F., VUILLARD, E., SIBONY, O., BLOT, P., SAIZOU, C. &

- LUTON, D. 2004. Amniotic fluid inflammatory proteins and digestive compounds profile in fetuses with gastroschisis undergoing amnioexchange. *BJOG: An International Journal of Obstetrics and Gynaecology*, 111, 292-297.
- BURGE, D. M. & ADE-AJAYI, N. 1997. Adverse outcome after prenatal diagnosis of gastroschisis: the role of fetal monitoring. *J Pediatr Surg*, 32, 441-4.
- BURNS, A. J. 2007. Disorders of interstitial cells of Cajal. *J Pediatr Gastroenterol Nutr*, 45 Suppl 2, S103-6.
- BURNS, A. J., HERBERT, T., WARD, S. M. & SANDERS, K. M. 1997. Interstitial cells of Cajal in the guinea-pig gastrointestinal tract as revealed by c-Kit immunohistochemistry. *Cell and Tissue Research*, 290, 11-20.
- BURNS, A. J., ROBERTS, R. R., BORNSTEIN, J. C. & YOUNG, H. M. 2009. Development of the enteric nervous system and its role in intestinal motility during fetal and early postnatal stages. *Semin Pediatr Surg*, 18, 196-205.
- BURREN, K. A., SAVERY, D., MASSA, V., KOK, R. M., SCOTT, J. M., BLOM, H. J., COPP, A. J. & GREENE, N. D. 2008. Gene-environment interactions in the causation of neural tube defects: folate deficiency increases susceptibility conferred by loss of Pax3 function. *Hum Mol Genet*, 17, 3675-85.
- BYRNE, J. L. & FELDKAMP, M. L. 2008. Seven-week embryo with gastroschisis, multiple anomalies, and physiologic hernia suggests early onset of gastroschisis. *Birth Defects Res A Clin Mol Teratol*, 82, 236-8.
- CAIN, M. A., SALEMI, J. L., PAUL TANNER, J., MOGOS, M. F., KIRBY, R. S., WHITEMAN, V. E. & SALIHU, H. M. 2014. Perinatal outcomes and hospital costs in gastroschisis based on gestational age at delivery. *Obstet Gynecol*, 124, 543-50.
- CARNAGHAN, H., BAUD, D., LAPIDUS-KROL, E., RYAN, G., SHAH, P. S., PIERRO, A. & EATON, S. 2016. Effect of gestational age at birth on neonatal outcomes in gastroschisis. *J Pediatr Surg*, 51, 734-8.
- CARNAGHAN, H., JESUDASON, E. & MINIATI, D. 2009. Mechanical compression with secondary ischemia as a possible cause of atresias associated with omphalocele. *J Pediatr Surg*, 44, e9-e11.
- CARNAGHAN, H., ONG, E., HORN, V., PIERRO, A. & EATON, S. 2012. The Long-Term Impact of Parenteral Nutrition on Growth in Surgical Infants. *Presented at International Conference on Nutrition & Growth, Paris, France.*
- CARNAGHAN, H., PEREIRA, S., JAMES, C. P., CHARLESWORTH, P. B., GHIONZOLI, M., MOHAMED, E., CROSS, K. M., KIELY, E., PATEL, S., DESAI, A., NICOLAIDES, K., CURRY, J. I., ADE-AJAYI, N., DE COPPI, P., DAVENPORT, M., DAVID, A. L., PIERRO, A. & EATON, S. 2014. Is early delivery beneficial in gastroschisis? *J Pediatr Surg*, 49, 928-33.
- CASALS, J. B., PIERI, N. C. G., FEITOSA, M. L. T., ERCOLIN, A. C. M., ROBALLO, K. C. S., BARRETO, R. S. N., BRESSAN, F. F., MARTINS, D. S., A., M. M. & AMBROSIO, C. E. 2011. The Use of Animal Models for Stroke Research: A Review. *Comp Med*, 61, 305-313.
- CASSINOTTI, A., ANNALORO, C., ARDIZZONE, S., ONIDA, F., DELLA VOLPE, A., CLERICI, M., USARDI, P., GRECO, S., MACONI, G., PORRO, G. B. & DELILIERIS, G. L. 2008. Autologous haematopoietic stem cell transplantation without CD34+ cell selection in refractory Crohn's disease. *Gut*, 57, 211-7.

- CASTILLA, E. E., MASTROIACOVO, P. & ORIOLI, I. M. 2008. Gastroschisis: international epidemiology and public health perspectives. *Am J Med Genet C Semin Med Genet*, 148c, 162-79.
- CHARLESWORTH, P., AKINNOLA, I., HAMMERTON, C., PRAVEENA, P., DESAI, A., PATEL, S. & DAVENPORT, M. 2014. Preformed silos versus traditional abdominal wall closure in gastroschisis: 163 infants at a single institution. *Eur J Pediatr Surg*, 24, 88-93.
- CHARLESWORTH, P., NJERE, I., ALLOTEY, J., DIMITROU, G., ADE-AJAYI, N., DEVANE, S. & DAVENPORT, M. 2007. Postnatal outcome in gastroschisis: effect of birth weight and gestational age. *J Pediatr Surg*, 42, 815-8.
- CHEN, Z. H., ZHANG, Y. C., JIANG, W. F., YANG, C., ZOU, G. M., KONG, Y. & CAI, W. 2014. Characterization of interstitial Cajal progenitors cells and their changes in Hirschsprung's disease. *PLoS One*, 9, e86100.
- CHEUNG, C. Y. & BRACE, R. A. 2005. Amniotic fluid volume and composition in mouse pregnancy. *J Soc Gynecol Investig*, 12, 558-62.
- CHU, G., HAGHIGHI, K. & KRANIAS, E. G. 2002. From mouse to man: understanding heart failure through genetically altered mouse models. *J Card Fail*, 8, S432-49.
- CHURCH, M. W., ADAMS, B. R., ANUMBA, J. I., JACKSON, D. A., KRUGER, M. L. & JEN, K. L. 2012. Repeated antenatal corticosteroid treatments adversely affect neural transmission time and auditory thresholds in laboratory rats. *Neurotoxicol Teratol*, 34, 196-205.
- CIFTCI, A. O., TANYEL, F. C., ERCAN, M. T., KARNAK, I., BUYUKPAMUKCU, N. & HICSONMEZ, A. 1996. In utero defecation by the normal fetus: a radionuclide study in the rabbit. *J Pediatr Surg*, 31, 1409-12.
- CODE, C. F. & MARLETT, J. A. 1975. The interdigestive myo-electric complex of the stomach and small bowel of dogs. *J Physiol*, 246, 289-309.
- COLLINS, F. S., ROSSANT, J. & WURST, W. 2007. A mouse for all reasons. *Cell*, 128, 9-13.
- CONSORTIUM, H. M. P. 2012. Structure, function and diversity of the healthy human microbiome. *Nature*, 486, 207-14.
- CONTRO, E., FRATELLI, N., OKOYE, B., PAPAGEORGHIU, A., THILAGANATHAN, B. & BHIDE, A. 2010. Prenatal ultrasound in the prediction of bowel obstruction in infants with gastroschisis. *Ultrasound Obstet Gynecol*, 35, 702-7.
- CORAN, A. G., CALDAMONE, A., ADZICK, N. S., KRUMMEL, T. M., LABERGE, J.-M. & SHAMBERGER, R. 2012. *Pediatric Surgery 7th ed.*: Elsevier.
- CORREIA-PINTO, J., TAVARES, M. L., BAPTISTA, M. J., HENRIQUES-COELHO, T., ESTEVÃO-COSTA, J., FLAKE, A. W. & LEITE-MOREIRA, A. F. 2002. Meconium dependence of bowel damage in gastroschisis. *Journal of Pediatric Surgery*, 37, 31-35.
- CRANE, J., ARMSON, A., BRUNNER, M., DE LA RONDE, S., FARINE, D., KEENAN-LINDSAY, L., LEDUC, L., SCHNEIDER, C., VAN AERDE, J. & OPINION, S. C. 2003. Antenatal Corticosteroid Therapy for Fetal Maturation. *Journal of Obstetrics and Gynaecology Canada*, 25, 45-48.



- CRAWFORD, R., RYAN, G., WRIGHT, V. & RODECK, C. 1992. The importance of serial biophysical assessment of fetal wellbeing in gastroschisis. *British Journal of Obstetrics and Gynaecology* 99, 899-902.
- CREASY, R. K., RENIK, R., IAMS, J. D., LOCKWOOD, C. J. & MOORE, T. R. 2009. *Creasy and Resnik's Maternal-Fetal Medicine Principles and Practice*, Saunders Elsevier.
- CURRY, J., LANDER, A. & STRINGER, M. 2004. A multicenter, randomized, double-blind, placebo-controlled trial of the prokinetic agent erythromycin in the postoperative recovery of infants with gastroschisis. *Journal of pediatric surgery*, 39, 565-569.
- D'ANTONIO, F., VIRGONE, C., RIZZO, G., KHALIL, A., BAUD, D., COHEN-OVERBEEK, T. E., KULEVA, M., SALOMON, L. J., FLACCO, M. E., MANZOLI, L. & GIULIANI, S. 2015. Prenatal Risk Factors and Outcomes in Gastroschisis: A Meta-Analysis. *Pediatrics*, 136, e159-69.
- DALTON, B. G., GONZALEZ, K. W., REDDY, S. R., HENDRICKSON, R. J. & IQBAL, C. W. 2016. Improved outcomes for inborn babies with uncomplicated gastroschisis. *J Pediatr Surg*.
- DANZER, E., LAYNE, M. D., AUBER, F., SHEGU, S., KREIGER, P., RADU, A., VOLPE, M., ADZICK, N. S. & FLAKE, A. W. 2010. Gastroschisis in mice lacking aortic carboxypeptidase-like protein is associated with a defect in neuromuscular development of the eviscerated intestine. *Pediatric research*, 68, 23-28.
- DAVENPORT, M. & PIERRO, A. 2009. *Paediatric Surgery*, Oxford Medical Publications.
- DAVID, A. L., HOLLOWAY, A., THOMASSON, L., SYNGELAKI, A., NICOLAIDES, K., PATEL, R. R., SOMMERLAD, B., WILSON, A., MARTIN, W. & CHITTY, L. S. 2014. A case-control study of maternal periconceptual and pregnancy recreational drug use and fetal malformation using hair analysis. *PLoS One*, 9, e111038.
- DAVID, A. L., TAN, A. & CURRY, J. 2008. Gastroschisis: sonographic diagnosis, associations, management and outcome. *Prenatal Diagnosis*, 28.
- DE BEAUFORT, A. J., PELIKAN, D. M., ELFERINK, J. G. & BERGER, H. M. 1998. Effect of interleukin 8 in meconium on in-vitro neutrophil chemotaxis. *Lancet*, 352, 102-5.
- DE COPPI, P., BARTSCH, G., JR., SIDDIQUI, M. M., XU, T., SANTOS, C. C., PERIN, L., MOSTOSLAVSKY, G., SERRE, A. C., SNYDER, E. Y., YOO, J. J., FURTH, M. E., SOKER, S. & ATALA, A. 2007. Isolation of amniotic stem cell lines with potential for therapy. *Nat Biotechnol*, 25, 100-6.
- DEGRUTTOLA, A. K., LOW, D., MIZOGUCHI, A. & MIZOGUCHI, E. 2016. Current Understanding of Dysbiosis in Disease in Human and Animal Models. *Inflamm Bowel Dis*, 22, 1137-50.
- DELEMOS, R. A., SHERMETA, D. W., KNELSON, J. H., KOTAS, R. & AVERY, M. E. 1970. Acceleration of appearance of pulmonary surfactant in the fetal lamb by administration of corticosteroids. *Am Rev Respir Dis*, 102, 459-61.
- DELLA TORRE, M., HIBBARD, J. U., JEONG, H. & FISCHER, J. H. 2010. Betamethasone in pregnancy: influence of maternal body weight and multiple gestation on pharmacokinetics. *Am J Obstet Gynecol*, 203, 254 e1-12.
- DELOOSE, E., JANSSEN, P., DEPOORTERE, I. & TACK, J. 2012. The migrating motor complex: control mechanisms and its role in health and disease. *Nat Rev Gastroenterol Hepatol*, 9, 271-85.

- DEMIR, N., CANDA, M. T., KUDAY, S., OZTURK, C., SEZER, O. & DANAOGU, N. 2013. Ferritin and bile acid levels during the intrauterine pre-treatment of gastroschisis by serial amnioexchange. *J Turk Ger Gynecol Assoc*, 14, 53-5.
- DENNISON, F. A. 2016. Closed gastroschisis, vanishing midgut and extreme short bowel syndrome: Case report and review of the literature. *Ultrasound*, 24, 170-174.
- DER-SILAPHET, T., MALYSZ, J., HAGEL, S., LARRY ARSENAULT, A. & HUIZINGA, J. D. 1998. Interstitial cells of cajal direct normal propulsive contractile activity in the mouse small intestine. *Gastroenterology*, 114, 724-36.
- DER, T., BERCIK, P., DONNELLY, G., JACKSON, T., BEREZIN, I., COLLINS, S. M. & HUIZINGA, J. D. 2000. Interstitial cells of Cajal and inflammation-induced motor dysfunction in the mouse small intestine. *Gastroenterology*, 119, 1590-1599.
- DEVRIES, P. A. 1980. The pathogenesis of gastroschisis and omphalocele. *J Pediatr Surg*, 15, 245-51.
- DEY, N., WAGNER, V. E., BLANTON, L. V., CHENG, J., FONTANA, L., HAQUE, R., AHMED, T. & GORDON, J. I. 2015. Regulators of gut motility revealed by a gnotobiotic model of diet-microbiome interactions related to travel. *Cell*, 163, 95-107.
- DICKSON, B. C., STREUTKER, C. J. & CHETTY, R. 2006. Coeliac disease: an update for pathologists. *J Clin Pathol*, 59, 1008-16.
- DOMMERGUES, M., ANSKER, Y., AUBRY, M. C., MACALEESE, J., LORTAT-JACOB, S., NIHOUL-FEKETE, C. & DUMEZ, Y. 1996. Serial transabdominal amnioinfusion in the management of gastroschisis with severe oligohydramnios. *J Pediatr Surg*, 31, 1297-9.
- DONNELL, A. M., DOI, T., HOLLWARTH, M., KALICINSKI, P., CZAUDERNA, P. & PURI, P. 2008. Deficient alpha-smooth muscle actin as a cause of functional intestinal obstruction in childhood. *Pediatr Surg Int*, 24, 1191-5.
- DUDRICK, S. J. & PALESTY, J. A. 2011. Historical highlights of the development of total parenteral nutrition. *Surg Clin North Am*, 91, 693-717.
- DUHAMEL, B. 1963. Embryology of Exomphalos and Allied Malformations. *Arch Dis Child*, 38, 142-7.
- DUPONT, S., MORSUT, L., ARAGONA, M., ENZO, E., GIULITTI, S., CORDENONSI, M., ZANCONATO, F., LE DIGABEL, J., FORCATO, M., BICCIATO, S., ELVASSORE, N. & PICCOLO, S. 2011. Role of YAP/TAZ in mechanotransduction. *Nature*, 474, 179-83.
- EATON, S., ZANI, A., PIERRO, A. & DE COPPI, P. 2013. Stem cells as a potential therapy for necrotizing enterocolitis. *Expert Opin Biol Ther*, 13, 1683-9.
- ERDOGAN, D., AZILI, M. N., CAVUSOGLU, Y. H., TUNCER, I. S., KARAMAN, I., KARAMAN, A. & OZGUNER, I. F. 2012. 11-year experience with gastroschisis: factors affecting mortality and morbidity. *Iran J Pediatr*, 22, 339-43.
- FAUSSONE-PELLEGRINI, M. S., VANNUCCHI, M. G., ALAGGIO, R., STROJNA, A. & MIDRIO, P. 2007. Morphology of the interstitial cells of Cajal of the human ileum from foetal to neonatal life. *J Cell Mol Med*, 11, 482-94.
- FELDKAMP, M. L., CARMICHAEL, S. L., SHAW, G. M., PANICHELLO, J. D., MOORE, C. A. & BOTTO, L. D. 2011. Maternal nutrition and gastroschisis:

- findings from the National Birth Defects Prevention Study. *American Journal of Obstetrics and Gynecology*, 204.
- FISHER, C. J. & SAWYER, R. H. 1980. The effect of triamcinolone on the development of the bursa of Fabricius in chick embryos. *Teratology*, 22, 7-12.
- FOSTER, F. S., HOSSACK, J. & ADAMSON, S. L. 2011. Micro-ultrasound for preclinical imaging. *Interface Focus*, 1, 576-601.
- FOSTER, F. S., ZHANG, M. Y., ZHOU, Y. Q., LIU, G., MEHI, J., CHERIN, E., HARASIEWICZ, K. A., STARKOSKI, B. G., ZAN, L., KNAPIK, D. A. & ADAMSON, S. L. 2002. A new ultrasound instrument for in vivo microimaging of mice. *Ultrasound Med Biol*, 28, 1165-72.
- FRASCOLI, M., JEANTY, C., FLECK, S., MATTIS, A. N. & MACKENZIE, T. C. 2013. T Cell Activation and Infiltration in Patients with Gastroschisis: Similarities to Inflammatory Bowel Disease. *Presented at American Association of Pediatrics, Orlando, Florida*.
- GELAS, T., GORDUZA, D., DEVONEC, S., GAUCHERAND, P., DOWNHAM, E., CLARIS, O. & DUBOIS, R. 2008. Scheduled preterm delivery for gastroschisis improves postoperative outcome. *Pediatr Surg Int*, 24, 1023-9.
- GEST, T. 2002. *Primitive Gut Tube* [Online]. University of Michigan Medical School. Available: <http://www.med.umich.edu/lrc/coursepages/m1/embryology/embryo/10digestivesystem.htm>.
- GHIONZOLI, M., CANANZI, M., ZANI, A., ROSSI, C. A., LEON, F. F., PIERRO, A., EATON, S. & DE COPPI, P. 2010. Amniotic fluid stem cell migration after intraperitoneal injection in pup rats: implication for therapy. *Pediatr Surg Int*, 26, 79-84.
- GHIONZOLI, M., JAMES, C. P., DAVID, A. L., SHAH, D., TAN, A. W., ISKAROS, J., DRAKE, D. P., CURRY, J. I., KIELY, E. M., CROSS, K., EATON, S., DE COPPI, P. & PIERRO, A. 2012. Gastroschisis with intestinal atresia--predictive value of antenatal diagnosis and outcome of postnatal treatment. *J Pediatr Surg*, 47, 322-8.
- GILBERT, W. & BRACE, R. 1993. Amniotic fluid volume and normal flows to and from the amniotic cavity. *Seminars in Perinatology*, 17, 150-157.
- GILL, S. K., BROUSSARD, C., DEVINE, O., GREEN, R. F., RASMUSSEN, S. A. & REEFHUIS, J. 2012. Association between maternal age and birth defects of unknown etiology: United States, 1997-2007. *Birth Defects Res A Clin Mol Teratol*, 94, 1010-8.
- GOETZINGER, K. R., TUULI, M. G., LONGMAN, R. E., HUSTER, K. M., ODIBO, A. O. & CAHILL, A. G. 2014. Sonographic predictors of postnatal bowel atresia in fetal gastroschisis. *Ultrasound Obstet Gynecol*, 43, 420-5.
- GOMEZ-PINILLA, P. J., GIBBONS, S. J., BARDSLEY, M. R., LORINCZ, A., POZO, M. J., PASRICHA, P. J., DE RIJN, M. V., WEST, R. B., SARR, M. G. & KENDRICK, M. L. 2009. Anol1 is a selective marker of interstitial cells of Cajal in the human and mouse gastrointestinal tract. *American Journal of Physiology-Gastrointestinal and Liver Physiology*, 296, G1370-G1381.
- GOMIS-RUTH, F. X., COMPANYS, V., QIAN, Y., FRICKER, L. D., VENDRELL, J., AVILES, F. X. & COLL, M. 1999. Crystal structure of avian carboxypeptidase D domain II: a prototype for the regulatory metallopeptidase subfamily. *Embo j*, 18, 5817-26.

- GRAY, J., MARSH, P. J., STEWART, D. & PEDLER, S. J. 1994. Enterococcal bacteraemia: a prospective study of 125 episodes. *J Hosp Infect*, 27, 179-86.
- GRIJALVA, J. L., HUIZENGA, M., MUELLER, K., RODRIGUEZ, S., BRAZZO, J., CAMARGO, F., SADRI-VAKILI, G. & VAKILI, K. 2014. Dynamic alterations in Hippo signaling pathway and YAP activation during liver regeneration. *Am J Physiol Gastrointest Liver Physiol*, 307, G196-204.
- GROVES, R., SUNDERAJAN, L., KHAN, A. R., PARIKH, D., BRAIN, J. & SAMUEL, M. 2006. Congenital anomalies are commonly associated with exomphalos minor. *J Pediatr Surg*, 41, 358-61.
- GUIBOURDENCHE, J., BERREBI, D., VUILLARD, E., DE LAGAUSIE, P., AIGRAIN, Y., OURY, J. F. & LUTON, D. 2006. Biochemical investigations of bowel inflammation in gastroschisis. *Pediatr Res*, 60, 565-8.
- GUO, W., SWANIKER, F., FONKALSRUD, E. W., VO, K. & KARAMANOUKIAN, R. 1995. Effect of intraamniotic dexamethasone administration on intestinal absorption in a rabbit gastroschisis model. *Journal of pediatric surgery*, 30, 983-987.
- GUTOVA, M., ELIS, J. & RASKOVA, H. 1971. Teratogenic effect of 6-azauridine in rats. *Teratology*, 4, 287-94.
- GYNAECOLOGISTS, R. C. O. O. A. Oct 2010. Antenatal Corticosteroids to Reduce Neonatal Morbidity and Mortality.
- HAKGUDER, G., OLGUNER, M., GUREL, D., AKGUR, F. M. & FLAKE, A. W. 2011. Induction of fetal diuresis with intraamniotic furosemide injection reduces intestinal damage in a rat model of gastroschisis. *Eur J Pediatr Surg*, 21, 183-7.
- HARPER, L. M., GOETZINGER, K. R., BIGGIO, J. R. & MACONES, G. A. 2014. Timing of Elective Delivery in Gastroschisis: A Decision and Cost Effectiveness Analysis. *Ultrasound Obstet Gynecol*.
- HARRISON, M. R., LANGER, J. C., ADZICK, N. S., GOLBUS, M. S., FILLY, R. A., ANDERSON, R. L., ROSEN, M. A., CALLEN, P. W., GOLDSTEIN, R. B. & DELORIMIER, A. A. 1990. Correction of congenital diaphragmatic hernia in utero, V. Initial clinical experience. *J Pediatr Surg*, 25, 47-55; discussion 56-7.
- HARTLEBEN, B., WIDMEIER, E., WANNER, N., SCHMIDTS, M., KIM, S. T., SCHNEIDER, L., MAYER, B., KERJASCHKI, D., MINER, J. H., WALZ, G. & HUBER, T. B. 2012. Role of the polarity protein Scribble for podocyte differentiation and maintenance. *PLoS One*, 7, e36705.
- HARTSHOME, D. 1987. Biochemistry of the contractile process in smooth muscle. *Johnson L (ed) Physiology of the gastrointestinal tract, vol. 2nd edn, Raven Press, New York*, 423-482.
- HILL, S. J. & DURHAM, M. M. 2011. Management of cryptorchidism and gastroschisis. *J Pediatr Surg*, 46, 1798-803.
- HIRST, G. D., GARCIA-LONDONO, A. P. & EDWARDS, F. R. 2006. Propagation of slow waves in the guinea-pig gastric antrum. *J Physiol*, 571, 165-77.
- HOBBS, C. A., CHOWDHURY, S., CLEVES, M. A., ERICKSON, S., MACLEOD, S. L., SHAW, G. M., SHETE, S., WITTE, J. S. & TYCKO, B. 2014. Genetic epidemiology and nonsyndromic structural birth defects: from candidate genes to epigenetics. *JAMA Pediatr*, 168, 371-7.
- HOFFMAN, D. J. & MOORE, J. M. 1979. Teratogenic effects of external egg applications of methyl mercury in the mallard, *Anas platyrhynchos*. *Teratology*, 20, 453-61.

- HOGAN, B. L. 1996. Bone morphogenetic proteins: multifunctional regulators of vertebrate development. *Genes Dev*, 10, 1580-94.
- HOLLISTER, E. B., RIEHLE, K., LUNA, R. A., WEIDLER, E. M., RUBIO-GONZALES, M., MISTRETTA, T. A., RAZA, S., DODDAPANENI, H. V., METCALF, G. A., MUZNY, D. M., GIBBS, R. A., PETROSINO, J. F., SHULMAN, R. J. & VERSALOVIC, J. 2015. Structure and function of the healthy pre-adolescent pediatric gut microbiome. *Microbiome*, 3, 36.
- HOMBALKAR, N. N., RAFF, A. & PRAKASH, G. D. 2015. Left-sided gastroschisis with caecal agenesis: A rare case report. *Afr J Paediatr Surg*, 12, 74-5.
- HOUBEN, C., DAVENPORT, M., ADE-AJAYI, N., FLACK, N. & PATEL, S. 2009. Closing gastroschisis: diagnosis, management, and outcomes. *J Pediatr Surg*, 44, 343-7.
- HOW, H. Y., HARRIS, B. J., PIETRANTONI, M., EVANS, J. C., DUTTON, S., KHOURY, J. & SIDDIQI, T. A. 2000. Is vaginal delivery preferable to elective cesarean delivery in fetuses with a known ventral wall defect? *Am J Obstet Gynecol*, 182, 1527-34.
- HOYME, H. E., HIGGINBOTTOM, M. C. & JONES, K. L. 1981. The vascular pathogenesis of gastroschisis: intrauterine interruption of the omphalomesenteric artery. *J Pediatr*, 98, 228-31.
- HOYME, H. E., JONES, K. L., DIXON, S. D., JEWETT, T., HANSON, J. W., ROBINSON, L. K., MSALL, M. E. & ALLANSON, J. E. 1990. Prenatal cocaine exposure and fetal vascular disruption. *Pediatrics*, 85, 743-7.
- HUH, N. G., HIROSE, S. & GOLDSTEIN, R. B. 2010. Prenatal intraabdominal bowel dilation is associated with postnatal gastrointestinal complications in fetuses with gastroschisis. *Am J Obstet Gynecol*, 202, 396 e1-6.
- HUIZINGA, J. D. & CHEN, J. H. 2014. Interstitial cells of Cajal: update on basic and clinical science. *Curr Gastroenterol Rep*, 16, 363.
- HUSEBYE, E. 1999. The patterns of small bowel motility: physiology and implications in organic disease and functional disorders. *Neurogastroenterol Motil*, 11, 141-61.
- IZRAELI, S., FREUD, E., MOR, C., LITWIN, A., ZER, M. & MERLOB, P. 1992. Neonatal intestinal perforation due to congenital defects in the intestinal muscularis. *Eur J Pediatr*, 151, 300-3.
- JANDHYALA, S. M., TALUKDAR, R., SUBRAMANYAM, C., VUYYYURU, H., SASIKALA, M. & NAGESHWAR REDDY, D. 2015. Role of the normal gut microbiota. *World J Gastroenterol*, 21, 8787-803.
- JAPARAJ, R. P., HOCKEY, R. & CHAN, F. Y. 2003. Gastroschisis: can prenatal sonography predict neonatal outcome? *Ultrasound Obstet Gynecol*, 21, 329-33.
- JAUNIAUX, E. & GULBIS, B. 2000. Fluid compartments of the embryonic environment. *Hum Reprod Update*, 6, 268-78.
- JOLIN-DAHEL, K., FERRETTI, E., MONTIVEROS, C., GRENON, R., BARROWMAN, N. & JIMENEZ-RIVERA, C. 2013. Parenteral nutrition-induced cholestasis in neonates: where does the problem lie? *Gastroenterol Res Pract*, 2013, 163632.
- K, V. S., MAMMEN, A. & VARMA, K. K. 2015. Pathogenesis of bladder exstrophy: A new hypothesis. *J Pediatr Urol*.
- KALFF, J. C., BUCHHOLZ, B. M., ESKANDARI, M. K., HIERHOLZER, C., SCHRAUT, W. H., SIMMONS, R. L. & BAUER, A. J. 1999a. Biphasic

- response to gut manipulation and temporal correlation of cellular infiltrates and muscle dysfunction in rat. *Surgery*, 126, 498-509.
- KALFF, J. C., CARLOS, T. M., SCHRAUT, W. H., BILLIAR, T. R., SIMMONS, R. L. & BAUER, A. J. 1999b. Surgically induced leukocytic infiltrates within the rat intestinal muscularis mediate postoperative ileus. *Gastroenterology*, 117, 378-87.
- KALFF, J. C., SCHRAUT, W. H., SIMMONS, R. L. & BAUER, A. J. 1998. Surgical manipulation of the gut elicits an intestinal muscularis inflammatory response resulting in postsurgical ileus. *Ann Surg*, 228, 652-63.
- KANAGAWA, T., TOMIMATSU, T., HAYASHI, S., SHIOJI, M., FUKUDA, H., SHIMOYA, K. & MURATA, Y. 2006. The effects of repeated corticosteroid administration on the neurogenesis in the neonatal rat. *Am J Obstet Gynecol*, 194, 231-8.
- KAPUR, R. P., YOST, C. & PALMITER, R. D. 1992. A transgenic model for studying development of the enteric nervous system in normal and aganglionic mice. *Development*, 116, 167-75.
- KASSA, A. M. & LILJA, H. E. 2011. Predictors of postnatal outcome in neonates with gastroschisis. *J Pediatr Surg*, 46, 2108-14.
- KAUFMAN, M. H. & BARD, J. B. L. 1999. the Anatomical Basis of Mouse Development *Academic Press, San Diego*, 28-30.
- KESSLER, E., TAKAHARA, K., BINIAMINOV, L., BRUSEL, M. & GREENSPAN, D. S. 1996. Bone morphogenetic protein-1: the type I procollagen C-proteinase. *Science*, 271, 360-2.
- KEYS, C., DREWETT, M. & BURGE, D. M. 2008. Gastroschisis: the cost of an epidemic. *J Pediatr Surg*, 43, 654-7.
- KHALIL, A. 2012. Report on the 11th World Congress in Fetal Medicine, 24-28 June 2012, Kos, Greece. *Ultrasound Obstet Gynecol*, 40, 489-94.
- KILBY, M. D. 2006. The incidence of gastroschisis: Is increasing in the UK, particularly among babies of young mothers. *BMJ: British Medical Journal*, 332, 250.
- KIRBY, R. S., MARSHALL, J., TANNER, J. P., SALEMI, J. L., FELDKAMP, M. L., MARENCO, L., MEYER, R. E., DRUSCHEL, C. M., RICKARD, R. & KUCIK, J. E. 2013. Prevalence and correlates of gastroschisis in 15 states, 1995 to 2005. *Obstet Gynecol*, 122, 275-81.
- KLOCKE, R., TIAN, W., KUHLMANN, M. T. & NIKOL, S. 2007. Surgical animal models of heart failure related to coronary heart disease. *Cardiovasc Res*, 74, 29-38.
- KNOWLES, C. H., SILK, D. B., DARZI, A., VERESS, B., FEAKINS, R., RAIMUNDO, A. H., CROMPTON, T., BROWNING, E. C., LINDBERG, G. & MARTIN, J. E. 2004. Deranged smooth muscle alpha-actin as a biomarker of intestinal pseudo-obstruction: a controlled multinational case series. *Gut*, 53, 1583-9.
- KOGA, Y., HAYASHIDA, Y., IKEDA, K., INOKUCHI, K. & HASHIMOTO, N. 1975. Intestinal atresia in fetal dogs produced by localized ligation of mesenteric vessels. *J Pediatr Surg*, 10, 949-53.
- KOH, S., BRADLEY, R. F., FRENCH, S. W., FARMER, D. G. & CORTINA, G. 2008. Congenital visceral myopathy with a predominantly hypertrophic pattern treated by multivisceral transplantation. *Hum Pathol*, 39, 970-4.
- KOHL, T., TCHATCHEVA, K., STRESSIG, R., GEMBRUCH, U. & KAHL, P. 2009. Is there a therapeutic role for fetoscopic surgery in the prenatal

- treatment of gastroschisis? A feasibility study in sheep. *Surg Endosc*, 23, 1499-505.
- KOMURO, T. 2006. Structure and organization of interstitial cells of Cajal in the gastrointestinal tract. *J Physiol*, 576, 653-8.
- KOTAS, R. V. & AVERY, M. E. 1971. Accelerated appearance of pulmonary surfactant in the fetal rabbit. *J Appl Physiol*, 30, 358-61.
- KRANZHOFFER, R., SCHMIDT, J., PFEIFFER, C. A., HAGL, S., LIBBY, P. & KUBLER, W. 1999. Angiotensin induces inflammatory activation of human vascular smooth muscle cells. *Arterioscler Thromb Vasc Biol*, 19, 1623-9.
- KREBS, T., BOETTCHER, M., SCHAFER, H., ESCHENBURG, G., WENKE, K., APPL, B., ROTH, B., ANDREAS, T., SCHMITZ, C., FAHJE, R., JACOBSEN, B., TIEMANN, B., REINSHAGEN, K., HECHER, K. & BERGHOLZ, R. 2014. Gut inflammation and expression of ICC in a fetal lamb model of fetoscopic intervention for gastroschisis. *Surg Endosc*, 28, 2437-42.
- KUNZ, S. N., TIEDER, J. S., WHITLOCK, K., JACKSON, J. C. & AVANSINO, J. R. 2013. Primary fascial closure versus staged closure with silo in patients with gastroschisis: a meta-analysis. *J Pediatr Surg*, 48, 845-57.
- LABERGE, J. M. 1986. Fetal Surgery. *College of Family Physicians of Canada*, 32, 2099-2103.
- LAI, S., YU, W., WALLACE, L. & SIGALET, D. 2014. Intestinal muscularis propria increases in thickness with corrected gestational age and is focally attenuated in patients with isolated intestinal perforations. *J Pediatr Surg*, 49, 114-9.
- LAM, P. K. & TORFS, C. P. 2006. Interaction between maternal smoking and malnutrition in infant risk of gastroschisis. *Birth Defects Research Part A-Clinical and Molecular Teratology*, 76, 182-186.
- LANGER, J. C., KHANNA, J., CACO, C., DYKES, E. H. & NICOLAIDES, K. 1993. Prenatal diagnosis of gastroschisis: Development of objective sonographic criteria for predicting outcome. *Obstetrics & Gynecology*, 81, 53-56.
- LANGER, J. C., LONGAKER, M. T., CROMBLEHOLME, T. M., BOND, S. J., FINKBEINER, W. E., RUDOLPH, C. A., VERRIER, E. D. & HARRISON, M. R. 1989. Etiology of intestinal damage in gastroschisis. I: Effects of amniotic fluid exposure and bowel constriction in a fetal lamb model. *J Pediatr Surg*, 24, 992-7.
- LARSEN, W. J. 1997. *Human Embryology*, Hong Kong, Churchill Livingstone.
- LAWSON, A. & DE LA HUNT, M. N. 2001. Gastroschisis and undescended testis. *J Pediatr Surg*, 36, 366-7.
- LAYNE, M. D., YET, S. F., MAEMURA, K., HSIEH, C. M., BERNFIELD, M., PERRELLA, M. A. & LEE, M. E. 2001. Impaired abdominal wall development and deficient wound healing in mice lacking aortic carboxypeptidase-like protein. *Mol Cell Biol*, 21, 5256-61.
- LEGAKI, E., ROUBELAKIS, M. G., THEODOROPOULOS, G. E., LAZARIS, A., KOLLIA, A., KARAMANOLIS, G., MARINOS, E. & GAZOULI, M. 2016. Therapeutic Potential of Secreted Molecules Derived from Human Amniotic Fluid Mesenchymal Stem/Stroma Cells in a Mice Model of Colitis. *Stem Cell Rev*, 12, 604-612.

- LEPIGEON, K., VAN MIEGHEM, T., VASSEUR MAURER, S., GIANNONI, E. & BAUD, D. 2014. Gastroschisis--what should be told to parents? *Prenat Diagn*, 34, 316-26.
- LI, S. W., SIERON, A. L., FERTALA, A., HOJIMA, Y., ARNOLD, W. V. & PROCKOP, D. J. 1996. The C-proteinase that processes procollagens to fibrillar collagens is identical to the protein previously identified as bone morphogenic protein-1. *Proc Natl Acad Sci U S A*, 93, 5127-30.
- LIGGINS, G. & HOWIE, R. 1972. A controlled trial of antepartum glucocorticoid treatment for prevention of the respiratory distress syndrome in premature infants. *Pediatrics*, 50, 515-525.
- LIGGINS, G. C. 1969. Premature delivery of foetal lambs infused with glucocorticoids. *J Endocrinol*, 45, 515-23.
- LIU, X., KIM, A. J., REYNOLDS, W. & WU, Y. 2017. Phenotyping cardiac and structural birth defects in fetal and newborn mice. 109, 778-790.
- LOANE, M., DOLK, H., KELLY, A., TELJEUR, C., GREENLEES, R. & DENSEM, J. 2011. Paper 4: EUROCAT statistical monitoring: identification and investigation of ten year trends of congenital anomalies in Europe. *Birth Defects Res A Clin Mol Teratol*, 91 Suppl 1, S31-43.
- LOCKWOOD, C. J., SCIOSCIA, A. L. & HOBBS, J. C. 1986. Congenital absence of the umbilical cord resulting from maldevelopment of embryonic body folding. *Am J Obstet Gynecol*, 155, 1049-51.
- LOGGHE, H. L., MASON, G. C., THORNTON, J. G. & STRINGER, M. D. 2005. A randomized controlled trial of elective preterm delivery of fetuses with gastroschisis. *J Pediatr Surg*, 40, 1726-31.
- LOUKOGEORGAKIS, S. P. & FLAKE, A. W. 2014. In utero stem cell and gene therapy: current status and future perspectives. *Eur J Pediatr Surg*, 24, 237-45.
- LOUW, J. H. & BARNARD, C. N. 1955. Congenital intestinal atresia; observations on its origin. *Lancet*, 269, 1065-7.
- LOW, B. C., PAN, C. Q., SHIVASHANKAR, G. V., BERSHADSKY, A., SUDOL, M. & SHEETZ, M. 2014. YAP/TAZ as mechanosensors and mechanotransducers in regulating organ size and tumor growth. *FEBS Lett*, 588, 2663-70.
- LUTON, D., DE LAGAUSIE, P., GUIBOURDENCHE, J., OURY, J., SIBONY, O., VUILLARD, E., BOISSINOT, C., AIGRAIN, Y., BEAUFILS, F., NAVARRO, J. & BLOT, P. 1999. Effect of amnioinfusion on the outcome of prenatally diagnosed gastroschisis. *Fetal Diagn Ther*, 14, 152-5.
- LUTON, D., GUIBOURDENCHE, J., VUILLARD, E., BRUNER, J. & DE LAGAUSIE, P. 2003. Prenatal management of gastroschisis: the place of the amnioexchange procedure. *Clin Perinatol*, 30, 551-72, viii.
- LYNCH, S. V. & PEDERSEN, O. 2016. The Human Intestinal Microbiome in Health and Disease. *N Engl J Med*, 375, 2369-2379.
- MAEDA, H., YAMAGATA, A., NISHIKAWA, S., YOSHINAGA, K., KOBAYASHI, S., NISHI, K. & NISHIKAWA, S. 1992. Requirement of c-kit for development of intestinal pacemaker system. *Development*, 116.
- MARAMREDDY, H., FISHER, J., SLIM, M., LAGAMMA, E. F. & PARVEZ, B. 2009. Delivery of gastroschisis patients before 37 weeks of gestation is associated with increased morbidities. *J Pediatr Surg*, 44, 1360-6.
- MASTROIACOVO, P., LISI, A., CASTILLA, E. E., MARTINEZ-FRIAS, M. L., BERMEJO, E., MARENGO, L., KUCIK, J., SIFFEL, C., HALLIDAY, J.,



- GATT, M., ANNEREN, G., BIANCHI, F., CANESSA, M. A., DANDERFER, R., DE WALLE, H., HARRIS, J., LI, Z., LOWRY, R. B., MCDONELL, R., MERLOB, P., METNEKI, J., MUTCHINICK, O., ROBERT-GNANSIA, E., SCARANO, G., SIPEK, A., POTZSCH, S., SZABOVA, E. & YEVTUSHOK, L. 2007. Gastroschisis and associated defects: an international study. *Am J Med Genet A*, 143a, 660-71.
- MATSUMARU, D., HARAGUCHI, R., MIYAGAWA, S., MOTOYAMA, J., NAKAGATA, N., MEIJLINK, F. & YAMADA, G. 2011. Genetic analysis of Hedgehog signaling in ventral body wall development and the onset of omphalocele formation. *PLoS One*, 6, e16260.
- MCBRIDE, W. G., VARDY, P. H. & FRENCH, J. 1982. Effects of scopolamine hydrobromide on the development of the chick and rabbit embryo. *Aust J Biol Sci*, 35, 173-8.
- MCCLELLAN, E. B., SHEW, S. B., LEE, S. S., DUNN, J. C. & DEUGARTE, D. A. 2011. Liver herniation in gastroschisis: incidence and prognosis. *J Pediatr Surg*, 46, 2115-8.
- MEARS, A. L., SADIQ, J. M., IMPEY, L. & LAKHOO, K. 2010. Antenatal bowel dilatation in gastroschisis: a bad sign? *Pediatr Surg Int*, 26, 581-8.
- MEYER, M. R., SHAFFER, B. L., DOSS, A. E., CAHILL, A. G., SNOWDEN, J. M. & CAUGHEY, A. B. 2014. Prospective risk of fetal death with gastroschisis. *J Matern Fetal Neonatal Med*, 1-4.
- MEYER, M. R., SHAFFER, B. L., DOSS, A. E., CAHILL, A. G., SNOWDEN, J. M. & CAUGHEY, A. B. 2015. Prospective risk of fetal death with gastroschisis. *J Matern Fetal Neonatal Med*, 28, 2126-9.
- MICHALOPOULOS, G. K. 2007. Liver regeneration. *J Cell Physiol*, 213, 286-300.
- MIDRIO, P., ALAGGIO, R., STROJNA, A., GAMBA, P., GIACOMELLI, L., PIZZI, S. & FAUSSONE-PELLEGRINI, M. S. 2010. Reduction of interstitial cells of Cajal in esophageal atresia. *J Pediatr Gastroenterol Nutr*, 51, 610-7.
- MIDRIO, P., FAUSSONE-PELLEGRINI, M. S., VANNUCCHI, M. G. & FLAKE, A. W. 2004. Gastroschisis in the rat model is associated with a delayed maturation of intestinal pacemaker cells and smooth muscle cells. *Journal of Pediatric Surgery*, 39, 1541-1547.
- MIDRIO, P., STEFANUTTI, G., MUSSAP, M., D'ANTONA, D., ZOLPI, E. & GAMBA, P. 2007. Amnioexchange for fetuses with gastroschisis: is it effective? *J Pediatr Surg*, 42, 777-82.
- MIDRIO, P., VANNUCCHI, M. G., PIERI, L., ALAGGIO, R. & FAUSSONE-PELLEGRINI, M. S. 2008. Delayed development of interstitial cells of Cajal in the ileum of a human case of gastroschisis. *Journal of cellular and molecular medicine*, 12, 471-478.
- MIKKELSEN, H., MALYSZ, J., HUIZINGA, J. D. & THUNEBERG, L. 1998. Action potential generation, Kit receptor immunohistochemistry and morphology of steel-Dickie (Sl/Sld) mutant mouse small intestine. *neurogastroenterology and motility*, 10, 11-26.
- MILLER, S. A. 1982. Differential proliferation in morphogenesis of lateral body folds. *J Exp Zool*, 221, 205-11.
- MIRZA, F. G., BAUER, S. T., VAN DER VEER, A. & SIMPSON, L. L. 2015. Gastroschisis: incidence and prediction of growth restriction. *J Perinat Med*, 43, 605-8.

- MOIR, C. R., RAMSEY, P. S., OGBURN, P. L., JOHNSON, R. V. & RAMIN, K. D. 2004. A prospective trial of elective preterm delivery for fetal gastroschisis. *Am J Perinatol*, 21, 289-94.
- MOLDENHAUER, J. S. & ADZICK, N. S. 2017. Fetal surgery for myelomeningocele: After the Management of Myelomeningocele Study (MOMS). *Semin Fetal Neonatal Med*, 22, 360-366.
- MOORE-OLUFEMI, S. D., OLSEN, A. B., HOOK-DUFRESNE, D. M., BANDLA, V. & COX, C. S., JR. 2015. Transforming growth factor-Beta 3 alters intestinal smooth muscle function: implications for gastroschisis-related intestinal dysfunction. *Dig Dis Sci*, 60, 1206-14.
- MOORE, K. L. & DALLEY, A. F. 1999. *Clinically Oriented Anatomy*, Lippincott Williams & Wilkins.
- MOORE, S. W., SCHNEIDER, J. W. & KASCHULA, R. O. 2002. Unusual variations of gastrointestinal smooth muscle abnormalities associated with chronic intestinal pseudo-obstruction. *Pediatr Surg Int*, 18, 13-20.
- MOORE, T. C., COLLINS, D. L., CATANZARITE, V. & HATCH, E. I., JR. 1999. Pre-term and particularly pre-labor cesarean section to avoid complications of gastroschisis. *Pediatr Surg Int*, 15, 97-104.
- MORRISON, J. J., KLEIN, N., CHITTY, L. S., KOCJAN, G., WALSH, D., GOULDING, M., GEARY, M. P., PIERRO, A. & RODECK, C. H. 1998. Intra-amniotic inflammation in human gastroschisis: possible aetiology of postnatal bowel dysfunction. *Br J Obstet Gynaecol*, 105, 1200-4.
- MORRISS, F. H., MOORE, M., WEISBRODT, N. W. & WEST, M. S. 1986. Ontogenic development of gastrointestinal motility: IV. Duodenal contractions in preterm infants. *Pediatrics*, 78, 1106-1113.
- MOSS, T. J. M., DOHERTY, D. A., NITSOS, I., HARDING, R. & NEWNHAM, J. P. 2003. Pharmacokinetics of betamethasone after maternal or fetal intramuscular administration. *American Journal of Obstetrics and Gynecology*, 189, 1751-1757.
- MOUSTY, E., CHALOUHI, G. E., EL SABBAGH, A., KHEN-DUNLOP, N., KULEVA, M., SALOMON, L. J. & VILLE, Y. 2012. Secondary bladder herniation in isolated gastroschisis justifies increased surveillance. *Prenat Diagn*, 32, 888-92.
- MULVIHILL, S. J., STONE, M. M., FONKALSRUD, E. W. & DEBAS, H. T. 1986. Trophic effect of amniotic fluid on fetal gastrointestinal development. *J Surg Res*, 40, 291-6.
- MURDOCH, J. N. 2003. Disruption of scribble (Scrb1) causes severe neural tube defects in the circletail mouse. *Human Molecular Genetics*, 12, 87-98.
- MURPHY, E. M., DEFONTGALLAND, D., COSTA, M., BROOKES, S. J. & WATTCHOW, D. A. 2007a. Quantification of subclasses of human colonic myenteric neurons by immunoreactivity to Hu, choline acetyltransferase and nitric oxide synthase. *Neurogastroenterol Motil*, 19, 126-34.
- MURPHY, K. E., HANNAH, M. E., WILLAN, A. R., HEWSON, S. A., OHLSSON, A., KELLY, E. N., MATTHEWS, S. G., SAIGAL, S., ASZTALOS, E., ROSS, S., DELISLE, M. F., AMANKWAH, K., GUSELLE, P., GAFNI, A., LEE, S. K. & ARMSON, B. A. 2008. Multiple courses of antenatal corticosteroids for preterm birth (MACS): a randomised controlled trial. *Lancet*, 372, 2143-51.

- MURPHY, V. E., FITTOCK, R. J., ZARZYCKI, P. K., DELAHUNTY, M. M., SMITH, R. & CLIFTON, V. L. 2007b. Metabolism of synthetic steroids by the human placenta. *Placenta*, 28, 39-46.
- NAGY, A. 2000. Cre recombinase: the universal reagent for genome tailoring. *Genesis*, 26, 99-109.
- NAIR, D. G., MILLER, K. G., LOURENSSEN, S. R. & BLENNERHASSETT, M. G. 2014. Inflammatory cytokines promote growth of intestinal smooth muscle cells by induced expression of PDGF-Rbeta. *J Cell Mol Med*, 18, 444-54.
- NICE 2013. Faecal calprotectin diagnostic tests for inflammatory diseases of the bowel. . *NICE Diagnostics Guidance*, nice.org.uk/guidance/dg11.
- NICHOL, P. F., CORLISS, R. F., YAMADA, S., SHIOTA, K. & SAJJOH, Y. 2012. Muscle patterning in mouse and human abdominal wall development and omphalocele specimens of humans. *Anat Rec (Hoboken)*, 295, 2129-40.
- NICK, A. M., BRUNER, J. P., MOSES, R., YANG, E. Y. & SCOTT, T. A. 2006. Second-trimester intra-abdominal bowel dilation in fetuses with gastroschisis predicts neonatal bowel atresia. *Ultrasound Obstet Gynecol*, 28, 821-5.
- NIEMAN, B. J. & TURNBULL, D. H. 2010. Ultrasound and magnetic resonance microimaging of mouse development. *Methods Enzymol*, 476, 379-400.
- NORBERG, H., STALNACKE, J., NORDENSTROM, A. & NORMAN, M. 2013. Repeat antenatal steroid exposure and later blood pressure, arterial stiffness, and metabolic profile. *J Pediatr*, 163, 711-6.
- NORRIS, F. C., MODAT, M., CLEARY, J. O., PRICE, A. N., MCCUE, K., SCAMBLER, P. J., OURSELIN, S. & LYTHGOE, M. F. 2013a. Segmentation propagation using a 3D embryo atlas for high-throughput MRI phenotyping: comparison and validation with manual segmentation. *Magn Reson Med*, 69, 877-83.
- NORRIS, F. C., WONG, M. D., GREENE, N. D., SCAMBLER, P. J., WEAVER, T., WENINGER, W. J., MOHUN, T. J., HENKELMAN, R. M. & LYTHGOE, M. F. 2013b. A coming of age: advanced imaging technologies for characterising the developing mouse. *Trends Genet*, 29, 700-11.
- O'RAHILLY, R. 1979. Early human development and the chief sources of information on staged human embryos. *Eur J Obstet Gynecol Reprod Biol*, 9, 273-80.
- OKAMOTO, R., YAJIMA, T., YAMAZAKI, M., KANAI, T., MUKAI, M., OKAMOTO, S., IKEDA, Y., HIBI, T., INAZAWA, J. & WATANABE, M. 2002. Damaged epithelia regenerated by bone marrow-derived cells in the human gastrointestinal tract. *Nat Med*, 8, 1011-7.
- OLGUNER, M., HAKGUDER, G., ATES, O., CAGLAR, M., OZER, E. & AKGUR, F. M. 2006. Urinary trypsin inhibitor present in fetal urine prevents intraamniotic meconium-induced intestinal damage in gastroschisis. *J Pediatr Surg*, 41, 1407-12.
- OVERCASH, R. T., DEUGARTE, D. A., STEPHENSON, M. L., GUTKIN, R. M., NORTON, M. E., PARMAR, S., PORTO, M., POULAIN, F. R. & SCHRIMMER, D. B. 2014. Factors associated with gastroschisis outcomes. *Obstet Gynecol*, 124, 551-7.
- OVERTON, T. G., PIERCE, M. R., GAO, H., KURINCZUK, J. J., SPARK, P., DRAPER, E. S., MARVEN, S., BROCKLEHURST, P. & KNIGHT, M. 2012. Antenatal management and outcomes of gastroschisis in the U.K. *Prenat Diagn*, 32, 1256-62.

- OYACHI, N., LAKSHMANAN, J., ROSS, M. G. & ATKINSON, J. B. 2004. Fetal gastrointestinal motility in a rabbit model of gastroschisis. *Journal of pediatric surgery*, 39, 366-370.
- PADMANABHAN, R. 1998. Retinoic acid-induced caudal regression syndrome in the mouse fetus. *Reprod Toxicol*, 12, 139-51.
- PALOMAKI, G. E., HILL, L. E., KNIGHT, G. J., HADDOW, J. E. & CARPENTER, M. 1988. Second-trimester maternal serum alpha-fetoprotein levels in pregnancies associated with gastroschisis and omphalocele. *Obstet Gynecol*, 71, 906-9.
- PAMPFER, S. & STREFFER, C. 1988. Prenatal death and malformations after irradiation of mouse zygotes with neutrons or X-rays. *Teratology*, 37, 599-607.
- PANCHENKO, M. V., STETLER-STEVENSON, W. G., TRUBETSKOY, O. V., GACHERU, S. N. & KAGAN, H. M. 1996. Metalloproteinase activity secreted by fibrogenic cells in the processing of prollysyl oxidase. Potential role of procollagen C-proteinase. *J Biol Chem*, 271, 7113-9.
- PARANJOTHY, S., BROUGHTON, H., EVANS, A., HUDDART, S., DRAYTON, M., JEFFERSON, R., RANKIN, J., DRAPER, E., CAMERON, A. & PALMER, S. R. 2012. The role of maternal nutrition in the aetiology of gastroschisis: an incident case-control study. *Int J Epidemiol*, 41, 1141-52.
- PAUL, C., ZOSMER, N., JURKOVIC, D. & NICOLAIDES, K. 2001. A case of body stalk anomaly at 10 weeks of gestation. *Ultrasound Obstet Gynecol*, 17, 157-9.
- PAYNE, N. R., SIMONTON, S. C., OLSEN, S., ARNESEN, M. A. & PFLEGHAAR, K. M. 2011. Growth restriction in gastroschisis: quantification of its severity and exploration of a placental cause. *BMC Pediatr*, 11, 90.
- PEARSON, H. B., PEREZ-MANCERA, P. A., DOW, L. E., RYAN, A., TENNSTEDT, P., BOGANI, D., ELSUM, I., GREENFIELD, A., TUVESON, D. A., SIMON, R. & HUMBERT, P. O. 2011. SCRIB expression is deregulated in human prostate cancer, and its deficiency in mice promotes prostate neoplasia. *J Clin Invest*, 121, 4257-67.
- PEREIRA, P. N., DOBREVA, M. P., GRAHAM, L., HUYLEBROECK, D., LAWSON, K. A. & ZWIJSEN, A. N. 2011. Amnion formation in the mouse embryo: the single amniochorionic fold model. *BMC Dev Biol*, 11, 48.
- PETIET, A. E., KAUFMAN, M. H., GODDEERIS, M. M., BRANDENBURG, J., ELMORE, S. A. & JOHNSON, G. A. 2008. High-resolution magnetic resonance histology of the embryonic and neonatal mouse: a 4D atlas and morphologic database. *Proc Natl Acad Sci U S A*, 105, 12331-6.
- POLNIK, D., BACEWICZ, L., JARON, W., KOWALSKI, A., ROSZKOWSKI, T., SZYSZKA, M., WILINSKA, M. & KALICINSKI, P. 2012. The effect of prenatally administered steroids on the treatment results of the newborns gastroschisis. *Presented at the Joint European Paediatric Surgeons' Association / British Association of Paediatric Surgeons congress, Rome.*
- QU, S., NISWENDER, K. D., JI, Q., VAN DER MEER, R., KEENEY, D., MAGNUSON, M. A. & WISDOM, R. 1997. Polydactyly and ectopic ZPA formation in Alx-4 mutant mice. *Development*, 124, 3999-4008.
- QUEMELO, P. R., LOURENCO, C. M. & PERES, L. C. 2007. Teratogenic effect of retinoic acid in swiss mice. *Acta Cir Bras*, 22, 451-6.

- RAMON Y CAJAL, C. L. & MARTINEZ, R. O. 2003. Defecation in utero: a physiologic fetal function. *Am J Obstet Gynecol*, 188, 153-6.
- RANKIN, J., DILLON, E. & WRIGHT, C. 1999. Congenital anterior abdominal wall defects in the north of England, 1986–1996: occurrence and outcome. *Prenatal diagnosis*, 19, 662-668.
- RASMUSSEN, S. A. & FRIAS, J. L. 2008. Non-genetic risk factors for gastroschisis. *American Journal of Medical Genetics Part C-Seminars in Medical Genetics*, 148C, 199-212.
- REID, K. P., DICKINSON, J. E. & DOHERTY, D. A. 2003. The epidemiologic incidence of congenital gastroschisis in Western Australia. *Am J Obstet Gynecol*, 189, 764-8.
- RENFREE, M. B., HENSLEIGH, H. C. & MCLAREN, A. 1975. Developmental changes in the composition and amount of mouse fetal fluids. *J Embryol Exp Morphol*, 33, 435-46.
- RICART, E. 2012. Current status of mesenchymal stem cell therapy and bone marrow transplantation in IBD. *Dig Dis*, 30, 387-91.
- RITTLER, M., VAUTHAY, L. & MAZZITELLI, N. 2013. Gastroschisis is a defect of the umbilical ring: evidence from morphological evaluation of stillborn fetuses. *Birth Defects Res A Clin Mol Teratol*, 97, 198-209.
- ROBERTS, D. & DALZIEL, S. 2006. Antenatal corticosteroids for accelerating fetal lung maturation for women at risk of preterm birth. *Cochrane Database Syst Rev*, 3.
- ROBERTS, J. P. & GOLLOW, I. J. 1990. Central venous catheters in surgical neonates. *J Pediatr Surg*, 25, 632-4.
- ROBERTS, R. R., ELLIS, M., GWYNNE, R. M., BERGNER, A. J., LEWIS, M. D., BECKETT, E. A., BORNSTEIN, J. C. & YOUNG, H. M. 2010. The first intestinal motility patterns in fetal mice are not mediated by neurons or interstitial cells of Cajal. *J Physiol*, 588, 1153-69.
- ROBERTS, T. A., NORRIS, F. C., CARNAGHAN, H., SAVERY, D., WELLS, J. A., SIOW, B., SCAMBLER, P. J., PIERRO, A., DE COPPI, P., EATON, S. & LYTHGOE, M. F. 2014. In amnio MRI of mouse embryos. *PLoS One*, 9, e109143.
- RODRIGUES, A. F., VAN MOURIK, I. D., SHARIF, K., BARRON, D. J., DE GIOVANNI, J. V., BENNETT, J., BROMLEY, P., PROTHEROE, S., JOHN, P., DE VILLE DE GOYET, J. & BEATH, S. V. 2006. Management of end-stage central venous access in children referred for possible small bowel transplantation. *J Pediatr Gastroenterol Nutr*, 42, 427-33.
- ROELOFS, L. A., GEUTJES, P. J., HULSBERGEN-VAN DE KAA, C. A., EGGINK, A. J., VAN KUPPEVELT, T. H., DAAMEN, W. F., CREVELS, A. J., VAN DEN BERG, P. P., FEITZ, W. F. & WIJNEN, R. M. 2013. Prenatal coverage of experimental gastroschisis with a collagen scaffold to protect the bowel. *J Pediatr Surg*, 48, 516-24.
- ROGERS, D. & BURNSTOCK, G. 1966. The interstitial cell and its place in the concept of the autonomic ground plexus. *Journal of Comparative Neurology*, 126, 255-284.
- ROMANO-KEELER, J. & WEITKAMP, J. H. 2015. Maternal influences on fetal microbial colonization and immune development. *Pediatr Res*, 77, 189-95.
- ROOT, E. D., MEYER, R. E. & EMCH, M. E. 2009. Evidence of localized clustering of gastroschisis births in North Carolina, 1999-2004. *Soc Sci Med*, 68, 1361-7.

- ROSS, M. G. & NIJLAND, M. J. 1998. Development of ingestive behavior. *Am J Physiol*, 274, R879-93.
- SADLER, T. W. 2004. Langman's Medical Embryology. Ninth ed.: Lippincott Williams & Wilkins.
- SADLER, T. W. 2010. The embryologic origin of ventral body wall defects. *Semin Pediatr Surg*, 19, 209-14.
- SADLER, T. W. & FELDKAMP, M. L. 2008. The embryology of body wall closure: relevance to gastroschisis and other ventral body wall defects. *Am J Med Genet C Semin Med Genet*, 148c, 180-5.
- SADLER, T. W. & RASMUSSEN, S. A. 2010. Examining the evidence for vascular pathogenesis of selected birth defects. *Am J Med Genet A*, 152A, 2426-36.
- SALIHU, H. M., EMUSU, D., ALIYU, Z. Y., PIERRE-LOUIS, B. J., DRUSCHEL, C. M. & KIRBY, R. S. 2004. Mode of delivery and neonatal survival of infants with isolated gastroschisis. *Obstet Gynecol*, 104, 678-83.
- SALLER, D. N., JR., CANICK, J. A., PALOMAKI, G. E., KNIGHT, G. J. & HADDOW, J. E. 1994. Second-trimester maternal serum alpha-fetoprotein, unconjugated estriol, and hCG levels in pregnancies with ventral wall defects. *Obstet Gynecol*, 84, 852-5.
- SAMARAWICKRAMA, G. P. & WEBB, M. 1981. The acute toxicity and teratogenicity of cadmium in the pregnant rat. *J Appl Toxicol*, 1, 264-9.
- SANTOS, M. M., TANNURI, U. & MAKSOUD, J. G. 2003. Alterations of enteric nerve plexus in experimental gastroschisis: is there a delay in the maturation? *J Pediatr Surg*, 38, 1506-11.
- SAPIN, E., MAHIEU, D., BORGNON, J., DOUVIER, S., CARRICABURU, E. & SAGOT, P. 2000. Transabdominal amniocentesis to avoid fetal demise and intestinal damage in fetuses with gastroschisis and severe oligohydramnios. *J Pediatr Surg*, 35, 598-600.
- SCHNEIDER, J. E., BAMFORTH, S. D., GRIEVE, S. M., CLARKE, K., BHATTACHARYA, S. & NEUBAUER, S. 2003. High-resolution, high-throughput magnetic paragraph sign resonance imaging of mouse embryonic paragraph sign anatomy using a fast gradient-echo sequence. *Magma*, 16, 43-51.
- SCHUSTER, S. R. 1967. A new method for the staged repair of large omphaloceles. *Surg Gynecol Obstet*, 125, 837-50.
- SCHWAB, M., COKSAYGAN, T., SAMTANI, M. N., JUSKO, W. J. & NATHANIELSZ, P. W. 2006. Kinetics of betamethasone and fetal cardiovascular adverse effects in pregnant sheep after different doses. *Obstetrics & Gynecology*, 108, 617-625.
- SEKAR, K. C. 2010. Iatrogenic complications in the neonatal intensive care unit. *J Perinatol*, 30 Suppl, S51-6.
- SENCAN, A., GUMUSTEKIN, M., GELAL, A., ARSLAN, O., OZER, E. & MIR, E. 2002. Effects of amnio-allantoic fluid exchange on bowel contractility in chick embryos with gastroschisis. *J Pediatr Surg*, 37, 1589-93.
- SERRA, A., FITZE, G., KAMIN, G., DINGER, J., KONIG, I. R. & ROESNER, D. 2008. Preliminary report on elective preterm delivery at 34 weeks and primary abdominal closure for the management of gastroschisis. *Eur J Pediatr Surg*, 18, 32-7.
- SHAH, S. K., AROOM, K. R., WALKER, P. A., XUE, H., JIMENEZ, F., GILL, B. S., COX, C. S., JR. & MOORE-OLUFEMI, S. D. 2012. Effects of

- nonocclusive mesenteric hypertension on intestinal function: implications for gastroschisis-related intestinal dysfunction. *Pediatr Res*, 71, 668-74.
- SHAW, A. 1975. The myth of gastroschisis. *J Pediatr Surg*, 10, 235-44.
- SHEA-DONOHUE, T., NOTARI, L., SUN, R. & ZHAO, A. 2012. Mechanisms of Smooth Muscle Responses to Inflammation. *Neurogastroenterology and Motility*, 24, 802-811.
- SINGH, J. 2003. Gastroschisis is caused by the combination of carbon monoxide and protein-zinc deficiencies in mice. *Birth Defects Res B Dev Reprod Toxicol*, 68, 355-62.
- SKARSGARD, E. D., CLAYDON, J., BOUCHARD, S., KIM, P. C., LEE, S. K., LABERGE, J. M., MCMILLAN, D., VON DADELSZEN, P. & YANCHAR, N. 2008. Canadian Pediatric Surgical Network: a population-based pediatric surgery network and database for analyzing surgical birth defects. The first 100 cases of gastroschisis. *J Pediatr Surg*, 43, 30-4; discussion 34.
- SLATTERY, J., MACFABE, D. F. & FRYE, R. E. 2016. The Significance of the Enteric Microbiome on the Development of Childhood Disease: A Review of Prebiotic and Probiotic Therapies in Disorders of Childhood. *Clin Med Insights Pediatr*, 10, 91-107.
- SMITH, V. V., LAKE, B. D., KAMM, M. A. & NICHOLLS, R. J. 1992. Intestinal pseudo-obstruction with deficient smooth muscle alpha-actin. *Histopathology*, 21, 535-42.
- SOUTH, A. P., STUTEY, K. M. & MEINZEN-DERR, J. 2013. Metaanalysis of the prevalence of intrauterine fetal death in gastroschisis. *Am J Obstet Gynecol*, 209, 114.e1-13.
- SRINATHAN, S. K., LANGER, J. C., BLENNERHASSETT, M. G., HARRISON, M. R., PELLETIER, G. J. & LAGUNOFF, D. 1995. Etiology of intestinal damage in gastroschisis. III: Morphometric analysis of the smooth muscle and submucosa. *J Pediatr Surg*, 30, 379-83.
- SRIVASTAVA, A. S., FENG, Z., MISHRA, R., MALHOTRA, R., KIM, H. S. & CARRIER, E. 2007. Embryonic stem cells ameliorate piroxicam-induced colitis in IL10<sup>-/-</sup> KO mice. *Biochem Biophys Res Commun*, 361, 953-9.
- STANGER, J., MOHAJERANI, N. & SKARSGARD, E. D. 2014. Practice variation in gastroschisis: factors influencing closure technique. *J Pediatr Surg*, 49, 720-3.
- STEVENSON, R. E., ROGERS, R. C., CHANDLER, J. C., GAUDERER, M. W. & HUNTER, A. G. 2009. Escape of the yolk sac: a hypothesis to explain the embryogenesis of gastroschisis. *Clin Genet*, 75, 326-33.
- STUBER, T. N., FRIEAUFF, E., WEISS, C., ZOLLNER, U., WOCKEL, A., MEYER, T. & REHN, M. 2016. Prenatal sonographic ultrasound predictors for the outcome in fetal gastroschisis: a retrospective analysis. *Arch Gynecol Obstet*, 293, 1001-6.
- SUITA, S., OKAMATSU, T., YAMAMOTO, T., HANDA, N., NIRASAWA, Y., WATANABE, Y., YANAGIHARA, J., NISHIJIMA, E., HIROBE, S., NIO, M., GOMI, A. & HORISAWA, M. 2000. Changing profile of abdominal wall defects in Japan: results of a national survey. *J Pediatr Surg*, 35, 66-71; discussion 72.
- SUKRA, Y., SASTROHADINOTO, S. & BUDIARSO, I. T. 1976. Effect of selenium and mercury on gross morphology and histopathology of chick embryos. *Poult Sci*, 55, 2424-33.

- SUZUKI, N., LABOSKY, P. A., FURUTA, Y., HARGETT, L., DUNN, R., FOGO, A. B., TAKAHARA, K., PETERS, D., GREENSPAN, D. S. & HOGAN, B. 1996. Failure of ventral body wall closure in mouse embryos lacking a procollagen C-proteinase encoded by *Bmp1*, a mammalian gene related to *Drosophila tolloid*. *Development*, 122, 3587-3595.
- SWAMINATHAN, M. & KAPUR, R. P. 2010. Counting myenteric ganglion cells in histologic sections: an empirical approach. *Hum Pathol*, 41, 1097-108.
- SZABO, K. T., DIFEBBO, M. E. & PHELAN, D. G. 1978. The effects of gold-containing compounds on pregnant rabbits and their fetuses. *Vet Pathol Suppl*, 15, 97-102.
- SZURSZEWSKI, J. H. 1969. A migrating electric complex of canine small intestine. *Am J Physiol*, 217, 1757-63.
- TAMADA, H. & KIYAMA, H. 2015. Existence of c-Kit negative cells with ultrastructural features of interstitial cells of Cajal in the subserosal layer of the W/W<sup>v</sup> mutant mouse colon. *J Smooth Muscle Res*, 51, 1-9.
- TAMBURINI, S., SHEN, N., WU, H. C. & CLEMENTE, J. C. 2016. The microbiome in early life: implications for health outcomes. 22, 713-22.
- TAN, K. B., TAN, K. H., CHEW, S. K. & YEO, G. S. 2008. Gastroschisis and omphalocele in Singapore: a ten-year series from 1993 to 2002. *Singapore Med J*, 49, 31-6.
- TAN, K. H., KILBY, M. D., WHITTLE, M. J., BEATTIE, B. R., BOOTH, I. W. & BOTTING, B. J. 1996. Congenital anterior abdominal wall defects in England and Wales 1987-93: retrospective analysis of OPCS data. *BMJ: British Medical Journal*, 313, 903.
- TANDER, B., BICAKCI, U., SULLU, Y., RIZALAR, R., ARITURK, E., BERNAY, F. & KANDEMIR, B. 2010. Alterations of Cajal cells in patients with small bowel atresia. *J Pediatr Surg*, 45, 724-8.
- THUNEBERG, L. 1999. One hundred years of interstitial cells of Cajal. *Microscopy research and technique*, 47, 223-238.
- TIBBOEL, D., VERMEY-KEERS, C., KLÜCK, P., GAILLARD, J., KOPPENBERG, J. & MOLENAAR, J. 1986. The natural history of gastroschisis during fetal life: development of the fibrous coating on the bowel loops. *Teratology*, 33, 267-272.
- TODROS, T., CAPUZZO, E. & GAGLIOTI, P. 2001. Prenatal diagnosis of congenital anomalies. *Images in Paediatric Cardiology*, 3, 3-18.
- TORIHASHI, S., NISHI, K., TOKUTOMI, Y., NISHI, T., WARD, S. M. & SANDERS, K. M. 1999. Blockade of kit signaling induces transdifferentiation of interstitial cells of Cajal to a smooth muscle phenotype. *Gastroenterology*, 117, 140-148.
- TORIHASHI, S., WARD, S. M. & SANDERS, K. M. 1997. Development of c-Kit-positive cells and the onset of electrical rhythmicity in murine small intestine. *Gastroenterology*, 112, 144-55.
- TORRAZZA, R. M. & NEU, J. 2013. The altered gut microbiome and necrotizing enterocolitis. *Clin Perinatol*, 40, 93-108.
- TOWER, C., ONG, S. S., EWER, A. K., KHAN, K. & KILBY, M. D. 2009. Prognosis in isolated gastroschisis with bowel dilatation: a systematic review. *Arch Dis Child Fetal Neonatal Ed*, 94, F268-74.
- TOWERS, C. V. & CARR, M. H. 2008. Antenatal fetal surveillance in pregnancies complicated by fetal gastroschisis. *Am J Obstet Gynecol*, 198, 686.e1-5; discussion 686.e5.



- TOYOSAKA, A., TOMIMOTOT, Y., NOSE, K., SEKI, Y. & OKAMOTO, E. 1994. Immaturity of the myenteric plexus is the aetiology of meconium ileus without mucoviscidosis: a histopathologic study. *Clinical Autonomic Research*, 4, 175-84.
- TUMELTY, K. E., SMITH, B. D., NUGENT, M. A. & LAYNE, M. D. 2014. Aortic carboxypeptidase-like protein (ACLP) enhances lung myofibroblast differentiation through transforming growth factor beta receptor-dependent and -independent pathways. *J Biol Chem*, 289, 2526-36.
- TURNBULL, D. H. & MORI, S. 2007. MRI in mouse developmental biology. *NMR Biomed*, 20, 265-74.
- UNDERWOOD, M., GILBERT, W. & MP, S. 2005. Amniotic Fluid: Not Just Fetal Urine Anymore. *Journal of Perinatology*, 25, 341-348.
- VACHHARAJANI, A. J., RAO, R., KESWANI, S. & MATHUR, A. M. 2009. Outcomes of exomphalos: an institutional experience. *Pediatric surgery international*, 25, 139-144.
- VAN DER VEEKEN, L., RUSSO, F. M., DE CATTE, L., GRATACOS, E., BENACHI, A., VILLE, Y., NICOLAIDES, K., BERG, C., GARDENER, G., PERSICO, N., BAGOLAN, P., RYAN, G., BELFORT, M. A. & DEPREST, J. 2018. Fetoscopic endoluminal tracheal occlusion and reestablishment of fetal airways for congenital diaphragmatic hernia. 15, 9.
- VAN DORP, D. R., MALLEIS, J. M., SULLIVAN, B. P. & KLEIN, M. D. 2010. Teratogens inducing congenital abdominal wall defects in animal models. *Pediatr Surg Int*, 26, 127-39.
- VAN MANEN, M., HENDSON, L., WILEY, M., EVANS, M., TAGHADDOS, S. & DINU, I. 2013. Early childhood outcomes of infants born with gastroschisis. *J Pediatr Surg*, 48, 1682-7.
- VAN TEEFFELEN, S., PAJKRT, E., WILLEKES, C., VAN KUIJK, S. M. & MOL, B. W. 2013. Transabdominal amnioinfusion for improving fetal outcomes after oligohydramnios secondary to preterm prelabour rupture of membranes before 26 weeks. *Cochrane Database Syst Rev*, Cd009952.
- VANDER, A., SHERMAN, J. & LUCIANO, D. 2001. Human Physiology, The Mechanisms of Body Function, Eighth Edition. *McGraw-Hill International Edition*.
- VARGUN, R., AKTUG, T., HEPER, A. & BINGOL-KOLOGLU, M. 2007. Effects of intrauterine treatment on interstitial cells of Cajal in gastroschisis. *J Pediatr Surg*, 42, 783-7.
- VRIJHEID, M., DOLK, H., STONE, D., ABRAMSKY, L., ALBERMAN, E. & SCOTT, J. 2000. Socioeconomic inequalities in risk of congenital anomaly. *Archives of Disease in Childhood*, 82, 349-352.
- WALLACE, A. S. & BURNS, A. J. 2005. Development of the enteric nervous system, smooth muscle and interstitial cells of Cajal in the human gastrointestinal tract. *Cell Tissue Res*, 319, 367-82.
- WANG, H., ZHANG, Y., LIU, W., WU, R., CHEN, X., GU, L., WEI, B. & GAO, Y. 2009. Interstitial cells of Cajal reduce in number in recto-sigmoid Hirschsprung's disease and total colonic aganglionosis. *Neurosci Lett*, 451, 208-11.
- WANG, X. Y., VANNUCCHI, M. G., NIEUWMEYER, F., YE, J., FAUSSONE-PELLEGRINI, M. S. & HUIZINGA, J. D. 2005. Changes in interstitial cells of Cajal at the deep muscular plexus are associated with loss of distention-

- induced burst-type muscle activity in mice infected by *Trichinella spiralis*. *Am J Pathol*, 167, 437-53.
- WARD, S. M., BURNS, A. J., TORIHASHI, S., HARNEY, S. C. & SANDERS, K. M. 1995. Impaired development of interstitial cells and intestinal electrical rhythmicity in steel mutants. *Am J Physiol*, 269, C1577-85.
- WATKINS, D. E. 1943. Gastroschisis. *Va Med*, 70, 42-45.
- WEBER, T. R., AU-FLIEGNER, M., DOWNARD, C. D. & FISHMAN, S. J. 2002. Abdominal wall defects. *Curr Opin Pediatr*, 14, 491-7.
- WESONGA, A. S., FITZGERALD, T. N., KABUYE, R., KIRUNDA, S., LANGER, M., KAKEMBO, N., OZGEDIZ, D. & SEKABIRA, J. 2016. Gastroschisis in Uganda: Opportunities for improved survival. *J Pediatr Surg*, 51, 1772-1777.
- WHO 2014. Child Causes of Death 2000-2013. *World Health Organisation*.
- WILLIAMS, J., MAI, C. T., MULINARE, J., ISENBURG, J., FLOOD, T. J., ETHEN, M., FROHNERT, B. & KIRBY, R. S. 2015. Updated estimates of neural tube defects prevented by mandatory folic Acid fortification - United States, 1995-2011. *MMWR Morb Mortal Wkly Rep*, 64, 1-5.
- WILSON, R. B. & HARTROFT, W. S. 1970. Pathogenesis of myocardial infarcts in rats fed a thrombogenic diet. *Arch Pathol*, 89, 457-69.
- WINN, H. N. & HOBBS, J. C. 2000. *Clinical Maternal-Fetal Medicine*, The Parthenon Publishing Group.
- WINTER, L. W., GIUSEPPETTI, M. & BREUER, C. K. 2005. A case report of midgut atresia and spontaneous closure of gastroschisis. *Pediatr Surg Int*, 21, 415-6.
- YAN, J. & HALES, B. F. 2006. Depletion of glutathione induces 4-hydroxynonenal protein adducts and hydroxyurea teratogenicity in the organogenesis stage mouse embryo. *J Pharmacol Exp Ther*, 319, 613-21.
- YARDLEY, I. E., BOSTOCK, E., JONES, M. O., TURNOCK, R. R., CORBETT, H. J. & LOSTY, P. D. 2012. Congenital abdominal wall defects and testicular maldescent--a 10-year single-center experience. *J Pediatr Surg*, 47, 1118-22.
- YOO, S. Y., JUNG, S. H., EOM, M., KIM, I. H. & HAN, A. 2002. Delayed maturation of interstitial cells of Cajal in meconium obstruction. *J Pediatr Surg*, 37, 1758-61.
- YOUSSEF, F., LABERGE, J. M. & BAIRD, R. J. 2015. The correlation between the time spent in utero and the severity of bowel matting in newborns with gastroschisis. *J Pediatr Surg*, 50, 755-9.
- YU, J., GONZALEZ-REYES, S., DIEZ-PARDO, J. A. & TOVAR, J. A. 2004. Local dexamethasone improves the intestinal lesions of gastroschisis in chick embryos. *Pediatric surgery international*, 19, 780-784.
- ZANI-RUTTENSTOCK, E., ZANI, A., PAUL, A., DIAZ-CANO, S. & ADE-AJAYI, N. 2015. Interstitial cells of Cajal are decreased in patients with gastroschisis associated intestinal dysmotility. *J Pediatr Surg*, 50, 750-4.
- ZANI, A., CANANZI, M., FASCETTI-LEON, F., LAURITI, G., SMITH, V. V., BOLLINI, S., GHIONZOLI, M., D'ARRIGO, A., POZZOBON, M., PICCOLI, M., HICKS, A., WELLS, J., SIOW, B., SEBIRE, N. J., BISHOP, C., LEON, A., ATALA, A., LYTHGOE, M. F., PIERRO, A., EATON, S. & DE COPPI, P. 2014. Amniotic fluid stem cells improve survival and enhance repair of damaged intestine in necrotising enterocolitis via a COX-2 dependent mechanism. *Gut*, 63, 300-9.

ZHAO, B., TUMANENG, K. & GUAN, K. L. 2011. The Hippo pathway in organ size control, tissue regeneration and stem cell self-renewal. *Nat Cell Biol*, 13, 877-83.

## **Appendix 1: Publications and Presentations Arising from the Work Contributing to this Thesis**

### **Publications**

**Carnaghan H**, Baud D, Lapidus-Krol E, Ryan G, Shah P, Pierro A, Eaton S. Effect of Gestational Age at Birth on Neonatal Outcomes in Gastroschisis, *J Pediatr Surg*. 2016 May;51(5):734-8.

Roberts TA, Norris FC, **Carnaghan H**, Savery D, Wells JA, Siow B, Scambler PJ, Pierro A, De Coppi P, Eaton S, Lythgoe MF. In amnio MRI of mouse embryos. *PLOS ONE*. 2014 Oct 15;9(10):e109143.

**Carnaghan H**, Pereira S, James CP, Charlesworth PB, Ghionzoli M, Mohamed E, Cross KM, Kiely E, Patel S, Desai A, Nicolaidis K, Curry JJ, Ade-Ajayi N, De Coppi P, Davenport M, David AL, Pierro A, Eaton S. Is Early Delivery Beneficial in Gastroschisis? *J Pediatr Surg*. 2014;49(6):928-33.

**Carnaghan H**, Roberts T, Savery D, Norris FC, McCann CJ, Copp AJ, Scambler PJ, Lythgoe MF, Greene ND, Decoppi P, Burns AJ, Pierro A, Eaton S. Novel exomphalos genetic mouse model: The importance of accurate phenotypic classification. *J Pediatr Surg*. 2013 Oct;48(10):2036-42.

### **International Invited Speaker**

**Carnaghan H**. Is dysmotility in gastroschisis secondary to deficiency in interstitial cells of Cajal? Evidence from animal models and human pathological specimens. Gastroschisis Symposium, British Association of Paediatric Surgeons Conference, Ljubljana, Slovenia 23<sup>rd</sup> July 2015.

### **International Oral Presentations**

**Carnaghan H**, Hart A, McCann CJ, De Coppi P, David AL, Pierro A, Burns AJ, Eaton S. Interstitial cells of Cajal and gut motility in abdominal wall defect mice

lacking aortic carboxypeptidase-like protein: Effects of pro-inflammatory cytokine il-8. British Association of Paediatric Surgeons Conference, London, UK, 20<sup>th</sup> July 2017.

**Carnaghan H**, Virasami A, Pierro A, De Coppi P, Burns AJ, Sebire NJ, Eaton S. Smooth muscle actin expression is decreased in small bowel longitudinal muscle in human gastroschisis: Possible implications for motility. Peter Paul Rickham Prize session, British Association of Paediatric Surgeons Conference, Amsterdam, Holond, 20<sup>th</sup> July 2016.

**Carnaghan H**, James CP, Charlesworth PB, Ghionzoli M, Pereira S, Mohamed E, Lapidus-Krol E, Baud D, Cros KMK, Kiely E, Patel S, Desai A, Nicolaidis K, Curry JI, Ade-Ajayi N, De Coppi P, Ryan G, Shah P, Davenport M, David AL, Pierro A, Eaton S. Do maternal antenatal corticosteroids decrease time to full enteral feeds in infants with gastroschisis? A multicentre retrospective study. President's Prize session winner, British Association of Paediatric Surgeons Conference, Cardiff, UK, 22<sup>nd</sup> July 2015

**Carnaghan H**, Virasami A, Copp AJ, Pierro A, De Coppi P, Sebire N, Burns AJ, Eaton S. Detailed phenotype classification of the ventral wall defect present in mice lacking aortic carboxypeptidase-like protein (ACL<sup>P</sup>): Neither gastroschisis or exomphalos. European Surgeons' Association Conference, Ljubljana, Slovenia, 20th June 2015

**Carnaghan H**, Virasami A, Pierro A, De Coppi P, Burns AJ, Sebire N, Eaton S. Analysis of Interstitial Cells of Cajal and Enteric Neurons in Human Gastroschisis. XXVIIth International Symposium on Paediatric Surgical Research, Toronto, Canada, Sept 2014

**Carnaghan H**, Pereira S, James CP, Charlesworth PB, Ghionzoli M, Mohamed E, Cross KMK, Kiely E, Patel S, Desai A, Nicolaidis K, Curry JI, Ade-Ajayi N, De Coppi P, Davenport M, David AL, Pierro A, Eaton S. Is Early Delivery Beneficial in Gastroschisis? Prize session, American Academy of Pediatrics National Conference and Exhibition, Orlando, USA, Oct 2013

**Carnaghan H**, Roberts T, Savery D, Norris F, Copp AJ, Lythgoe M, De Coppi P, Eaton S, Pierro A. Novel exomphalos genetic mouse model: The importance of accurate phenotypic classification. Joint European Paediatric Surgeons' Association/ British Association of Paediatric Surgeons Annual Paediatric Surgery Congress, Jun 2012.

### **International Poster Presentations**

**Carnaghan H**, Virasami A, Pierro A, De Coppi P, Burns AJ, Sebire N, Eaton S. Bowel wall thickening and prolonged time to full enteral feeds in gastroschisis: A new hypothesis for the cause of gastroschisis-related gut dysfunction. International Symposium on Pediatric Surgical Research, Dublin, 24-26 September 2015.

**Carnaghan H**, Baud D, Lapidus-Krol E, Ryan G, Shah P, Pierro A, Eaton S. Effect of gestational age at birth on neonatal outcomes in gastroschisis. Canadian Association of Paediatric Surgeons, Niagara Falls, Canada, 18<sup>th</sup> September 2015.

Roberts T, Norris FC, **Carnaghan H**, Savery D, Wells JA, Siow B, Scambler PJ, Pierro A, Eaton S, Lythgoe MF. *In amnio* MRI of mouse embryos for the identification of abdominal pathologies. International Society for Magnetic Resonance in Medicine: British Chapter, Cambridge, UK, Sep 2012.

Roberts T, Norris F, **Carnaghan H**, Savery D, Wells JA, Siow B, Scambler PJ, Pierro A, Eaton S, Lythgoe MF. *In amnio* MRI for the identification of abdominal pathologies. International Society for Magnetic Resonance in Medicine, Melbourne Australia, May 2012.

# Appendix 2: The Long-Term Impact of Parenteral Nutrition on Growth in Surgical Infants.

## The Long-Term Impact of Parenteral Nutrition on Growth in Surgical Infants

Helen Carnaghan, Evelyn Ong, Venetia Horn, Agostino Pierro, Simon Eaton  
Surgery Unit, UCL Institute of Child Health and Great Ormond Street Hospital,  
London, United Kingdom



### Background

It is known that surgical infants on PN exhibit poor growth. However, relatively little is known about the long-term impact on growth in this population and whether catch-up growth occurs following establishment of full enteral feeds.

### Aim

Our aim was to determine the pattern of growth of surgical infants both during PN and following attainment of full enteral feeds.



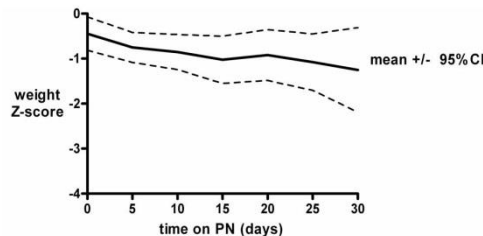
Infant with gastroschisis, an example of an abdominal wall defect requiring PN

### Methods

- This was a retrospective study with IRB approval.
- Investigating infants <3 months (n=38) of age receiving PN following surgery and who went on to achieve full enteral feeds.
- The following data were collected from the patient case notes:
  - Date of birth
  - Gestational age
  - Sex
  - Birth weight
  - Weights prior, during, and after PN including the date of measurement.
- Weight Z-scores were calculated and analysed using paired t-tests and multi-level regression modelling.
- Data displayed as mean  $\pm$  SEM.

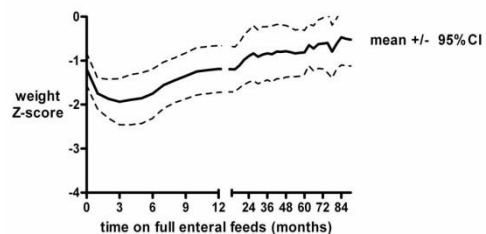
### Results

#### Parenteral Feeds



- Surgical infants at commencement of PN were slightly under the 50<sup>th</sup> centile with a mean Z-score of  $-0.45 \pm 0.18$ .
- During PN surgical infants lost  $0.10 \pm 0.01$  Z-scores per week of PN ( $p < 0.001$ ).
- At the end of PN this cohort had a weight Z-score of  $-1.4 \pm 0.21$ .
- Follow-up duration following establishment of full enteral feeds was  $50 \pm 5.4$  months.

#### Full Enteral Feeds



- Following attainment of full enteral feeds, surgical infants continued to grow poorly resulting in further significant loss of weight Z-scores for approximately 3-6 months.
- Following this period, catch-up growth did occur but at a slower rate than it was initially lost with on average  $0.19 \pm 0.03$  Z-scores being gained per year ( $p < 0.001$ ).
- Weight Z-scores at last follow-up were  $-0.7 \pm 0.3$ , significantly greater than that at end of PN ( $p = 0.013$ ).

### Conclusions

- Surgical infants are known to exhibit poor growth during periods of PN as confirmed by this study.
- However, although full enteral feeds have been reached, there is a further loss of weight Z-scores lasting a further 3-6 months.
- We hypothesise even though full enteral feeds are tolerated, the intestine may not have reached full absorptive capacity. Catch-up growth does eventually occur but weight gain is at slower rate than the initial weight loss exhibited during PN, presumably as intestinal adaptation takes place.

- As these surgical infants experience an extended period of sub-optimal growth and nutrition during a critical period of development, there may be long-term adverse consequences. A long-term follow-up study of body composition and cardiovascular risk markers is necessary to assess these long-term consequences.

### Acknowledgements

- Action Medical Research
- British Association of Paediatric Surgeons
- Royal College of Surgeons of England
- Great Ormond Street Hospital Children's Charity